S-block metal chemistry of iminophosphoranes, phosphonium ylides and related systems: a synthetic and structural investigation

Price, Richard D.

S-block metal chemistry of iminophosphoranes, phosphonium ylides and related systems: a synthetic and structural investigation.

by

Richard D. Price
(Collingwood College)

A thesis submitted in part fulfilment of the requirements for the degree of Doctor of Philosophy in the University of Durham.

August 1999

Statement of Copyright

Declaration

The work described in this thesis was carried out in the Department of Chemistry at the University of Durham between October 1996 and July 1999. All the work is my own unless stated to the contrary and it has not been submitted previously for a degree at this or any other university.

Financial Support

The EPSRC and ICI are gratefully acknowledged for their financial support.

Table of Contents

Dedication		i
Acknowledgements		ii
List of Publications		iii
Abstract		iv
List of Abbreviations		v
	CHAPTER 1	
1.	Introduction	1
1.1	Ylides	2
1.2	Phosphonium Ylides	3
1.3	Iminophosphoranes	19
	CHAPTER 2	
2.	General Experimental Techniques	29
2.1	Inert Atmosphere Techniques	29
2.2	Starting materials and solvents	31
2.3	Nuclear Magnetic Resonance (NMR) Spectroscopy	32
2.4	Infra-Red Spectroscopy	32
2.5	Melting Points	33
2.6	Elemental Analysis	33
2.7	X-ray Diffraction Studies	33
2.8	Neutron Diffraction	34
2.9	Cryoscopy	35
2.10	Gas Chromatography (GC)	37

CHAPTER 3

3.	Experimental	38
3.1	Preparation of Starting Materials 1-8	40
3.2	Synthesis and characterisation of complexes 9-24	47
3.3	Synthesis and characterisation of complexes 25-28	68
3.4	Synthesis and characterisation of complexes 29-35	74
3.5	Synthesis and characterisation of complexes 36-40	83
3.6	Synthesis and characterisation of complexes 41-44	89

CHAPTER 4

4.	Complexation of s-block metal aryloxides	95
4.1	Background	96
4.2	Structural features of ligands 1-8	100
4.3	NMR data of complexes 9 to 24	104
4.4	Structural discussion of complexes 9-27	106
4.5	Conclusions	130

CHAPTER 5

5.	Phosphonium ylide-alkali metal amide complexes	131
5.1	Alkali metal amides	131
5.2	Solid-state structure of complexes 25 and 27	134
5.3	Solution-state studies of complexes 25-28	140
5.4	Studies of the Wittig reaction	143
5.5	Conclusions	148

CHAPTER 6

6.	*N*-metallated iminophosphoranes	149
6.1	Background	149
6.2	Solid and solution-state studies of 29	152
6.3	Solid-state studies of complexes 30-35	160
6.4	Solid-state NMR studies	180
6.5	Conclusions	184

CHAPTER 7

7.	Alkyldiphenylphosphonium ylides and imines	186
7.1	Introduction	186
7.2	Solid-state structures of complexes 36-38	188
7.3	Solid-state structures of A, 39 and 40	196
7.4	Conclusions	201

CHAPTER 8

8.	Miscellaneous reactions	202
8.1	Solid-state structure of complexes 41 and 42	203
8.2	Solid-state structure and *in situ* NMR studies of 43	211
8.3	Solid-state structure of complex 44	218
8.4	Conclusions	220

Appendix A	Supplementary Crystallographic Data	221
Appendix B	Research Colloquia, Lectures and Conferences Attended	288

Dedication

I would like to dedicate this thesis to Mum and Dad for all their love and encouragement.

Acknowledgements

Firstly, I would like to thank my supervisor Dr. Matthew G. Davidson for his support during the last four years in Durham, his ideas, enthusiasm and plentiful supply of alcoholic beverages.

On the academic side, there are a whole host of people to whom I am gratefully indebted, most notably Prof. Judith A. K. Howard and the Durham University Crystallographic Service. From the latter, a large amount of work was undertaken by Charlie Broder, John Cowan and Drs. Andrei S. Batsanov, Andrés E. Goeta, Christian W. Lehmann, Dmitri Yufit, Royston C. B. Copley and Vanessa Hoy. Also, thanks to the departmental analytical services: Jarika Dostal, Lenny Lauchlan, Judith Magee and Dr. Alan Kenwright. Extensive solid-state nmr studies were performed in collaboration with Prof. Robin K. Harris and Dr. Julian C. Cherryman.

Thanks to Gordon and Ray, the departmental glassblowers, who have exceptional skill and have been invaluable.

Prof. Fernando López-Ortiz (University of Almeria) is thanked for both his hospitality during my three-week stay and his painstaking work on variable- temperature and - concentration nmr. A mention is also worthy of Luis (a truly unique individual), Emma and Nacho, for their camaraderie and help during my visit.

Various lab colleagues have helped make the last three years enjoyable and interesting. Thanks to Christian, Patrick, Markus, Marina and the other members of the section. Special thanks to Sarah and Phil for their friendship and help throughout my PhD, in particular for their crossword-solving abilities, quiz machine addiction and for sharing the odd drink after work.

Thanks also to the many people I have met in Durham during the past six years - too numerous to mention, but in particular the support and encouragement of Simon, Alex, Charlie, Helen, Angus, Liz, Dave, Rich and Steve.

Finally, I must thank my family, especiallly Mum, Dad and Vic, who continue to encourage and support me in everything I do.

List of Publications

(1) Synthesis and X-ray structures of *N*-lithioiminophosphorane·lithium bromide adducts.
Andrei. S. Batsanov, Matthew G. Davidson, Judith A. K. Howard, Sarah Lamb, Christian Lustig and Richard D. Price.
J. Chem. Soc., Chem. Commun., 1211, 1997.

(2) The metallation of imino(triphenyl)phosphorane by ethylmagnesium chloride: The synthesis, isolation and X-ray structure of $[Ph_3P{=}NMgCl{\cdot}O{=}P(NMe_2)_3]_2$.
Andrei. S. Batsanov, Philip D. Bolton, Royston C. B. Copley, Matthew G. Davidson, Judith A. K. Howard, Christian Lustig and Richard D. Price.
J. Organomet. Chem., **550**, 445, 1998.

(3) Low temperature neutron and X-ray diffraction study of imino(triphenyl)phosphorane.
Matthew G. Davidson, Andrés E. Goeta, Judith A. K. Howard, Christian Lehmann, Garry M. McIntyre and Richard D. Price.
J. Organomet. Chem., **550**, 449, 1998.

(4) One pot synthesis and X-ray structure of a chiral *N*-phosphine substituted iminophosphorane.
Andrei. S. Batsanov, Matthew G. Davidson, Judith A. K. Howard, Fernando López-Ortiz, Ignacio Fernández and Richard D. Price.
J. Chem. Soc., Dalton Trans., **submitted for publication**.

(5) MAS solid-state nmr studies of s-block metal-iminophosphorane complexes.
Julian A. Cherryman, Robin K. Harris, Matthew G. Davidson and Richard D. Price.
J. Braz. Chem. Soc., **in press**.

Abstract

This thesis details the synthesis and characterisation of s-block metal (lithium, sodium and magnesium) phosphonium ylide, R_3PCHR', and iminophosphorane complexes, R_3PNR', together with some related phosphine oxide, R_3PO, and sulfide, R_3PS, species, where R= Ph or Me_2N and R' = H, Me or Ph.

The first three chapters of the thesis provide an introduction to the topic, with details of the experimental methods employed and results obtained. Chapter 4 presents a systematic study of Lewis base complexed s-block metal aryloxides, $(ArOM{\cdot}L)_2$ where Ar = $C_6H_3Ph_2$ or $MeC_6H_2(^tBu)_2$, L = R_3PCHR', R_3PNR', R_3PO or R_3PS, and M = Li, Na, and $(ArO)_2Mg{\cdot}(L)_2$ where Ar = $MeC_6H_2(^tBu)_2$ and L = R_3PCHR' or R_3PNR'. This includes a discussion of the single crystal XRD structures of the eight neutral ligands used, L, and ten new complexes containing either lithium or sodium.

Chapter 5 describes the application of some related s-block metal ylide complexes, e.g. $Ph_3PCHMe{\cdot}LiN(CH_2Ph_2)_2$ and $Ph_3PCHMe{\cdot}NaN(SiMe_3)_2$, to the Wittig reaction, together with some solution-state and solid-state discussions (two single crystal XRD structures) of s-block metal amide-phosphonium ylide complexes, $R_3PCHR'.MNR''_2$ where R = Ph or Me_2N, R' = H or Me, and R'' = $SiMe_3$ or CH_2Ph. Chapter 6 details a range of *N*-s-block metallated iminophosphorane complexes (e.g. $Ph_3PNLi{\cdot}LiBr.2thf$ and $R_3PNMgX{\cdot}L$ where R = Ph or Me_2N and L = Lewis base) their application to transmetallation reactions with copper(I) compounds, solution-state and solid-state NMR studies and six new single-crystal XRD structures. Chapter 7 describes some very recent work involving alkyldiphenylphosphonium ylides, $MePh_2PCHPh$, and imines, $MePh_2PNPh$, including a single crystal XRD structural study of the latter and three of its lithium derivatives, e.g. $[CH_2LiPh_2PNPh]_4$. Chapter 8 is concerned with a number of unexpected results, including the synthesis, solid-state structure and proposed mechanism of a novel *N*-phosphino-iminophosphorane, $Ph_2(C_3H_4Ph)PNP(C_3H_5)Ph$, and two aminophosphonium salts, $[R_3PNH_2]^+[OC_6H_3Ph_2]^-$ where R = Ph or Me_2N.

List of Abbreviations

Ave.	average
Ar	aryl
^{n}BuLi	*n*-butyllithium
^{t}Bu	*tert*-butyl
COSY	correlation spectroscopy
CSD	Cambridge Structural Database
δ	chemical shift
DSC	differential scanning calorimetry
Et	ethyl
FT	Fourier transform
GC	gas chromatography
HMDS	hexamethyldisilylamide
hmpa	hexamethylphosphorictriamide
IR	infra-red
K_b	cryoscopic constant (for benzene)
L	Lewis base
M	generic metal
Me	methyl
m.p.	melting point
M_r	relative molecular mass
NMR	nuclear magnetic resonance
Ph	phenyl
ppm	parts per million
R	generic aliphatic hydrocarbon group
thf	tetrahydrofuran
tol	toluene
TMS	trimethylsilane
VC	variable concentration
VT	variable temperature
XRD	X-ray Diffraction

1. Introduction

This thesis is concerned with phosphorus species of the general type $R_2R'PX$, where X can be CH_2, NH, O or S. Their use in synthesis and, in particular, the generation of metal complexes and their solid-state structures are discussed. This chapter provides a very general overview of the topic. More detailed background information is given in the relevant discussion chapters.

The reader is referred to the following excellent monographs and review articles in the field for further reading.

Phosphonium Ylides:

D. G. Gilheany, *Chem. Rev.*, **94**, 1339 (1994).
O. I. Kolodiazhnyi, *Russ. Chem. Rev.*, **3**, 225 (1997).
A. W. Johnson with special contributions by W. C. Kaska, K. A. O. Starzewski and D. A. Dixon, '*Ylides and Imines of Phosphorus*', John Wiley & Sons Inc., New York, (1993).
O. O. Kolodiazhnyi, *Tetrahedron*, **52**, 1855 (1996).

Iminophosphoranes:

K. Dehnicke, M. Krieger and W. Massa, *Coord. Chem. Rev.*, **182**, 19 (1999).
K. Dehnicke and F. Weller, *Coord. Chem. Rev.*, **158**, 103 (1997).
K. Dehnicke and J. Stahle, *Polyhedron*, **8**, 707 (1989).

Phosphine Oxides:

J. A. Dobado, H. Martinez-Garcia, J. Molina-Molina and M. R. Sundberg, *J. Am. Chem. Soc.*, **120**, 8461 (1998).
D. B. Chesnut, *J. Am. Chem. Soc.*, **120**, 10504 (1998).

1.1 Ylides

Ylides have been known for over a century being first discovered by Michaelis et al.,[1] however, it was Staudinger et al. who first proposed the ylide structure in 1919.[2] The later finding in 1953 by Georg Wittig[3] of his Nobel Prize Winning olefination reaction, initiated a hitherto little known branch of chemistry (*Wittig Chemistry*), incorporating the organic, inorganic and organometallic disciplines. The Wittig reaction provides an unparalleled method for olefination during organic syntheses, being '***of unmatched importance for specific introduction of C-C double bonds in a known location***'.[4]

An ylide may be defined[5] as '***a substance in which a carbanion is attached directly to a heteroatom carrying a substantial degree of positive charge and in which the positive charge is created by the sigma bonding of substituents to the heteroatom***', and is most easily represented by the two resonance canonical forms (**Fig. 1.1**).

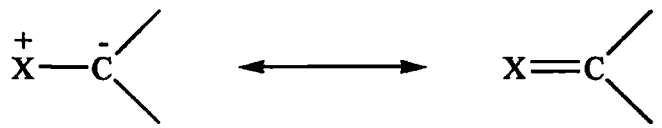

ylide ylene

Figure 1.1 Two resonance canonical forms of an ylide

The ylide canonical form highlights the zwitterionic nature of an onium moiety attached to a carbanionic centre, whilst the ylene form indicates a degree of electronic delocalisation of the charge. Ylide† is the anglicised, and now widely accepted, version of '*ylid*' that Wittig originally coined in his native German tongue - '*yl*' meaning open valence (c.f. methyl) and '*id*' referring to anionicity (c.f. acetylid).[6]

---

[1] A. Michaelis and H. V. Gimborn, *Chem. Ber.*, **27**, 272 (1894).
[2] H. Staudinger and J. Meyer, *Helv. Chim. Acta*, **2**, 635 (1919).
[3] G. Wittig and G. Geissler, *Leibigs Ann. Chem.*, **580**, 44 (1953); G. Wittig's Nobel Prize Lecture, *Science*, **210**, 600 (1980).
[4] E. Vedejs, *Science*, **210**, 42 (1980).
[5] A. W. Johnson with special contributions by W. C. Kaska, K. A. O. Starzewski and D. A. Dixon, '*Ylides and Imines of Phosphorus*', John Wiley & Sons Inc., New York, (1993).
† A phosphonium ylide is defined as '***an easily pyramidalised carbanion, stabilised by an adjacent, tetrahedral phosphonium centre.***'[7]

The heteroatom, X, may be from any one of a variety of atoms, including phosphorus,[7] arsenic[8] and sulfur,[9] amongst others. The most common, useful and extensively studied ylides are those containing a phosphorus heteroatom (*vide infra*), such ylides being the subject of much of this thesis. This introduction will now focus on phosphonium ylides, although much of the discussion concerning structure, bonding and reactivity is applicable to other heteroatoms.

1.2 Phosphonium Ylides

1.2.1 Background

Phosphonium ylides were the first to be discovered in 1894 when Michaelis[1] et al. managed to isolate $Ph_3P{=}CHCO_2Et$. However, its structure[10] wasn't determined until 1961, by which time the identity of the simplest phosphonium ylide, viz. triphenylphosphonium methylide ($Ph_3P{=}CH_2$), had already been elucidated by Staudinger et al.,[2] and Wittig had reported the essential use of ylides in organic synthesis.

Phosphonium ylides can be loosely divided into one of three types:[11] stabilised, semi-stabilised and non-stabilised, which reflect both the degree of delocalisation and basicity. Stabilised ylides are weak bases and generally unreactive, even with moisture and oxygen, whereas, in stark contrast, non-stabilised ylides need to be isolated in the strict absence of oxygen and moisture.

Stabilised ylides contain strongly electron withdrawing groups, such as cyanide, carbonyl or cyclopentadienyl, on the ylidic carbon atom. These are capable of delocalising the negative charge on the carbanion, hence providing added stability.

Semi-stabilised ylides contain moderately conjugating groups, such as phenyl, on the ylidic carbon and are of intermediate reactivity.

---

[6] D. G. Dilheany, *Chem. Rev.*, **94**, 1339 (1994).
[7] H. Schmidbaur, A. Schier, W. Graf, D. L. Wilkinson and G. Muller, *New J. Chem.*, **13**, 341 (1989).
[8] D. Lloyd, *Chem. Soc. Rev.*, **16**, 45 (1987).
[9] B. F. Yates, W. J. Bouma and L. Radom, *J. Am. Chem. Soc.*, **109**, 2250 (1987).
[10] G. Asknes, *Scand. Chem. Acta*, **15**, 438 (1961).

Non-stabilised ylides include those which contain alkyl groups (or hydrogen) on the ylidic carbon, e.g. Ph_3P=CHR (R=alkyl). Their ease of reaction with moisture and oxygen often necessitates their formation (as reactive intermediates) *in situ*. They also tend to be highly coloured from yellow through to red-purple, and as a consequence colour changes may be used to monitor their reactions.

1.2.2 Structure and Bonding

The molecular geometry of a typical phosphonium ylide contains a R_3P fragment bonded to a CXY fragment (**Fig. 1.2**).[6] The CXY group was originally considered to be planar, based on XRD and ED results,[12,13,14] but more recently has been shown to deviate from planarity by as much as 30°.[7,15] Evidence now suggests that stabilised ylides have trigonal planar carbanions, whereas non-stabilised ylides are slightly pyramidalised.[16] The structures exhibit a unique phosphorus substituent, R^*, whose P-R bond is elongated and has a wider RPC_{ylidic} angle in comparison to the other two substituents. The plane defined by R^*, P and C_{ylidic}, is orientated perpendicular to the plane defined by C_{ylidic}, X and Y, thereby relieving steric strain and revealing a possible site of attack beneath and perpendicular to the $C_{ylidic}XY$ plane, where the lone pair resides.

The P-C_{ylidic} bond is shorter than a classical P-C single bond (1.87 Å),[17] typically falling in the range 1.63-1.71 Å.[15] Despite this abbreviated P-C_{ylidic} distance and the resulting inferred P-C double bond character, there is little resistance to rotation around the bond. The barrier to rotation for the hypothetical phosphonium ylide H_3PCH_2 was calculated to be 0.24kcal mol^{-1}.[18,19] This is significantly lower than that of the sulfonium ylide, H_2SCH_2 (21.2 kcal mol^{-1}),[16,18] and lower even than the ammonium ylide, H_3NCH_2 (2.0

---

[11] B. E. Maryanoff and A. B. Reitz, *Chem. Rev.*, **89**, 863 (1989).
[12] J. C. J. Bart, *J. Chem. Soc.*, 350 (1969).
[13] E. A. V. Ebsworth, T. E. Fraser and D. W. H. Rankin, *Chem. Ber.*, **110**, 3494 (1977).
[14] E. A. V. Ebsworth, T. E. Fraser, D. W. H. Rankin, O. Gasser and H. Schmidbaur, *Chem. Ber.*, **110**, 3508 (1977).
[15] Ref. 5 (Chp. 2) and references cited therein.
[16] Ref. 5 (Chp. 3) and references cited therein.
[17] F. H. Allen, O. Kennard, D. G. Watson, L. Brammer, A. G. Orpen and R. Taylor, *J. Chem. Soc. Perkin Trans. II*, S1-S19 (1987).
[18] D. A. Dixon, T. H. Dunning, R. A. Eades and P. G. Gassman, *J. Am. Chem. Soc.*, **105**, 7011 (1983).
[19] R. A. Eades, P. G. Gassman and D. A. Dixon, *J. Am. Chem. Soc.*, **103**, 1066 (1981).

kcal mol^{-1}),[16,18] whose C-N distance (1.457) is typical of a carbon-nitrogen single bond.[15,17]

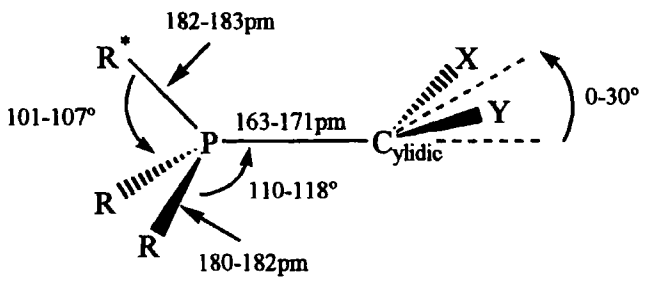

Figure 1.2 Molecular geometry of a typical phosphonium ylide

Phosphonium ylides give special stabilisation to the ylidic carbon, thus rendering them particularly stable carbanions in comparison to other ylides. This observation has been attributed to the ability to delocalise the negative charge on the carbanion. There are several theories as to how this delocalisation occurs, the majority of which discuss it in terms of a hybrid between the dipolar 'ylide' species and localised 'ylene' form (**Fig. 1.3**).

ylide ylene

Figure 1.3 Dipolar and localised double bond forms of a phosphonium ylide

One such theory,[6,20] which suggests that d_π-p_π bonding, arising from back-donation of electron density from the doubly occupied 2p orbital on the carbanion into a vacant 3d orbital on phosphorus, could explain why phosphonium ylides are more stable than their nitrogen (ammonium) analogues. Nitrogen has no low-lying 3d orbitals in which to receive electron density, thereby precluding any extra stabilisation that back-bonding could supply.[11,16] However, recent theoretical studies indicate that d-orbitals play little or no role in the ylidic bond.[6,21]

---

[20] See for example: A. W. Johnson, *'Ylid Chemistry'*, Academic Press, New York (1966).
[21] E. Magnusson, *J. Am. Chem. Soc.*, **112**, 7940 (1990).

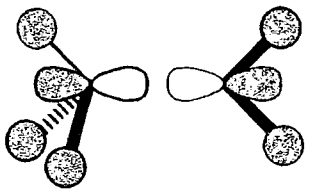

σ PR_3 σ CXY

Figure 1.4 σ-bonding in a phosphonium ylide

Alternatively, the lone pair on phosphorus may form a σ-bond to carbon, thus completing its octet. The extra charge on carbon, formally a lone pair, is in a p-orbital which can then overlap with two possible acceptor orbitals (anti-bonding with respect to the other ligands) on phosphorus to form a π back-bond, i.e. a π-σ^* bond (negative hyperconjugation). There is now considerable support for this theory. [6,22]

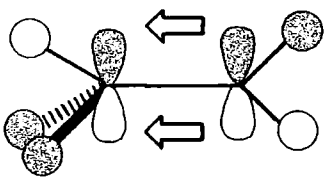

σ^* PR_3 p_π CXY

Figure 1.5 π-σ^* back donation (negative hyperconjugation)

It is worthy of note that this type of back-bonding from the p_π (HOMO) of the carbanion into the σ^* (LUMO) of the PR_3 fragment would lead to an anti-bonding interaction with the unique R^* substituent, thereby rendering its P-R bond weaker. Consequently, the bond vector would become more elongated and tend to a wider RPC_{ylidic} angle. This, coupled with analogies to negative hyperconjugation in phosphine oxides and transition metal phosphine complexes,[23] provides strong corroboration for this theory. Back donation to the antibonding LUMO orbitals is also possible in the perpendicular orientation (**Fig. 1.6**) to that shown in **Fig. 1.5**, which is a possible explanation for the ease of rotation around the $P\text{-}C_{ylidic}$ bond.[24]

---

[22] N. Sandblom, T. Ziegler and T. Chivers, *Can. J. Chem.*, **74**, 2363 (1996).
[23] A. E. Reed and P. von R. Schleyer, *J. Am. Chem. Soc.*, **112**, 1434 (1990).
[24] D. J. Mitchell, S. Wolfe and H. B. Schlegel, *Can. J. Chem.*, **59**, 3280 (1981).

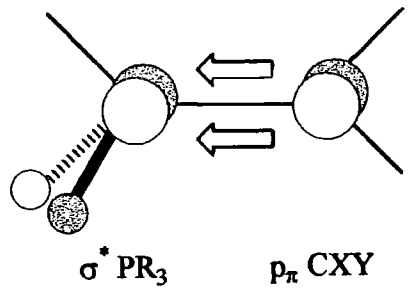

Figure 1.6 Alternative π-σ* back donation (negative hyperconjugation)

Another possible theory suggests banana[25] or bent multiple bonds (Ω or τ) as a model.[18,26] These describe the bonding as two curved areas of electron density in between the phosphorus and carbon centres (**Fig. 1.7**). Calculations indicate that both bond pairs are close to carbon, one being marginally closer than the other.[27]

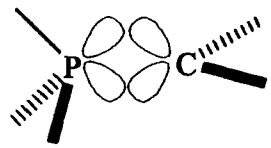

Figure 1.7 Banana bond representation for phosphonium ylides

A final alternative could be to attribute the length of the ylidic bond to simple electrostatic shortening.[6] This assumes the bonding to be a -interaction between the phosphorus and carbon centres, with a resulting coulombic attraction between the positively charged phosphonium centre and negatively charged carbanion centre producing a reduction in the P-C_{ylidic} separation.

---

[25] I. N. Levine, '*Quantum Chemistry*', 3rd Edn., Allyn & Bacon, Boston, (1983).
[26] R. P. Messmer, P. A. Schultz, R. C. Tatar and H-J. Freund, *Chem. Phys. Lett.*, **126**, 176 (1986).
[27] P. Molina, M. Alajarin, C. L. Leonardo, R. M. Claramunt, M. C. Foces, F. H. Cano, J. Catalan, J. L. G. de Paz and J. Elguero, *J. Am. Chem. Soc.*, **111**, 355 (1989); H. Lischka, *J. Am. Chem. Soc.*, **99**, 353 (1977).

1.2.3 Preparation of Phosphonium ylides and their salts

There are several methods available for the preparation of phosphonium ylides depending on the nature of the desired substituents, but that most predominantly used is the 'salt' method.

The 'salt' method involves the conversion of a phosphonium salt to a phosphonium ylide via the removal of an α-proton from the carbon atom later to become the ylidic carbon. The phosphonium salt may sometimes be commercially available or alternatively can often be made via a S_N2 quaternisation reaction (nucleophilic addition) at a trialkyl or triaryl phosphine by an alkyl halide (**Scheme 1.1**).

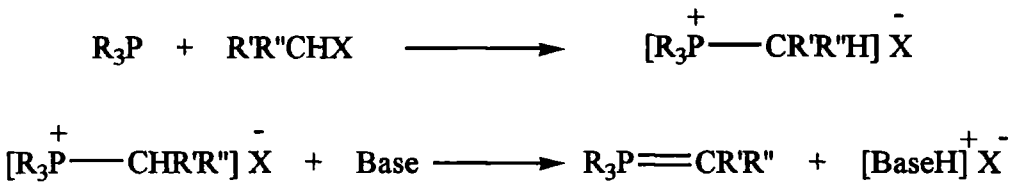

Scheme 1.1 Formation of a phosphonium salt and ylide

Reaction conditions for the formation of ylides tend to be mild - heat is seldom required. The choice of base is extremely important since it (and its conjugate acid) must (i) be inert to reaction with the ylide, (ii) produce easily separable by-products and (iii) be tolerant to any further reaction (ylides are often generated *in situ*). Generally carbon, nitrogen or oxygen bases, such as BuLi, sodium amide and potassium tert-butoxide, are employed in the deprotonation step. Solvents used vary widely depending on the substituents, but the most frequently used are hydrocarbons or ethers. They must also be inert to reaction with the ylide and base.

Originally phosphonium ylides were prepared using organolithium bases. It was soon realised, however, that lithium salts are capable of forming complexes with ylides (*vide infra*) and also have dramatic effects on the nature of Wittig products. Koster et al.[28] advocated the use of sodium amide as base, thereby avoiding the undesirable side-effects

[28] R. Koster, D. Simic and M. Grassberger, *Liebigs Ann. Chem.*, 739, 281 (1970).

caused by organolithium bases, and also used thf as solvent. A similar strategy was employed by Schmidbaur et al.,[29] who used sodium hydride and thf. Bestmann[30] discovered a method of avoiding metal bases completely with transylidation. This relies on the basicity of phosphonium ylides and involves the reaction of a phosphonium ylide with a phosphonium salt yielding the least basic phosphonium ylide as the product. However, the ylide must initially be prepared via an alternative route (**Scheme 1.2**).

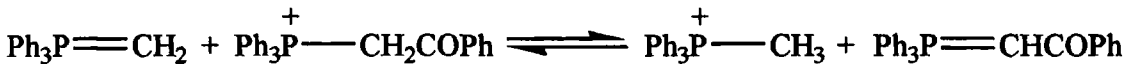

Scheme 1.2 Transylidation reaction

There are other methods of phosphonium ylide formation, but they tend to be more specific to individual cases. These include direct reaction of a carbene and phosphine, effectively linking the two fragments of a phosphonium ylide, and decomposition of a *N*-iminoiminophosphorane.[31]

The most commonly used precursor for ylide salts is triphenylphosphine, Ph_3P. It has the advantages of being cheap, easy and safe to handle, crystalline and air-stable. Also, phosphorus-bound carbon atoms are tertiary and, therefore, do not offer competing sites for deprotonation. This is in contrast to trialkylphosphines, which are often liquids, less safe to handle and may contain α-protons.

1.2.4 General reactions of Phosphonium ylides

Phosphonium ylides can function chemically as carbanions (due to their basicity and nucleophilicity), undergoing both addition and substitution reactions. The ability to create new C-C single bonds, with subsequent loss of the phosphonium group, makes phosphonium ylides very useful synthetic reagents (**Scheme 1.3**).

Ylides, especially non-stabilised, are susceptible to hydrolytic cleavage, yielding a hydrocarbon and phosphine oxide. The highly stable phosphorus-oxygen bond drives the

---

[29] H. Schmidbaur, H. Stuher and W. Vornberger, *Chem. Ber.*, **105**, 1084 (1972).
[30] H. J. Bestmann, *Chem. Ber.*, **95**, 58 (1962).
[31] Ref. 5 (Chp. 4) and references cited therein.

reaction, with the susceptibility of an ylide towards hydrolysis paralleling its basicity. In general, the most basic ylide is the most susceptible to hydrolysis.

Oxidation of phosphonium ylides also cleaves the carbanion-phosphorus bond. The carbanion portion of the ylide is able, in some instances, to react with any unconverted ylide to produce a symmetrical alkene; the phosphorus part is similarly converted to a phosphine oxide. Reduction also cleaves the ylidic bond, but is not generally as regiospecific as hydrolysis and oxidation reactions. However, by employing $LiAlH_4$, it is possible to generate an alkane and tertiary phosphine.

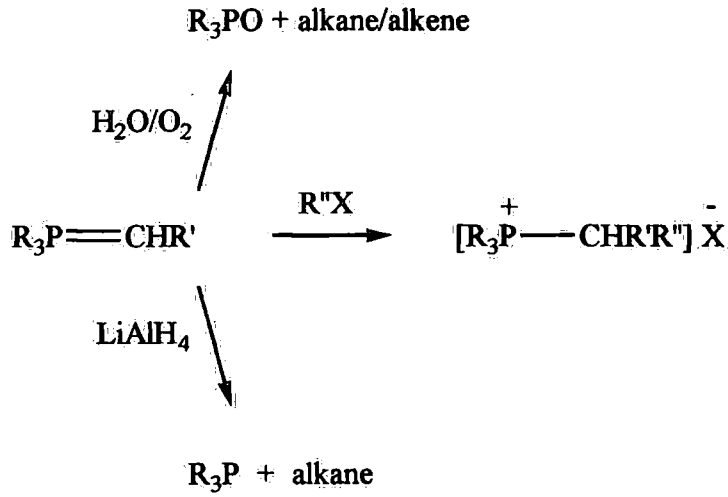

Scheme 1.3 Selection of reactions of phosphonium ylides

1.2.5 The Wittig Reaction

1.2.5.1 Background

The Wittig Reaction,[3] first reported by Georg Wittig in 1953, is undoubtedly one of the most useful ways of generating olefins, proceeding via the condensation of a phosphonium ylide with a carbonyl compound. Amongst its advantages are its simplicity and efficiency - being performed under mild conditions (often -78°C) and with short reaction times. Starting materials are easily generated and it is usually trivial to separate the phosphine oxide by-product.

As well as being regiospecific (c.f. methods such as Grignard addition[32]), the reaction can often be highly stereoselective. Selectivity is dependent on ylide substituents: as a guideline, non-stabilised ylides afford Z-alkenes; stabilised ylides afford E-alkenes; semi-stabilised ylides generate a mixture. Reaction conditions, solvent, carbonyl substituents, temperature and pressure also affect the E/Z ratio.

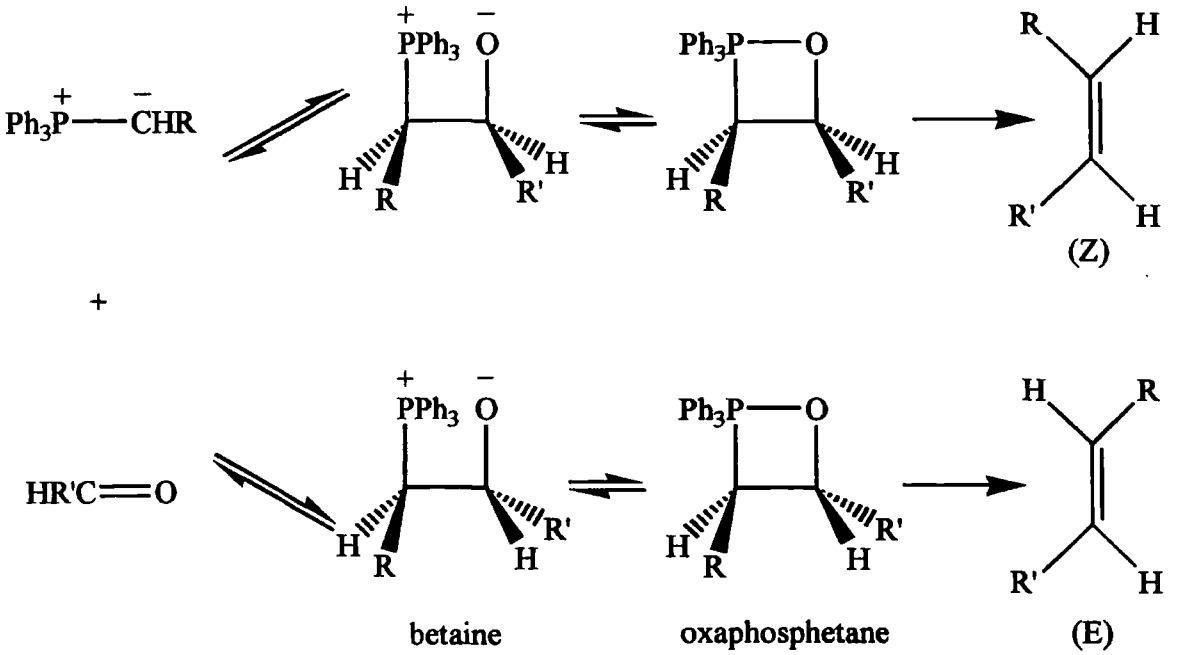

Scheme 1.4 Schematic of the Wittig reaction mechanism

[32] G. S. Silverman and P.E. Rakita (Eds.), '*Handbook of Grignard Reagents*', Marcel Dekker, Inc., Monticello (1996).

The mechanism has historically been viewed as reversible nucleophilic addition of the ylide carbanion to the carbonyl species affording a betaine intermediate. Cyclisation to the respective oxaphosphetane is then followed by dissociation to a phosphine oxide and the desired olefin (**Scheme 1.4**).

Many modifications have been proposed[5] and current thinking suggests that oxaphosphetanes may be the intermediates, with the betaine being a model for a transition state.

The Wittig reaction provides scope for a wide range of alternative reactions based on a similar theme. One such reaction is the Schlosser-Wittig reaction,[33] in which the expected stereochemistry of the olefin is reversed by the presence of a lithium salt and organolithium base.[‡]

1.2.5.2 The effect of lithium on Wittig reactions

Phosphonium ylides are very useful in organic synthesis (*vide supra*) but due to only moderate nucleophilic character, especially in stabilised ylides, their reactions have tended to be limited to those with the most electrophilic and sterically unhindered carbonyl compounds, viz. aldehydes and ketones. This inherent lack of reactivity has led to a search for more nucleophilic organophosphorus reagents - recent attention has turned to metallated phosphonium ylides.

Phosphorus ylides can form complexes with the majority of metals (*vide infra*), but the most synthetically useful are those containing lithium. The ylide anions, $R_2P^+(CR_2^-)_2M^+$, are more nucleophilic than the ylide and potentially provide scope for altering stereochemical outcomes.[34] Lithium is known to provide enhanced reactivity in Wittig

---

[33] M. Schlosser, *Topics Stereochem.*, **5**, 1 (1970).

[‡] Lithium cations were found to have an effect on the production of ylides and on Wittig reactions in the 1950s due to the ability of lithium halides to complex to ylides and Wittig intermediates. This resulted in the use of sodium and potassium bases for the production of ylides.

[34] H-J. Cristau, Y. Ribeill, F. Plenat and L. Chiche, *Phosphorus and Sulfur*, **30**, 135 (1987).

reactions. One such example of this is in the reaction of hindered ketones with lithiated ylides.[35]

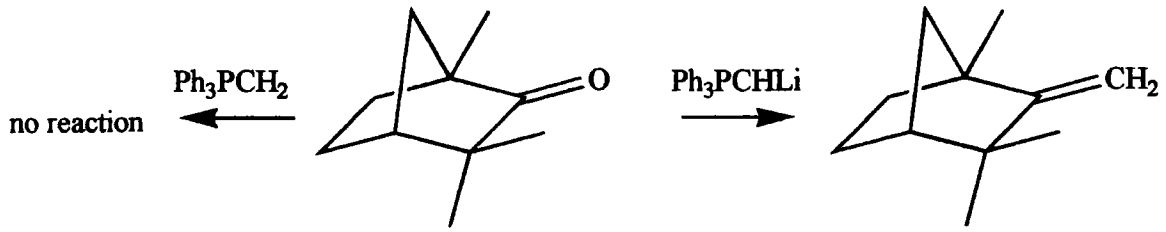

Scheme 1.5 Effect of "lithiated" phosphonium ylides on Wittig reactivity

The reaction of fenchone with the unstabilised ylide, triphenylphosphonium methylide, yields no Wittig products, whereas using an α-lithiated species converts the hindered ketone to the respective alkene in good yield (**Scheme 1.5**). The metallated ylide, Ph_3PCHLi,[35,36] has a marked effect on reactivity in Wittig reactions, although there has been a degree of controversy surrounding its actual structure.

Corey et al.[35] describe the synthesis of α-lithio(triphenyl)phosphonium methylide from the parent phosphonium salt and two equivalents of tert- or sec-butyllithium in thf or diethylether at -78 °C. The "lithiated" phosphonium ylide was then reacted (at -78 °C) with a variety of hindered ketones and epoxides, which were inert to reaction with solely (triphenyl)phosphonium methylide (e.g. **Scheme 1.5**).

Schlosser et al.,[36] however, refute this claim and, on the basis of nmr experiments and quenching reactions, propose a structure in which the ortho-position of one phenyl group is lithiated. It is also claimed that above 25 °C the "ortho-lithiated" species decomposes to a lithiated-phosphine species, Ph_2PCH_2Li.

Grützmacher et al.,[37] in a recent communication, report the synthesis of an α-zincated phosphonium ylide, which upon heating converts to an ortho-zincated species. On the basis of this evidence, and the claims of Corey and Schlosser, it is quite likely that both

---

[35] E. J. Corey and J. Kang, *J. Am. Chem. Soc.*, **104**, 4724 (1982); E. J. Corey, J. Kang and K. Kyler, *Tet. Lett.*, **26**, 555 (1985).
[36] B. Schaub, T. Jenny and M. Schlosser, *Tet. Lett.*, **25**, 4097 (1984); B. Schaub and M. Schlosser, *Tet. Lett.*, **26**, 1623 (1985).

proposals for the structure are correct (**Scheme 1.6**). The α-lithio species proposed by Corey could be a kinetic product, which upon heating reverts to the more stable o-lithio species suggested by Schlosser (thermodynamic product).

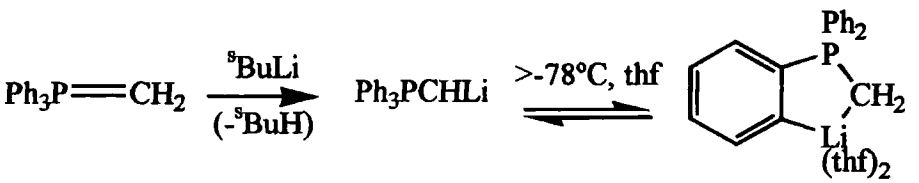

Scheme 1.6 Lithiation of (triphenyl)phosphonium methylide

However, attempts to determine the molecular structure of either species by single crystal XRD have so far been unsuccessful and there are no simple and few known structures of lithiated phosphonium ylides with which to compare.

Several other lithiated phosphonium ylides have been reported. $Ph_2P(CH_2)_2Li$ can perform the same activation of fenchone (**Scheme 1.5**) as Ph_3PCHLi, yielding a hindered olefin.[38] The single crystal XRD structure of $Ph_2P(CH_2)_2Li$ has also been determined.[39]

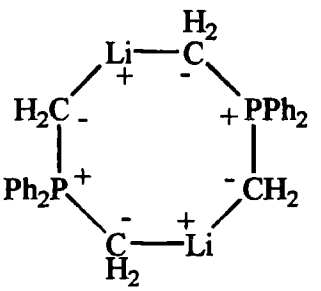

Figure 1.8 Dimer of $Ph_2P(CH_2)_2Li$ in the solid-state

Lithium salts are known to have a marked effect on stereochemistry when present in Wittig reactions. Ester ylides (stabilised) and aldehydes react to form an approximate E/Z ratio of 94:6 in 'lithium salt-free' conditions, whilst a ratio of 78:22 is achieved with a lithium halide present. In general, stabilised ylides give more Z isomer when lithium is present, the reverse being true for non-stabilised ylides. The effect of lithium salts on the latter is exemplified below (**Fig. 1.9**).[5]

---

[37] M. Steiner, H. Grützmacher, H. Prtizkow and L. Ksolnai, *J. Chem. Soc., Chem. Comm.*, 285 (1998).
[38] H-J, Cristau, *J. Organomet. Chem.*, **352**, C47 (1988).

Lithium Salt	E/Z ratio
None	4:96
LiCl	10:90
LiI	17:83
$LiBF_4$	48:52

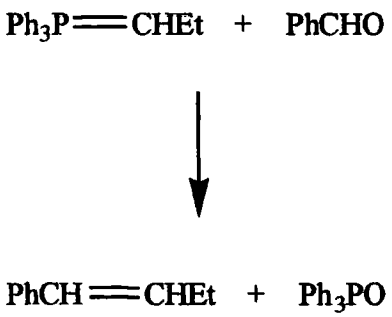

Figure 1.9 Effect of lithium salts on Wittig product stereochemistry

1.2.6 Coordination Chemistry of Phosphonium Ylides

1.2.6.1 Main Group Metals

The coordination chemistry of phosphonium ylides has been mostly limited to transition metals, although more recently examples of s-block and main group metal coordinated ylides have been characterised (**Fig. 1.10**).[37,40]

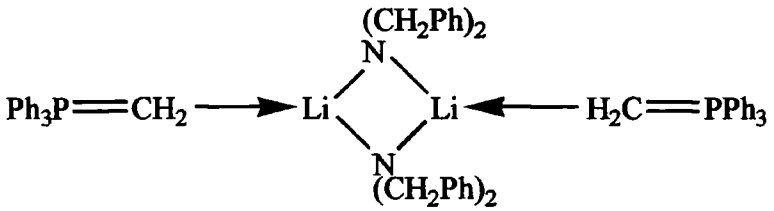

Figure 1.10 A phosphonium ylide-lithium amide complex

Metals can interact with the ylidic carbanion in two ways (**Fig. 1.11**):

(1) Metals with σ-donor properties can increase the electron-density at the ylidic carbon (B), thereby increasing its nucleophilicity and leading to increased reactivity.

(2) Main group metals with suitable acceptor orbitals, such as metals of the silicon group, can interact with filled carbon centred p-orbitals of the ylide (C). This results in a M-C bond and subsequent π-back donation gives some partial M=C bonding, leading to decreased electron density at the ylidic carbon and reduced ylide nucleophilicity.

---

[39] R. E. Cramer, M. A. Bruck and J. W. Gilje, *Organometallics*, **5**, 1497 (1986).
[40] D. R. Armstrong, M. G. Davidson and D. Moncrieff, *Angew. Chem., Int. Ed. Engl.*, **34**, 478 (1995).

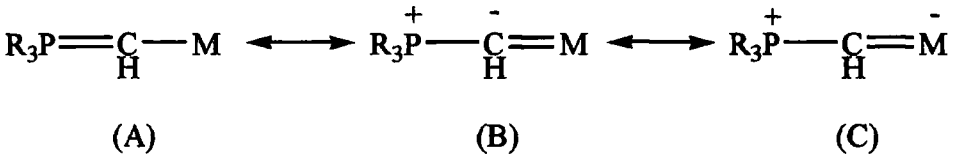

(A) (B) (C)

Figure 1.11 Interactions of metals with phosphonium ylides

The relative contribution of the two opposing effects is dependent on both the metal centre and its surrounding ligands.[41]

1.2.6.2 Transition Metals

Transition metals possessing a high π-acceptor capacity, stabilise ylidic carbanions and, due to their propensity for high coordination numbers, tend to form dimers and higher oligomers with ylides. These types of complexes are thought to have potential uses in pharmacology and as catalysts.[42,43,44,45]

The reaction of Cu^{I}, Ag^{I} and Au^{I} compounds with phosphonium ylides proceed in a 2:1 geometry (ylide:M^{I}), resulting in complexes that have an unusually high stability to hydrolysis, oxidation and heat (**Scheme 1.7**).[46,47,48,49,50] However, complexes that contain these metals at the α-carbon have not been reported.

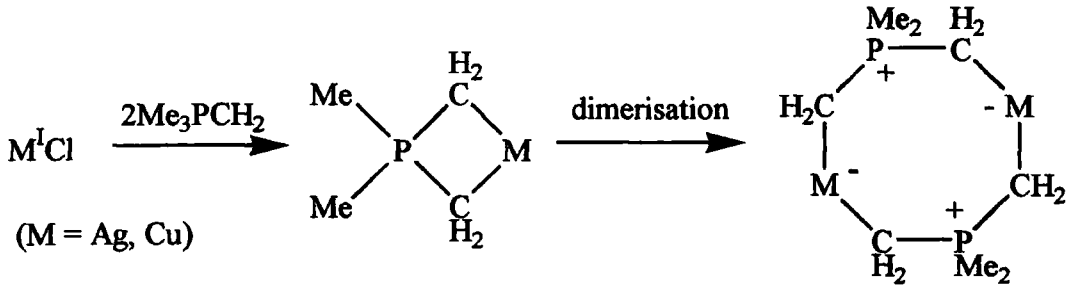

Scheme 1.7 Dimers formed by Group 11-phosphonium ylide complexes

---

[41] O. O. Kolodiazhnyi, *Tetrahedron*, **52**, 1855 (1996) and references cited therein.
[42] R. P. Grey and L. R. Anderson, *Inorg. Chem.*, **16**, 3187 (1977).
[43] W. Keyn, F. H. Kowaldt, R. Goddart and C. Kruger, *Angew. Chem.*, **90**, 493 (1978).
[44] N. Holy, N. C. Baeziger and R. M. Flynn, *Angew. Chem.*, **90**, 732 (1978).
[45] H. Schmidbaur, J. R. Mandl, A. Wohlleben-Hammer and A. Fugner, *Z. Natursforsch*, **33b**, 1325 (1978).
[46] H. Schmidbaur and R. Franke, *Chem. Ber.*, **108**, 1321 (1975).
[47] H. Schmidbaur and R. Franke, *Angew. Chem.*, **85**, 449 (1973).
[48] Y. Yamamoto and H. Schmidbaur, *J. Organomet. Chem.*, **96**, 133 (1975).
[49] Y. Yamamoto and H. Schmidbaur, *J. Organomet. Chem.*, **97**, 479 (1975).

In contrast, mercury compounds, due to their propensity to form σ-bonds and have low coordination number, give non-associated monomeric complexes, co-ordinated at the α-carbon (**Scheme 1.8**).[51]

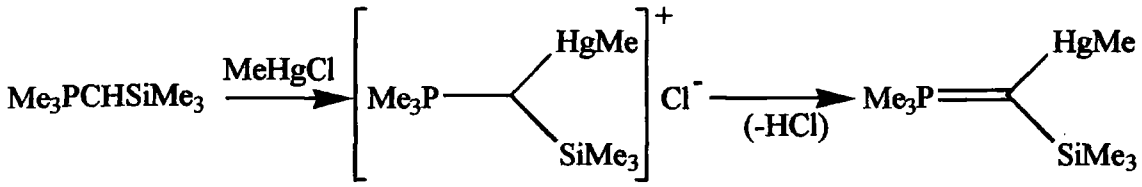

Scheme 1.8 Mercury-phosphonium ylide complex

Reaction of phosphonium ylides with metal carbonyls[41] leads to a diversity of possible structures, for example the reaction of tris(ruthenium tetracarbonyl) with (triphenyl)phosphonium methylide in thf yields a μ_3-ylidic carbon atom in a cluster-type structure (**Fig. 1.12**).[52]

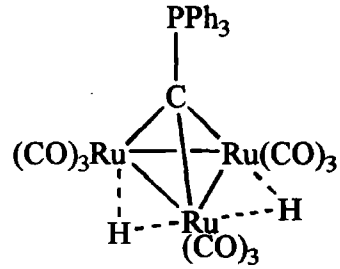

Figure 1.12 A ruthenium carbonyl-phosphonium ylide cluster complex

Group 4 metals have an uncompleted orbital set enabling them to form donor-acceptor bonds. There are many examples of Group 4 metal-phosphonium ylide complexes, depending on the choice of phosphonium ylide and the group 4 metal precursor (**Scheme 1.9**).[41,53,54]

---

[50] Y. Yamamoto, *Chem. Lett.*, **11**, 311 (1980).
[51] H. Schmidbaur and R. H. Rothlein, *Chem. Ber.*, **107**, 102 (1974).
[52] D. S. Bohle, D. Heinike and A. Tiripicchio, *Angew. Chem.*, **102**, 938 (1990).
[53] H. Schmidbaur, W. Scharf and H. J. Fuller, *Z. Natursforsch*, **32**, 858 (1977).
[54] Ref. 5 (Chp. 14), pp 489-497, and references cited therein.

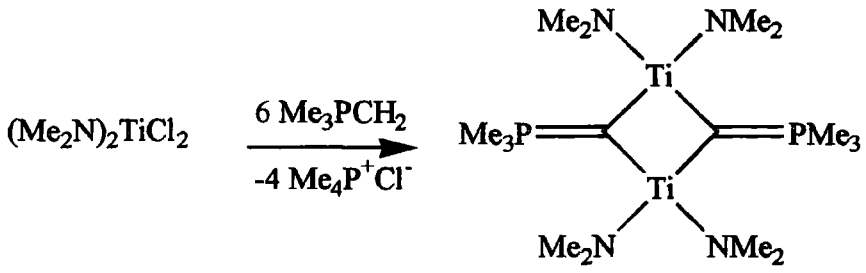

Scheme 1.9 A titanium-phosphonium ylide complex

1.2.6.3 Actinides

The coordination of actinide metals to phosphonium ylides is also possible. Several complexes have been reported and, in particular, much of this work has involved organouranium compounds.[55]

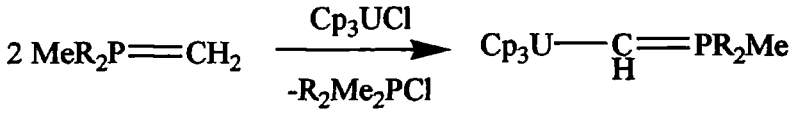

Scheme 1.10 A uranium-phosphonium ylide complex

The complex shown (**Scheme 1.10**) is a flammable, dark green, crystalline solid that is highly air- and moisture-sensitive.[55]

There are many metal-complexes of phosphonium ylides that are now known[41] and their investigation continues, especially that of the main group and s-block metals. The latter, as intimated earlier, have been shown to have a dramatic effect on the stereochemical outcome of Wittig and other related reactions.

[55] R. E. Cramer, R. B. Maynard, J. C. Paw and J. W. Gilje, *J. Am. Chem. Soc.*, **103**, 3589 (1981); R. E. Cramer, J. H. Jeong, P. N. Richmann and J. W. Gilje, *Organometallics*, **9**, 1141 (1990).

1.3 Iminophosphoranes

1.3.1 Background

Iminophosphoranes, or phosphinimines, were first reported in 1919 by Staudinger et al.,[2] but detailed investigations only started around 40 years later. They have since found use in a variety of organic applications,[56] especially the formation of C=N bonds via the aza-Wittig reaction.

Iminophosphoranes are isoelectronic with phosphonium ylides, with the general formula R_3PNR' and show largely analogous chemistry. They can be considered as containing a single phosphorus-nitrogen bond with a degree of electronic delocalisation, although the $P\text{-}N_{iminic}$ bond is considerably more delocalised than the $P\text{-}C_{ylidic}$ bond (**Fig. 1.13**).

$$R_3P{=}NR' \longleftrightarrow R_3\overset{+}{P}{-}\overset{-}{N}R'$$

Figure 1.13 Two resonance canonical forms of an iminophosphorane

Stability to air and moisture is substantially greater than for phosphonium ylides, which can be attributed to the nature of the phosphorus-nitrogen bond and, in particular, the greater delocalisation of electron density from nitrogen to phosphorus. They are also basic, nitrogen being the site of attack[57] - $[(Me_2N)_3P{=}N]_3P{=}NBu^t$, for example, is the strongest known neutral organic base.[58]

1.3.2 Structure and Bonding

The bonding in iminophosphoranes can be considered in an analogous fashion to that in phosphonium ylides, due to the isolobality of the frontier orbitals for CH_2 and NH fragments (**Fig. 1.14**).[22]

---

[56] Ref. 5 (Chp. 13) and references cited therein; H-J. Cristau, *Chem. Rev.*, **94**, 1299 (1994).
[57] R. D. Wilson and R. Bau, *J. Am. Chem. Soc.*, **96**, 7601 (1974).
[58] R. Schwesinger and H. Schlemper, *Angew. Chem.*, **26**, 1167 (1987); R. Link and R. Schwesinger, *Angew. Chem.*, **31**, 850 (1992).

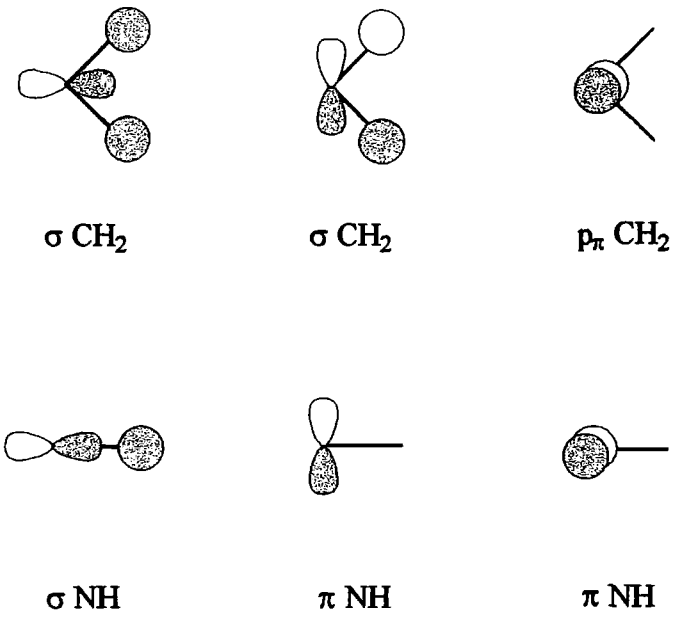

Figure 1.14 Isolobality of frontier orbitals in CH_2 and NH fragments

The bonding may, similarly, be described using several models. Again, there is the possibility of d_π-p_π bonding due to back-donation from the two, singly occupied 2p orbitals on nitrogen into a vacant 3d orbital on phosphorus. Electrostatic shortening of the P-N_{iminic} bond is an alternative possibility.[6] However, as was the case for phosphonium ylides, the most widely accepted model describes the bonding in terms of negative hyperconjugation, again involving π-σ^* donation - for iminophosphoranes there are two possibilities (**Fig. 1.15**).[22]

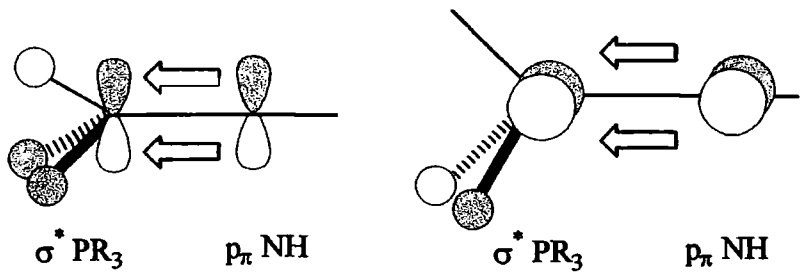

Figure 1.15 Negative hyperconjugation in iminophosphoranes.

The molecular geometry (**Fig. 1.16**) of iminophosphoranes is based on a tetrahedral phosphorus environment bonded to a trigonal nitrogen. The P-N_{iminic} bond is thought to be almost a double bond, the range of known lengths (1.54-1.64 Å) comparing

favourably with the sum of covalent radii for a P=N double bond.[59] The existence of a unique P-R bond vector was a feature also observed in phosphonium ylides. This will be discussed later, but it is worthy of note that as a consequence of negative hyperconjugation there is an anti-bonding interaction between the σ^* orbital on nitrogen and the unique phosphorus substituent, R^*. Subsequently the P-R^* bond vector is more elongated and has a wider NPR^* angle than the other two P-R vectors.

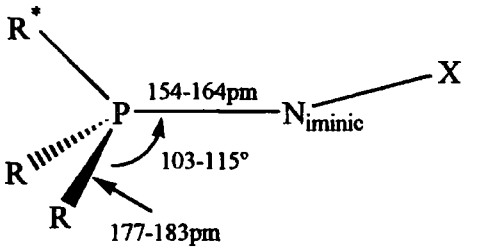

Figure 1.16 Molecular geometry of an iminophosphorane

It is interesting to note that the P-N bond length in reported structures of aminophosphonium salts, generally $[R_3PNR''_2]^+X^-$,[60] are only marginally longer than those for iminophosphoranes (approximately 1.62-1.63 Å). This suggests a degree of iminic character is already present in the phosphonium cations, which could be due to the overlap of nitrogen's lone pair of electrons with a suitable phosphorus acceptor orbital.

The ease of rotation around the P-N_{iminic} bond has been discussed in terms of ^{31}P NMR spectroscopy and theoretical calculations. A rotational barrier of approximately 2 kcal mol^{-1} was calculated for $Ph_3P{=}NCH{=}CH_2$.[61] This is greater than calculated for phosphonium ylides,[17,18] indicating a greater degree of electronic delocalisation, but nonetheless suggests there is little restriction to rotation. ^{31}P nmr spectroscopy performed on $Ph_3P{=}NPh$ revealed only one set of resonances and a rapid rotation around the P-N_{iminic} bond was concluded.[62]

---

[59] L. Pauling, '*Nature of the Chemical Bond*', 3rd ed., Cornell University Press, Ithaca, NY, pp 224 & 228 (1960).
[60] See for example: M. B. Hursthouse, N. P. C. Walker, C. P. Warrens and J. D. Woolins, *J. Chem. Soc. Dalton*, 1043 (1985); A. L. Llamas-Saiz, C. Foces-Foces, J. Elguero, P. Molina, M. Alajarin and A. Vidal, *J. Chem. Soc. Perkin Trans. II*, 1667 (1991); C. Imrie, T. A. Modro, P. H. van Rooyen, C. C. P. Wagener, K. Wallace, H. R. Hudson, M. McPartlin, J. B. Nasirin and L. Powroznyk, *J. Phys. Org. Chem.*, **8**, 41 (1995).
[61] J. Bragin, S. Chan, E. Mazzola and H. Goldwhite, *J. Phys. Chem.*, **77**, 1506 (1973).
[62] T. A. Albright, W. J. Freeman and E. E. Schweizer, *J. Org. Chem.*, **41**, 2716 (1976).

1.3.3 Preparation of Iminophosphoranes

Iminophosphoranes have been synthesised via two major routes. The Staudinger reaction (**Scheme 1.11**) uses a direct combination of nitrogen (via azide) and phosphorus (via phosphine) fragments to yield the product in a one-step synthesis. The Kirsanov reaction[63] is similar to the 'salt' method used to prepare phosphonium ylides.

During the Staudinger reaction, there is nucleophilic attack by phosphorus on the terminal nitrogen of an azide, via a four-centred transition-state, to yield a linear phosphazide, which spontaneously loses nitrogen to generate the iminophosphorane product.

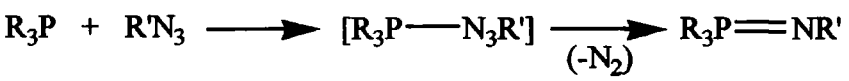

Scheme 1.11 The Staudinger reaction

The Kirsanov reaction uses the dihalide (usually the dibromide) salt of the phosphine and reacts it with an amine and was employed by Horner et al.[64] to convert arylamines directly to *N*-aryliminophosphoranes (**Scheme 1.12**).

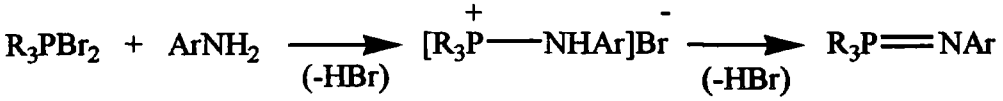

Scheme 1.12 Kirsanov reaction using arylamines

In the case of aliphatic amines, deprotonation is not spontaneous, necessitating the addition of a strong base, such as sodamide (**Scheme 1.13**).[65]

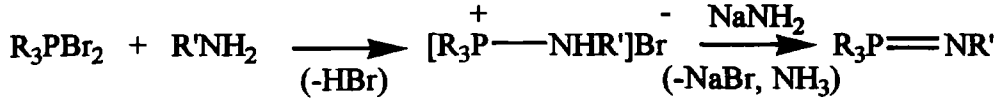

Scheme 1.13 Kirsanov reaction using aliphatic amines

---

[63] A. V. Kirsanov, *Isv. Akad. Nauk SSSR*, 426 (1950); *Chem. Abstr.*, **45**, 1503 (1951); *Zh. Obshch. Khim.*, **22**, 269 (1952); *Chem. Abstr.*, **46**, 11135 (1952).
[64] L. Horner and H. Oediger, *Liebigs Ann. Chem.*, **627**, 142 (1959).
[65] H-J Cristau, J. Kadoura, L. Chiche and E. Toreilles, *Bull. Soc. Chim. Fr.*, **4**, 515 (1989).

Other syntheses have been reported, but these are specific to a small number of examples, such as the use of chloroamines or azocarboxylates[56] with tertiary phosphines or the reaction of phosphorus ylides and azides/carbonyl imines to yield iminophosphoranes.[66,67]

1.3.4 Reactions of Iminophosphoranes

Directly analogous to phosphonium ylides is the ability of iminophosphoranes to undergo hydrolysis, yielding amines and phosphine oxides under acidic/basic conditions. The nitrogen substituent dictates the ease of hydrolysis. Generally, iminophosphoranes are more resilient to hydrolysis than their ylide analogues, as can be seen by the lower reactivity of imino(triphenyl)phosphorane in comparison to (triphenyl)phosphonium methylide. *N*-aryl imines are generally quite stable in air, and sometimes in water, but readily hydrolyse in dilute acid/base conditions.

Oxidation and reduction reactions are analogous to those discussed for phosphonium ylides - imines with electron withdrawing groups are more difficult to oxidise; reduction is usually carried out using $LiAlH_4$.

Of more synthetic importance, however, is the aza-Wittig reaction,[68] which is the nitrogen equivalent of the Wittig reaction, discussed earlier for phosphonium ylides (**Scheme 1.14**):

$$Ph_3P{=}NR \;+\; R''R'C{=}O \longrightarrow R''R'C{=}NR \;+\; Ph_3P{=}O$$

Scheme 1.14 The aza-Wittig reaction

The reaction generally proceeds under mild conditions, in a neutral solvent and without catalysis, affording a high yield of products. The mechanism is thought to proceed via nucleophilic attack of the iminic nitrogen on the carbonyl, although no evidence of a betaine or oxaphosphetane intermediate has yet been found. Intramolecular aza-Wittig reactions, leading to cyclisations, have been reported (**Scheme 1.15**).[69]

---

[66] H. Hoffmann, *Chem. Ber.*, **95**, 2563 (1962).
[67] H. J. Bestmann and F. Seng, *Tetrahedron*, **21**, 1373 (1965).
[68] Ref. 5 (Chp. 13), p. 423.
[69] T. Sasaki, S. Eguchi and T. Okano, *J. Am. Chem. Soc.*, **105**, 3912 (1983).

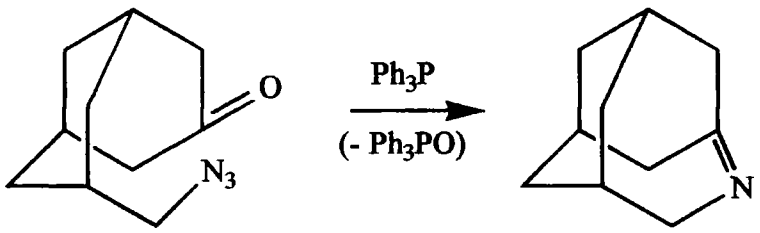

Scheme 1.15 Intramolecular aza-Wittig reaction

1.3.5 Coordination Chemistry of Iminophosphoranes

This area had, until recently, received very little attention - the first reported compounds were poorly characterised and considered relatively unimportant. The phosphorane iminato ligand, R_3PN^-, can behave as a 1, 2 or 4 electron donor, and is isoelectronic with the corresponding phosphine oxide, $R_3P{=}O$. With metals, iminophosphoranes can interact as either neutral Lewis bases, viz. R_3PNH, or as a counter-anionic ligand (reacting as a protic acid), viz. the phosphorane iminato ligand, R_3PN^-.

With Lewis acids, iminophosphoranes are able to form 1:1 adducts, particularly with boron halides,[70] boranes[71] and group 3 metal halides/alkyls[72] (**Scheme 1.16**).

$$Ph_3P{=}NH + BF_3 \longrightarrow Ph_3P{=}NH.\,BF_3$$

$$Ph_3P{=}NH + BPh_3 \longrightarrow Ph_3P{=}NH.\,BPh_3$$

$$Ph_3P{=}NH + AlCl_3 \longrightarrow Ph_3P{=}NH.\,AlCl_3$$

Scheme 1.16 Iminophosphorane-Lewis acid adduct formation

The coordination chemistry of iminophosphoranes with transition metals is much more extensive[72] and complexes have been synthesised by a variety of routes. That most widely used is the reaction of a *N*-(trimethylsilyl)iminophosphorane and a metal halide. This is

[70] H. Zimmer and G. Singh, *J. Org. Chem.*, **29**, 3412 (1964).
[71] R. Appel and A. Hauss, *Z. Anorg. Allg. Chem.*, **311**, 290 (1961).
[72] K. Dehnicke and J. Stahle, *Polyhedron*, **8**, 707 (1989); K. Dehnicke and F. Weller, *Coord. Chem. Rev.*, **158**, 103 (1997).

often driven by the formation of a stable halo(trimethyl)silane, but this depends on the metal centre and its surrounding ligands (**Scheme 1.17**).[72,73]

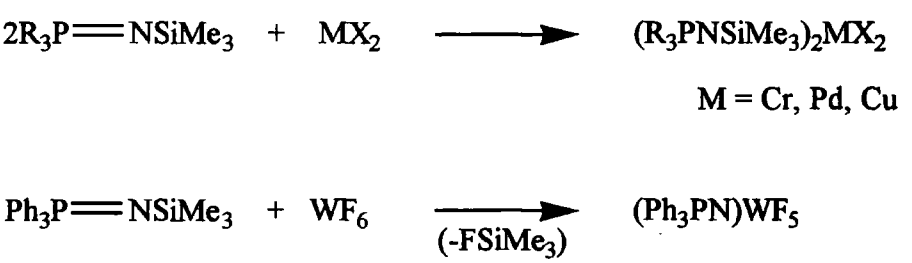

Scheme 1.17 Transition metal complexes of iminophosphoranes

There are several coordination modes with a metal that are possible for both the neutral and anionic ligand. It can be terminal (μ_1) or bridging two (μ_2) or three (μ_3) metal centres. The mode depends upon the metal centre and the phosphorus substituents (**Fig. 1.17**).

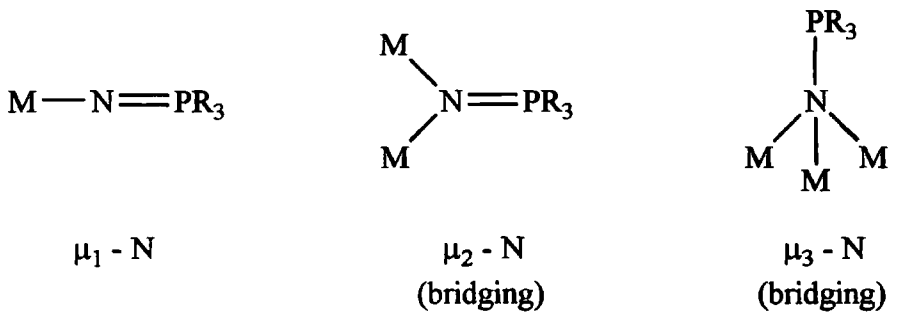

Figure 1.17 Different modes of metal coordination for Ph_3PN^-

The varying modes of coordination are most easily seen by coordination to metal carbonyl compounds. With group 6 metal carbonyls, the iminophosphorane ligand is able to replace one or more CO groups (**Scheme 1.18**).[74] In the final product, the molybdenum atoms have octahedral coordination, arranged around a face of three bridging atoms, with the iminophosphorane ligand adopting the dipolar form, allowing it to be a $4e^-$ donor and thus complete the $18e^-$ rule for the complex (**Fig. 1.18**).

---

[73] T. Miekisch, H. J. Mai, R. M. zu Kocker, K. Dehnicke, J. Magull and H. Goesmann, *Z. Anorg. Allg. Chem.*, **622**, 583 (1996).
[74] M. Grun, F. Weller and K. Dehnicke, *Z. Anorg. Allg. Chem.*, **623**, 224 (1997); W. Kolitsch and K. Dehnicke, *Z. Natursforsch*, **25b**, 1080 (1970).

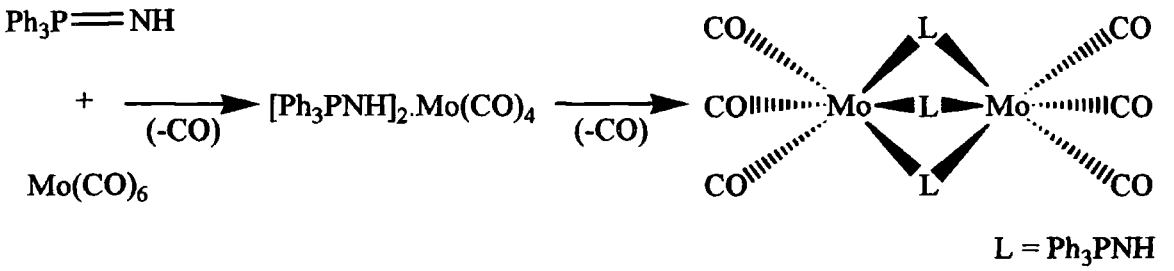

Scheme 1.18 Molybdenum carbonyl-iminophosphorane complex

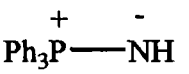

Figure 1.18 Dipolar form of the imino(triphenyl)phosphorane ligand

Other nitrogen containing species, such as azido, nitrosyl and nitrido compounds, have been used in the synthesis of metal co-ordinated iminophosphorane complexes (**Scheme 1.19**).[72,73]

Scheme 1.19 Synthesis of phosphorane iminato-group 6 complexes from metal azido compounds

A non-metallocene ethylene polymerisation catalyst that contains phosphorane iminato ligands has recently been shown to be highly active [(^{t}Bu$_3$PN)$_2$TiMe$_2$].[75]

Iminophosphorane complexes with zinc,[76,77] cadmium,[76] mercury,[76] lead[78] and tin[79] have been reported, and there continues to be considerable interest in the coordination chemistry of iminophosphoranes and phosphorane iminato ligands to metals, especially those of the s-block (*vide infra*).

---

[75] D. W. Stephan, F. Guérin, R. E. v. H. Spence, L. Koch, X. Gao, S. J. Brown, J. W. Swabey, Q. Wang, W. Xu, P. Zoricak and D. G. Harrison, *Organometallics*, **18**, 2046 (1999).
[76] E. W. Abel and S. A. Mucklejohn, *Inorg. Chim. Acta*, **37**, 107 (1979).
[77] M. Krieger, R. O. Gould, K. Harms, S. Parsons and K. Dehnicke, *Chem. Ber.*, **129**, 1621 (1996); H. Ackermann, F. Weller, B. Neumuller and K. Dehnicke, *Z. Anorg. Allg. Chem.*, **625**, 147 (1999).
[78] P. B. Hitchcock, M. F. Lappert and W. Zhong-Wia, *J. Chem. Soc., Chem. Comm.*, 1113 (1997).
[79] M. Veith and V. Huch, *J. Organomet. Chem.*, **293**, 161 (1985); H. W. Roesky, U. Seseke, M. Noltemeyer and G. M. Sheldrick, *Z. Natursforsch*, **43b**, 1130 (1988).

1.3.6 S-block metallated Iminophosphoranes

There are several reports of s-block metallated iminophosphoranes (some of which are discussed in more detail later) that have been described recently. In most cases, coordination of an alkali metal to an iminophosphorane is achieved through both the iminic nitrogen and a carbanion also bound to phosphorus, i.e. α-metallation (**Fig. 1.19**).[80,81,82]

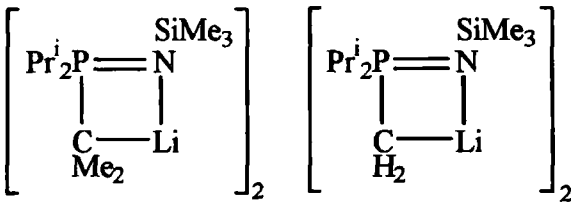

Figure 1.19 α-lithiated iminophosphoranes

An analogous structure for sodium[83] has been reported and there are examples of potassium, rubidium and caesium complexes containing α-metallated amido phosphorus substituents (**Fig. 1.20**).[82]

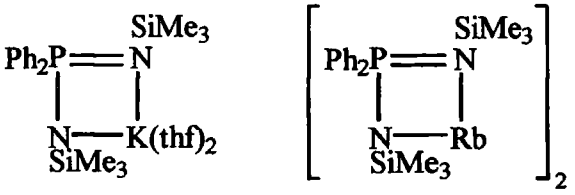

Figure 1.20 Heavier alkali metal iminophosphorane complexes

The single crystal XRD structures of $(LiNPPh_3)_6$ and $(KNPPh_3)_6$, determined by Dehnicke et al., will be discussed in more detail later (**Chapter 6**).[84,85]

---

[80] A. Muller, B. Neumuller and K. Dehnicke, *Chem. Ber.*, **129**, 253 (1996).
[81] F. López-Ortiz, E. Peláez-Arango, B. Tejerina, E. Pérez-Carreño and S. García-Granda, *J. Am. Chem. Soc.*, **117**, 9972 (1995).
[82] A. Steiner and D. Stalke, *Inorg. Chem.*, **32**, 1977 (1993).
[83] A. Steiner and D. Stalke, *Angew. Chem., Int. Ed. Engl.*, **34**, 1752 (1995).
[84] S. Anfang, G. Seybert, K. Harms, G. Geisler, W. Massa and K. Dehnicke, *Z. Anorg. Allg. Chem.*, **624**, 1187 (1998).
[85] S. Chitsaz, B. Neumuller and K. Dehnicke, *Z. Anorg. Allg. Chem.*, **625**, 9 (1999).

Examples of group 2 iminophosphorane complexes are equally rare. Once more, the most common instances are those containing phosphorus-bound carbanions. The latter type have been prepared for beryllium, magnesium, calcium, strontium and barium (**Fig. 1.21**), with the degree of thf-solvation increasing down the group from beryllium (none) to calcium (one) and finally strontium/barium (two).[86]

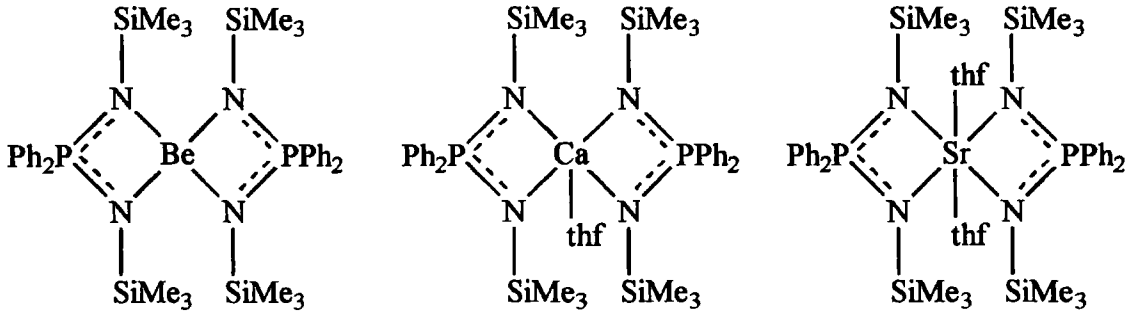

Figure 1.21 Group 2 amido-iminophosphorane complexes

There are few examples of coordination by neutral iminophosphoranes (**Fig. 1.22**),[87] but there are, however, several cases of *N*-metallation at the imino nitrogen by magnesium, e.g. $(Me_3PNMgBr)_4$.[87]

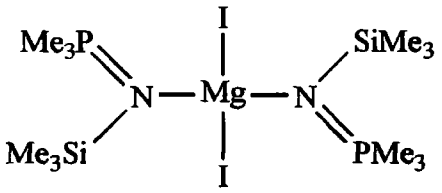

Figure 1.22 Coordination of a neutral iminophosphorane ligand to magnesium

The use of metallated iminophosphoranes in organic synthesis, particularly those containing alkali metals,[65,81] is still in the preliminary stages of investigation. Similarly to phosphonium ylides, it is the increased reactivity that these species provide that is initiating considerable interest in their study.

---

[86] R. Fleischer and D. Stalke, *Inorg. Chem.*, **36**, 2413 (1997).
[87] A. Muller, M. Krieger, B. Neumuller, K. Dehnicke and J. Magull, *Z. Anorg. Allg. Chem.*, **623**, 1081 (1997).

2. General Experimental Techniques

2.1 Inert Atmosphere Techniques

Due to the air-sensitive and hygroscopic nature of the complexes studied in this work, it was necessary to employ inert atmosphere techniques in order to facilitate their study. Standard vacuum line techniques (**Fig. 2.1**) were, therefore, used for all synthetic work.[1] Syntheses were performed under an atmosphere of argon or nitrogen from the manifold supply, using pre-dried solvents and, where appropriate, pre-dried starting materials.

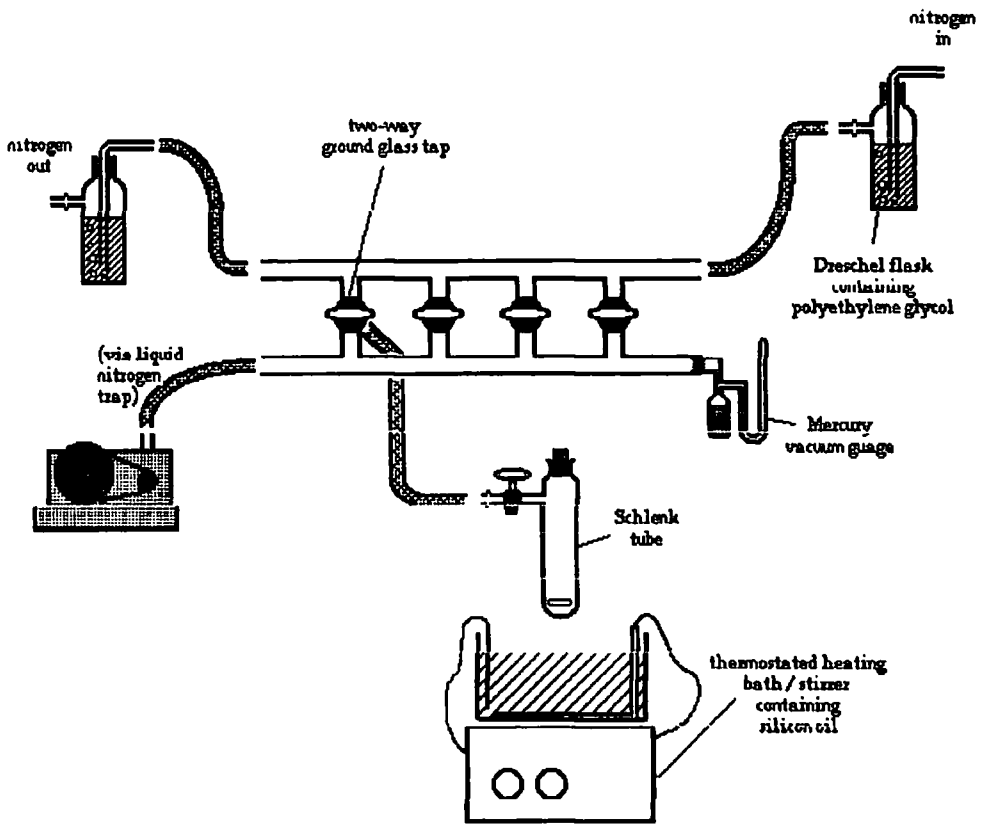

Figure 2.1 Schematic representation of a vacuum line

[1] D. F. Schriver and M. A. Drezdon, *'The Manipulation of Air Sensitive Compounds.'*, 2nd Edn., Wiley, New York (1986).

Reactions were generally carried out in Schlenk tubes (or similar vessels), dried in an oven at 130 °C for several hours, evacuated to approximately 10^{-2} Torr three times and flushed with dry argon or nitrogen from the manifold supply. Solids were pre-weighed in a dry, oxygen-free glove box (**Fig. 2.2**) either into an airtight vial (being then introduced under a positive pressure of inert gas) or directly into the Schlenk tube. Air-sensitive and hygroscopic liquid reagents and solvents were introduced via a dry syringe.

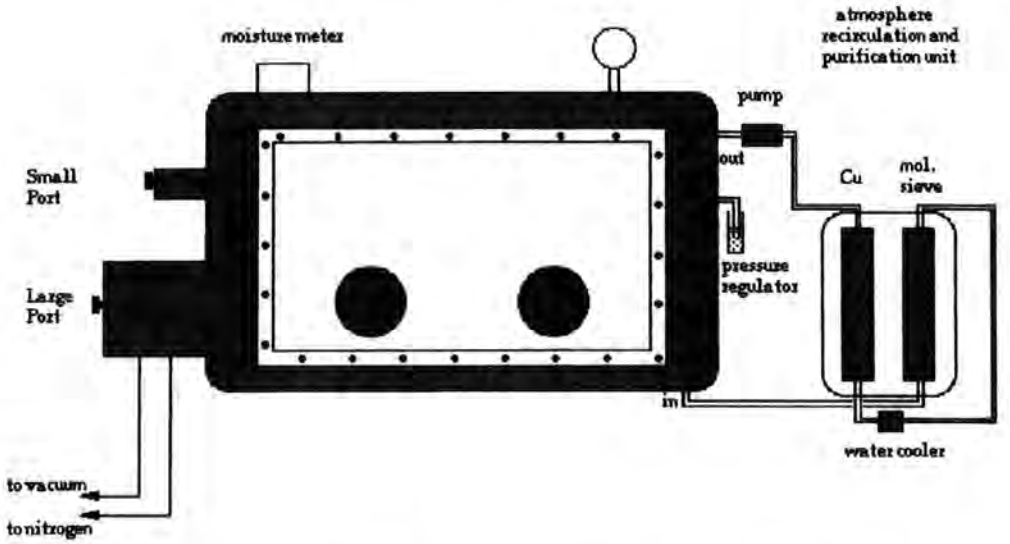

Figure 2.2 Schematic representation of a glove box

Products were isolated in a glove box using filter apparatus of varying porosities. The latter were evacuated on a vacuum line and flushed with an inert gas. The separation of desired product and filtrate could then be achieved by inversion of the filter apparatus, and subsequent separation. Products were dried *in vacuo* before transferral to a glove box for analysis.

Introduction of products to the glove box was through one of its two ports, which must be evacuated and flushed with argon at least three times, in order to maintain the inert atmosphere inside the box. The moisture and oxygen levels were monitored by meters (moisture levels were maintained between 2 and 4ppm and oxygen levels kept below 10ppm).

Argon in the glove box is constantly recirculated through two purification columns by a vacuum pump. Initially, a copper catalyst (BASF Cu catalyst R11) at 200 °C removes oxygen as copper oxide. On cooling, argon is passed through a molecular sieve (BDH 3,16") which removes moisture.

The purification columns must be occasionally regenerated when they cease to function efficiently, i.e. oxygen and moisture levels become too high. This is achieved by heating the columns to 180 °C. The copper column is treated with a reforming gas (80% N_2, 20% H_2), whilst the molecular sieve is evacuated with a rotary pump - the steam removed being condensed into a cold trap.

2.2 Starting materials and solvents

Starting materials were of the highest quality available. Solvents used (e.g. thf, benzene, hexane, toluene, acetonitrile) were freshly distilled over the appropriate drying agents, but degassed only in certain instances. Deuterated solvents, used for NMR spectroscopy, were stored over molecular sieves in the glove box or supplied in glass ampoules, which were opened in a glove box as required. They were also, on occasion, distilled over appropriate drying agents (e.g. alkali metal).

Air-sensitive and hygroscopic reagents, such as *n*-butyllithium, *t*-butyllithium, ethylmagnesium chloride and methylmagnesium bromide, were purchased as standard solutions in Sure-Seal bottles and manipulated via the recommended procedure.

Certain liquid starting materials (e.g. hmpa) were stored over an appropriate grade of molecular sieve (either 4A or 13X), since they could not be purchased as anhydrous reagents.

2.3 Nuclear Magnetic Resonance (NMR) Spectroscopy

Due to the presence of phosphorus in many of the complexes investigated, it was possible to record ^{31}P NMR spectra in the majority of cases, as well as standard ^{1}H experiments.

All samples were prepared in a glove box, typically by dissolution of between 1 and 5mg of sample in a suitable dry, deuterated solvent. For most cases suitable protection from air and moisture was afforded by using a standard nmr tube fitted with a plastic cap, Teflon tape and plastic film.

Room temperature ^{1}H NMR studies were generally performed at 200MHz, on the Varian VXR200 and Mercury 200, or at 250MHz on a Bruker AC250 spectrometers.[†] All chemical shifts (δ) are reported relative to TMS; all coupling constants are quoted in Hz.

^{31}P NMR studies were performed on the Bruker AC250 (101.2MHz) or Mercury 200 spectrometers (80.9MHz) at ambient temperature with proton decoupling. Values are reported relative to 85% H_3PO_4; coupling constants are quoted in Hz.

Variable temperature and concentration NMR spectra were recorded in collaboration with Professor Fernando López-Ortiz (University of Almeria). These included ^{7}Li, ^{15}N and ^{29}Si nmr studies, as well as a number of correlation experiments. These are discussed in more detail in the main text (*vide infra*).

2.4 Infra-Red Spectroscopy

The IR. spectra of isolated products were prepared as nujol mulls on NaCl plates using a Perkin Elmer 1720 x FTIR spectrometer. The nujol mulls were prepared in the glove box where necessary, using nujol that had been previously dried over molecular sieves. Spectra were re-recorded after air exposing samples, following the recording of the initial spectra, to gauge the resistance of the sample to air and moisture.

[†] Selected nmr experiments were performed at higher field and different temperatures.

2.5 Melting Points

Melting points were determined by differential scanning calorimetry (DSC) using a Mettler FP80 control unit coupled to a Mettler FP85 thermal analysis cell. DSC capsules were prepared in the glove box by loading between 5-10mg of sample into an aluminium crucible, which was then sealed and placed in the furnace whilst maintaining a constant flow of nitrogen through the system.

2.6 Elemental Analysis

Carbon, hydrogen, nitrogen and phosphorus content (percentage by mass), were determined for nearly all characterised products. These were prepared in the glove box, with the CHN analysis being performed on between 1-2mg of sample sealed in an aluminium capsule, using an Exeter Analytical CE-440 apparatus.

Phosphorus analysis was performed on between 6-10mg of sample placed in a gelatine capsule. This was digested using a 1:1 solution of sulphuric:perchloric acids. A portion of this solution was reacted with ammonium molybdate, forming a coloured phosphomolybdate complex, which could be determined spectroscopically using a Pye Unicam UV spectrophotometer.

2.7 X-ray Diffraction Studies

This technique gives the best, readily available information about solid-state structure. Suitable single crystals (they must be generally no smaller than 0.1 x 0.1 x 0.1 mm^3 and no larger than 0.5 x 0.5 x 0.5 mm^3) were grown in Schlenk tubes under nitrogen or argon atmospheres and at various temperatures (-40 to 20 °C).

Due to the air-sensitivity of these crystals they must be carefully treated before undertaking a diffraction study. One much employed way is to coat a suitably sized crystal with a perfluorinated ether oil which is inert to reaction and transparent to the X-rays. A

crystal treated in this way may then be mounted onto the goniometer by means of a glass fibre. The oil is frozen by the introduction of cold, nitrogen gas, which also prevents decomposition and fixes the orientation of the crystal.

Collection of data was undertaken (using a Siemens CCD Area Detector) at low temperature (153K in Durham), so as to minimise lattice vibrations and reduce the likelihood of decomposition.

2.8 Neutron Diffraction

Neutron diffraction gives the most accurate crystallographic data, but is very expensive due to the necessity for a neutron source and, hence, less accessible than X-ray diffraction. It is isotope dependent, but not molecular mass dependent and is, therefore, very useful in the study of light atoms, especially hydrogen. Crystals suitable for study by neutron diffraction need to be slightly larger than those used in X-ray diffraction experiments, typically 2 x 2 x 2 mm^3.

Air-sensitive samples for neutron diffraction were manipulated in a glove-box under an inert atmosphere of dry, oxygen-free, nitrogen. They are mounted on an aluminium pin by the use of a low temperature epoxy glue (Oxford Instruments, TRZ0004) and sealed under a quartz dome in order to maintain the inert atmosphere throughout subsequent transport to the neutron source.

The neutron diffraction experiment at Grenoble was performed on a D10 four-circle diffractometer using a wavelength of 1.2658(4) Å obtained by a Cu(200) monochromator. Data collection was carried out at 20K using a liquid-He flow cryostat.

2.9 Cryoscopy

The widespread use of organolithium compounds, especially those containing C-Li and N-Li bonds, in organic synthesis (often as proton abstractors)[2] has necessitated the study of their solution behaviour. This can be monitored by variable-temperature/concentration NMR studies on a variety of nuclei and by the use of cryoscopy. The most useful information is gained by comparing results from both.

Cryoscopy is a colligative measurement, relying on the depression in freezing point caused by an added solute. The cryoscopic equation (**Equation 2.1**) relates the freezing point depression (ΔT) to the mass of solute (w_s).

$$\Delta T = \frac{1000\, K_b w_s}{w_b M_r}$$

Equation 2.1 Cryoscopic equation

(K_b denotes the cryoscopic constant,[3] which is related to the solvent; w_b denotes the mass of solvent; M_r denotes the relative molecular mass of the solute).

The apparatus consists of a flat-bottomed inner vessel surrounded by an outer cooling jacket filled with constantly recycled ethanol (**Fig. 2.3**). The temperature of the cooling jacket is adjusted via the cryostat, whilst the side-arm allows a dry, nitrogen atmosphere to be introduced. A magnetic vortex stirrer is used to homogenise the solution.

Measurements are taken using a Beckmann thermometer, which is accurate to ±0.001 °C, with the aid of an eyepiece. A known mass of very pure, cryoscopic-grade benzene is placed in the inner vessel and allowed to freeze (initiated by scratching the sides of the glassware), whilst the mercury level equilibrates to a steady value. A value is accepted when three readings within ±0.002 °C have been obtained.

---

[2] L. Hegedus, B. Lipshutz, H. Nozaki, M. Reetz, P. Rittmeyer, K. Smith, F. Totter and H. Yamamoto, *'Organometallics in Synthesis.'*, Ed. M. Schlosser, Wiley, New York (1994); A. Loupy and B. Tchoubar, *'Salt Effects in Organic and Organometallic Chemistry.'*, VCH, Weinheim (1992).

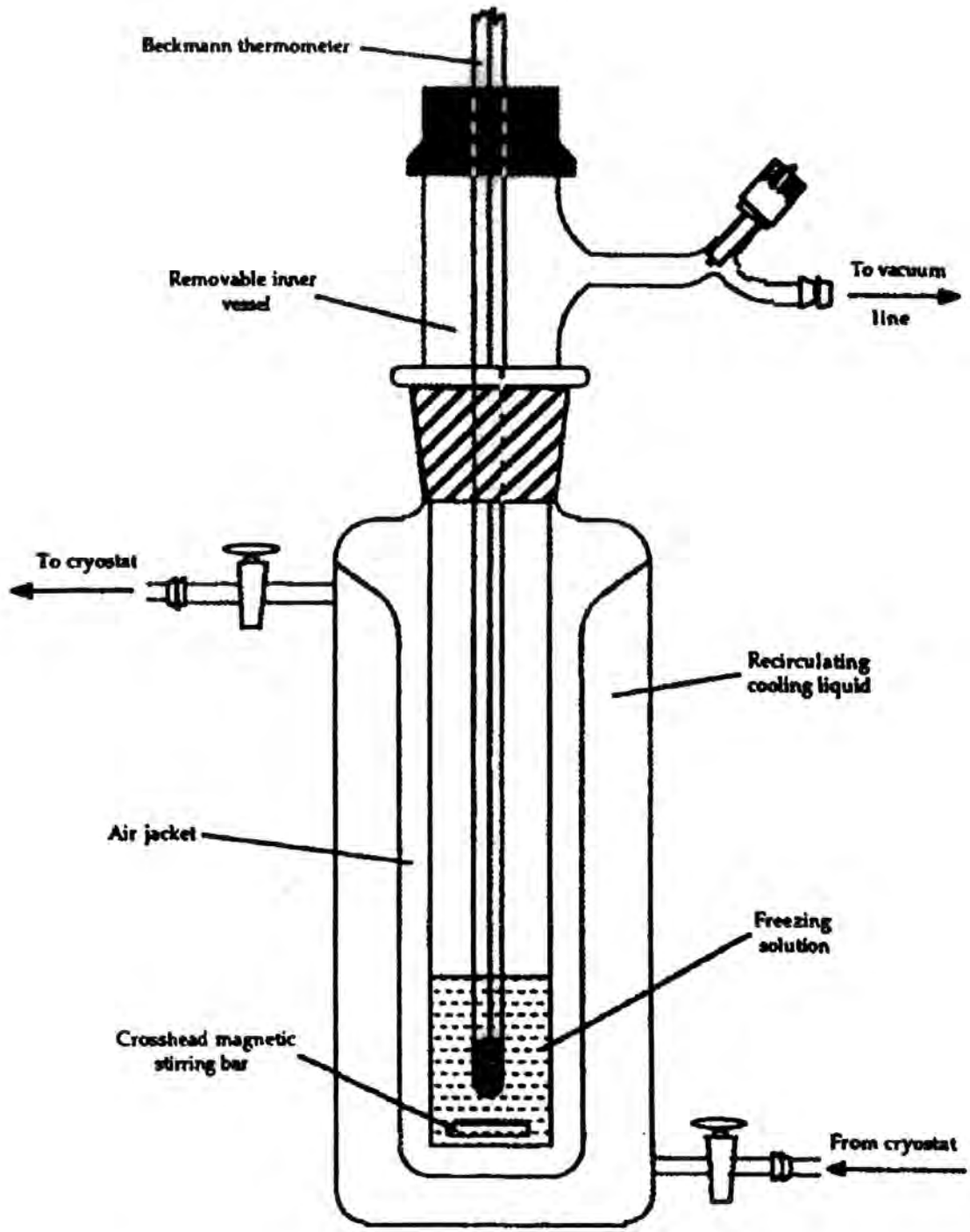

Figure 2.3 Schematic representation of a cryoscopy apparatus

[3] K_b = 5.12 K Kg mol^{-1}, P. W. Atkins, *'Physical Chemistry'*, O. U. P., 4th Ed., p. 169 (1990).

An accurately known mass of solute, contained in an air-tight vial under nitrogen, is then added to the system and the process repeated to ascertain the new freezing point. Once a new value has been obtained, progressively more and more solute can be added and a range of freezing points and thus freezing point depressions determined. The relative molecular mass of the solute can, therefore, be calculated for each result and a model for the solution state equilibria postulated.

Errors can be minimised by increasing the speed of the stirrer close to the approximately known freezing point and by the prompt reading of the temperature following the freezing process, such that any effects due to super-cooling are kept to a minimum. It should also be noted that the majority of the errors incurred from this technique arise from the thermometer readings, i.e. it is not necessary to know the mass of solute present too precisely.

2.10 Gas Chromatography (GC)

Gas chromatography measurements were performed on a HP 5890A Gas Chromatograph using 0.2μl injection of sample. The column was heated from 40 to 220°C using a heating rate of 15°C/min. and then held at that temperature for approx. 15 minutes.

3. Experimental

This chapter details the preparation of all starting materials, together with the synthesis of the complexes formed in their subsequent reactions. In the cases where single crystal X-ray analysis was possible the relevant parameters are discussed in the following chapters, together with a summary of the crystallographic data in Appendix A. The chapter is partitioned into six sections: the first details the synthesis of starting materials **1-8**; the remaining sections describe the preparation of complexes **9-44**. All syntheses were, unless otherwise stated, carried out under an inert atmosphere, using either an argon or nitrogen manifold supply. Materials were all stored in an argon-filled glove box.

Number used in text	Empirical Formula	Discussion Chapter
1	Ph_3PCH_2	-
2	Ph_3PCHMe	-
3	$(Me_2N)_3PCH_2$	-
4	Ph_3PNH	-
5	$(Me_2N)_3PNH$	-
6	Ph_3PO	-
7	$(Me_2N)_3PO$	-
8	Ph_3PS	-
9	$Ph_3PCH_2{\cdot}LiOC_6H_2(Me)^tBu_2$	4
10	$Ph_3PCH_2{\cdot}NaOC_6H_2(Me)^tBu_2$	4
11	$Ph_3PCHMe{\cdot}LiOC_6H_2(Me)^tBu_2$	4
12	$(Me_2N)_3PCH_2{\cdot}LiOC_6H_2(Me)^tBu_2$	4
13	$Ph_3PNH{\cdot}LiOC_6H_2(Me)^tBu_2$	4
14	$Ph_3PNH{\cdot}NaOC_6H_2(Me)^tBu_2$	4
15	$(Me_2N)_3PNH{\cdot}LiOC_6H_2(Me)^tBu_2$	4
16	$(Me_2N)_3PNH{\cdot}LiOC_6H_3(Ph)_2$	4
17	$(Me_2N)_3PNH{\cdot}NaOC_6H_2(Me)^tBu_2$	4
18	$(Me_2N)_3PNH{\cdot}NaOC_6H_3(Ph)_2$	4
19	$Ph_3PO{\cdot}LiOC_6H_2(Me)^tBu_2$	4

20	$Ph_3PO{\cdot}NaOC_6H_2(Me)^tBu_2$	4
21	$(Me_2N)_3PO{\cdot}LiOC_6H_3(Ph)_2$	4
22	$Ph_3PS{\cdot}LiOC_6H_2(Me)^tBu_2$	4
23	$[Ph_3PCH_2]_2{\cdot}Mg[OC_6H_2(Me)^tBu_2]_2$	4
24	$[Ph_3PNH]_2{\cdot}Mg[OC_6H_2(Me)^tBu_2]_2$	4
25	$Ph_3PCHMe{\cdot}LiN(CH_2Ph)_2$	5
26	$Ph_3PCHMe{\cdot}LiN(SiMe_3)_2$	5
27	$Ph_3PCHMe{\cdot}NaN(SiMe_3)_2$	5
28	$(Me_2N)_3PCH_2{\cdot}LiN(CH_2Ph)_2$	5
29	$Ph_3PNLi{\cdot}LiX.2thf$[1]	6
30	$(Me_2N)_3PNLi$	6
31	Ph_3PNCu	6
32	$(Me_2N)_3PNCu$	6
33	$(Me_2N)_3PO{\cdot}MgClNPPh_3$	6
34	$(Me_2N)_3PNH{\cdot}MgBrNP(NMe_2)_3$	6
35	$[(Me_2N)_3PNH]_2MgBr_2$	6
36	$[Ph_2P(=NPh)CH_2Li]_4$	7
37	$\{[Ph_2P(=NPh)CH_2(Me)_2PNLi]_3$ $[Ph_2P(=NPh)CH_2Li]\}$	7
38	$[Ph_2P(=NPh)CH_2Li{\cdot}LiO$ $C_6H_2(Me)^tBu_2]_2$	7
39	$Ph_2(Me)PCHPh$	7
40	$[Ph_2(Me)PCH_2Ph]^+[C_6H_2(Me)^tBu_2O]^-$	7
41	$[Ph_3PNH_2]^+[Ph_2C_6H_2O]^-$	8
42	$[(Me_2N)_3PNH_2]^+[Ph_2C_6H_2O]^-$	8
43	$Ph_2(C_3H_4Ph)PNP(C_3H_5)Ph$	8
44	$(Ph_2PS)_2NLi{\cdot}OPPh_2Me$	8

Table 3.1 Ligand, Compound and Complex numbering scheme for this thesis

[1] X = Br or Cl - refers to complexes **29a**, **29b** and **29c**.

3.1 Preparation of Starting Materials 1-8

Preparation of the ylides **1-3** was performed using the standard 'lithium salt-free' method of preparation.[2] The preparation of iminotriphenylphosphorane was modified from syntheses found in the literature.[3,4] Compounds **5** and **7** were purchased from *Fluka Synthesis* and *Aldrich* respectively, and were dried over 13X molecular sieves. Compound **8** was purchased from *Aldrich* and used as supplied. Phosphonium salts for compounds **1** and **2** were purchased from *Lancaster*, the other phosphonium salts (used to synthesise ligands **3, 4, 6** and **45**) were prepared through quaternisation of the corresponding phosphine (purchased from *Aldrich*) as described in **Chapter 1**.

3.1.1 Triphenylphosphonium methylide 1

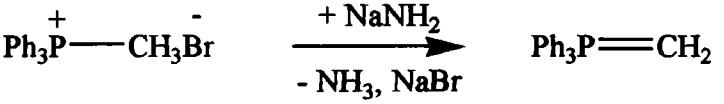

Dry thf (150 mL) was added to methyltriphenylphosphonium bromide (35.6 g, 100 mmol) and sodium amide (4.6 g, 110 mmol). Heating to 40 °C was followed by agitation of the mixture for 24 hours at ambient temperature. The resulting yellow solution was filtered, thereby removing NaBr and any unreacted $NaNH_2$. Thf was evaporated under reduced pressure to approximately 2mL. Addition of hexane (80 mL) and toluene (8 mL), with gentle heating, afforded a yellow solution. On cooling a crop of yellow crystals was produced.

Yield: 19.8 g (72 %)

Melting point: 101-2 °C

---

[2] R. Koster, D. Simic and M. Grassberger, *Liebigs Ann. Chem.*, **739**, 281 (1970); H. Schmidbaur, H. Stuhler and W. Vornberger, Chem. Ber., **105**, 1084 (1972).

[3] H. Staudinger and J. Meyer, *Helv. Chim. Acta.*, **2**, 635 (1919); L. Bickofer and S. M. Kim, *Chem. Ber.*, **96**, 3099 (1963); H-J. Cristau, J. Kadoura, L. Chiche and E. Toreilles, *Bull. Soc. Chim. Fr.*, **4**, 515 (1989).

[4] R. Appel and A. Hauss, *Chem. Ber.*, **93**, 405 (1960).

IR Spectrum: ν/cm^{-1} 880 P-C_{ylidic} stretch.

^{1} H NMR spectrum: 200 MHz, solvent C_6D_6

δ (ppm)	Integral	Multiplicity	Assignment
0.9	2H	Doublet	Ph_3PCH_2
7.2-7.8	15H	Multiplet	ArH

^{31}P NMR spectrum: 101.2 MHz, solvent C_6D_6

δ (ppm)	Multiplicity	Assignment
20.7	singlet	Ph_3PCH_2

3.1.2 Triphenylphosphonium ethylide 2

$$Ph_3\overset{+}{P}-\overset{-}{C}H_2MeBr \xrightarrow[-\ NH_3,\ NaBr]{+\ NaNH_2} Ph_3P{=}CHMe$$

Dry thf (180 mL) was added to ethyltriphenylphosphonium bromide (37.0 g, 100 mmol) and sodium amide (4.6 g, 110 mmol). Heating to 40 °C was followed by agitation of the mixture for 24 hours at ambient temperature. The resulting red solution was filtered, thereby removing NaBr and any unreacted $NaNH_2$. Thf was evaporated under reduced pressure to approximately 2mL. Addition of hexane (20 mL), with gentle heating, afforded a red solution. On cooling a crop of red crystals was produced.

Yield: 16.0 g (55 %)

Melting point: 112-3 °C

IR Spectrum: ν/cm^{-1} 820 P-C_{ylidic} stretch.

^{1}H NMR spectrum: 200 MHz, solvent C_6D_6

δ (ppm)	Integral	Multiplicity	Assignment
1.0	1H	doublet of quartets	$Ph_3PC(Me)\mathbf{H}$
2.1	3H	doublet of doublets	$Ph_3PC(\mathbf{Me})H$
7.0 - 7.1	9H	Multiplet	m,p-ArH
7.1-7.7	6H	Multiplet	o-ArH

^{31}P NMR spectrum: 101.2 MHz, solvent C_6D_6

δ (ppm)	Multiplicity	Assignment
14.6	Singlet	$Ph_3PC(Me)H$

3.1.3 Tris(dimethylamino)phosphonium methylide 3

$$(Me_2N)_3\overset{+}{P}-\overset{-}{C}H_3Br \xrightarrow[-\ NH_3,\ NaBr]{+\ NaNH_2} (Me_2N)_3P{=}CH_2$$

Dry thf (150mL) was added to a mixture of 24.3g (100mmol) methyltris(dimethylamino) phosphonium bromide (or iodide) and sodium amide (4.2g, 108mmol) under an inert atmosphere. The solution was vigorously stirred at ambient temperature for 24 hours, before filtration to remove the solid residues. The solvent was removed *in vacuo* and the product distilled (39°C, 10^{-3} Torr).

Yield: 12.5g (75% for the bromide salt)

^{1}H NMR spectrum: 200 MHz, solvent C_6D_6

δ (ppm)	Integral	Multiplicity	Coupling/Hz	Assignment
0.13	2H	broad singlet	-	$(Me_2N)_3PCH_2$
2.46	18H	doublet	8.8	$(Me_2N)_3PCH_2$

^{31}P NMR spectrum: 101.2 MHz, solvent C_6D_6

δ (ppm)	Multiplicity	Assignment
71.3	singlet	$(Me_2N)_3PCH_2$

3.1.4 Iminotriphenylphosphorane 4

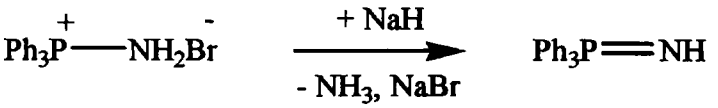

Dry toluene (15 mL) was added to amino(triphenyl)phosphonium bromide (1.79 g, 5 mmol) and sodium hydride (0.20 g, 5 mmol). Agitation of the solution, at 100 °C for 48 hours, was followed by filtration and reduction of the solvent *in vacuo* to approximately 3mL. Storage of this solution at -40 °C for 24 hours yielded a crop of colourless crystals.

Yield: 1.0 g (75 %)

Melting point: 128 °C

IR Spectrum: ν/cm^{-1} 1189 P-N stretch of imine

ν/cm^{-1} 3349 N-H stretch

^{1}H NMR spectrum: 200 MHz, solvent C_6D_6

δ (ppm)	Integral	Multiplicity	Assignment
1.1	1H	Broad singlet	Ph_3PNH
7.1-7.3	9H	multiplet	m,p-ArH
7.34	6H	multiplet	o-ArH

^{31}P NMR spectrum: 101.2 MHz, solvent C_6D_6

δ (ppm)	Multiplicity	Assignment
17.5	Singlet	Ph_3PNH

3.1.5 Iminotris(dimethylamino)phosphorane 5

^{1}H NMR spectrum: 200 MHz, solvent C_6D_6

δ (ppm)	Integral	Multiplicity	Assignment
0.3	1H	Multiplet	NH
2.3-2.5	18H	Multiplet	Me_2N

^{31}P NMR spectrum: 101.2 MHz, solvent C_6D_6

δ (ppm)	Multiplicity	Assignment
40.0	Singlet	$(Me_2N)_3PNH$

3.1.6 Triphenylphosphine oxide 6

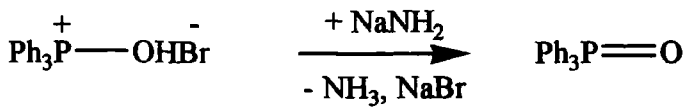

Dry thf (100 mL) was added to hydroxytriphenylphosphonium bromide (14.0 g, 39 mmol) and sodium amide (1.64 g, 42 mmol). Agitation for 24 hours was followed by filtration and reduction of the solvent *in vacuo* to approximately 2mL. Addition of toluene (10 mL), with heating, resulted in complete dissolution of the residue. Colourless, transparent blocks were produced upon standing at ambient temperature for several hours.

Yield: 7.6 g (70 %)

Melting point: 156-7 °C

^{1}H NMR spectrum: 200 MHz, solvent C_6D_6

δ (ppm)	Integral	Multiplicity	Assignment
7.0-7.1	9H	Multiplet	m,p-**Ph_3PO**
7.8-7.9	6H	Multiplet	o-**Ph_3PO**

^{31}P NMR spectrum: 101.2 MHz, solvent C_6D_6

δ (ppm)	Multiplicity	Assignment
25.9	Singlet	**Ph_3PO**

3.1.7 Hexamethylphosphorictriamide 7

^{1}H NMR spectrum: 200 MHz, solvent C_6D_6

δ (ppm)	Integral	Multiplicity	Coupling/Hz	Assignment
2.41	18H	Doublet	$^{3}J_{PH} = 9.4$	$(Me_2N)_3PO$

^{31}P NMR spectrum: 101.2 MHz, solvent $CDCl_3$

δ (ppm)	Multiplicity	Assignment
25.0	Singlet	$(Me_2N)_3PO$

3.1.8 Triphenylphosphine sulfide 8

Melting point: 162-4 °C

^{1}H NMR spectrum: 200 MHz, solvent C_6D_6

δ (ppm)	Integral	Multiplicity	Assignment
6.9-7.0	9H	Multiplet	m,p-Ph_3PS
7.7-7.8	6H	Multiplet	o-Ph_3PS

^{31}P NMR spectrum: 101.2 MHz, solvent C_6D_6

δ (ppm)	Multiplicity	Assignment
43.8	Singlet	Ph_3PS

3.2 Synthesis and characterisation of complexes 9-24

3.2.1 Formation of 9

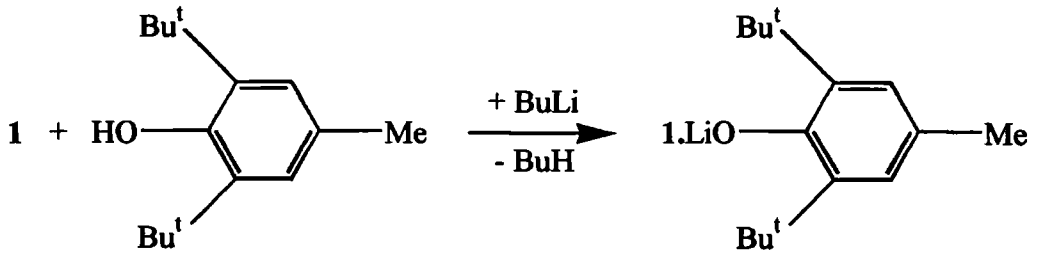

Dry toluene (40mL) was added to a cooled mixture (to approximately 0°C) of 2,6-di-tert-butyl-4-methylphenol (0.550g, 2.5mmol), *n*-butyllithium (1.6mL, 2.5mmol, 1.6M solution in hexanes) and **1** (0.693 g, 2.5mmol). Following agitation of the solution for 1 hour at ambient temperature, a yellow precipitate formed. Heating, to approximately 70°C, accomplished complete dissolution. Storage of the orange solution for 24 hours, at ambient temperature, induced the formation of transparent, yellow blocks.

Yield: 1.1 g (87 %)

Melting Point: 282-3 °C

^{1}H NMR spectrum: 200 MHz, solvent C_6D_6

δ/ppm	Integral	Multiplicity	Coupling/Hz	Assignment
0.35	2H	Broad singlet	$^2J_{PH} = 4.5$	Ph_3PCH_2
1.7	18H	Singlet	-	**^{t}Bu**
2.6	3H	Singlet	-	**Me**
6.8-7.5	17H	Multiplet	-	**Aromatic**

^{31}P NMR spectrum: 101.2 MHz, solvent C_6D_6

δ (ppm)	Multiplicity	Assignment
30.6	Singlet	Ph_3PCH_2

Elemental Analysis: $C_{34}H_{40}POLi$

	C	H	P	O	Li
Calculated % by mass	81.3	8.0	6.2	3.2	1.4
Observed % by mass	80.2	8.1	-	-	-

3.2.2 Formation of 10

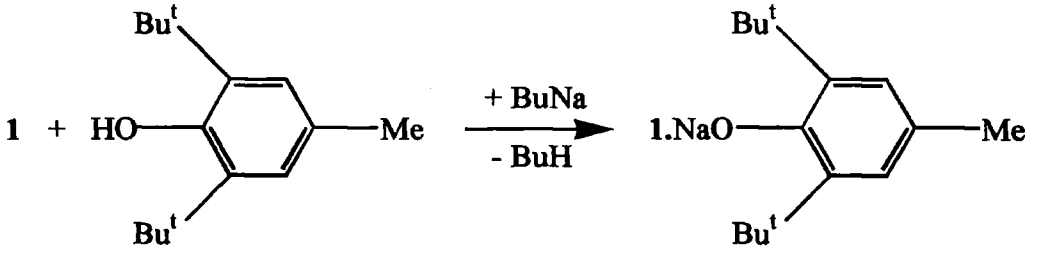

Dry toluene (40mL) was added to a cooled mixture (to approximately 0°C) of 2,6-di-tert-butyl-4-methylphenol (0.550g, 2.5mmol), *n*-butyl sodium (0.197g, 2.5mmol) and 1 (0.693 g, 2.5mmol). Following agitation of the solution for 1 hour at ambient temperature, a yellow precipitate formed. Heating, to approximately 70°C, accomplished complete dissolution. Storage of the yellow solution for 24 hours, at ambient temperature, induced the formation of transparent, yellow blocks.

Yield: 0.87 g (61%)

Melting Point: 222 °C

^{1}H NMR spectrum: 200 MHz, solvent C_6D_6

δ/ppm	Integral	Multiplicity	Assignment
0.2	2H	Broad singlet	Ph_3PCH_2
1.6	18H	Singlet	**^{t}Bu**
2.6	3H	Singlet	**Me**
6.7-7.3	17H	Multiplet	**Aromatic**

^{31}P NMR spectrum: 101.2 MHz, solvent C_6D_6

δ (ppm)	Multiplicity	Assignment
30.6	Singlet	Ph_3PCH_2

Elemental Analysis: $C_{34}H_{40}PONa$

	C	H	P	O	Na
Calculated % by mass	78.7	7.8	6.0	3.1	4.5
Observed % by mass	77.2	7.8	-	-	-

3.2.3 Formation of 11

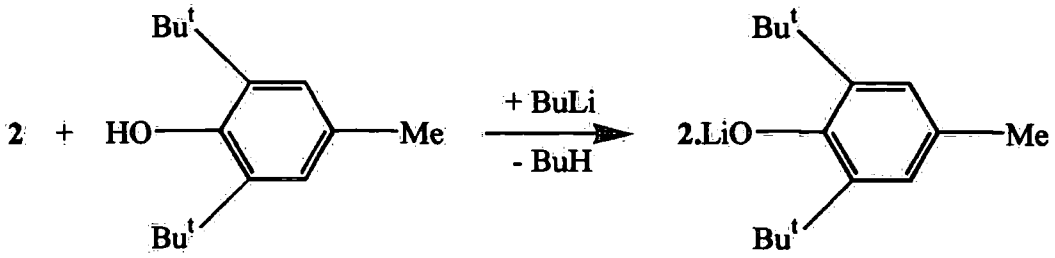

Dry toluene (6mL) was added to 2,6-di-tert-butyl-4-methylphenol (0.550g, 2.5mmol) and **1** (0.72 g, 2.5mmol). Addition of *n*-butyllithium (1.6mL, 2.5mmol, 1.6M solution in hexanes) yielded an orange precipitate which, upon heating to approximately 70°C, achieved complete dissolution. Storage of the yellow/orange solution for 4 hours, at ambient temperature, afforded orange crystalline blocks.

Yield: 0.90 g (70 %)

Melting Point: 194-5°C

^{1}H NMR spectrum: 200 MHz, solvent C_6D_6

δ/ppm	Integral	Multiplicity	Coupling/Hz	Assignment
0.80	1H	Quartet of doublets	$^{2}J_{PH} = 3.7$, $^{3}J_{HH} = 6.8$	Ph_3PCHMe
1.58	3H	Doublet of doublets	$^{3}J_{HH} = 6.7$, $^{3}J_{PH} = 20.6$	Ph_3PCHMe
1.65	18H	Singlet	-	**^{t}Bu**
2.52	3H	Singlet	-	**Me**
6.8-7.4	17H	Multiplet	-	**Aromatic**

^{31}P NMR spectrum: 101.2 MHz, solvent C_6D_6

δ (ppm)	Multiplicity	Assignment
27.4	Singlet	Ph_3PCHMe

Elemental Analysis: $C_{38.5}H_{46}PNOLi{\cdot}0.5C_7H_8$)

	C	H	P	O	Li
Calculated % by mass	82.2	8.2	5.5	2.8	1.2
Observed % by mass	82.7	8.5	-	-	-

3.2.4 Formation of 12

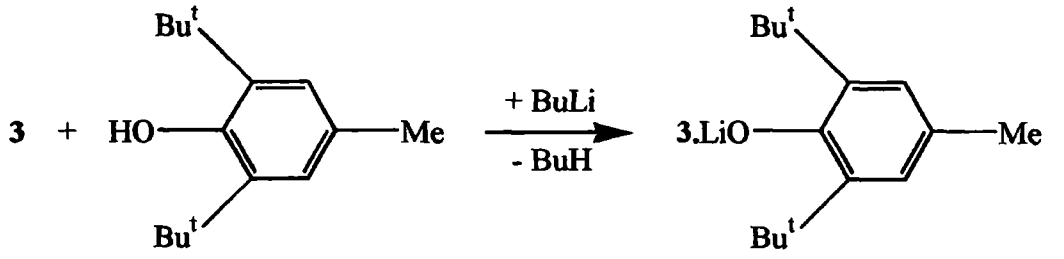

Dry toluene (15mL) was added to a mixture of **3** (0.32g, 2mmol) and 2,6-di-tert-butyl-4-methbylphenol (0.44g, 2mmol). Addition of *n*-butyllithium (1.28mL, 1.6M solution in hexanes, 2mmol) afforded a white precipitate, which dissolved, upon heating to approximately 70°C, leaving a yellow solution. Upon cooling to ambient temperature and standing for several hours, a crop of transparent blocks was produced.

Yield: 0.44g (55 %)

Melting Point: 245°C

^{1}H NMR spectrum: 200 MHz, solvent C_6D_6

δ/ppm	Integral	Multiplicity	Coupling/Hz	Assignment
-0.40	2H	doublet	$^{2}J_{PH} = 9.8$	$(Me_2N)_3PCH_2$
1.88	18H	singlet	-	**^{t}Bu**
2.07	18H	doublet	$^{3}J_{PH} = 9.4$	$(Me_2N)_3PCH_2$
2.47	3H	singlet	-	**Me**
7.31	2H	singlet	-	**Aromatic**

^{31}P NMR spectrum: 101.2 MHz, solvent C_6D_6

δ (ppm)	Multiplicity	Assignment
79.0	Singlet	$(Me_2N)_3PCH_2$

Elemental Analysis: $C_{22}H_{43}N_3POLi$

	C	H	N	P	O	Li
Calculated % by mass	65.5	10.7	10.4	7.7	4.0	1.7
Observed % by mass	65.4	11.0	10.8	-	-	-

3.2.5 Formation of 13

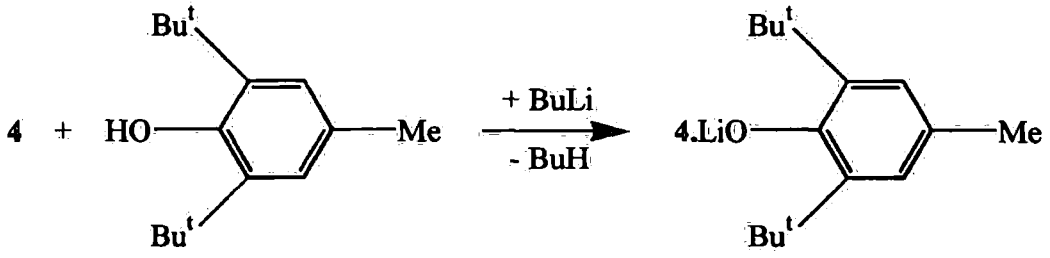

Dry toluene (10mL) was added to iminotriphenylphosphorane (5mmol, 1.39g) and 2,6-di-tert-butyl-4-methylphenol (5mmol, 1.10g). Addition of *n*-butyllithium (3.2mL, 5mmol, 1.6M solution in hexanes) afforded a white precipitate. Addition of a further 35mL toluene, with heating, caused complete dissolution. After 24h at ambient temperature a crop of colourless crystals was produced.

Yield: 1.9g (74 %)

Melting Point: 317-318 °C

^{1}H NMR spectrum: 200 MHz, solvent C_6D_6

δ/ppm	Integral	Multiplicity	Coupling/Hz	Assignment
0.6-0.65	1H	Doublet	$^{2}J_{PH} = 9.9$	N-**H**
1.8	18H	Singlet	-	**^{t}Bu**
2.5	3H	Singlet	-	**Me**
6.8-7.0	9H	Multiplet	-	m,p-**Ph_3**PNH
7.25-7.4	8H	Multiplet	-	**Aromatic**

^{31}P NMR spectrum: 101.2 MHz, solvent C_6D_6

δ (ppm)	Multiplicity	Assignment
29.0	Singlet	Ph_3PNH

Elemental Analysis: $C_{33}H_{39}PNOLi$

	C	H	N	P	O	Li
Calculated % by mass	78.7	7.8	2.8	6.2	3.2	1.4
Observed % by mass	78.8	8.0	3.4	7.0	-	-

3.2.6 Formation of 14

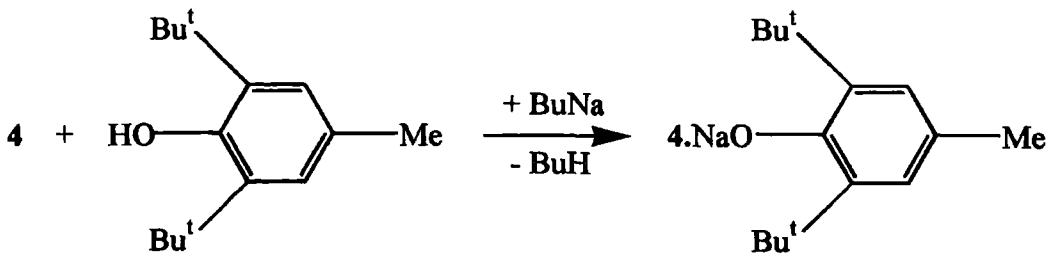

Dry toluene (8mL) was added to a mixture of 2,6-di-tert-butyl-4-methylphenol (0.220 g, 1 mmol), *n*-butyl sodium (0.086 g, 1 mmol) and **4** (0.277g, 1mmol). Following agitation of the solution for 1 hour, at ambient temperature, a white precipitate formed. Heating, to approximately 70 °C, accomplished complete dissolution. Storage of the pale yellow solution for 24 hours, at ambient temperature, induced the formation of transparent, colourless blocks.

Yield: 0.34g (66 %)

Melting Point: 269°C

^{1}H NMR spectrum: 200 MHz, solvent C_6D_6

δ/ppm	Integral	Multiplicity	Coupling/Hz	Assignment
0.3	1H	Broad singlet	-	Ph_3PNH
1.6-2.0	18H	Broad doublet	-	**^{t}Bu**
2.6	3H	Broad singlet	-	**Me**
7.2-7.8	17H	Multiplet	-	**aromatic**

^{31}P NMR spectrum: 101.2 MHz, solvent C_6D_6

δ (ppm)	Multiplicity	Assignment
21.5	Singlet	Ph_3PNH

Elemental Analysis: $C_{33}H_{39}NPONa$

	C	H	N	P	O	Na
Calculated % by mass	74.5	8.1	2.9	6.4	3.3	4.8
Observed % by mass	73.8	7.3	2.0	-	-	-

3.2.7 Formation of 15

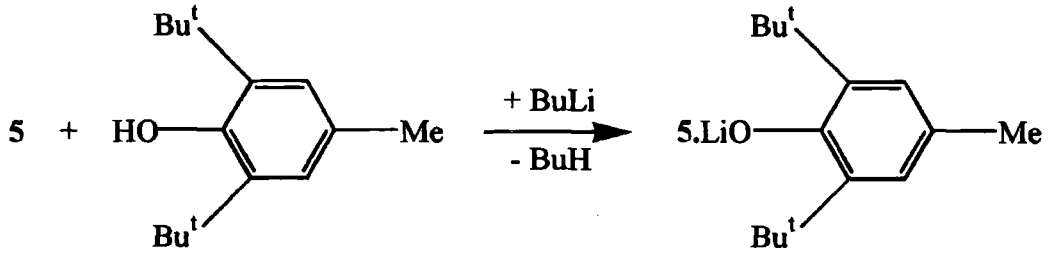

Toluene (10 mL) was added to 2,6-di-tert-butyl-4-methylphenol (0.22 g, 1 mmol) and **5** (0.18 mL, 1 mmol). Addition of *n*-butyllithium (0.64 mL, 1.6M solution in hexanes, 1 mmol) yielded a white precipitate, which dissolved with gentle heating. After standing for several days at ambient temperature, a crop of transparent blocks was formed.

Yield: 0.22 g (54 %)

Melting Point: 150-1 °C

^{1}H NMR spectrum: 200 MHz, solvent C_6D_6

δ/ppm	Integral	Multiplicity	Coupling/Hz	Assignment
-0.025-0	2H	Multiplet	-	$(Me_2N)_3PNH$
1.9	18H	Singlet	-	**^{t}Bu**
2.05-2.1	18H	Doublet	-	$(Me_2N)_3PNH$
2.5	3H	Singlet	-	**Me**
7.3	2H	Singlet	-	**aromatic**

^{31}P NMR spectrum: 101.2 MHz, solvent C_6D_6

δ (ppm)	Multiplicity	Assignment
50.0	Singlet	$(Me_2N)_3PNH$

Elemental Analysis: $C_{21}H_{42}N_4POLi$

	C	H	N	P	O	Li
Calculated % by mass	62.4	10.5	13.9	7.7	4.0	1.7
Observed % by mass	61.5	10.5	12.8	8.5	-	-

3.2.8 Formation of 16

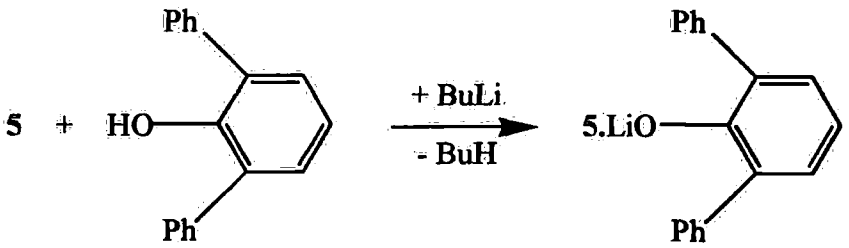

Toluene (3 mL) was added to diphenylphenol (0.492 g, 2 mmol) and *n*-butyllithium (1.28 mL, 1.6M solution in hexanes, 2 mmol) to give a white precipitate. Addition of **5** (0.36 mL, 2 mmol), together with a further 7mL toluene and gentle heating, yielded a colourless solution. Cooling to -30 °C, for a period of 72 hours, afforded a crop of transparent block-like crystals.

Yield: 0.2g (23.3%)

Melting Point: 126-7 °C

^{1}H NMR spectrum: 200 MHz, solvent C_6D_6

δ/ppm	Integral	Multiplicity	Coupling/Hz	Assignment
-0.5	1H	Broad singlet	-	$(Me_2N)_3PNH$
2.04	18H	Doublet	$^{3}J_{PH}$ = 7.6	$(Me_2N)_3PNH$
6.82	1H	Triplet	$^{3}J_{HH}$ = 6.0	p-$C_6H_3(Ph)_2$
7.15-7.20	6H	Multiplet	-	m,p-$C_6H_3(Ph)_2$
7.45	2H	Doublet	$^{3}J_{HH}$ = 6.0	m-$C_6H_3(Ph)_2$
8.0	4H	Doublet	$^{3}J_{HH}$ = 7.5	o-$C_6H_3(Ph)2$

^{31}P NMR spectrum: 101.2 MHz, solvent C_6D_6

δ (ppm)	Multiplicity	Assignment
44.8	Singlet	$(Me_2N)_3PNH$

Elemental Analysis: $C_{24}H_{32}N_4POLi$

	C	H	N	P	O	Li
Calculated % by mass	67.0	7.5	13.0	7.2	3.7	1.6
Observed % by mass	65.8	7.6	12.7	7.9	-	-

3.2.9 Formation of 17

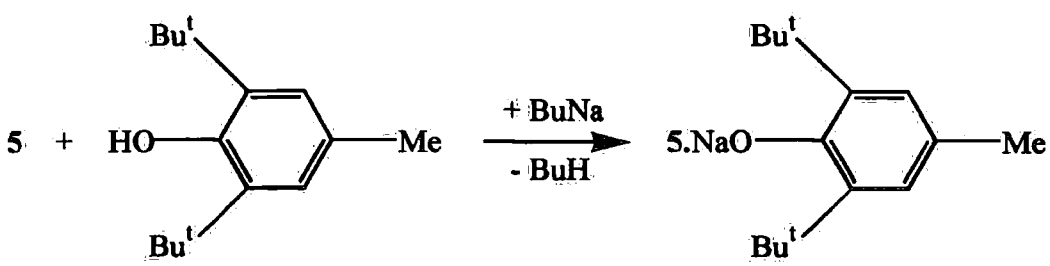

Dry toluene (10 mL) was added to a cooled mixture (to approximately 0 °C) of 2,6-di-tert-butyl-4-methylphenol (0.220 g, 1 mmol), *n*-butyl sodium (0.086 g, 1 mmol) and **5** (0.17 mL, 1 mmol). Following agitation of the solution for 1 hour, at ambient temperature, a white precipitate formed. Heating, to approximately 70°C, accomplished complete dissolution. Storage of the colourless solution for 24 hours, at ambient temperature, induced the formation of transparent, colourless blocks.

Yield: 0.18g (43 %)

Melting Point: 305°C

^{1}H NMR spectrum: 200 MHz, solvent C_6D_6

δ/ppm	Integral	Multiplicity	Coupling/Hz	Assignment
-0.3	1H	broad singlet	-	$(Me_2N)_3PN\mathbf{H}$
1.84	18H	singlet	-	**^{t}Bu**
2.07	18H	doublet	$^{3}J_{PH} = 7.6$	$(\mathbf{Me_2N})_3PNH$
2.49	3H	singlet	-	**Me**
7.28	2H	singlet	-	**meta**-phenyl

^{31}P NMR spectrum: 101.2 MHz, solvent C_6D_6

δ (ppm)	Multiplicity	Assignment
45.3	singlet	$(Me_2N)_3PNH$

Elemental Analysis: $C_{21}H_{42}N_4PONa$

	C	H	N	P	O	Na
Calculated % by mass	60.0	10.1	13.3	7.4	3.7	5.5
Observed % by mass	58.1	9.3	13.2	-	-	-

3.2.10 Formation of 18

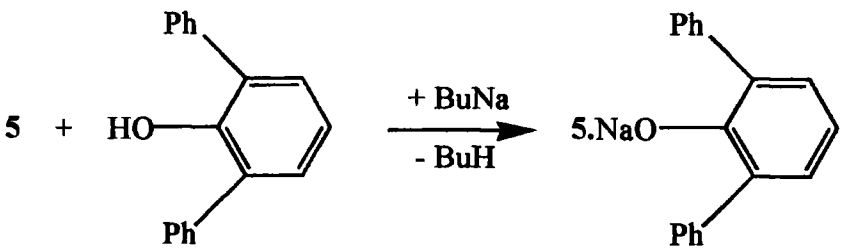

Dry toluene (5 mL) was added to a cooled mixture (to approximately 0 °C) of 2,6-di-phenylphenol (0.246 g, 1 mmol), *n*-butylsodium[5] (0.086 g, 1 mmol) and **5** (0.17 mL, 1 mmol). Agitation of the solution for 1 hour, at ambient temperature, afforded a white precipitate. Heating, to approximately 70 °C, accomplished complete dissolution. Storage of the colourless solution for 48 hours, at -30°C, induced the formation of transparent, colourless blocks.

Yield: 0.26 g (58 %)

Melting Point: 277-8 °C

^{1}H NMR spectrum: 200 MHz, solvent C_6D_6

δ/ppm	Integral	Multiplicity	Coupling/Hz	Assignment
-0.34	1H	Broad singlet	-	$(Me_2N)_3PNH$
2.10	18H	Doublet	$^{3}J_{PH} = 7.6$	$(Me_2N)_3PNH$
6.7-7.9	13H	Multiplet	-	**aromatic**

^{31}P NMR spectrum: 101.2 MHz, solvent C_6D_6

δ (ppm)	Multiplicity	Assignment
44.0	singlet	$(Me_2N)_3PNH$

[5] BuNa synthesised from ^{n}BuLi and NaOBu^{t} in hexanes. Personal communication - *K. W. Henderson.*

Elemental Analysis: $C_{24}H_{32}N_4PONa$

	C	H	N	P	O	Na
Calculated % by mass	64.6	7.2	12.6	6.9	3.6	5.2
Observed % by mass	63.3	7.1	12.7	-	-	-

3.2.11 Formation of 19

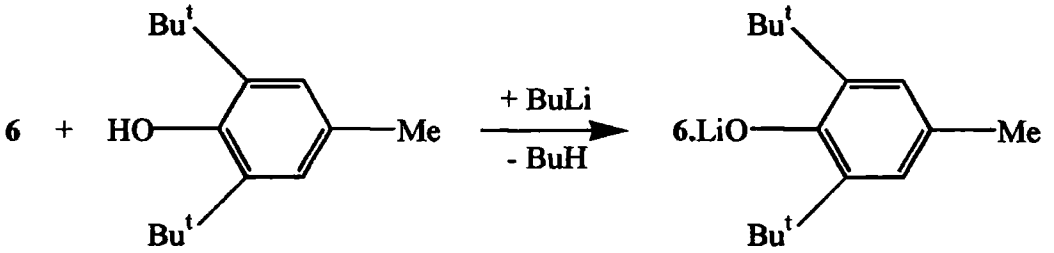

Toluene (5mL) was added to 2,6-di-tert-butyl-4-methylphenol (0.220 g, 1 mmol) and **6** (0.28 g, 1 mmol). Addition of *n*-butyllithium (0.64 mL, 1.6M solution in hexanes, 1 mmol) afforded a white precipitate which, on addition of a further 15mL toluene (with heating), gave a colourless solution. Storage of the colourless solution at ambient temperature yielded a crop of transparent blocks after 24 hours.

Yield: 0.38 g (75.0 %)

Melting Point: 287-8 °C

^{1}H NMR spectrum: 200 MHz, solvent C_6D_6

δ/ppm	Integral	Multiplicity	Coupling/Hz	Assignment
1.83	18H	Singlet	-	**^{t}Bu**
2.59	3H	Singlet	-	**Me**
6.9-7.0	8H	Multiplet	-	**Aromatic**
7.15-7.40	9H	Multiplet	-	**Aromatic**

^{31}P NMR spectrum: 101.2 MHz, solvent C_6D_6

δ (ppm)	Multiplicity	Assignment
31.8	Singlet	Ph_3PO

Elemental Analysis: $C_{30}H_{38}PO_2Li$

	C	H	P	O	Li
Calculated % by mass	76.9	8.2	6.61	6.81	1.48
Observed % by mass	77.5	7.6	-	-	-

3.2.12 Formation of 20

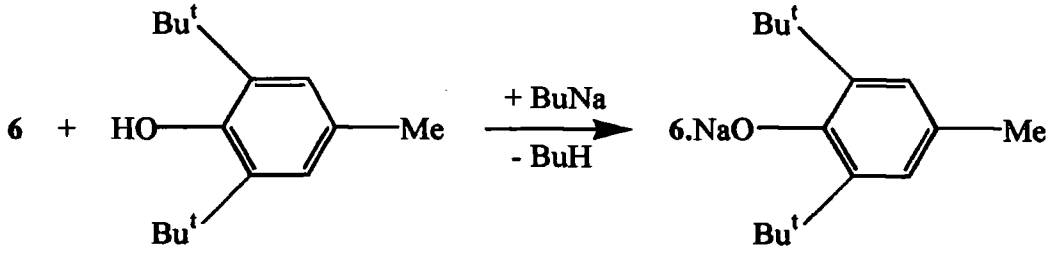

Toluene (5mL) was added to 2,6-di-tert-butyl-4-methylphenol (0.220 g, 1 mmol), *n*-butylsodium (0.86 g, 1 mmol) and **6** (0.28 g, 1 mmol), to give a white precipitate. Addition of a further 25mL toluene (with heating), gave a pale green solution. Storage of this solution at ambient temperature yielded a crop of transparent blocks after 24 hours.

Yield: 0.32 g (62.0 %)

Melting Point: 293-4 °C

^{1}H NMR spectrum: 200 MHz, solvent C_6D_6

δ/ppm	Integral	Multiplicity	Coupling/Hz	Assignment
1.70	18H	Singlet	-	**^{t}Bu**
2.48	3H	Singlet	-	**Me**
6.8-7.3	17H	Multiplet	-	**Aromatic**

^{31}P NMR spectrum: 101.2 MHz, solvent C_6D_6

δ (ppm)	Multiplicity	Assignment
31.8	singlet	**Ph_3PO**

Elemental Analysis: $C_{30}H_{38}PO_2Na$

	C	H	P	O	Na
Calculated % by mass	74.2	7.9	6.4	6.6	4.7
Observed % by mass	75.5	7.3	-	-	-

3.2.13 Formation of 21

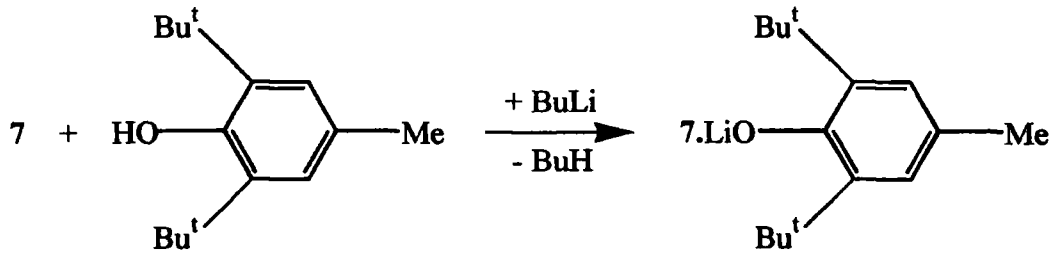

Toluene (5mL) was added to 2,6-di-tert-butyl-4-methylphenol (0.220 g, 1 mmol) and 7 (0.18 mL, 1 mmol). Addition of *n*-butyllithium (0.64 mL, 1.6M solution in hexanes, 1 mmol), together with a further 15 mL toluene (and heating), gave a colourless solution. Storage of this solution at ambient temperature yielded a crop of transparent blocks after 24 hours.

Yield: 0.31 g (80.0 %)

Melting Point: 341-2 °C

^{1}H NMR spectrum: 200 MHz, solvent C_6D_6

δ/ppm	Integral	Multiplicity	Coupling/Hz	Assignment
1.7	18H	Singlet	-	^{t}Bu
1.9	18H	Doublet	$^{3}J_{PH} = 4.7$	Me_2N
2.35	3H	Singlet	-	Me
7.00	2H	Multiplet	-	Aromatic

^{31}P NMR spectrum: 101.2 MHz, solvent C_6D_6

δ (ppm)	Multiplicity	Assignment
24.1	Singlet	$(Me_2N)_3PO$

Elemental Analysis: $C_{21}H_{41}N_3PO_2Li$

	C	H	N	P	O	Li
Calculated % by mass	62.2	10.2	10.4	7.6	7.9	1.7
Observed % by mass	61.8	10.3	10.2	-	-	-

3.2.14 Formation of 22

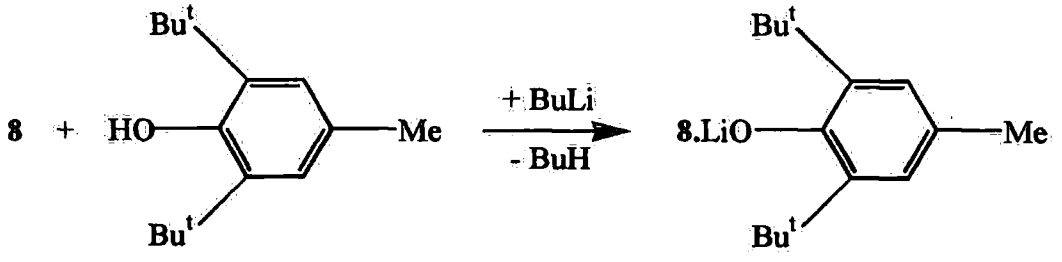

Toluene (5mL) was added to 2,6-di-tert-butyl-4-methylphenol (0.220 g, 1 mmol) and **8** (0.294 g, 1 mmol). The solution was cooled (to approximately 0 °C) before the addition of *n*-butyllithium (0.64 mL, 1.6M solution in hexanes, 1 mmol) gave a white precipitate. Heating, with a further 10mL toluene, resulted in complete dissolution. Storage of the pale yellow solution at ambient temperature yielded a crop of transparent blocks after 24 hours.

Yield: 0.31 g (%)

Melting Point: 237-8 °C

^{1}H NMR spectrum: 200 MHz, solvent C_6D_6

δ/ppm	Integral	Multiplicity	Coupling/Hz	Assignment
1.55	18H	Singlet	-	**^{t}Bu**
2.4	3H	Singlet	-	**Me**
6.8-7.8	20H	Multiplet	-	**Aromatic**

^{31}P NMR spectrum: 101.2 MHz, solvent C_6D_6

δ (ppm)	Multiplicity	Assignment
44.1	Singlet	**Ph_3PS**

Elemental Analysis: $C_{33}H_{38}POSLi$

	C	H	P	O	S	Li
Calculated % by mass	76.1	7.4	6.0	3.1	6.2	1.3
Observed % by mass	77.0	7.5	-	-	-	-

3.2.15 Formation of 23

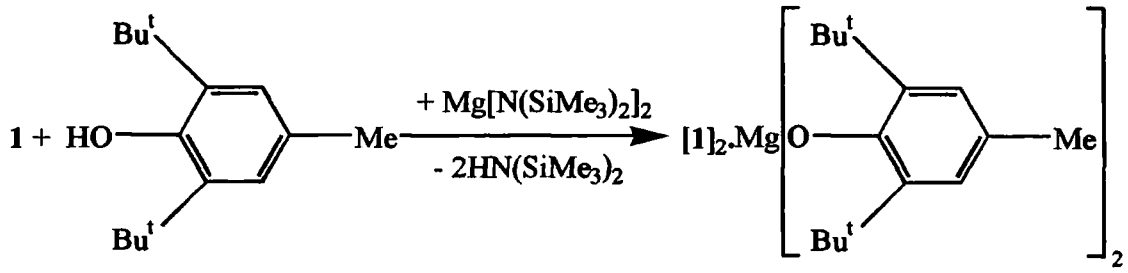

Toluene (5 mL) was added to 2,6-di-tert-4-methylphenol (0.44 g, 2 mmol), 1 (0.56 g, 2 mmol) and magnesium bis[bis(trimethylsilyl)amide][6] (0.34 g, 1 mmol), to give a yellow precipitate. Heating, to approximately 70 °C, together with the addition of a further 3 mL toluene yielded a red solution. On cooling to ambient temperature a yellow product could be isolated.

Yield: 0.74 g (72 %)

Melting Point: 130-1 °C

^{1}H NMR spectrum: 200 MHz, solvent C_6D_6

δ/ppm	Integral	Multiplicity	Coupling/Hz	Assignment
1.63	18H	Singlet	-	**^{t}Bu**
2.46	3H	Singlet	-	**Me**
3.4	2H	Singlet	-	**CH_2**
6.8-7.4	17H	Multiplet	-	**aromatic**

^{31}P NMR spectrum: 101.2 MHz, solvent C_6D_6

δ (ppm)	Multiplicity	Assignment
24.5	Singlet	Ph_3PCH_2

[6] K. W. Henderson, J. F. Allan and A. R. Kennedy, *J. Chem. Soc., Chem. Commun.*, 1149 (1997).

Elemental Analysis: $C_{68}H_{76}P_2O_2Mg$

	C	H	P	O	Mg
Calculated % by mass	80.7	7.6	6.1	3.2	2.4
Observed % by mass	78.4	8.1	-	-	-

3.2.16 Formation of 24

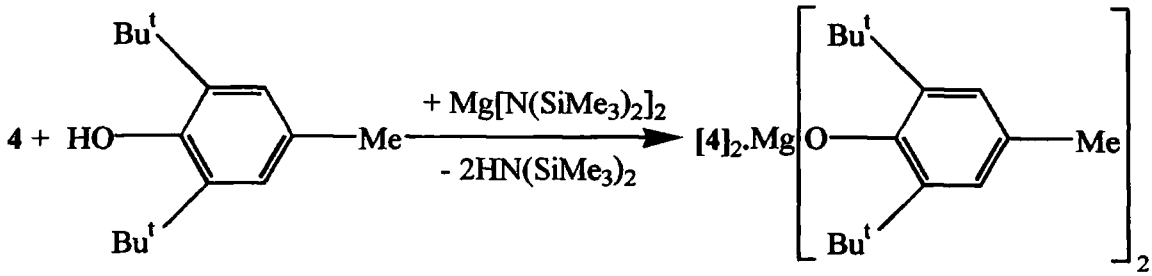

Toluene (20 mL) was added to 2,6-di-tert-4-methylphenol (0.44 g, 2 mmol), **4** (0.56 g, 2 mmol) and magnesium bis[bis(trimethylsilyl)amide][6] (0.2 g, 1 mmol), to give a yellow precipitate. Heating, to approximately 70 °C, together with the addition of a further 35 mL toluene yielded a pale yellow solution. On cooling to ambient temperature a yellow product could be isolated.

Yield: 0.56 g (55 %)

Melting Point: 238-9 °C

^{1}H NMR spectrum: 200 MHz, solvent C_6D_6

δ/ppm	Integral	Multiplicity	Coupling/Hz	Assignment
1.38	1H	Singlet	-	**NH**
1.70	18H	Singlet	-	**^{t}Bu**
2.53	3H	Singlet	-	**Me**
6.8-7.6	17H	Multiplet	-	**aromatic**

^{31}P NMR spectrum: 101.2 MHz, solvent C_6D_6

δ (ppm)	Multiplicity	Assignment
32.5	Singlet	Ph_3PNH

Elemental Analysis: $C_{66}H_{78}N_2P_2O_2Mg$

	C	H	N	P	O	Mg
Calculated % by mass	77.9	7.7	2.8	6.1	3.1	2.4
Observed % by mass	76.4	7.2	2.4	-	-	-

3.3 Synthesis and characterisation of complexes 25-28

3.3.1 Formation of 25

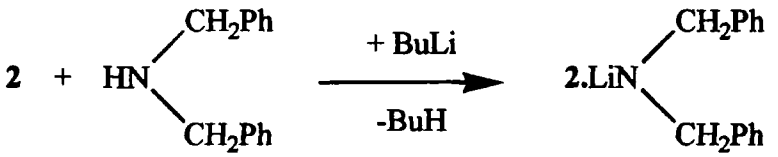

N-butyllithium (1.6 mL, 1.6M solution in hexanes, 2.5 mmol) was added to a cooled (0 °C), stirred solution of **2** (0.73 g, 2.5 mmol) and dibenzylamine† (0.55 mL, 2.5 mmol) in hexane:toluene (1:1, 10 mL). The yellow solution immediately turned deep purple and with further agitation precipitated a red solid. Addition of 15mL toluene, with heating to 70 °C, caused complete dissolution of the solid. After standing at ambient temperature for several hours a crop of dark red/purple crystals was produced.

Yield: 0.9 g (73 %)

Melting Point: 130 °C

^{1}H NMR spectrum: 200 MHz, solvent C_6D_6

δ/ppm	Integral	Multiplicity	Coupling/Hz	Assignment
1.0-1.1	1H	Doublet of quartets	$^3J_{HH} = 6.8$, $^2J_{PH} = 11.2$	Ph_3PCHMe
2.0-2.1	3H	Doublet of doublets	$^3J_{HH} = 6.8$, $^3J_{PH} = 20.4$	Ph_3PCHMe
3.8	4H	Broad singlet	-	$(PhCH_2)_2NLi$
7.0-7.7	25H	Multiplet	-	phenyl

† Dibenzylamine dried over 4A molecular sieves.

^{31}P NMR spectrum: 101.2 MHz, solvent C_6D_6

δ (ppm)	Multiplicity	Assignment
14.3	Singlet	Ph_3PCHMe

Elemental Analysis: $C_{34}H_{33}PNLi$

	C	H	N	P	Li
Calculated % by mass	82.7	6.7	2.8	6.3	1.4
Observed % by mass	81.6	6.7	3.0	-	-

3.3.2 Formation of 26

Dry hexane (5 mL) was added to a mixture of **2** (0.58 g, 2 mmol) and lithium bis(trimethylsilyl)amide (0.34g, 2mmol) under nitrogen. The resulting orange precipitate was dissolved with heating (to 70 °C) and the solution allowed to cool to ambient temperature. After 24 hours, a red and a colourless product had co-crystallised, which were separated and analysed by n.m.r. spectroscopy.

Red Product:

^{1}H NMR spectrum: 200 MHz, solvent C_6D_6

δ/ppm	Integral	Multiplicity	Coupling/Hz	Assignment
1.05-1.24	1H	Doublet of quartets	$^{2}J_{PH}$ = 17.5, $^{3}J_{HH}$ = 6.8	Ph_3PCHMe
2.19-2.36	3H	Doublet of doublets	$^{3}J_{PH}$ = 19.0, $^{3}J_{HH}$ = 6.8	Ph_3PCHMe
7.0-7.2	9H	Multiplet	-	m,p-Ph_3PCHMe
7.7-7.9	6H	Multiplet	-	o-Ph_3PCHMe

^{31}P NMR spectrum: 101.2 MHz, solvent C_6D_6

δ (ppm)	Multiplicity	Assignment
14.9	Singlet	Ph_3PCHMe

Colourless Product:

Melting Point: 103-4 °C

^{1}H NMR spectrum: 200 MHz, solvent C_6D_6

δ/ppm	Integral	Multiplicity	Coupling/Hz	Assignment
0.3	18H	Singlet	-	$LiN(SiMe_3)_2$
1.0	1H	Doublet of quartets	$^{2}J_{PH}$ = 4.1, $^{3}J_{HH}$ = 6.8	Ph_3PCHMe
2.0	3H	Doublet of doublets	$^{3}J_{PH}$ = 21.4, $^{3}J_{HH}$ = 6.8	Ph_3PCHMe
7.1-7.2	9H	Multiplet	-	m,p-Ph_3PCHMe
7.5-7.8	6H	Multiplet	-	o-Ph_3PCHMe

^{31}P NMR spectrum: 101.2 MHz, solvent C_6D_6

δ (ppm)	Multiplicity	Assignment
22.4	Singlet	Ph_3PCHMe

3.3.3 Formation of 27

Dry toluene (5 mL) was added to **2** (0.73 g, 2.5 mmol) and sodium bis(trimethylsilyl)amide (0.45 g, 2.5 mmol). Agitation for 15 min. yielded an orange precipitate, which dissolved in a further 5ml toluene with heating (to 70 °C). On standing at ambient temperature for 48 hours a crop of orange crystals was afforded.

Yield: 0.69 g (58 %)

Melting Point: 177 °C

^{1}H NMR spectrum: 200 MHz, solvent C_6D_6

δ/ppm	Integral	Multiplicity	Coupling/Hz	Assignment
0.2	18H	Singlet	-	$NaN(SiMe_3)_2$
0.95	1H	Doublet	$^{3}J_{HH} = 6.7$,	$Ph_3P{=}C(CH_3)H$
		Of quartets	$^{2}J_{PH} = 13.1$	
2.3	3H	Doublet	$^{3}J_{HH} = 6.8$,	$Ph_3P{=}C(CH_3)H$
		Of doublets	$^{3}J_{PH} = 19.9$	
7.0-7.15	9H	Multiplet	-	m,p **aromatic**
7.6	6H	Multiplet	-	o- **aromatic**

^{31}P NMR spectrum: 101.2 MHz, solvent C_6D_6

δ (ppm)	Multiplicity	Assignment
16.29	Singlet	Ph_3PCHMe

Elemental Analysis: $C_{26}H_{37}PNSi_2Na$

	C	H	N	P	Si	Na
Calculated % by mass	65.9	7.9	3.0	6.5	11.9	4.9
Observed % by mass	64.8	7.8	3.1	-		-

3.3.4 Formation of 28

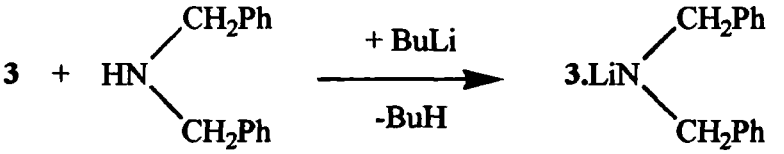

Dry hexane (5 mL) was added to **3** (0.32 g, 2 mmol) and the solution cooled (to approximately 0 °C). Addition of dibenzylamine (0.44 mL, 2 mmol) and *n*-butyllithium (1.28 mL, 1.6M solution in hexanes, 2 mmol) afforded a red precipitate, which dissolved, upon heating, to leave a red/purple solution. On cooling to ambient temperature and standing for several hours, a crop of red crystals was produced.[‡]

Yield: 0.30 g (38%)

[‡] Crystals form a molten flow upon isolation, thereby precluding XRD and m.p. studies.

^{1}H NMR spectrum: 200 MHz, solvent C_6D_6

δ/ppm	Integral	Multiplicity	Coupling/Hz	Assignment
-0.4	2H	Singlet	-	$(Me_2N)_3PCH_2$
2.2	18H	Doublet	$^{3}J_{PH} = 9.8$	$(Me_2N)_3PCH_2$
4.1	4H	Broad singlet	-	$LiN(CH_2Ph)_2$
7.0-7.6	10H	Multiplet	-	$LiN(CH_2Ph)_2$

^{31}P NMR spectrum: 101.2 MHz, solvent C_6D_6

δ (ppm)	Multiplicity	Assignment
75.5	Singlet	$(Me_2N)_3PCH_2$

3.4 Synthesis and characterisation of complexes 29-35

3.4.1 Formation of 29a

$$Ph_3P^{+}-NH_2Br^{-} \xrightarrow[-\ 2^nBuH]{+\ 2^nBuLi,\ tol/thf} (Ph_3P{=}NLi.LiBr.2thf)_2.1.5tol$$

Dry toluene (15 mL) was added to aminotriphenylphosphonium bromide[7] (0.90 g, 2.5 mmol) and the solution cooled (to approximately 0 °C). Addition of *n*-butyllithium (3.2 mL, 1.6M solution in hexanes, 5 mmol) yielded a white precipitate, which upon heating to 70 °C and addition of 2mL thf, gave a yellow solution. On cooling to ambient temperature a crop of transparent blocks was produced.

Yield: 0.58 g (45.0 %)

Melting Point: 166 °C

^{1}H NMR spectrum: 200 MHz, solvent C_6D_6

δ/ppm	Integral	Multiplicity	Assignment
1.2	8H	Quintet	β–thf
2.1	-	Singlet	Tol
3.6	8H	Quintet	α–thf
6.9-7.6	9H	Multiplet	m,p-**aromatic**
7.9-8.0	6H	Multiplet	o-**aromatic**

[7] Prepared by a modification of the literature synthesis: H-J Cristau, J. Kadoura, L. Chiche and E. Toreilles, *Bull. Soc. Chim. Fr.*, 4, 515 (1989).

3.4.2 Formation of 29b

$$Ph_3P^{+}—NH_2Br^{-} \xrightarrow[-\ 2^nBuH]{+\ 2^nBuLi,\ ArH/thf} (Ph_3P{=}NLi.LiBr.2thf)_2.2ArH$$

Dry benzene (15 mL) was added to aminotriphenylphosphonium bromide (2.08 g, 5.8 mol) and the solution cooled (to approximately 0 °C). Addition of *n*-butyllithium (11.6 mL, 1.6M solution in hexanes, 11.6 mmol) yielded a white precipitate, which upon heating to 70 °C and addition of 4mL thf, afforded a yellow solution. On cooling to ambient temperature afforded a crop of transparent blocks formed.

Yield: 2.1 g (72.0 %)

Melting Point: 166 °C

^{1}H NMR spectrum: 200 MHz, solvent C_6D_6

δ/ppm	Integral	Multiplicity	Assignment
1.2-1.3	-	Quintet	β–thf
3.5-3.6	-	Quintet	α–thf
7.2	-	Multiplet	m,p **aromatic**
8.0	-	Multiplet	o-**aromatic**

Elemental Analysis: $C_{26}H_{31}NPO_2Li_2Br$

	C	H	N	P	Li	O	Br
Calculated % by mass	60.7	6.1	2.7	6.0	2.7	6.2	16.0
Observed % by mass	62.2	6.1	2.4	6.4	2.6	-	-

3.4.3 Formation of 29c

$$Ph_3\overset{+}{P}-\overset{-}{N}H_2Cl \xrightarrow[-\ 2^nBuH]{+\ 2^nBuLi,\ ArH/thf} (Ph_3P{=}NLi.LiCl.2thf)_2.2ArH$$

Dry toluene (10 mL) was added to amino(triphenyl)phosphonium chloride[8] (0.38 g, 1.2 mmol) and cooled (to 0 °C). Addition of *n*-butyllithium (1.44 mL, 1.6M solution in hexanes, 5 mmol) yielded a white precipitate, which on heating (to approximately 70 °C) and addition of 0.5mL thf, yielded a yellow solution. Upon cooling to -30 °C for 2 weeks a crop of transparent crystals formed.

Yield: 0.3 g (63.0 %)

Melting Point: 104 °C

^{1}H NMR spectrum: 200 MHz, solvent C_6D_6

δ/ppm	Integral	Multiplicity	Assignment
1.4	8H	Quintet	β–thf
2.1	-	Singlet	Tol
3.5-3.6	8H	Quintet	α–thf
6.9-7.7	15H	Multiplet	**aromatic**

^{31}P NMR spectrum: 101.2 MHz, solvent C_6D_6

δ (ppm)	Multiplicity	Assignment
-4.8	3P	Ph_3PNLi
-1.1	1P	Ph_3PNLi

[8] R. Appel, G. Kohnlein and R. Schollhorn A., *Chem. Ber.*, **98**, 1355 (1965).

3.4.4 Formation of 30

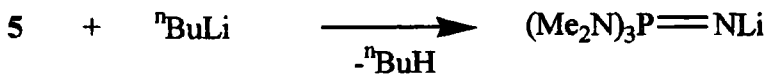

Dry toluene (10 mL) was added to **5** (2.73 mL, 15 mmol) and cooled (to 0 °C). Addition of *n*-butyllithium (9.6 mL, 1.6M solution in hexanes, 15 mmol) gave a white precipitate, complete dissolution was achieved upon addition of a further 60mL toluene, with heating (to 70 °C). After several days, transparent block-like crystals were isolated.

Yield: 1.55 g (56.0 %)

Melting Point: 135 °C

^{1}H NMR spectrum: 200 MHz, solvent C_6D_6

δ/ppm	Multiplicity	Assignment
2.4-2.7	Doublets	Me_2N

^{31}P NMR spectrum: 101.2 MHz, solvent C_6D_6

δ (ppm)	Multiplicity	Assignment
13.2	1P	$(Me_2N)_3PNLi$
17.9	4P	$(Me_2N)_3PNLi$

Elemental Analysis: $C_6H_{18}N_4PLi$

	C	H	N	P	Li
Calculated % by mass	39.2	9.9	30.4	16.8	3.8
Observed % by mass	38.4	9.9	29.9	-	-

3.4.5 Formation of 31

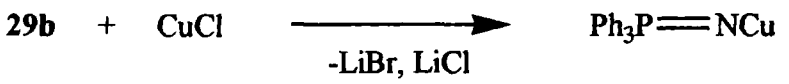

Dry toluene (5 mL) was added to **29b** (1 mmol, 0.513 g) and heated, whereupon lithium bromide precipitated and was filtered after cooling to ambient temperature. The filtrate was cooled to -20 °C, before copper (I) chloride (1 mmol, 0.099 g) was added resulting in a colour change from yellow/brown to bright pink and then yellow. After stirring at room temperature for several hours the solution was filtered cold, at 0 °C. Upon standing at ambient temperature for 72 hours, a crop of green blocks was obtained.

Yield: 0.14 g (41.0 %)

Melting Point: 156 °C

^{1}H NMR spectrum: 200 MHz, solvent C_6D_6

δ/ppm	Integral	Multiplicity	Assignment
2.1	-	Singlet	Tol
6.8-7.1	9H	Multiplet	m,p- **aromatic**
7.8-7.9	6H	Multiplet	o- **aromatic**

^{31}P NMR spectrum: 101.2 MHz, solvent C_6D_6

δ/ppm	Assignment
17.0	Ph_3**P**NCu

Elemental Analysis: $C_{21.5}H_{19}PNCu$

	C	H	N	P	Cu
Calculated % by mass	66.9	5.2	3.4	8.0	16.4
Observed % by mass	66.9	5.0	3.2	-	-

3.4.6 Formation of 32

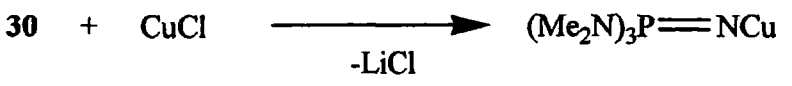

Dry toluene (5 mL) was added to **5** (0.18 mL, 1 mmol) and cooled to 0 °C. Addition of *n*-butyllithium (0.64 mL, 1.6M solution in hexanes, 1 mmol) gave a white precipitate (**30**), which dissolved upon gentle heating. The solution was then cooled to -196 °C and a slight excess of copper (I) chloride added (0.108 g, 1.1 mmol). Upon warming to room temperature and stirring for several hours a yellow solution formed, which was separated from the lithium chloride precipitate by filtration and cooled to -30 °C. After 48 hours a crop of crystals was produced.

Yield: 0.05 g (21.0 %)
Melting Point: 215-6 °C

^{1}H NMR spectrum: 200 MHz, solvent C_6D_6

δ/ppm	Multiplicity	Assignment
2.20-2.65	Multiplet	Me_2N

^{31}P NMR spectrum: 101.2 MHz, solvent C_6D_6

δ/ppm	Assignment
43.4	$(Me_2N)_3PNCu$

Elemental Analysis: $C_6H_{18}N_4PCu$

	C	H	N	P	Cu
Calculated % by mass	29.9	7.5	23.3	12.9	26.4
Observed % by mass	30.4	7.6	23.4	-	-

3.4.7 Formation of 33

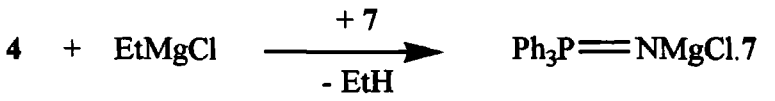

Dry toluene (15 mL) was added to **4** (0.55 g, 2 mmol) and cooled to approximately 0 °C. Addition of ethylmagnesium chloride (1.0 mL, 2M solution in diethylether, 2 mmol) afforded a yellow precipitate, which dissolved on addition of hmpa (0.35 mL, 2 mmol) and heating (to 70 °C). Cooling the solution overnight (5 °C) gave a crop of transparent crystals.

Yield: 0.73 g (71.0 %)

Melting Point: 161-2 °C

^{1}H NMR spectrum: 200 MHz, solvent C_6D_6

δ/ppm	Integral	Multiplicity	Coupling/Hz	Assignment
2.0	18H	Doublet	$^{2}J_{PH} = 9.7$	**Me_2N**
7.2-8.3	15H	Multiplet	-	**aromatic**

^{31}P NMR spectrum: 101.2 MHz, solvent C_6D_6

δ/ppm	Integral	Assignment
2.6	1P	**$(Me_2N)_3PO$**
23.3	1P	**$Ph_3PNMgCl$**

Elemental Analysis: $C_{24}H_{33}N_4P_2OMgCl$

	C	H	N	P	O	Mg	Cl
Calculated % by mass	56.0	6.5	10.9	12.0	3.1	4.7	6.9
Observed % by mass	56.0	6.7	10.6	11.7	-	-	-

3.4.8 Formation of 34

$$5 \quad + \quad MeMgBr \xrightarrow[-\ MeH]{+\ 5} (Me_2N)_3P{=}{=}NMgBr.5$$

Dry toluene (5 mL) was added to 5 (0.36 mL, 2 mmol) and cooled to 0 °C. Addition of methyl magnesium bromide (0.33 mL, 3M solution in diethylether, 1 mmol) afforded a white precipitate, which dissolved upon gentle heating. Storage of the colourless solution at -30 °C for 72 hours yielded a crop of transparent blocks.

Yield: 0.21g (46 %)

Melting Point: 95-6 °C

^{1}H NMR spectrum: 200 MHz, solvent C_6D_6

δ/ppm	Integral	Multiplicity	Coupling/Hz	Assignment
1.3	1H	Singlet	-	$(Me_2N)_3PNH$
2.43	18H	Doublet	$^2J_{PH} = 3.9$	$(Me_2N)_3PNH$
2.87	18H	Doublet	$^2J_{PH} = 3.6$	$(Me_2N)_3PNMgBr$

^{31}P NMR spectrum: 101.2 MHz, solvent C_6D_6

δ/ppm	Integral	Assignment
24.1	1P	$(Me_2N)_3PNMgBr$
45.0	1P	$(Me_2N)_3PNH$

Elemental Analysis: $C_{12}H_{37}N_8P_2MgBr$

	C	H	N	P	Mg	Br
Calculated % by mass	31.4	8.1	24.4	13.5	5.3	17.4
Observed % by mass	32.2	8.7	22.3	15.0	-	-

3.4.9 Formation of 35

$$5 + 1/2\ MgBr_2 \longrightarrow 1/2\ [5]_2.MgBr_2$$

Diethyl ether (10 mL) was added to a solution of anhydrous magnesium bromide (0.092 g, 0.5 mmol) and **5** (0.18 mL, 1 mmol). Agitation for approximately 30min. was followed by reduction of the ether *in vacuo* to dryness. The residue was re-dissolved in toluene (20 mL) and cooled to -30 °C.

Yield: 0.25g (46 %)

Melting Point: 166 °C

^{1}H NMR spectrum: 200 MHz, solvent C_6D_6

δ/ppm	Integral	Multiplicity	Assignment
1.0	2H	Broad singlet	$[(Me_2N)_3PNH]_2{\cdot}MgBr_2$
2.3-2.6	36H	Broad singlet	$[(Me_2N)_3PNH]_2{\cdot}MgBr_2$

^{31}P NMR spectrum: 101.2 MHz, solvent C_6D_6

δ/ppm	Multiplicity	Assignment
46.0	Singlet	$[(Me_2N)_3PNH]_2{\cdot}MgBr_2$

Elemental Analysis: $C_{12}H_{38}N_8P_2MgBr_2$

	C	H	N	P	Mg	Br
Calculated % by mass	26.7	7.1	20.7	11.5	4.5	29.6
Observed % by mass	27.1	7.6	18.1	-	-	-

3.5 Synthesis and characterisation of complexes 36-40

3.5.1 Formation of 36

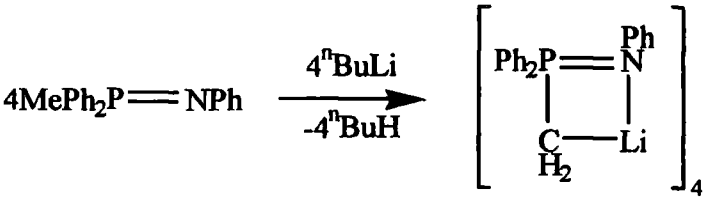

Dry toluene (2mL) was added to a cooled (to approx. 0°C) mixture of $MePh_2PNPh$[9] (0.291g, 1mmol) and *n*-butyllithium (0.64mL, 1mmol, 1.6M solution in hexanes) to yield a white precipitate. Gentle heating aided dissolution to a colourless solution. On cooling to ambient temperature, a crop of transparent blocks was produced.

Yield: 0.18 g (61 %)

Melting Point: 197-8°C

^{1}H NMR spectrum: 200 MHz, solvent C_6D_6

δ/ppm	Integral	Multiplicity	Coupling/Hz	Assignment
0.16	2H	Doublet	$^2J_{PH}$ = 9.8	$Ph_2P(=NPh)CH_2Li$
2.1	-	Singlet	-	tol
6.8-7.8	15H	Multiplet	-	**Aromatic**

^{31}P NMR spectrum: 101.2 MHz, solvent C_6D_6

δ/ppm	Assignment
32.9	$Ph_2P(=NPh)CH_2Li$

[9] $MePh_2PNPh$ prepared by Staudinger reaction and supplied by Prof. López-Ortiz (University of Almeria).

Elemental Analysis: $C_{19}H_{17}NPLi$

	C	H	N	P	Li
Calculated % by mass	76.8	5.8	4.7	10.4	2.3
Observed % by mass	76.8	6.0	4.4	-	-

3.5.2 Formation of 37

$$\{[Ph_2P(=NPh)CH_2(Me)_2PNLi]_3[Ph_2P(=NPh)CH_2Li]\}$$

N-butyllithium (0.64mL, 1mmol, 1.6M solution in hexanes) was added to a cooled (approx. 5°C) solution of $MePh_2PNPh$ (0.291g, 1mmol) in hexane:benzene (2mL:10mL) to yield a white precipitate. Filtration to remove a small amount of precipitate was followed by gentle heating of the solution to give complete dissolution. Upon cooling to ambient temperature a crop of transparent blocks was produced.

^{1}H NMR spectrum: 200 MHz, solvent C_6D_6

δ/ppm	Integral	Multiplicity	Assignment
0.0-1.8	20H	multiplet	Aliphatic CH_2/CH_3
3.5	6H	Singlet	"PCH_2"
6.7-8.0	60H	multiplet	**Aromatic**

^{31}P NMR spectrum: 101.2 MHz, solvent C_6D_6

δ/ppm	Assignment
21.0, 22.3, 23.0	$Ph_2P(=NPh)CH_2P(Me)_2=NPhLi$, $Ph_2P(=NPh)CH_2Li$

3.5.3 Formation of 38

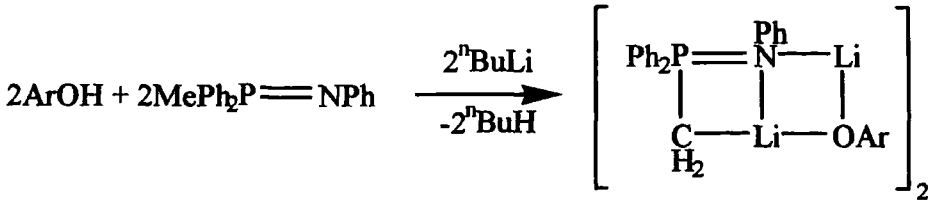

Dry toluene (10mL) was added to a cooled (to approx. 0°C) solution of $MePh_2PNPh$ (0.291g, 1mmol) and 2,6-di-tert-butyl-4-methylphenol (0.220g, 1mmol). Addition of *n*-butyllithium (1.28mL, 2mmol, 1.6M solution in hexanes) afforded a white precipitate. Gentle warming gave a colourless solution and on cooling to ambient temperature a crop of transparent blocks was produced.

Yield: 0.25 g (48 %)

Melting Point: 250-2 °C

^{1}H NMR spectrum: 200 MHz, solvent C_6D_6

δ/ppm	Integral	Multiplicity	Coupling/Hz	Assignment
0.08	2H	Doublet	$^2J_{PH}$ = 13.4	$Ph_2P(=NPh)CH_2Li$
1.68	18H	Singlet	-	$LiOC_6H_2(Me)^tBu_2$
2.39	3H	Singlet	-	$LiOC_6H_2(\mathbf{Me})^tBu_2$
6.5-7.6	17H	Multiplet	-	**aromatic**

^{31}P NMR spectrum: 101.2 MHz, solvent C_6D_6

δ/ppm	Assignment
29.0	$Ph_2P(=NPh)CH_2Li$

Elemental Analysis: $C_{34}H_{40}NPOLi_2$

	C	H	N	P	O	Li
Calculated % by mass	78.0	7.7	2.7	5.9	3.1	2.7
Observed % by mass	79.0	7.7	3.1	-	-	-

3.5.4 Formation of 39

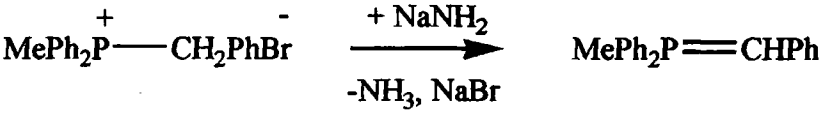

Dry thf (50 mL) was added to benzyl(methyl)diphenylphosphonium bromide[10] (7.4g, 20mmol) and sodium amide (0.975g, 25mmol). Heating to 40 °C was followed by agitation of the mixture for 24 hours at ambient temperature. The resulting orange solution was filtered, thereby removing NaBr and any unreacted $NaNH_2$. Thf was evaporated under reduced pressure to approximately 2mL. Addition of toluene (5 mL), with gentle heating, afforded an orange solution, which on cooling produced a crop of orange crystals.

Yield: 3.8 g (66%)

Melting Point: 113-4°C

^{1}H NMR spectrum: 200 MHz, solvent C_6D_6

δ/ppm	Integral	Multiplicity	Coupling/Hz	Assignment
1.57	3H	doublet	$^2J_{PH} = 12.6$	Ph_2**(Me)**PCHPh
2.8	1H	doublet	$^2J_{PH} = 20.0$	Ph_2(Me)PC**H**Ph
6.8-7.6	15H	multiplet	-	**Ph_2**(Me)PCHPh

[10] Prepared by quarternisation reaction of methyldiphenylphosphine and benzyl bromide in acetonitrile.

^{31}P NMR spectrum: 101.2 MHz, solvent C_6D_6

δ (ppm)	Multiplicity	Assignment
0.3	Singlet	$Ph_2(Me)PCHPh$

Elemental Analysis: $C_{20}H_{19}P$

	C	H	P
Calculated % by mass	82.7	6.6	10.7
Observed % by mass	81.2	6.6	-

3.5.5 Formation of 40

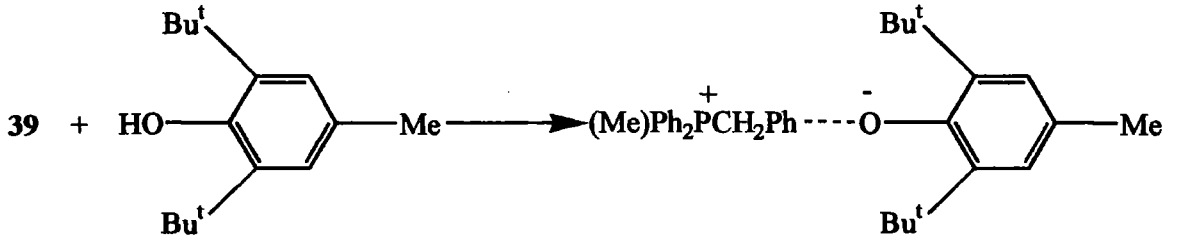

Dry toluene (5mL) was added to a mixture of 2,6-di-tert-butyl-4-methylphenol (0.220g, 1mmol) and **45** (0.290 g, 1mmol). Following agitation of the solution for 15 min. at ambient temperature, a red precipitate formed. Heating, to approximately 70°C, accomplished complete dissolution. Storage of the orange solution at ambient temperature, induced the formation of orange/red crystals.

Yield: 0.3 g (59 %)

Melting Point: 135-6 °C

^{1}H NMR spectrum: 200 MHz, solvent C_6D_6

δ/ppm	Integral	Multiplicity	Assignment
0.0	2H	Singlet	$Ph_2(Me)PCH_2Ph$
1.1	3H	Singlet	$Ph_2(Me)PCH_2Ph$
1.5	18H	Singlet	$C_6H_2Me(^tBu)_2O$
2.3	3H	Singlet	$C_6H_2Me(^tBu)_2O$
6.9-7.9	17H	multiplet	**Aromatic**

^{31}P NMR spectrum: 101.2 MHz, solvent C_6D_6

δ (ppm)	Multiplicity	Assignment
1.1	singlet	$Ph_2(Me)PCH_2Ph$

Elemental Analysis: $C_{35}H_{43}PO$

	C	H	P	O
Calculated % by mass	82.3	8.5	6.1	3.1
Observed % by mass	80.9	8.4	-	-

3.6 Synthesis and characterisation of complexes 41-44

3.6.1 Formation of 41

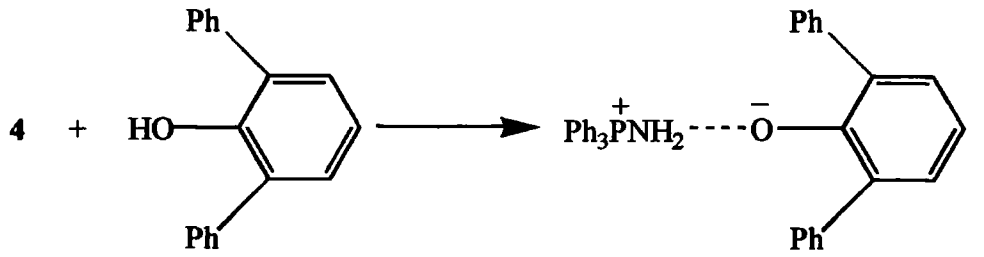

Dry toluene (5 mL) was added to **4** (0.277 g, 1 mmol) and diphenylphenol (0.246 g, 1 mmol) to yield a white precipitate. Complete dissolution was achieved on addition of further toluene (2 mL) and thf (4 mL), with heating. Transparent, colourless crystals formed after 48 hours at ambient temperature.

Yield: 0.31 g (59 %)

Melting Point: 145 °C

^{1}H NMR spectrum: 200 MHz, solvent C_6D_6

δ/ppm	Integral	Multiplicity	Assignment
5.0	2H	Broad singlet	Ph_3PNH_2
6.7-7.6	28H	Multiplet	**aromatic**

^{31}P NMR spectrum: 101.2 MHz, solvent C_6D_6

δ/ppm	Multiplicity	Assignment
21.8	Singlet	Ph_3PNH_2

Elemental Analysis: $C_{36}H_{30}NPO$

	C	H	N	P	O
Calculated % by mass	82.6	5.8	2.7	5.9	3.1
Observed % by mass	82.0	5.7	2.8	-	-

3.6.2 Formation of 42

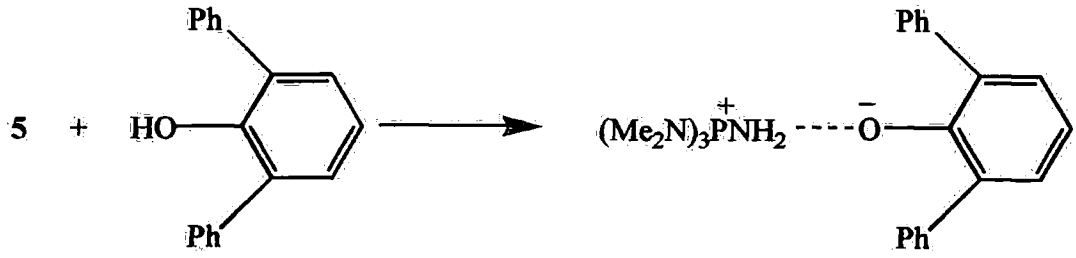

Toluene (3.5 mL) was added to **5** (0.18 mL, 1 mmol) and diphenylphenol (0.246 g, 1 mmol) to give a white precipitate. Addition of further toluene (7 mL), with heating, yielded a green solution and upon cooling to ambient temperature and storing for 24 hours, a crop of transparent, colourless crystals was produced.

Yield: 0.29 g (68 %)

Melting Point: 168 °C

^{1}H NMR spectrum: 200 MHz, solvent C_6D_6

δ/ppm	Integral	Multiplicity	Coupling/Hz	Assignment
2.1	18H	Doublet	$^{3}J_{PH}$ = 7.6	$(\mathbf{Me_2}N)_3PNH_2$
6.3	2H	Singlet	$^{3}J_{HH}$ = 6.3	$(Me_2N)_3P\mathbf{NH_2}$
6.9	1H	Triplet	-	p-$C_6\mathbf{H_3}(Ph)_2O$
7.1-7.4	6H	Multiplet	-	m,p-$C_6H_3(\mathbf{Ph})_2O$
7.4	2H	Doublet	$^{3}J_{HH}$ = 6.3	m-$C_6\mathbf{H_3}(Ph)_2O$
7.9	4H	Doublet	-	o-$C_6H_3(\mathbf{Ph})_2O$

^{31}P NMR spectrum: 101.2 MHz, solvent C_6D_6

δ/ppm	Multiplicity	Assignment
41.6	Singlet	$(Me_2N)_3\mathbf{P}NH_2$

Elemental Analysis: $C_{24}H_{33}N_4PO$

	C	H	N	P	O
Calculated % by mass	67.9	7.8	13.2	7.3	3.8
Observed % by mass	67.9	8.2	13.4	-	-

3.6.3 Formation of 43

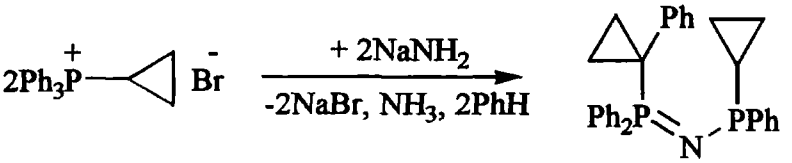

Dry thf (50 mL) was added to cyclopropylphosphonium bromide (10.1 g, 26.4 mmol) and sodium amide (1.1 g, 28.2 mmol). The solution was agitated overnight at ambient temperature, after which time an orange-brown solution had formed with a white precipitate. Filtration of the precipitate, followed by removal of approximately 45 mL of solvent *in vacuo*, gave a slurry. Dissolution of the slurry was achieved on addition of hexane (10 mL) and toluene (10mL), with heating. Crystals were grown at -30 °C after 1 week.

Yield: 2.8 g (46 %)

Melting Point: 144-5 °C

^{1}H NMR spectrum: 400 MHz, solvent C_6D_6

δ/ppm	Integral	Multiplicity	Assignment
0.5	3H	Multiplet	Cyclopropyl
0.6	1H	Multiplet	Cyclopropyl
0.9	2H	Multiplet	Cyclopropyl
1.1	1H	Multiplet	Cyclopropyl
2.1	2H	Multiplet	Cyclopropyl
6.7-8.1	20H	Multiplet	**Aromatic**

^{31}P NMR spectrum: 161.9 MHz, solvent C_6D_6

δ/ppm	Integral	Multiplicity	Coupling/Hz	Assignment
57.8	1P	Doublet	$^{2}J_{PP} = 89$	$\mathbf{P^{V}}$=N
24.3	1P	Doublet	$^{2}J_{PP} = 89$	$\mathbf{P^{III}}$-N

Elemental Analysis: $C_7H_{22}N_4P$

	C	H	N	P
Calculated % by mass	77.4	6.3	3.0	13.3
Observed % by mass	75.2	6.3	2.5	14.0

3.6.4 Formation of 44

$$Ph_2P(=O)Me + (Ph_2PS)_2NH \xrightarrow{^nBuLi} Ph_2P(=O)Me.LiN(SPPh_2)_2$$

N-butyllithium (1.24mL, 2mmol, 1.6M solution in hexanes) was added to a cooled solution of methyldiphenylphosphine oxide (0.43g, 2mmol)[11] and tetraphenyl-dithioimidodiphosphinate (0.45g, 2mmol) $[(Ph_2PS)_2NH]$[12] in toluene (25mL). Gentle heating afforded a colourless solution, which on cooling yielded a crop of transparent blocks **39**, suitable for a single crystal XRD study.

Yield: 1.1 g (82 %)

Melting Point: 285-6 °C

^{1}H NMR spectrum: 200 MHz, solvent C_6D_6

δ/ppm	Integral	Multiplicity	Coupling/Hz	Assignment
1.67	3H	Doublet	$^2J_{PH}$ = 13.4	**MeP(=O)Ph$_2$**
6.9-8.3	30H	Multiplet	-	**aromatic**

[11] Purchased from *Lancaster Synthesis* and used as supplied.

[12] F. T. Wang, *Synth. React. Inorg. Met. Chem.*, **8**, 120 (1978).

^{31}P NMR spectrum: 101.2 MHz, solvent C_6D_6

δ/ppm	Integral	Assignment
39.4	2P	P=S
24.9	1P	P=O

Elemental Analysis: $C_{37}H_{33}NP_3OS_2Li$

	C	H	N	P	O	S	Li
Calculated % by mass	66.2	5.0	2.1	4.6	2.4	9.5	1.0
Observed % by mass	63.9	4.7	2.1	-	-	-	-

4. Discussion: Complexation of s-block metal aryloxides by phosphorus Lewis bases.

The compounds discussed in this section were prepared as described in the experimental section. In all cases the metal aryloxide species was generated *in situ*, using either ^{n}BuLi, ^{n}BuNa, $NaNH_2$ or $Mg[N(SiMe_3)_2]_2$ and a substituted phenol. The phosphorus bases used (**1-8**) are of the general formula, R_3PX, where X = CHR, NR, O or S. These bases have been incorporated in complexes (**9-24**).

Complex	Empirical Formula
9	$Ph_3PCH_2{\cdot}LiOC_6H_2(Me)^tBu_2$
10	$Ph_3PCH_2{\cdot}NaOC_6H_2(Me)^tBu_2$
11	$Ph_3PCHMe{\cdot}LiOC_6H_2(Me)^tBu_2$
12	$(Me_2N)_3PCH_2{\cdot}LiOC_6H_2(Me)^tBu_2$
13	$Ph_3PNH{\cdot}LiOC_6H_2(Me)^tBu_2$
14	$Ph_3PNH{\cdot}NaOC_6H_2(Me)^tBu_2$
15	$(Me_2N)_3PNH{\cdot}LiOC_6H_2(Me)^tBu_2$
16	$(Me_2N)_3PNH{\cdot}LiOC_6H_3(Ph)_2$
17	$(Me_2N)_3PNH{\cdot}NaOC_6H_2(Me)^tBu_2$
18	$(Me_2N)_3PNH{\cdot}NaOC_6H_3(Ph)_2$
19	$Ph_3PO{\cdot}LiOC_6H_2(Me)^tBu_2$
20	$Ph_3PO{\cdot}NaOC_6H_2(Me)^tBu_2$
21	$(Me_2N)_3PO{\cdot}LiOC_6H_3(Ph)_2$
22	$Ph_3PS{\cdot}LiOC_6H_2(Me)^tBu_2$
23	$[Ph_3PCH_2]_2{\cdot}Mg[OC_6H_2(Me)^tBu_2]_2$
24	$[Ph_3PNH]_2{\cdot}Mg[OC_6H_2(Me)^tBu_2]_2$

Table 4.1 Complexes discussed in this chapter

4.1 Background

Phosphorus Lewis bases of type R_3PX, have been widely used in synthetic inorganic,[1] organic[2] and organometallic chemistry.[2] In particular, the use of phosphine oxides R_3PO,[1] has generated families of complexes of the type $R_x^{y-}M_y^{x+}\cdot zL$ (where R^{y-} is an organic anion; M^{x+} is a metal cation; L is a Lewis base), most notably with transition metals.[3] The emergence of their utility in s-block chemistry, mostly as hmpa,[4] has produced a fascinating diversity of structural types, prompting their further investigation.

Since much of this work has focussed on phosphine oxides, limited use has been made of the isoelectronic phosphonium ylides R_3PCH_2, iminophosphoranes R_3PNH and phosphine sulfides R_3PS. This chapter presents a systematic study of the complexation of s-block metal aryloxides by phosphorus Lewis bases of type R_3PX. Firstly, however, it commences with a summary of the structural types that have been found in alkoxy- and aryloxy- s-block metal compounds/complexes.

Considering only complexes of the general type $(RO)^-Li^+\cdot zL$, the observed solid-state (and solution-state) structures can be explained in terms of the Ring Stacking[5] and Ring Laddering[6] Principles proposed and developed by Mulvey, Snaith and Wade in the 1980s. In the case of the uncomplexed alkoxy- and aryloxy- lithiums (i.e. $z = 0$), the degree of aggregation (or association) is largely dependent on the steric demands of the anion substituents (the stereochemistry of the lithium-oxygen fragment being fixed - **Fig. 4.1**). For these types of lithiated organics the organic anion substituents are essentially coplanar with the lithium-anion fragment.

---

[1] W. Setzer and P. von R. Schleyer, *Adv. Organomet. Chem.*, **24**, 353 (1985); C. Shade and P. von R. Schleyer, *Adv. Organomet. Chem.*, **27**, 169 (1987); R. Snaith and D. S. Wright, *'Lithium Chemistry- A Theoretical and Experimental Overview'*, ed. A. M. Sapse, P. von R. Schleyer, Wiley, New York (1995).
[2] A. Loupy and B. Tchoubar, *'Salt Effects in Organic and Organometallic Chemistry'*, VCH, New York (1992).
[3] A. E. Reed and P. von R. Schleyer, *J. Am. Chem. Soc.*, **112**, 1434 (1990).
[4] K. Gregory, P. von R. Schleyer and R. Snaith, *Adv. Inorg. Chem.*, **37**, 47 (1991).
[5] D. R. Armstrong, D. Barr, R. Snaith, W. Clegg, R. E. Mulvey, K. Wade and D. Reed, *J. Chem. Soc., Dalton*, 1071 (1987).

Figure 4.1 Representation of an Alkoxy/aryloxylithium

Rings are not necessarily dimeric - this depends on the size of the anion substituents. Surprisingly, there are no known structures of uncomplexed aryloxylithiums (lithium aryloxides), although a single crystal XRD structure of PhONa (**Fig. 4.2**) has very recently been reported,[7] from which the lithium aryloxide structure can be extrapolated. (Unit-cell dimensions have been reported for PhOLi, but no reasonable solution could be produced from the final data set).[8]

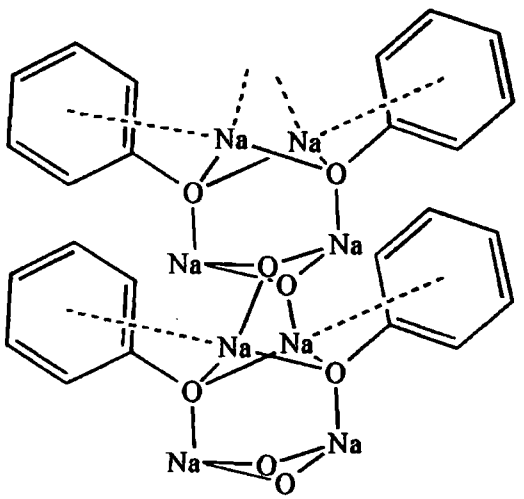

Figure 4.2 Solid-state structure in $(PhONa)_\infty$

Therefore, one might expect the structure of PhOLi to be similar - an infinite stack of Li_2O_2 dimers perpendicular to the Li_2O_2 plane; further aggregation along the plane is prevented by the phenyl substituents of the anion. The polymeric structure that these simple aryloxylithiums (and aryllithiums) form explains why they are difficult to characterise in the solid-state. They are often amorphous and hydrocarbon-insoluble, inhibiting the isolation of pure, crystalline materials.[9]

---

[6] D. R. Armstrong, D. Barr, W. Clegg, R. E. Mulvey, D. Reed, R. Snaith and K. Wade, *J. Chem. Soc., Chem. Commun.*, 869 (1986).
[7] M. Kunert, E. Dinjus, M. Nauck and J. Sieler, *Chem. Ber.*, **130**, 1461 (1997).
[8] R. E. Dinnbier, M. Pnik, J. Sieler and P. W. Stephens, *Inorg. Chem.*, **36**, 3398 (1997).

On addition of a simple Lewis base, however, deaggregation occurs. In the case of thf, for example, the structure is hexameric (**Fig. 4.3**), $[PhOLi{\cdot}thf]_6$.[10]

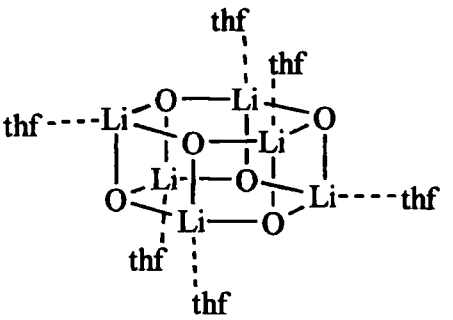

Figure 4.3 Hexameric unit of $[PhOLi{\cdot}thf]_6$ (phenyl groups omitted for clarity).

If we now consider the solid-state structure of lithium 2,6-di-tert-butyl,4-methylphenoxide (a compound that is the building block for many of the complexes to be discussed later), then there are several possibilities (**Fig. 4.4**), but unfortunately no single crystal XRD structural determination has yet been possible.

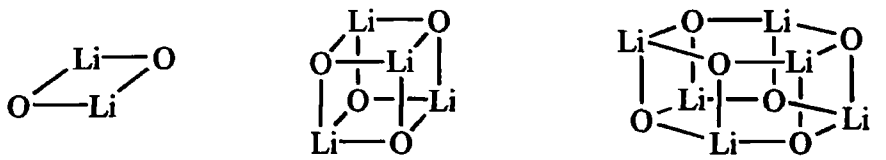

(a) **(b)** **(c)**

Figure 4.4 Schematic showing three possible aggregation states of $C_6H_2(Bu^t)_2MeOLi$

The lithium aryloxide may form solely a dimeric fragment (**Fig. 4.4a**), although this is unlikely since lithium will only be two coordinate and, hence, coordinatively unsaturated. Alternatively, aggregation could occur to give a tetramer (**Fig. 4.4b**), or even a hexamer (**Fig. 4.4c** - conceptually derived from an original trimeric unit which is unknown as a structural type, except in lithium amides).[9]

---

[9] R. E. Mulvey, *Chem. Soc. Rev.*, **20**, 167 (1991).
[10] L. M. Jackman, D. Cizmeciyan, P. G. Williard and M. A. Nichols, *J. Am. Chem. Soc.*, **115**, 6262 (1993).

Whatever its exact identity, the uncomplexed aggregate is easily deaggregated, indeed it is this feature that makes it such a useful complex for the reactions discussed later in the chapter. For example, synthesis of the lithium aryloxide with diethylether (a monodentate ligand), yields a dimeric structure in which each lithium is coordinated by one molecule of diethylether (**Fig. 4.5**).[11] The analogous thf complex is also now known.†

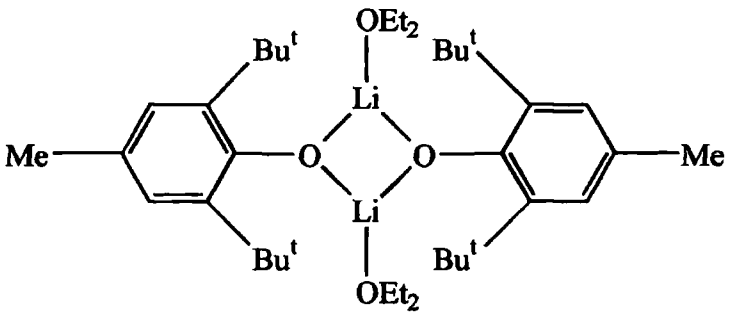

Figure 4.5 Dimeric structure of $C_6H_2(Bu^t)_2MeOLi{\cdot}OEt_2$

Bidentate and tridentate Lewis bases are able to cause further deaggregation of alkoxy/aryloxyllithiums. Therefore, it could be envisaged in some cases that 'intercepted' ladders or stacks could be formed [c.f. group 1 metal amides],[9,12] although none have been reported to date.

Although there are far fewer examples of other alkali (and alkaline-earth) metal alkoxides and aryloxides,[13] these have been shown to exhibit many of the same general features and follow similar structural principles to their lithium analogues. Thus, we can compare the structures of their complexes to those of lithium on this basis. For example, a dimeric magnesium complex, with bridging phenoxide and terminal diethylether and bromide ligands, has been structurally characterised [**Fig. 4.6**].[13d]

---

[11] B. Cetinkaya, I. Gumrukcu, M. F. Lappert, J. L. Atwood and R. Shakir, *J. Am. Chem. Soc.*, **102**, 2086 (1980).

† See Appendix A - compound 45.

[12] R. E. Mulvey, *Chem. Soc. Rev.*, **27**, 339 (1998).

[13] See for example: *(a)* S. R. Drake, W. E. Streib, M. H. Chisholm and K. G. Caulton, *Inorg. Chem.*, **29**, 2707 (1990); *(b)* K. G. Caulton, M. H. Chisholm, S. R. Drake, K. Folting and J. C. Huffman, *Inorg. Chem.*, **32**, 816 (1993); *(c)* K. G. Caulton, M. H. Chisholm, S. R. Drake, K. Folting, J. C. Huffman and W. E. Streib, *Inorg. Chem.*, **32**, 1970 (1993); *(d)* G. Bocelli, A. Cantoni, G. Sartori, R. Maggi and F. Bigi, *Chem. Eur. J.*, **3**, 1269 (1997).

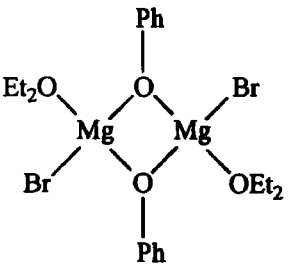

Figure 4.6 A magnesium aryloxide

4.2 Structural features of ligands 1-8

The solid-state structures of the eight starting ligands **1-8** have all been determined by single-crystal XRD studies.[14,15,16,17,18,19,20,21] A brief treatise of their relevant structural parameters will precede a discussion of the structure and properties of some of their s-block metal aryloxide complexes **9-24**.

Ligand **1** exhibits the classic structural features of an unstabilised phosphonium ylide, as discussed in the introduction (**Chapter 1**).[14] The ylidic carbon deviates from planarity, i.e. the methylene protons are bent out of the plane, whilst the phosphonium centre is pyramidalised [sum of angles around phosphorus = 341 °]. The P-C_{ylidic} bond distance [1.693 Å (ave.)] is also in the range of known phosphonium ylides.[22] The existence of a unique C_{ipso}-P-C_{ylidic} bond, that is both elongated and has a wider C_{ipso}-P-C_{ylidic} angle in comparison to the other two bonds, was explained in the introduction (**page 4**) and is situated perpendicular to the methylene plane. **1** has been observed to aggregate through

---

[14] H. Schmidbaur, J. Jeong, A. Schier, W. Graf, D. L. Wilkinson, G. Muller and C. Krüger, *New. J. Chem.*, **13**, 341 (1989).
[15] M. G. Davidson, *Unpublished results.*
[16] N. W. Mitzel, B. A. Smart, K-H. Dreihaupl, D. W. H. Rankin and H. Schmidbaur, *J. Am. Chem. Soc.*, **118**, 12673 (1996).
[17] M. G. Davidson, A. E. Goeta, J. A. K. Howard, C. W. Lehmann, G. M. McIntyre and R. D. Price, *J. Organomet. Chem.*, **550**, 449 (1998).
[18] N. W. Mitzel, *Personal Communication.*
[19] G. Bandoli, G. Bartolozzo, D. A. Clemente, U. Croatto and C. Panattoni, *J. Chem. Soc. A*, 2778 (1970); G. Ruban and V. Zabel, *Cryst. Struc. Commun.*, **5**, 671 (1976); A. L. Spek, *Acta Crystallogr.* **C43**, 1233 (1987).
[20] N. W. Mitzel, *Personal Communication.*
[21] P. W. Codding and K. A. Kerr, *Acta Crystallogr.*, **C34**, 3785 (1978); C. Foces-Foces and A. L. Llamas-Saiz, *ibid.*, **C54**, cif access (1998).

C-H...π interactions, unlike the C-H...C interactions proposed for triphenylphosphonium benzylide,[23] which forms dimeric aggregates, although a thorough examination of such interactions is beyond the scope of this work.

Ligand Number	Empirical Formula
1	Ph_3PCH_2
2	Ph_3PCHMe
3	$(Me_2N)_3PCH_2$
4	Ph_3PNH
5	$(Me_2N)_3PNH$
6	Ph_3PO
7	$(Me_2N)_3PO$
8	Ph_3PS

Table 4.2 Ligands 1-8 used to prepare complexes 9-24

Ylide **2** shows largely analogous structural features to **1** in the solid state.[15] The P-C_{ylidic} bond length [1.661(6) Å] is slightly abbreviated in comparison and the ylidic carbon similarly non-planar. However, one difference is the presence of three unique phenyl substituent groups [P-C_{ipso}: 1.794(4) to 1.847(5) Å; C_{ipso}-P-C_{ylidic}: 106.4(2) to 114.3(3) °]. This is in contrast to the general structural behaviour of phosphonium ylides that was discussed in the introduction (*vide supra*). The basis for this deviation is unclear and may be a result of crystal packing distortions, or simply a manifestation of the supramolecular ordering of the structure through C-H...C and C-H...π interactions.

The solid-state structure of **3**, a liquid at ambient temperature, has recently highlighted some fundamental characteristics of these structural types.[16] The parent phosphine, $P(NMe_2)_3$, was shown by single crystal XRD and *ab initio* MO calculations to have a local C_s symmetry around phosphorus, rather than an idealised C_3 (**Fig. 4.7**).

---

[22] D. G. Gilheany, *Chem. Rev.*, **94**, 1339 (1994) and references cited therein.
[23] A. S. Batsanov, M.G. Davidson, J. A. K. Howard, S. Lamb and C. Lustig, *J. Chem. Soc., Chem. Commun.*, 1791 (1996).

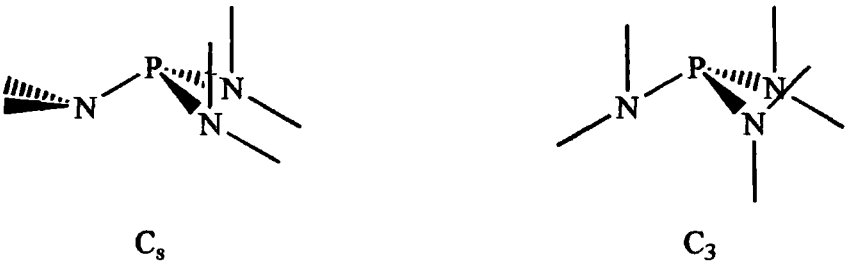

C_s C_3

Figure 4.7 C_s and C_3 symmetry for $P(NMe_2)_3$

The local symmetry around phosphorus in **3** is also C_s, i.e. there are two planar, vertical dimethylamino groups [ave. sum of angles = 353 °] and one pyramidal, horizontal dimethylamino group [sum of angles = 337 °]. The reasons for C_s symmetry are not yet fully understood - it may be attributable to electronic effects. The other structural parameters in **3** are fairly unremarkable [P-C_{ylidic} 1.655(6) Å; sum of angles around phosphorus = 342 °]. It has been suggested[16] that the PCH_2 unit is planar, although the positions of the protons are not well determined. Such planarity would be in disagreement with most other unstabilised phosphonium ylide structures containing a pyramidalised ylide carbanion (**Chapter 1**).

Iminophosphorane **4** was subject to a single crystal X-ray and neutron diffraction study[17] in order to locate precisely the position of the proton on nitrogen. It also contains a pyramidalised phosphonium centre [C_{ipso}-P-N: 109.1(1) to 115.6(1) °] and has a P-N_{iminic} bond length [1.582(2) Å] in the range for previously reported iminophosphoranes.[24] The P-N_{iminic}-H bond angle [115.0(2) °] is smaller than seen in $Ph_3PN(p\text{-}BrC_6H_4)$ and Ph_3PNPh [124.2(6) and 130.4(3) ° respectively].[24] This may be due to reduced steric demands, or indicative of the pyramidalisation of the iminic nitrogen, such as was seen in the phosphonium ylide structures **1** to **3**. There is also the existence of N-H...N bridges and C-H...N contacts, the latter of which form layers of molecules parallel to the bc-plane (**Fig. 4.8**).

---

[24] M. J. E. Hewlins, *J. Chem. Soc. B*, 942 (1971); E. Bohm, K. Dehnicke, J. Beck, W.Hiller, J. Strahler, A. Maurer and D. Fenske, *Z. Natursforsch*, **43B**, 138 (1988).

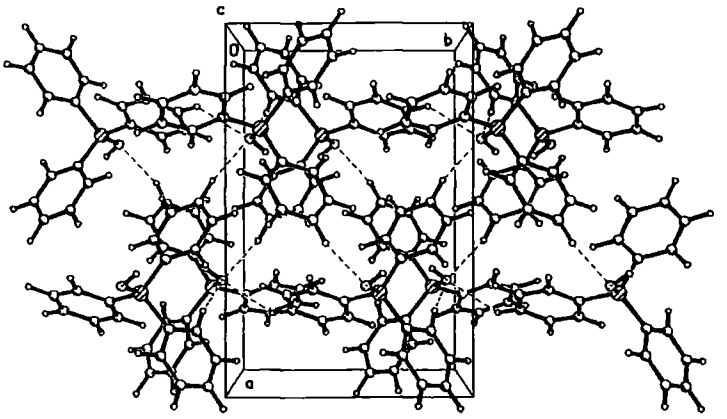

Figure 4.8 C-H...N interactions in 4

Considering **5**,[18] the P-N_{iminic} bond length is similarly in the expected range [1.557(1) Å] and, as for the isoelectronic ylide **3**, there is local C_s symmetry around phosphorus, [sum of angles around pyramidal dimethylamino group = 344 °]. The phosphonium centre is also pyramidalised [sum of angles around phosphorus = 341 °].

There are three known polymorphs of triphenylphosphine oxide **6**,[19] that have slightly differing structural parameters. The average P-O distance is 1.494 Å, the orthorhombic polymorph contains a unique P-C_{ipso} bond and there is a pyramidalised phosphonium centre.

Phosphine oxide **7**, hmpa, displays many of the same features as **5** and **3**,[20] the directly related isoelectronic ylide and iminophosphorane ligands. There is a local C_s symmetry [sum of angles around pyramidal dimethylamino group = 347 °] around the phosphorus, which is also pyramidalised, with the deviation from C_3 being slightly less in this case. The P-O distance [1.477(1) Å] is similar to that found for **6**, as one would expect.

Ligand **8** (a phosphine sulfide) has an unremarkable structure,[21] with a pyramidalised phosphonium centre [sum of angles around phosphorus = 339 °]. The P-S bond length [1.950 Å] is in the range of known phosphine sulfide lengths.[25]

The decrease in P-X bond length (**Table 4.3**) across the isoelectronic series of R_3PX compounds from X = BH_3 to O can be attributed to a number of factors: a decrease in covalent radius, an increase in electronegativity (and possible increased amount of electrostatic shortening) and an increase in multiple bonding. The relative contribution of each factor is not definite, however. The increase in the P-X length on going from X = O to S, is due to the increase in covalent radius, although a reduced amount of multiple bonding may also be a factor.[26]

R_3PX	X = BH_3	X = CH_2	X = NH	X = O	X = S
R = Ph	1.917[27]	1.693 - **1**	1.582 - **4**	1.494 - **6**	1.950 - **8**
R = Me_2N	1.913[28]	1.655 - **3**	1.557 - **5**	1.477 - **7**	1.954[29]

Table 4.3 P-X bond lengths for various neutral P(V) Lewis bases

4.3 NMR data of complexes 9 to 24

All complexes were analysed by ^{31}P and ^{1}H nmr spectroscopy (using d^6-benzene as solvent) and, where possible, single crystal XRD studies. The ^{31}P nmr chemical shift (a singlet in all the complexes discussed in this chapter) is the simplest method for detecting complexation. Below is shown (**Table 4.4**) a ^{31}P nmr shift comparison between the parent, uncoordinated compounds **1-8**, and their derived complexes **9-24**.

---

[25] T. S. Cameron, K. D. Howlett, R. A. Shaw and M. Woods, *Phosphorus*, **3**, 71 (1973); W. Dreissig and K. Pleith, *Acta Cryst.*, **B28**, 3478 (1972); W. Dreissig, K. Pleith and P. Zaske, *Acta Cryst.*, **A27**, 368 (1972).
[26] J. A. Dobado, H. Martinez-Garcia, J. M. Molina and M. R. Sundberg, *J. Am. Chem. Soc.*, **120**, 8461 (1998); D. B. Chesnut, *J. Am. Chem. Soc.*, **120**, 10505 (1998).
[27] J. C. Huffman, W. A. Skupinski and K. G. Caulton, *Cryst. Struct. Commun.*, **11**, 1435 (1982).
[28] N. W. Mitzel, *Personal Communication*.

Complex	Formula	^{31}P chemical shift (δ/ppm.)	
		Complex	Ligand
9	$Ph_3PCH_2{\cdot}LiOC_6H_2(Me)^tBu_2$	30.6	20.7 **(1)**
10	$Ph_3PCH_2{\cdot}NaOC_6H_2(Me)^tBu_2$	30.6	20.7 **(1)**
11	$Ph_3PCHMe{\cdot}LiOC_6H_2(Me)^tBu_2$	27.4	14.6 **(2)**
12	$(Me_2N)_3PCH_2{\cdot}LiOC_6H_2(Me)^tBu_2$	79.0	71.3 **(3)**
13	$Ph_3PNH{\cdot}LiOC_6H_2(Me)^tBu_2$	29.0	17.5 **(4)**
14	$Ph_3PNH{\cdot}NaOC_6H_2(Me)^tBu_2$	21.5	17.5 **(4)**
15	$(Me_2N)_3PNH{\cdot}LiOC_6H_2(Me)^tBu_2$	50.0	40.0 **(5)**
16	$(Me_2N)_3PNH{\cdot}LiOC_6H_3(Ph)_2$	44.8	40.0 **(5)**
17	$(Me_2N)_3PNH{\cdot}NaOC_6H_2(Me)^tBu_2$	45.3	40.0 **(5)**
18	$(Me_2N)_3PNH{\cdot}NaOC_6H_3(Ph)_2$	44.0	40.0 **(5)**
19	$Ph_3PO{\cdot}LiOC_6H_2(Me)^tBu_2$	31.8	25.9**(6)**
20	$Ph_3PO{\cdot}NaOC_6H_2(Me)^tBu_2$	31.8	25.9 **(6)**
21	$(Me_2N)_3PO{\cdot}LiOC_6H_3(Ph)_2$	24.1	25.3 **(7)**
22	$Ph_3PS{\cdot}LiOC_6H_2(Me)^tBu_2$	44.1	43.8 **(8)**
23	$[Ph_3PCH_2]_2{\cdot}Mg[OC_6H_2(Me)^tBu_2]_2$	24.5	20.7 **(1)**
24	$[Ph_3PNH]_2{\cdot}Mg[OC_6H_2(Me)^tBu_2]_2$	32.5	17.5 **(2)**

Table 4.4 NMR data for ligands 1-8 and complexes 9-24

It can be clearly seen in the vast majority of cases[‡] that there is a shift to higher frequency (i.e. the ^{31}P chemical shift is higher) on forming a complex in which the ligand behaves as a neutral Lewis base donor. In simple terms this can be explained by the deshielding of phosphorus as electron density is drawn from the P-X bond to the electropositive metal centre.

[29] M. D. Rudd, S. V. Lindeman and S. Husebye, *Acta Chem. Scand.*, **50**, 759 (1996)

[‡] With one notable exception being the hmpa complex **21**.

4.4 Structural discussion of complexes 9-27

Reaction of ^{n}BuLi with a toluene solution containing 2,6-di-tert-butyl-4-methylphenol and triphenylphosphonium methylide **1** affords a yellow precipitate, which dissolves upon heating. From the resulting solution a crop of yellow crystals **9** could be isolated. **9** is the first example of a phosphonium ylide s-block metal aryloxide complex and is dimeric in the solid state. It can be considered as a model-intermediate for Wittig reactions involving lithiated phosphonium ylides.[30,31] One possible mechanism for this is shown below **(Scheme 4.1)**.

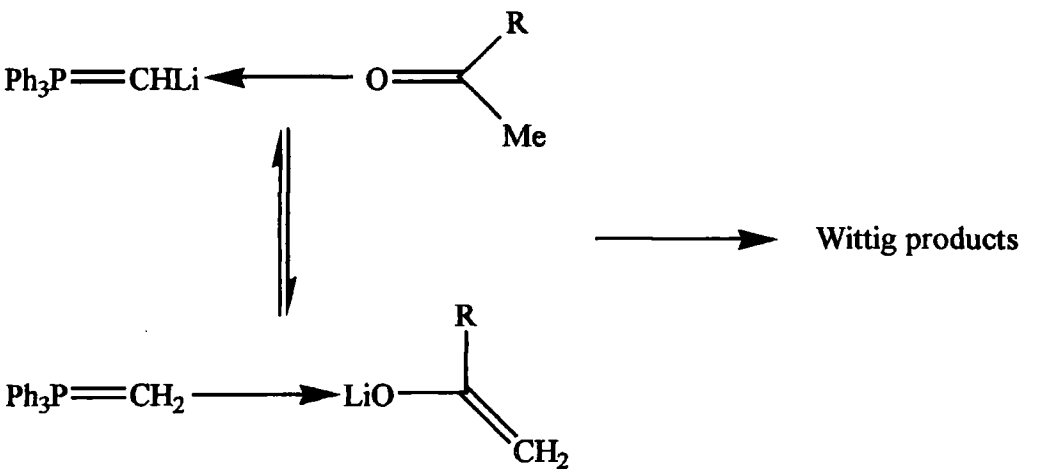

Scheme 4.1 Schematic of Wittig reaction with lithiated-ylide

Initially, the carbonyl compound complexes the lithiated ylide. Enolisation follows, resulting in a phosphonium ylide-complexed lithium enolate. This species is similar to **9**, in that it contains a phosphonium ylide Lewis base moiety and a lithium alkoxide species.

---

[30] E. J. Corey and J. Kang, *J. Am. Chem. Soc.*, **104**, 4724, (1982); E. J. Corey, J. Kang and K. Kyler, *Tet. Lett.*, **26**, 555 (1985).

[31] B. Schaub, T. Jenny and M. Schlosser, *Tet. Lett.*, **25**, 4097 (1984); B. Schaub and M. Schlosser, *ibid.*, **26**, 1623 (1985).

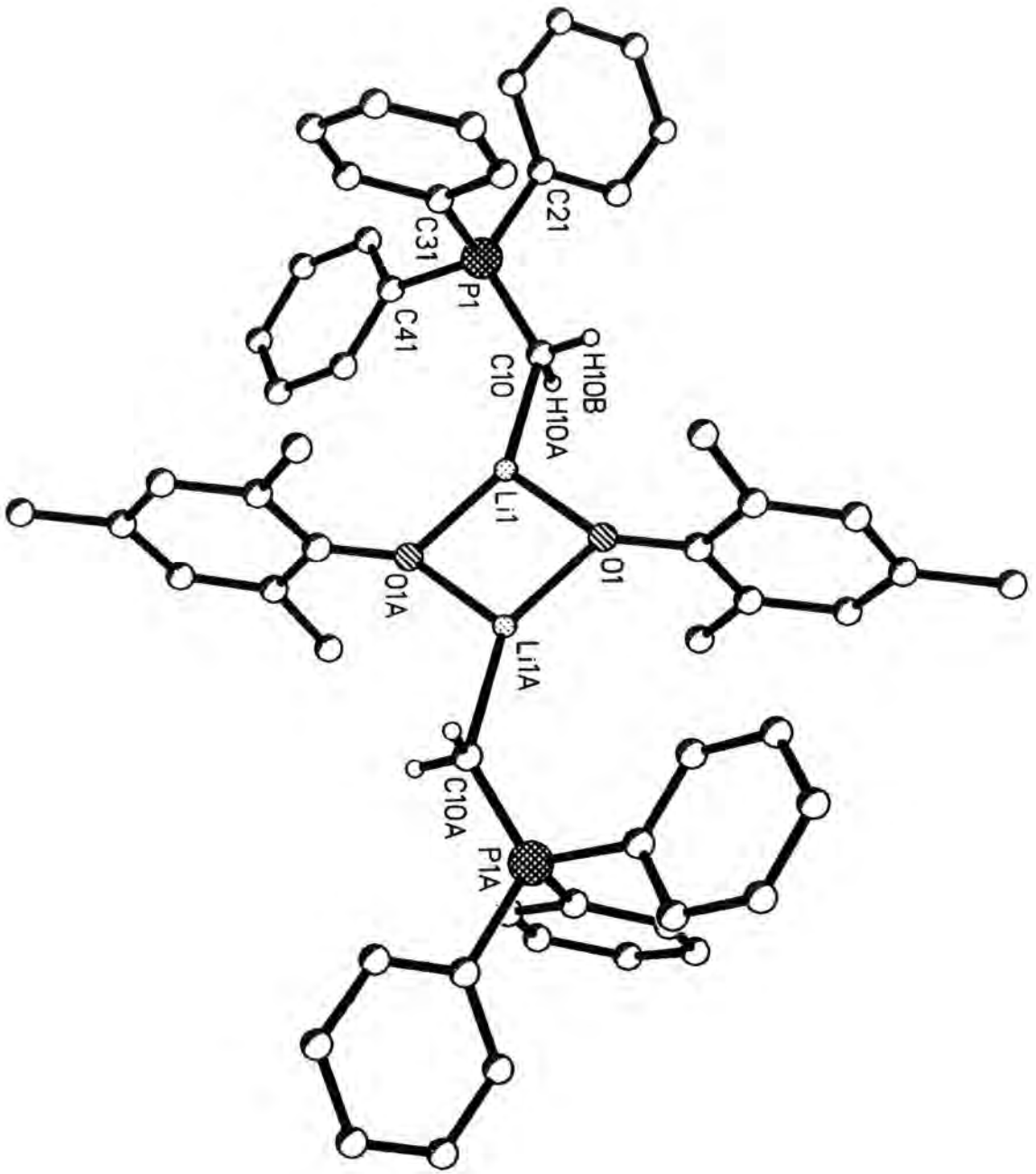

Figure 4.9 Single crystal XRD structure of 9 (methyl group of tert-butyl groups omitted for clarity)

The solid-state structure of **9** (**Fig. 4.9**) contains an unremarkable Li_2O_2 core [Li(1)-O(1) 1.887(4), Li(1)-O(1a) 1.910(4) Å; Li(1)-O(1)-Li(1a) 84.14(17), O(1)-Li(1)-O(1a) 95.86(17) °].[32]

However, the completion of the lithium coordination sphere by two neutral triphenylphosphonium methylide units, results in a short Li-C_{ylidic} bond length indicative of the high Li-C bond strength in **9** [Li(1)-C(10) 2.213(4) Å].[1] The short Li-C bond length was also a feature of the only previously isolated and structurally characterised phosphonium ylide-lithium complex [Li-C 2.207(4) Å].[33] Despite this remarkably short Li-C distance, there is little change in the P-C_{ylidic} bond distance upon complexation [P(1)-C(10) 1.715(2) Å] when compared to the parent ylide [average P-C 1.693 Å - **Table 4.3**].[14]

That there is little disruption of the ylidic bond length and, therefore, the ylidic bonding is not particularly surprising. As was discussed in the introduction on phosphonium ylides, they can be considered as pyramidalised cationic phosphonium centres with a large degree of electronic delocalisation.[14] Coupling this to the evidence concerning Li-C bonding,[34] which even the most conservative models estimate to be at least 70% ionic in nature (and more realistically 80%), then the interaction here between lithium and the ylidic carbon is essentially an ionic bond (**Fig. 4.10**). This model explains both the short approach of lithium to the ylidic carbon and the lack of disruption in the ylidic bonding.

$$Ph_3\overset{+}{P}-\overset{-}{C}H_2\overset{+}{Li}$$

Figure 4.10 Ionic Li-C_{ylidic} interaction

The local geometry around phosphorus is also little affected by complexation to lithium: deviations from an "idealised" C_{3v} symmetry have also been previously observed.[14,35] There

---

[32] J. C. Huffman, R. L. Geerts and K. G. Caulton, *J. Crystallogr. Spectro. Res.*, **14**, 541 (1984).
[33] D. R. Armstrong, M. G. Davidson and D. Moncrieff, *Angew. Chem., Int. Ed. Engl.*, **34**, 478 (1995).
[34] A. E. Reed, R. B. Weinstock and F. Weinhold, *J. Chem. Phys.*, **83**, 735 (1985).
[35] A. S. Batsanov, P. D. Bolton, R. C. B. Copley, M. G. Davidson, J. A. K. Howard, C. Lustig and R. D. Price, *J. Organomet. Chem.*, **550**, 445 (1998).

is, however, a unique P-C_{ipso} bond (**Fig. 4.11**) perpendicular to the methylene plane. This bond [P(1)-C(21)] is both elongated and has a wider C_{ipso}-P-C bond angle [P(1)-C(21) 1.828(2), P(1)-C(31) 1.810(2), P(1)-C(41) 1.812(2) Å; C(10)-P(1)-C(21) 118.23(12), C(10)-P(1)-C(31) 111.40(12), C(10)-P(1)-C(41) 108.74(12) °] in comparison to the other two. This was a feature of many of the parent ligands discussed earlier (**Section 4.2**) and is now considered a general structural feature in unstabilised phosphonium ylides.[14,15,22]

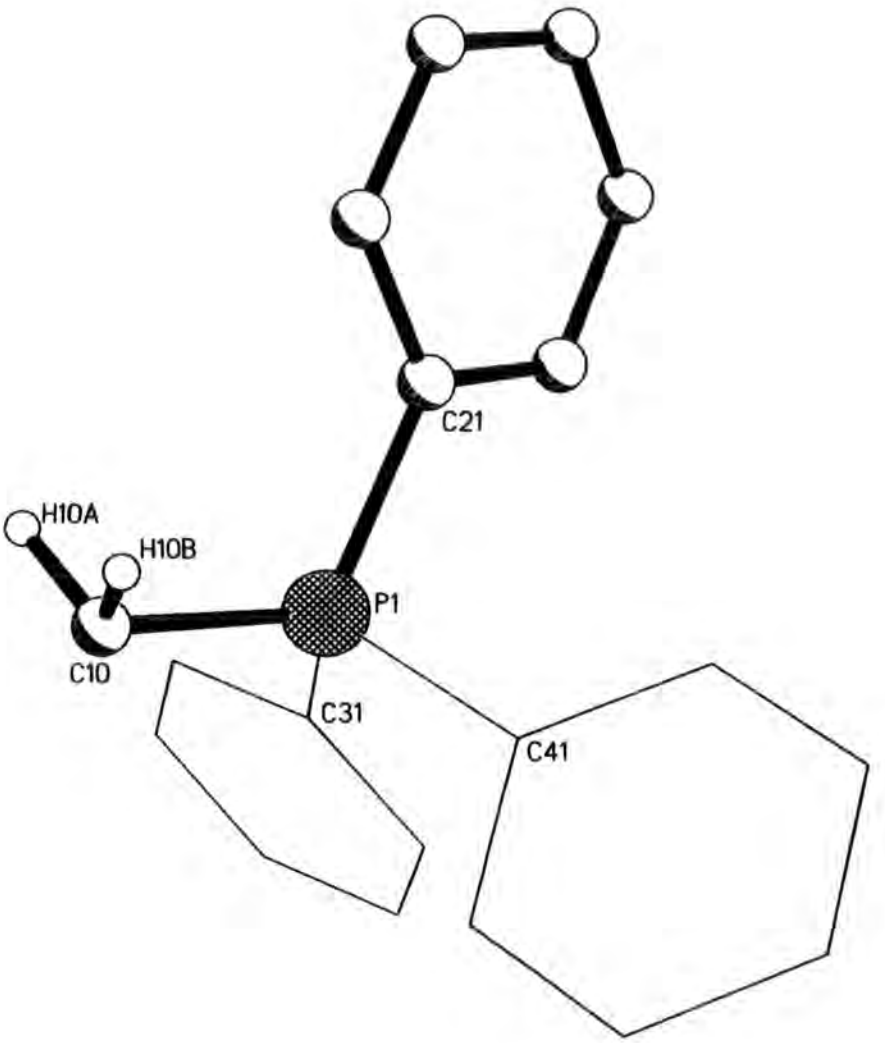

Figure 4.11 Unique P-C_{ipso} bond perpendicular to CH_2 plane

Whilst **9** is the first example of an s-block metal aryloxide-phosphonium ylide complex, there are five related examples of s-block metals interacting with phosphonium ylides.[34,36,37,38,39] One is a dioxane coordinated-lithium bis-ylide compound (**Fig. 4.12**).[36]

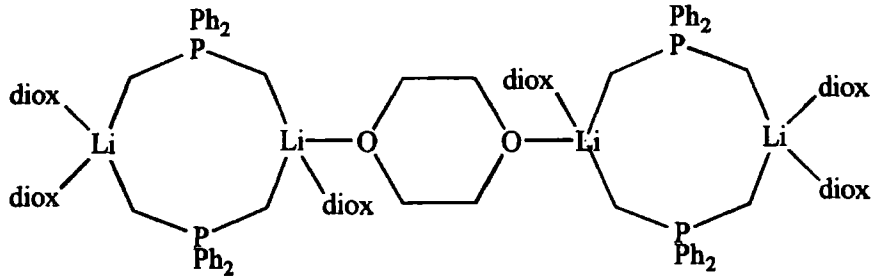

Figure 4.12 Structure of $Ph_2P(CH_2)_2Li(diox)_2$

The example shown below contains a delocalised aromatic system, with a potassium counter-ion (**Fig. 4.13**).[37] A bis(bisphosphoniumbenzylide) barium structure is also now known.[38]

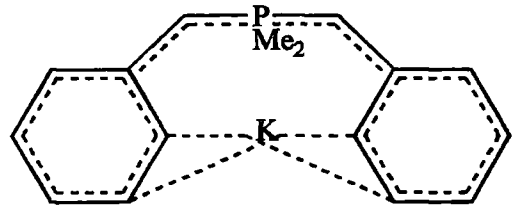

Figure 4.13 Structure of $Me_2P(CHPh)_2K$

The remaining two are a magnesium-uranium complex serendipitously crystallised in an nmr tube[39] and a triphenylphosphonium methylide-lithium dibenzylamide complex.[33] The latter two are the only previous examples in which the ylidic species behave as neutral Lewis bases.

---

[36] R. E. Cramer, M. A. Bruck and J. W. Gilje, *Organometallics*, **5**, 1496 (1986).
[37] H. Schmidbaur, U. Deschler, B. Milewski-Mahria and B. Zimmer-Gasser, *Chem. Ber.*, **114**, 612 (1981).
[38] S. Harder and M. Lutz, *Organometallics*, **16**, 225 (1997).
[39] R. E. Cramer, M. A. Bruck and J. W. Gilje, *Organometallics*, **7**, 1465 (1988).

Reaction of ^{n}BuNa[40] with a toluene solution containing 2,6-di-tert-butyl-4-methylphenol and triphenylphosphonium methylide **1** affords a yellow precipitate, which dissolves upon heating. On cooling to ambient temperature crystals of **10** could be isolated. **10** is the sodium analogue of **9** and displays many of the same features in the solid-state. This is the first sodium aryloxide-phosphonium ylide complex to be structurally characterised and is dimeric, with a Na_2O_2 core. In this case it is the coordination sphere of sodium that is completed by the neutral phosphonium ylide Lewis base.

Complex **10** is isostructural with its lithium analogue **9**, having a P-C_{ylidic} bond distance slightly more elongated than in **9** [P(1)-C(8) 1.703(1) Å] (**Table 4.3**), but similarly is essentially unchanged due to the ionic nature of the interaction (c.f. **Fig. 4.10**). The Na_2O_2 core is, again, fairly unremarkable [Na(1)-O(1) 2.244(1), Na(1)-O(1a) 2.200 Å; Na(1)-O(1)-Na(1a) 88.32(4), O(1)-Na(1)-O(1a) 91.68(4) °],[7,41] with a transoid arrangement of ylide fragments (**Fig. 4.14**). The Na-C bond [2.489(2) Å] is at the lower end of known sodium organometallic bonds,[42] indicative of a strong sodium-ylide interaction. There is a unique P-C_{ipso} bond [P(1)-C(10) 1.825(1), P(1)-C(20) 1.810(1), P(1)-C(30) 1.810(1) Å; C(8)-P(1)-C(10) 118.3(3), C(8)-P(1)-C(20) 108.3(3), C(8)-P(1)-C(10) 110.8(3) °], a feature also noted in **9** and a pyramidalised phosphonium centre.

---

[40] ^{n}BuNa synthesised from ^{n}BuLi and NaOBu^{t} in hexanes. Personal communication - *K. W. Henderson.*

[41] I. Cragg-Hine, M. G. Davidson, O. Kocian, T. Kottke, F. S. Mair, R. Snaith and J. F. Stoddart, *J. Chem. Soc., Chem. Commun.*, 1355 (1993).

[42] See for example: R. den Besten, M. T. Lakin, N. Veldman, A. L. Spek and L. Brandsma, *J. Organomet. Chem.*, **514**, 191 (1996); V. Jordan, U. Behrens, F. Olbrich and E. Weiss, *ibid.*, **517**, 81 (1996); H. Viebrock, U. Behrens and E. Weiss, *Chem. Ber.*, **127**, 1399 (1994).

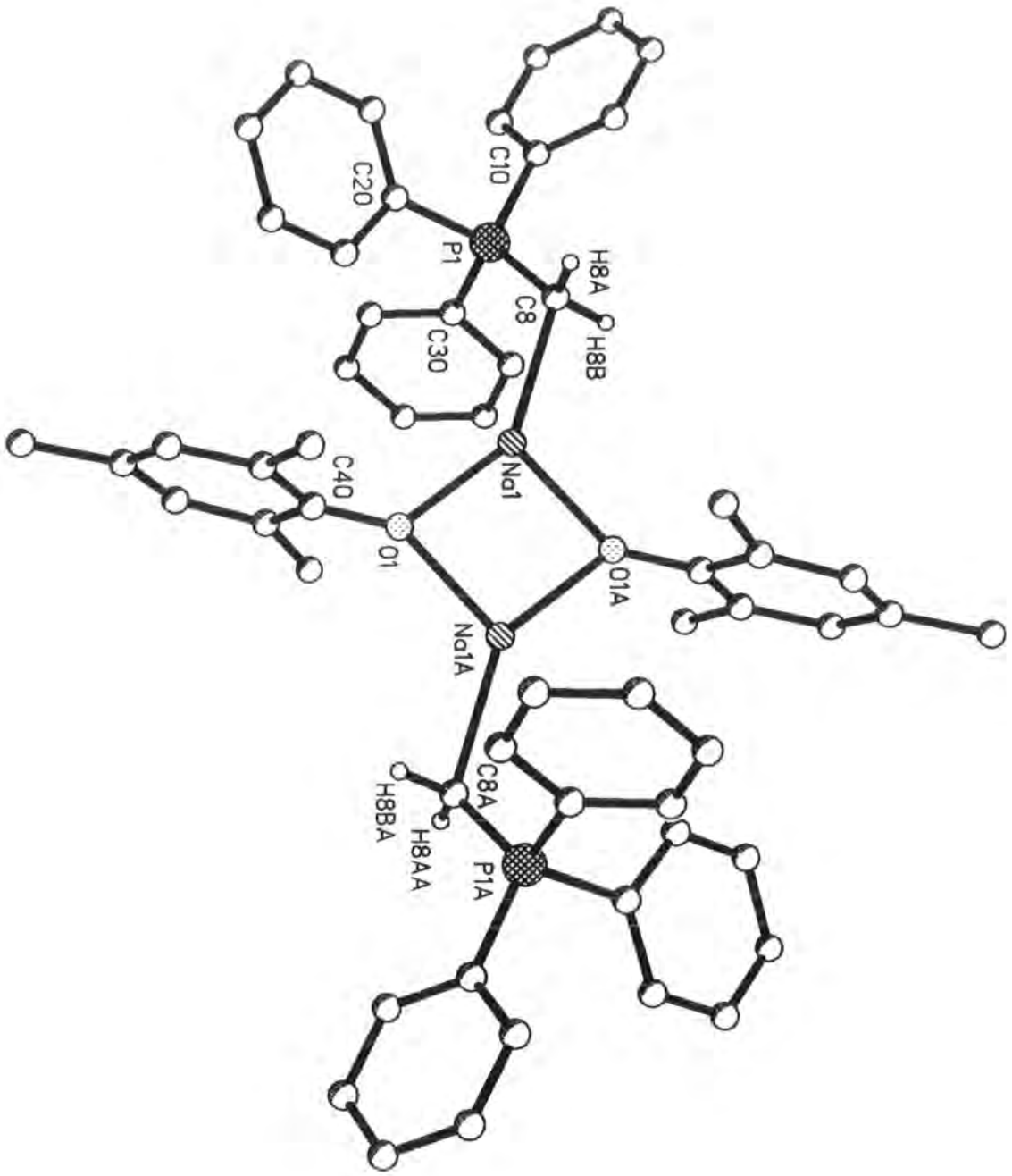

Figure 4.14 Single crystal XRD structure of 10 (methyl group of tert-butyl groups omitted for clarity)

In order to assess the effect of substitution at the ylidic carbon, **11** was synthesised. It is a further example of a phosphonium ylide-lithium aryloxide complex, namely triphenylphosphonium ethylide **2** coordinated to lithium 2,6-di-tert-butyl-4-methylphenoxide. The structure is analogous to **9**, in that it is dimeric and contains a Li_2O_2 core. There is also a transoid arrangement of ylide units across the bridge (most clearly seen with the β-ethyl ylidic carbon atoms). This compound is likewise a model-intermediate in Wittig reactions involving lithiated ylides,[30,31] as well as a useful reagent for studying the effects of lithium salts on the stereochemical outcome in Wittig transformations (**Chapter 5**).[43]

At the molecular level (**Fig. 4.15**) the core follows the same trend as **9** and **10**, being slightly unsymmetrical and having Li-O bond distances and angles of a similar magnitude [Li(1)-O(1) 1.866(3), Li(1)-O(1a) 1.909(3) Å; Li(1)-O(1)-Li(1a) 83.88(14), O(1)-Li(1)-O(1a) 96.12(14) °]. The P-C_{ylidic} distance [1.720(2) Å] is little changed upon complexation from the structure of the ethylide **2** (1.661 Å),[15] which is due to the essentially ionic nature of the interaction (**Fig. 4.10**). The Li-C_{ylidic} [Li(1)-C(1) 2.227(3) Å] is very close to the previously determined Li-C_{ylidic} interactions.[33] Whether the basis for this lengthening (and, therefore, weakening) of the Li-C bond is a steric or electronic factor (or a combination) is unclear, but it is noteworthy that complexes of **2** are not as readily accessible as for **1** (c.f. complex **26** - **Chapter 5**, which co-crystallises with the ligand **2**).

There is a unique phenyl group, perpendicular to the ethylene plane, which has both an elongated P-C_{ipso} bond and a more obtuse C_{ylide}-P-C_{ipso} angle [P(1)-C(11) 1.816(2), P(1)-C(21) 1.812(2), P(1)-C(31) 1.828(2) Å; C(1)-P(1)-C(11) 113.98(9), C(1)-P(1)-C(21) 111.72(9), C(1)-P(1)-C(31) 114.72(9) °]. This feature can be attributed to a pyramidalisation of the phosphonium centre (sum of angles around P(1) = 340 °).[14] The unique bond is slightly more pronounced for **11** than in the parent ligand **2**.

---

[43] A. W. Johnson with special contributions by W. C. Kaska, K. A. O. Starzewski and D. A. Dixon, *'Ylides and Imines of Phosphorus'*, John Wiley & Sons Inc., New York (1993).

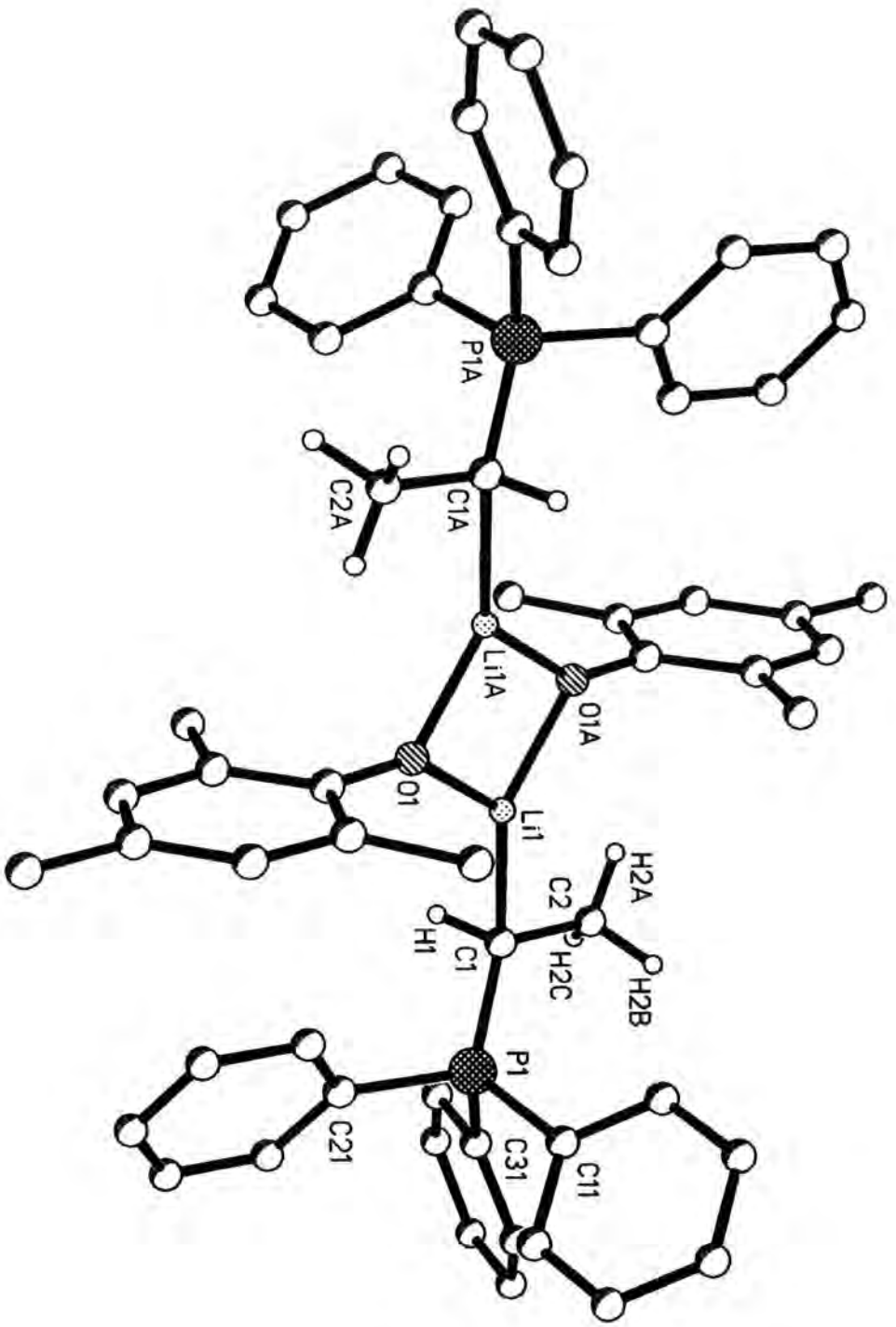

Figure 4.15 Single crystal XRD structure of 11 (methyl group of tert-butyl groups omitted for clarity)

Complex **12** is an example of tris(dimethylamino)phosphonium methylide behaving as a P(V) Lewis base. It is analogous to **9** and **11**, but with **3** as the neutral ylide-Lewis base. Many of the same structural features persist in this case, i.e. a dimeric structure with an Li_2O_2 core (**Fig. 4.16**). There is a cisoid arrangement of ylide units across the bridging core (**Fig. 4.17**), unlike previous cases **9** and **11** (with Ph_3P moieties). The CH_2 groups rotate, such that they are situated approximately perpendicular to each other. The P-C_{ylidic} bond lengths [P(2)-C(37) 1.698(2), P(1)-C(44) 1.700(2) Å] are similarly little changed (**Table 4.3**), upon complexation from the XRD and electron diffraction (ED) determined distances for **3**.[16] Li-C_{ylidic} distances are somewhat shorter than previous examples, being 2.187(3) and 2.174(3) Å, respectively.[33] Whether or not this reflects a stronger interaction between the negatively-charged ylide canonical form (**Fig. 4.10**) and the cationic lithium centre is not clear. It may be attributable to reduced steric demands, especially in comparison with **11**, or a greater degree of inductive pull by the dimethylamino compared to phenyl groups, thereby increasing the negative charge on the ylidic carbon.

The unique dimethylamino group (**Fig. 4.18**) is pyramidalised (sum of angles = 342 °) and even more pronounced in this instance than in previous examples: P(2)-N(1) 1.658(2), P(2)-N(2) 1.688(2), P(2)-N(3) 1.645(2) Å; C(37)-P(2)-N(1) 110.1(2), C(37)-P(2)-N(2) 119.9(1), C(37)-P(2)-N(3) 109.8(2) °, the difference in the bond parameters (N-P length and N-P-C angle) here being considerably larger than seen for the phenyl cases (C_{ipso}-P length and C_{ipso}-P-C angle). This implies a greater contribution from the ylide lone pair to phosphorus (σ^* orbital) than in the phenyl-substituted ylide complexes. The ylidic carbon atom is clearly non-planar [sum of angles = 324 °], which is a large deviation from the parent ligand in which the carbon is planar.

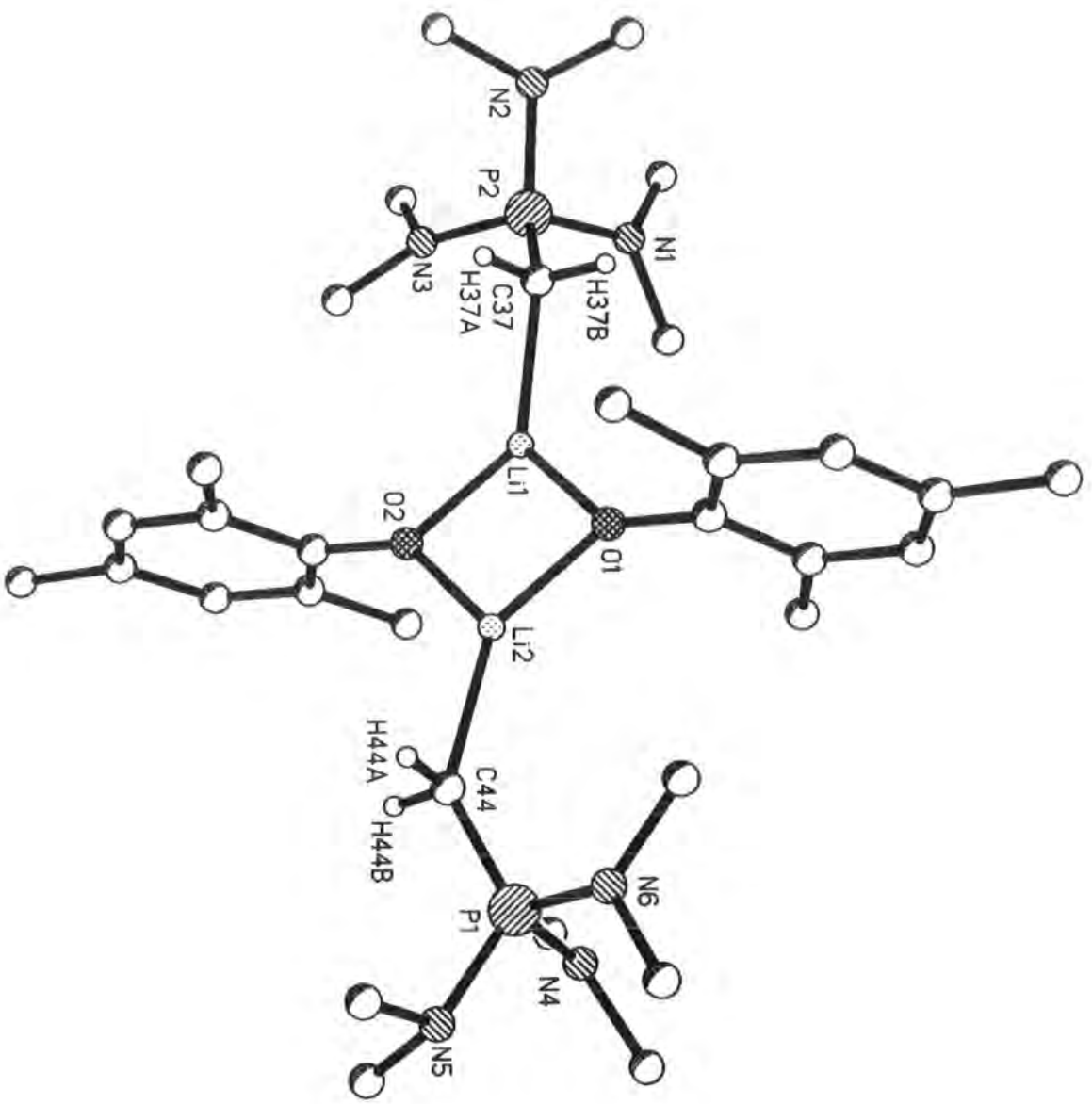

Figure 4.16 Single crystal XRD structure of 12 (methyl group of tert-butyl groups omitted for clarity)

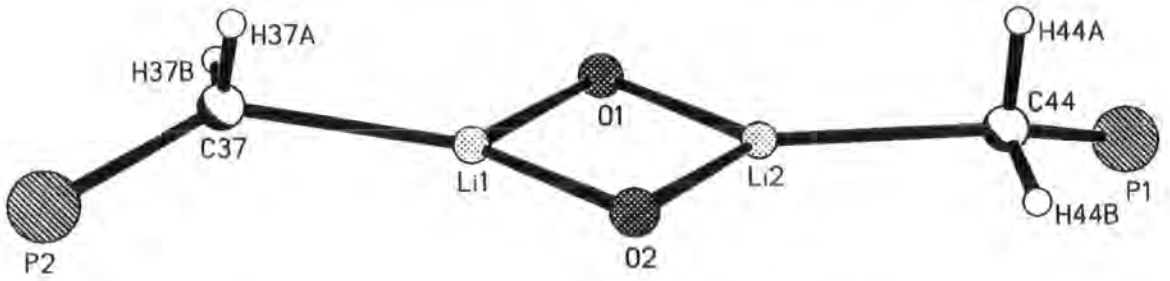

Figure 4.17 Cisoid arrangement of ylide units in 12
(oxygen substituents omitted for clarity)

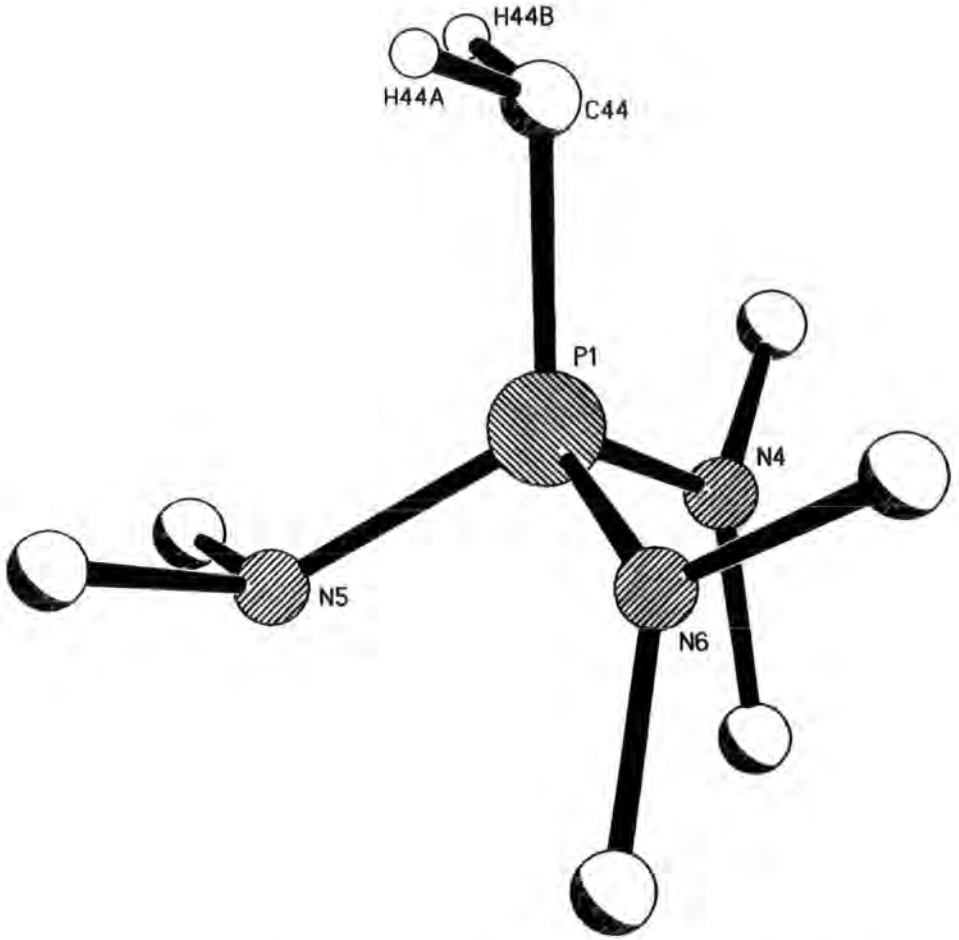

Figure 4.18 Unique P-NMe_2 bond [N(5)] perpendicular to CH_2 plane

There are only two previously isolated and structurally characterised transition (or main-group) metal derivatives of **3**,[44,45] in comparison to the vast number that have been reported for **1**, especially of transition metals.[46] Both are complexes of **3** with titanium, one containing bridging ylidic carbon atoms,[44] the other bridging chlorines (**Fig. 4.19**).[45]

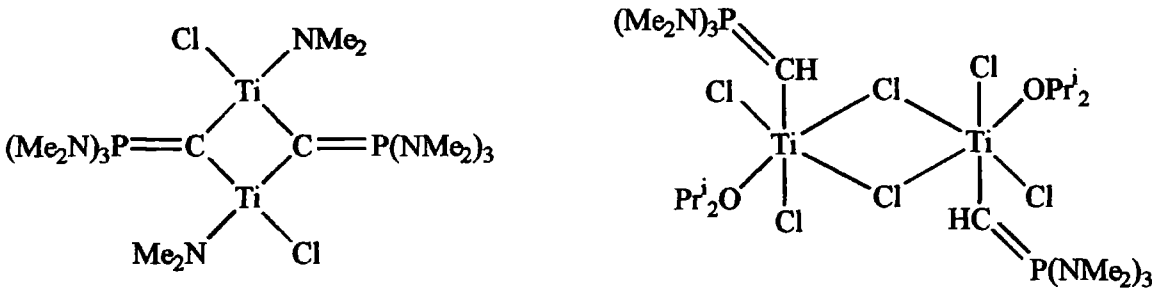

Figure 4.19 Titanium complexes of 3

Moving along the isoelectronic series from phosphonium ylides to iminophosphoranes an analogous strategy can be employed. Reaction of ^{n}BuLi with a toluene solution of **4** and 2,6-di-tert-butyl-4-methylphenol yields a colourless solution from which crystals of **13** can be isolated. A single crystal XRD study (**Fig. 4.22**) revealed the structure to be isostructural with **9** and **11.** This is the first simple example of an iminophosphorane behaving as a neutral Lewis base to an s-block metal, although it has been shown to interact in such a manner with transition metals.[47,48]

The P-N bond length [1.578(2)Å] is little changed upon coordination from that of the parent iminophosphorane (**Table 4.3**).[17] This is a feature of all of the complexes discussed so far and can be explained once more in terms of electrostatics (**Fig. 4.20**).[34] The P-N-H angle [109(2)°] is more acute than in the parent ligand **5** [115.0(2)°], but caution must be exercised when discussing XRD determined hydrogen positions.

---

[44] K. A. Reynolds and M. G. Finn, *J. Org. Chem.*, **62**, 2574 (1997).
[45] K. A. Hughes, P. G. Dopico, M. Sabat and M. G. Finn, *Angew. Chem., Int. Ed. Engl.*, **32**, 554 (1993).
[46] O. O. Kolodiazhnyl, *Tetrahedron*, **52**, 1855 (1996).
[47] M. Grün, F. Weller and K. Dehnicke, *Z. Anorg. Allg. Chem.*, **623**, 224 (1997).
[48] W. Kolitsch and K. Dehnicke, *Z. Natursforsch*, **25b**, 1080 (1970).

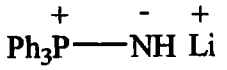

Figure 4.20 Ionic Li-N interaction in 13

Whilst the O-Li bond lengths are fairly typical of lithium aryloxides [Li(1)-O(1) 1.890(4) Å, Li(1)-O(1a) 1.893(4) Å],[32] the N-Li distance [Li(1)-N(1) 1.982(4) Å] is shorter than generally seen for the common bridging mode found for lithium amides.[49] However, it does compare well with N-Li bond lengths for other terminal lithium amides. For example, $[Li(12\text{-crown-4})N(SiMe_3)_2]$[50] and $[Li(12\text{-crown-4})NPh_2]$[51] have respective N-Li distances of 1.965(4) Å and 2.007(5) Å. Mixed-metal complexes $[Co(N_2)(PPh_3)_3]Li(Et_2O)_3$ and $[Co(N_2)(PPh_3)_3]Li(thf)_3$ are also in this range, the respective N-Li distances being 1.96(4) Å and 2.06(9) Å.[52]

Whilst $LiNPPh_3$ was first reported by Schmidbaur et al. in 1967 (but not isolated)[53] and Ph_3PNPh can be o-lithiated (but only detected by trapping experiments),[54] previously observed lithium-iminophosphorane structures all exhibit intramolecular coordination, i.e. lithiation at either nitrogen or carbon atoms α to phosphorus substituents. Comparably, the N-Li distances for $[LiCH_2PMe_2NSiMe_3]_4$ and $[LiCMe_2P(^iPr)_2NSiMe_3]_2$ (intramolecular iminophosphorane N-Li coordination - **Fig. 4.21a**) are 2.03Å (ave.) and 1.928(6)Å.[55] There are three other known examples of lithium-iminophosphorane complexes that have been isolated, viz. $[LiCH_2PPh_2NPh].2thf$ (**Fig. 4.21a**),[56] $[LiNSiMe_3PPh_2NSiMe_3].2thf$ (**Fig. 4.21b**)[57] and $[Li(C_6H_4PPh_2NSiMe_3)_2.LiOEt_2]$ (**Fig. 4.21c**),[58] respectively.

---

[49] M. F. Lappert, P. P. Power, A. R. Sanger and R. C. Sryvastava, *'Metal and Metalloid Amines'*, Ellis Horwood-John Wiley: Chichester (1980).
[50] P. P. Power and X. Xu, *J. Chem. Soc., Chem. Commun.*, 358 (1984).
[51] R. A. Bartlett, H. V. Raiska Dias, H. Hope, B. D. Murray, M. M. Olmstead and P. P. Power, *J. Am. Chem. Soc.*, **106**, 6921 (1986).
[52] A. Yamamoto, Y. Miura, T. Ito, H-L. Chen., K. Iri, F. Ozawa, K. Miki, T. Sei, N. Tanaka and N. Kasai, *Organometallics*, **2**, 1429 (1983).
[53] H. Schmidbaur and G. Jonas, *Chem. Ber.*, **100**, 1120 (1967).
[54] C. G. Stuckwisch, *J. Org. Chem.*, **41**, 1173 (1976).
[55] A. Müller, B. Neumüller and K. Dehnicke, *Chem. Ber.*, 253 (1996).
[56] F. López-Ortiz, E. Peláez-Arango, B. Tejerina, E. Pérez-Carreño and S. García-Granda, *J. Am. Chem. Soc.*, **117**, 9972 (1995).
[57] A. Steiner and D. Stalke, *Inorg. Chem.*, **32**, 1977 (1993).
[58] A. Steiner and D. Stalke, *Angew. Chem., Int. Ed. Engl.*, **34**, 1752 (1995).

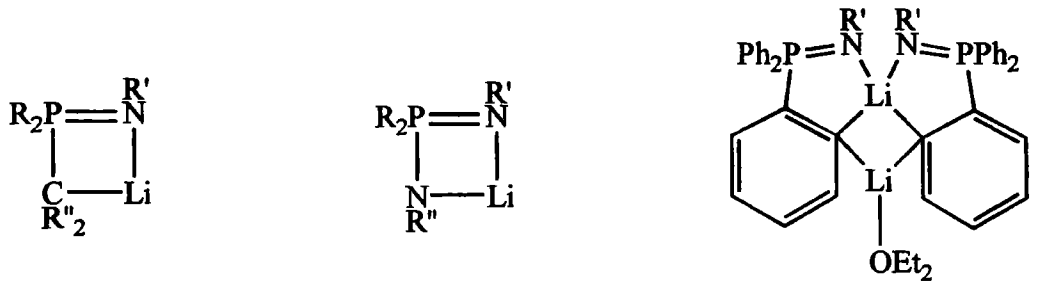

(a) (b) (c)

Figure 4.21 Intramolecular coordination in other lithium-iminophosphoranes

Reaction of ^{n}BuNa with a toluene solution of **4** and 2,6-di-tert-butyl-4-methylphenol yields a white precipitate **14**, which dissolves upon heating and on cooling affords a crop of transparent blocks. **14** is the first example of an iminophosphorane behaving as a simple Lewis base donor to sodium (**Fig. 4.23**), although there is, similarly to **13**, a case of intramolecular N-Na coordination, viz. $[Na(thf)_6]^+[\{Ph_2PNSiMe_3)_2\}_2Na]^-\cdot thf$.[57]

Complex **14** is the iminophosphorane analogue of ylide complex **10** and the sodium equivalent of **13**. The structural motif displayed in the previous structures also forms the basis of the solid-state arrangement of **14**. The Na-N_{iminic} distance, 2.307(2) Å, is at the lower end of known sodium amide bond lengths,[9,59] which once more reflects the strength of this ionic interaction and the P-N bond length, 1.581(2) Å, which itself is virtually unaffected upon complexation (**Table 4.3**).

The unique P-C_{ipso} bond in **14** is unusual in that it is abbreviated and has a smaller C_{ipso}-P-C_{ylidic} angle in comparison to the other two [P(1)-C(21) 1.822(2), P(1)-C(31) 1.809(2), P(1)-C(41) Å 1.821(2); N(1)-P(1)-C(21) 115.0(1), N(1)-P(1)-C(31) 106.6(1), N(1)-P(1)-C(41) 116.2(1) °]. This may be due to a reduction in electron density in the phosphorus σ^* orbital (see pages 4-7) compared to both the parent iminophosphorane and other related complexes. The phosphonium centre is also more pyramidalised than in previous examples: sum of angles around P(1) = 338 °.

---

[59] See for example: W. Clegg, K. W. Henderson, L. Horsburgh, F. M. Mackenzie and R. E. Mulvey, *Chem. Eur. J.*, **4**, 53 (1998); M. Driess, H. Pritzkow, M. Skipinski and U. Winkler, *Organometallics*, **16**, 5108 (1997); P. C. Andrews, N. D. R. Barnett, R. E. Mulvey, W. Clegg, P. A. O'Neill, D. Barr, L. Cowton, A. J. Dawson and B. J. Wakefield, *J. Organomet. Chem.*, **518**, 85 (1996).

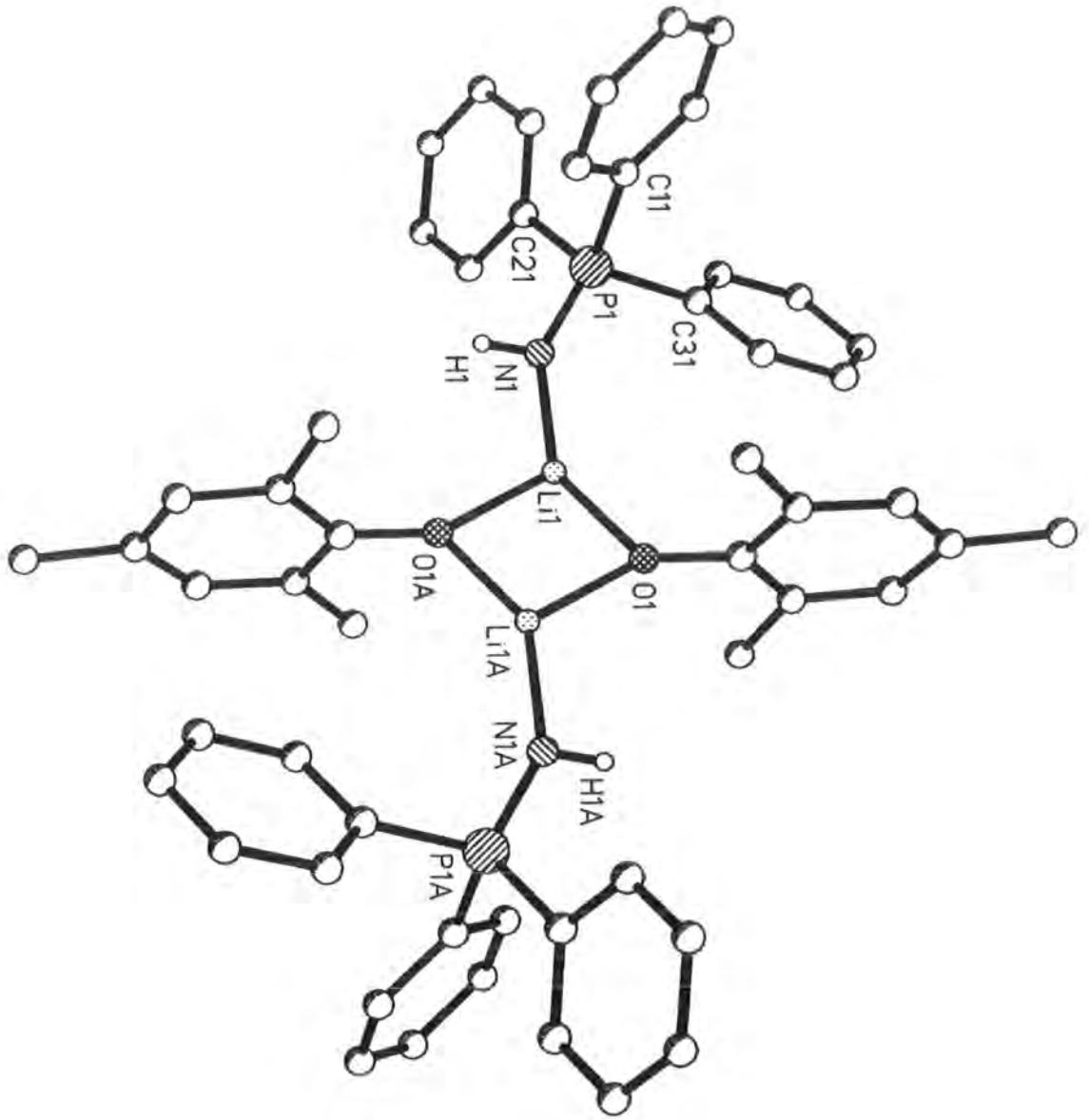

Figure 4.22 Single crystal XRD structure of 13 (methyl group of tert-butyl groups omitted for clarity)

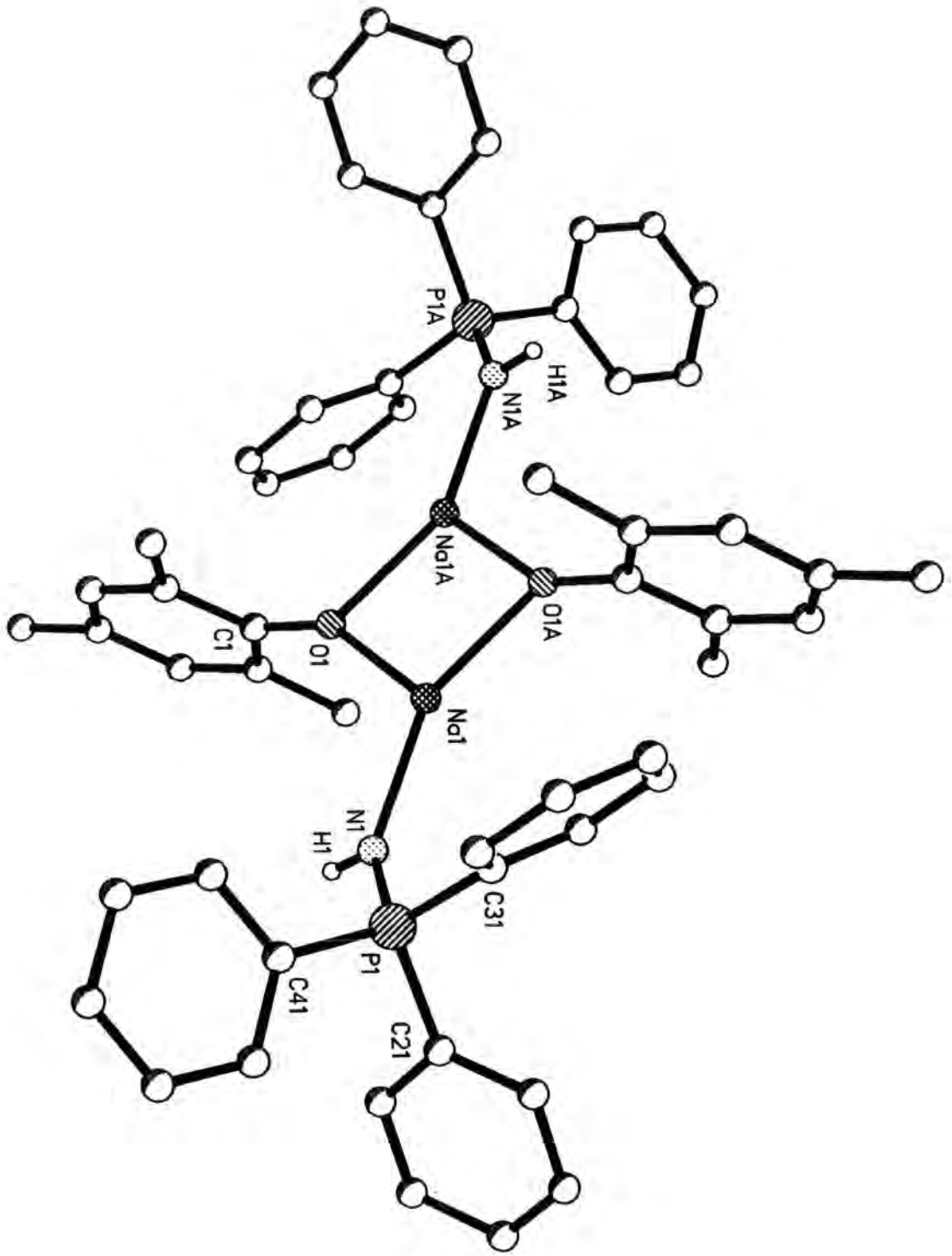

Figure 4.23 Single crystal XRD structure of 14 (methyl group of tert-butyl groups omitted for clarity)

Reaction of ^{n}BuLi with a toluene solution of **5** and either 2,6-di-tert-butyl-4-methylphenol or 2,6-diphenylphenol yields a white precipitate. On heating, the precipitate dissolves affording a crop of transparent blocks upon cooling. Analysis of these crystals, ultimately by single crystal XRD studies revealed them to be iminophosphorane complexed-lithium aryloxides **15** and **16** respectively.

Complexes **15** and **16** display very similar structural features to **13**, **16** is shown in **Fig. 4.24** and **15** is not shown here. The iminophosphorane P-N bond lengths [**15**: P(1)-N(1) 1.566(4) Å; **16**: P(1)-N(1) 1.574(2) Å] are little changed from the parent iminophosphorane (**Table 4.3**)[18] and there is a transoid arrangement of the iminophosphorane units across the Li_2O_2 core. The N-Li distances are similarly short [**15**: Li(1)-N(1) 1.945(7) Å; **16**: Li(1)-N(1) 1.999(4)Å], c.f. **13**. Both **15** and **16** have a unique P-NMe_2 bond that is elongated and has a wider imino-phosphorus-amino bond angle compared with the other two amino groups. For **16** only this group is at N(5) [P(1)-N(2) 1.654(2), P(1)-N(3) 1.676(2), P(1)-N(4) 1.655(2) Å; N(1)-P(1)-N(2) 113.7(1), N(1)-P(1)-N(3) 118.8(1), N(1)-P(1)-N(4) 106.8(1) °]. The unique amino group in **16** is pyramidalised (sum of angles = 344 °), whilst the other two amino groups are planar, as is the iminic nitrogen environment.[§]

Reaction of ^{n}BuNa with a toluene solution of tris(dimethylamino)iminophosphorane **5** and 2,6-di-tert-butyl-4-methylphenol, with heating, yields a colourless solution. Storage of the solution at ambient temperature produces a crop of crystals, which following ^{1}H and ^{31}P nmr spectroscopy (**Table 4.4**) and a single crystal XRD study were shown to be **17**. In the solid-state **17** is unexceptional in the context of the other complexes discussed in this work and is very similar to **15** and **16**, but not shown here. The P-N_{iminic} bond length [1.569(2) Å] is similar to that of its lithium equivalent **15**, whilst the N-Na distance [2.315(2) Å] is short for sodium amide structures,[59] due to the reasons discussed above (**Fig. 4.20**). The unique P-N_{amino} bond in this structure, is less pyramidalised than in previous cases (sum of angles = 351 °).

---

§ Disorder of the dimethylamino groups in **16** inhibit a more thorough discussion of their geometry.

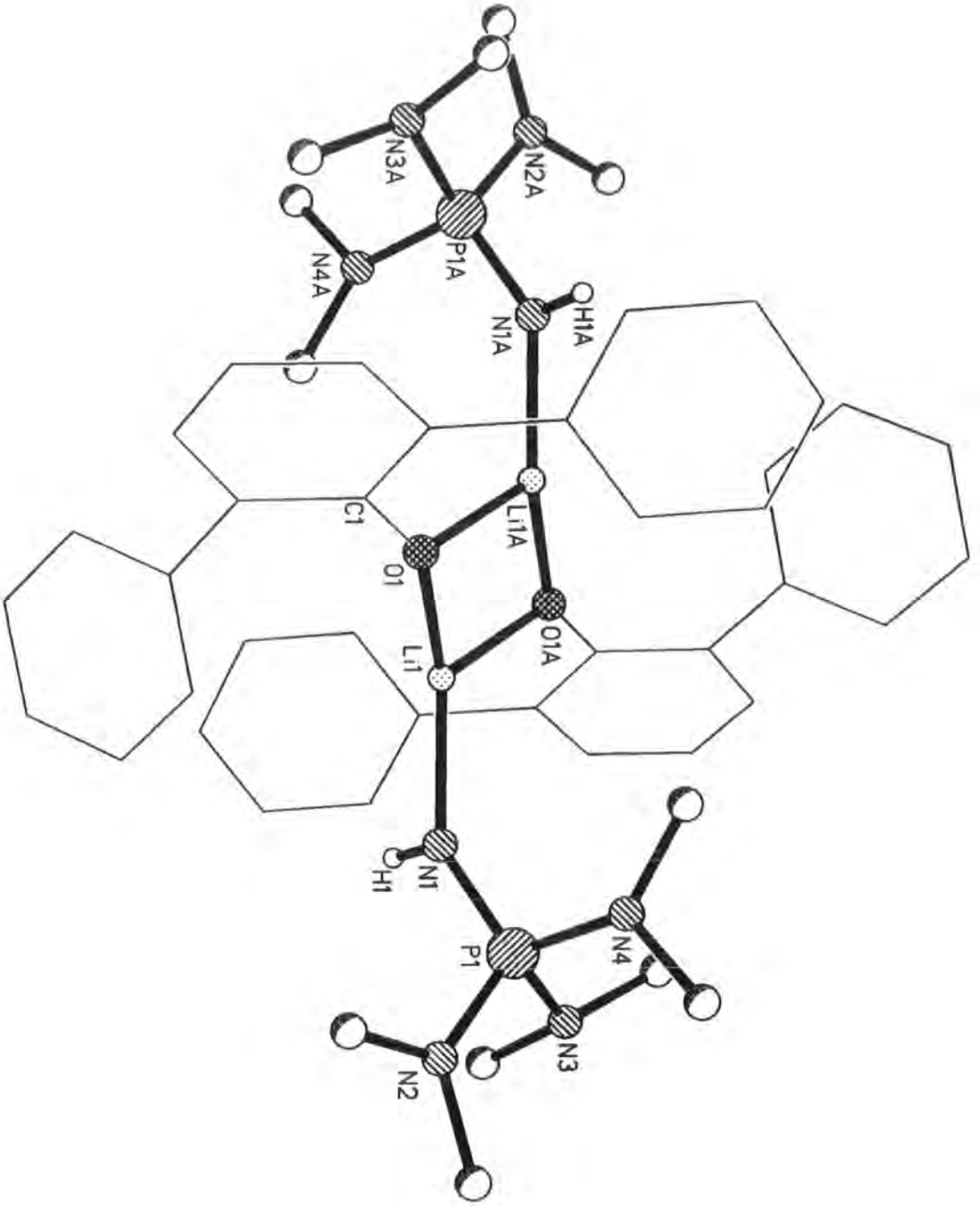

Figure 4.24 Single crystal XRD structure of 16 (phenyl rings of diphenylphenoxide in outline)

Complex **18**, formed by a similar reaction using 2,6-diphenylphenol is the sodium equivalent of **16**. Analysis by ^{1}H and ^{31}P nmr spectroscopy (**Table 4.4**), together with the information discussed so far, infer its solid-phase structure to be dimeric, with a pyramidalised phosphonium centre and transoid arrangement of the iminic moieties across the Na_2N_2 bridge (although its single crystal XRD structure has not been determined).

Phosphine oxide complexes **19-21** are isoelectronic with the phosphonium ylide structures **9**, **10** and **12** and the iminophosphorane structures **13-15**. Analysis by ^{1}H and ^{31}P nmr spectroscopy (**Table 4.4**) show evidence for complexes of the type discussed so far. Complexes **19** and **20** contain triphenylphosphine oxide **6** units and provide useful comparisons for the s-block metal complexes of ylide **1** and iminophosphorane **4**. Complex **21** contains tris(dimethylamino)phosphine oxide units (hmpa) and provides useful comparisons for the ylide and iminophosphorane s-block metal complexes of **3** and **5**, respectively.

Reaction of ^{n}BuLi with a toluene solution of triphenylphosphine sulfide **7** and 2,6-di-tert-butyl-4-methylphenol yields a white precipitate, which dissolves on heating. Cooling of the resulting pale yellow solution affords a crop of transparent blocks of **22**. Surprisingly, **22** is the first example of a neutral phosphine sulfide co-ordinating to a lithium salt. The solid-state structure is dimeric, with a transoid arrangement of the phosphine sulfide (**Fig. 4.26**). The P-S bond length, 1.976(1) Å, is little changed upon complexation (**Table 4.3**)[21] - this indicates that the P-S bonding is of a similar nature to the P-X bonding in the second row, since it must also be an essentially ionic interaction (**Fig. 4.25**).[60] The Li-S distance [2.504(3) Å] is in the same range as previously reported lengths,[61] the majority of which contain anionic sulfur fragments. This offers another indication of the strength of this interaction.

---

[60] P. Azavant, A. Lichanot, M. Repat and C. Pisani, *Acta Cryst.*, **B50**, 279 (1994); T. Ouazzani, A. Lichanot, C. Pisani and C. Roetti, *J. Phys. Chem. Solids*, **54**, 1603 (1993).

[61] See for example: J. J. Ellison and P. P. Power, *Inorg. Chem.*, **33**, 4231 (1994); A. J. Banister, D. Barr, A. T. Brooker, W Clegg, M. J. Cunnington, M. J. Doyle, S. Drake, W. R. Gill, K. Manning, P. R. Raithby, R. Snaith, K. Wade and D. S. Wright, *J. Chem. Soc., Chem. Commun.*, 105 (1990); G. A. Sigel and P. P. Power, *Inorg. Chem.*, **26**, 2819 (1987).

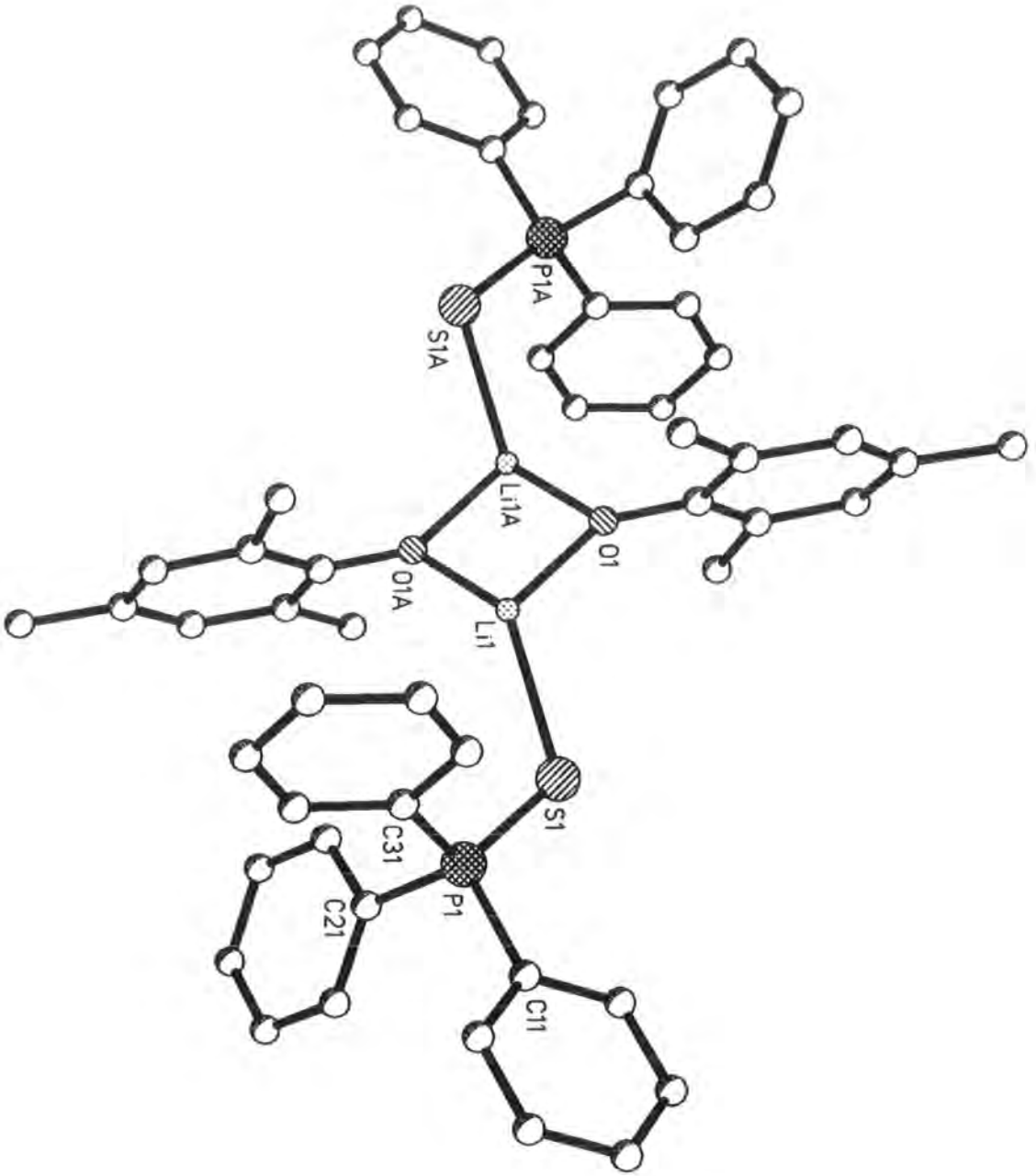

Figure 4.25 Single crystal XRD structure of 22 (methyl group of tert-butyl groups omitted for clarity)

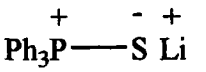

Figure 4.26 Ionic interaction between phosphine sulfide and lithium cation

Due to the increased steric demands of the phosphine sulfide compared to its second row analogues, the Li_2O_2 core is more distorted from an ideal square arrangement [Li(1)-O(1) 1.856(3), Li(1)-O(1a) 1.883(3) Å; Li(1)-O(1)-Li(1a) 82.24(14), O(1)-Li(1)-O(1a) 97.76(14) °]. There is no particularly unique P-C_{ipso} bond in this case. This may be due to a poorer overlap between the sulfur p_π and phosphorus σ^* orbital (negative hyperconjugation - **Chapter 1**) in comparison to the second row cases.

There are only two examples of phosphine sulfide-lithium complexes that have been structurally characterised (**Fig. 4.27**).[62,63] Both are examples of α-lithiation at an alkyl side-chain, i.e. analogous to the examples for iminophosphoranes.

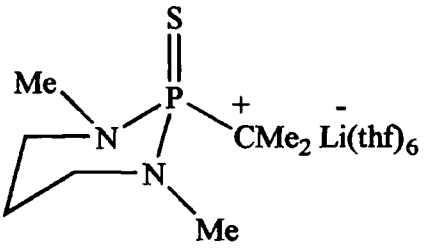

Figure 4.27 α-lithiated phosphine sulfide

22 is the first example of a phosphine sulfide behaving as a neutral P(V) Lewis base to lithium (and indeed to any s-block metal). Moreover, there are similarly few examples of phosphine sulfide-transition metal complexes[64] since there is a tendency for cleavage of the phosphorus-sulfur bond leaving discrete phosphine and sulfur donors attached to the metal centre.[65]

---

[62] M. Kranz, S. E. Denmark, K. A. Swiss and S. R. Wilson, *J. Org. Chem.*, **61**, 8551 (1996).
[63] S. E. Denmark, K. A. Swiss and S. R. Wilson, *J. Am. Chem. Soc.*, **115**, 3826 (1993).
[64] see for example: H. W. Roesky, K. K. Pandey, M. Noltemeyer and G. M. Sheldrick, *Acta Cryst.*, **C40**, 1555 (1984); M. E. Olmos, A. Schier and H. Schmidbaur, *Z. Natursforsch*, **52b**, 385 (1997).
[65] L. Ma, D. P. S. Rodgers, S. R. Wilson and J. R. Shapley, *Inorg. Chem.*, **30**, 3593 (1991).

Reaction of magnesium bis[bis(trimethylsilyl)]amide[66] with a toluene solution of **1** (or **4**) and 2,6-di-tert-butyl-4-methylphenol yields a yellow (or white precipitate), which dissolves on heating. Cooling of the solution yields a non-crystalline product, which following ^{1}H and ^{31}P nmr spectroscopy (**Table 4.4**), was identified as **23** (or **24**). **23** and **24** are magnesium complexes analogous to their lithium and sodium equivalents, ylide complexes **9** and **13**, iminophosphorane complexes **10** and **14**, respectively. **23** represents the first isolable phosphonium ylide-magnesium complex (if one discounts a serendipitous crystal grown in an nmr tube),[39] whilst **24** is a neutral magnesium complex of the type $[R_3PNR]_2MgX_2$. They are both likely to be monomeric, and are analogous to the complexes of the heavier alkaline earth metals, whose single crystal XRD structures have been determined (**Fig. 4.28**).[67]

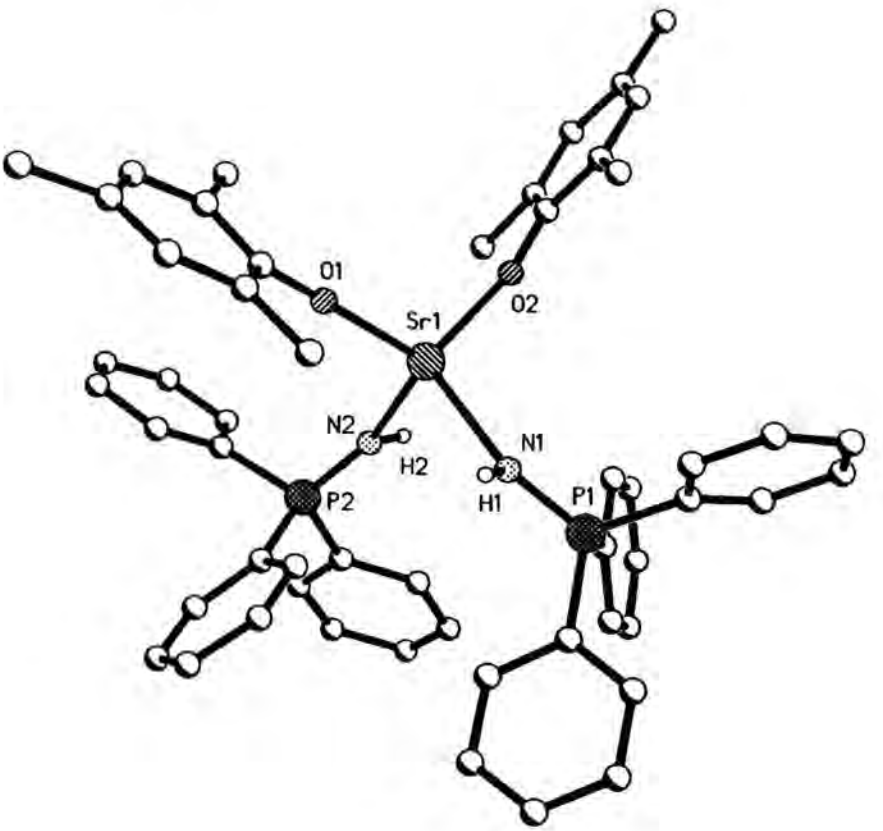

Figure 4.28 Single crystal XRD structure of a Strontium aryloxide-iminophosphorane complex (methyl group of tert-butyl groups omitted for clarity)

[66] K. W. Henderson, J. F. Allan and A. R. Kennedy, *J. Chem. Soc. Chem. Commun.*, 1149 (1997).
[67] P. D. Bolton, C. K. Broder, M. G. Davidson, J. A. K. Howard and R. D. Price, *Unpublished results.*

Complex	Formula	Average P-X bond distance / Å		
		Complex	Ligand	Ref
9	$Ph_3PCH_2{\cdot}LiOC_6H_2(Me)^tBu_2$	1.715	1.693	**15**
10	$Ph_3PCH_2{\cdot}NaOC_6H_2(Me)^tBu_2$	1.703	1.693	**15**
11	$Ph_3PCHMe{\cdot}LiOC_6H_2(Me)^tBu_2$	1.720	1.661	**16**
12	$(Me_2N)_3PCH_2{\cdot}LiOC_6H_2(Me)^tBu_2$	1.700	1.655	**17**
13	$Ph_3PNH{\cdot}LiOC_6H_2(Me)^tBu_2$	1.578	1.582	**18**
14	$Ph_3PNH{\cdot}NaOC_6H_2(Me)^tBu_2$	1.581	1.582	**18**
15	$(Me_2N)_3PNH{\cdot}LiOC_6H_2(Me)^tBu_2$	1.566	1.557	**19**
16	$(Me_2N)_3PNH{\cdot}LiOC_6H_3(Ph)_2$	1.574	1.557	**19**
17	$(Me_2N)_3PNH{\cdot}NaOC_6H_2(Me)^tBu_2$	1.569	1.557	**19**
22	$Ph_3PS{\cdot}LiOC_6H_2(Me)^tBu_2$	1.976	1.950	**22**

Table 4.5 Summary of P-X bond distances for complexes 9-17 and 22

The detailed synthetic and structural investigation given above allows a number of comparisons to be drawn. As can be seen above (**Table 4.5**), the P-X bond distance is little affected upon complexation to lithium or sodium in all cases. The iminophosphorane structures, have the smallest elongation (generally 0.01 Å for the trisdimethylamino substituted cases **15-17**; the phenyl substituted cases **13** and **14** are unchanged within experimental error). One explanation could be that the neutral iminophosphorane **4** can use two orbitals for π-σ^* back-bonding (and, therefore, still has one available for this upon complexation to lithium), whereas for the neutral ylides there is only one available orbital for negative hyperconjugation (thus, whatever π-σ^* interaction there is will be disrupted following complexation to lithium). However, the difference is very small and no true comparison of differing electronic effects can be drawn from this.

For the phenyl substituted examples, the P-X-Li bond angle changes markedly from X = S [117.90(7)° **22**], X = CH_2 [130.64(17)° **9**] to X = NH [146.3(2)° **13**]. Whether or not this is significant is unclear.

4.5 Conclusions

(i) A range of complexes containing neutral P(V) Lewis bases has been prepared using 2,6-di-tert-butyl-4-methylphenol.

(ii) In the majority of cases these represent the first reported complexes of their type.

(iii) In the case of the alkali metals, the structures are dimeric, often with a transoid arrangement of the Lewis base across the bridging core. Based on similar structures of other alkaline-earth metals, the magnesium complexes **23** and **24** are expected to be monomeric.

(iv) Structures should be accessible with a wide-range of phenols: 2,6-diphenylphenol has also been used. Other less sterically demanding phenols may lead to more open, extended chain/ladder-type structures.

(v) The ylide complexes **9-12**, are model intermediates for Wittig reactions and may provide information about the effects of alkali metal salts on the course of Wittig reactions (see following chapter).

5. Discussion: Phosphonium ylide-alkali metal amide complexes and their application to the Wittig reaction.

This chapter will commence with a brief, general overview of the structural types found for alkali metal amides and related complexes. A discussion of the solid-state structures of complexes **25** and **27** will follow, including a comparison with analogous alkali metal amide complexes of **1** that have been previously structurally characterised. This will be followed by a consideration of the solution-state behaviour of complexes **25-28** and an investigation of their role during Wittig transformations.

Complex	Empirical Formula
A	$Ph_3PCH_2{\cdot}LiN(CH_2Ph)_2$
B	$Ph_3PCH_2{\cdot}NaN(SiMe_3)_2$
25	$Ph_3PCHMe{\cdot}LiN(CH_2Ph)_2$
26	$Ph_3PCHMe{\cdot}LiN(SiMe_3)_2$
27	$Ph_3PCHMe{\cdot}NaN(SiMe_3)_2$
28	$(Me_2N)_3PCH_2{\cdot}LiN(CH_2Ph)_2$

Table 5.1 Complexes discussed in this chapter

5.1 Alkali metal amides

Alkali metal amides are unable to stack, unlike aryloxylithiums (**Chapter 4**), due to their stereochemistry and instead associate via rings sharing edges to give ladders. There are several possible modes of aggregation in the solid-state, some of which are shown below (**Fig. 5.1**). These are in accordance with the Ring Laddering Principle.[1]

[1] D. R. Armstrong, D. Barr, W. Clegg, R. E. Mulvey, D. Reed, R. Snaith and K. Wade, *J. Chem. Soc., Chem. Commun.*, 869 (1986).

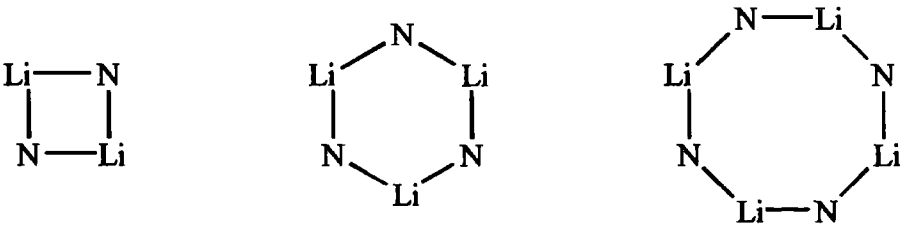

Figure 5.1 Some possible aggregation states for an uncomplexed lithium amide

Trimeric rings are common for uncomplexed lithium amides that are soluble in non-polar hydrocarbon solvents, such as $[(PhCH_2)_2NLi]_3$[2] and $[(Me_3Si)_2NLi]_3$.[3] The resulting two coordinate lithium undergoes agostic Li...H-C interactions where possible. There is an example of both an uncomplexed dimeric[4] and tetrameric[5] lithium amide. These are unusual, however, being caused by specific steric instances. Lithium amides with smaller and flatter substituent groups are predicted to form polymeric infinite ladders. Inevitably, this precludes the use of single crystal XRD methods to determine their solid-state structures and only two examples of uncomplexed oligomeric ladder structures are known.[6] There are also uncomplexed sodium[7] and potassium[8] amide structures known, $[(Me_3Si)_2NNa]_\infty$ being a polymer (or trimer) and $[(Me_3Si)_2NK]_2$ a dimer. (The latter, infact, is strictly a toluene-solvated dimeric complex).[8]

Uncomplexed lithium amide structures have mainly arisen as a result of bulky amine substituents preventing further association into polymeric ladders. The majority of lithium amides require addition of a donor to facilitate dissolution in non-polar hydrocarbon solvents. In general, this leads to dimeric or monomeric species upon complexation (**Fig. 5.2**). Accordingly, the structures of both $[(PhCH_2)_2NLi.OEt_2]_2$ and $[(PhCH_2)_2NLi.hmpa]_2$ are dimers.[2]

---

[2] D. Barr, W. Clegg, R. E. Mulvey and R. Snaith, *J. Chem. Soc., Chem. Commun.*, 285 (1984); D. Barr, W. Clegg, R. E. Mulvey and R. Snaith, *ibid.*, 287 (1984).
[3] R. D. Rogers, J. L. Atwood and R. Grüning, *J. Organomet. Chem.*, **157**, 229 (1978).
[4] D. Kennepohl, S. Brooker, G. M. Sheldrick and H. W. Roesky, *Chem. Ber.*, **124**, 2223 (1991).
[5] M. F. Lappert, M. J. Slade, A. Singh, J. L. Atwood, R. D. Rogers and R. Shakir, *J. Am. Chem. Soc.*, **105**, 302 (1983).
[6] R. Snaith, D. Barr, D. S. Wright, W. Clegg, S. M. Hodgson, G. R. Lammin, A. J. Scott and R. E. Mulvey, *Angew. Chem., Int. Ed. Engl.*, **28**, 1241 (1989); N. D. R. Barnett, W. Clegg, L. Horsburgh, D. M. Lindsay, Qi-Yong Liu, F. M. Mackenzie, R. E. Mulvey and P. G. Williard, *J. Chem. Soc., Chem. Commun.*, 2321 (1996).
[7] R. Grüning and J. L. Atwood, *J. Organomet. Chem.*, **137**, 101 (1977).

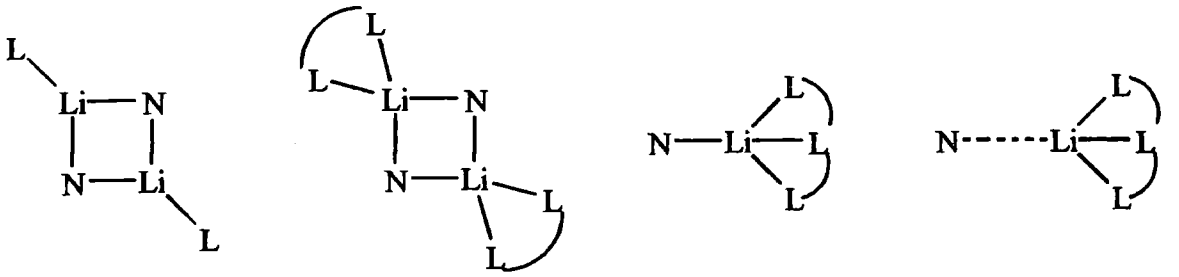

Figure 5.2 Some possible aggregation states of complexed lithium amides

In the presence of a less than stoichiometric amount of donor, intercepted ladder structures, in which only some of the lithium centres are complexed, can be formed. The form of the ladder is dictated by the denticity of the donor. One such example **(Fig. 5.3)** shows a bidentate Lewis base, such as TMEDA, in a 1:2 stoichiometry. The latter case was found for the solid-state structure of $[(pyrrolidinoLi)_2.TMEDA]_2$.[1]

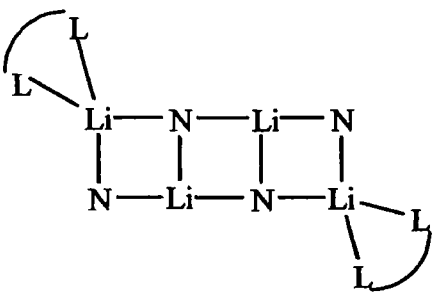

Figure 5.3 An intercepted ladder structure

There are now a considerable number of alkali metal amide structures known[9] and, in particular, mixed metal (lithium/heavier alkali metal) amides are being prepared as a consequence of the widespread use of superbases (alkyllithium/heavier metal alkoxide) in organic synthesis.[10] More recently a new class of complexes in this field has emerged.[11]

---

[8] P. G. Williard, *Acta Cryst.*, **C44**, 270 (1988).
[9] For a review of the topic see: R. E. Mulvey, *Chem. Soc. Rev.*, **20**, 167 (1991); *ibid.*, **27**, 339 (1998).
[10] A. Mordini, *Advances in Carbanion Chemistry*, ed. V. Snieckus, JAI Press, London (1992), Vol. 1, 1; L. Brandsma, *Preparative Polar Organometallic Chemistry*, Springer, Berlin, Vol. 1 (1990).
[11] A. R. Kennedy, R. E. Mulvey, C. L. Raston, B. A. Roberts and R. B. Rowlings, *J. Chem. Soc., Chem. Commun.*, 353 (1999); A. R. Kennedy, R. E. Mulvey and R. B. Rowlings, *Angew. Chem., Int. Ed. Engl.*, **37**, 3180 (1998); A. R. Kennedy, R. E. Mulvey and R. B. Rowlings, *J. Am. Chem. Soc.*, **120**, 7816 (1998).

These (inverse crown-ethers) are mixed s-block metal amides containing a central atom or molecule, such as O^{2-} (**Fig. 5.4**) or tolyl anions.

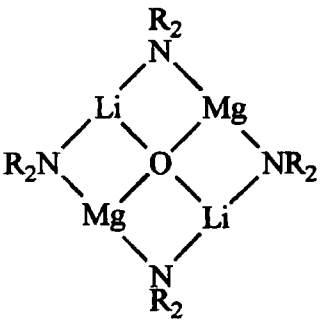

Figure 5.4 Schematic of a mixed lithium/magnesium amide with an oxo anion core

The use of these complexes in synthesis/reaction chemistry has not yet been reported, but may provide some interesting applications.

5.2 Solid-state structure of complexes 25 and 27

Addition of ^{n}BuLi to a cooled (to approx. 0 °C) solution of **2** and dibenzylamine in hexane/toluene (1:1) affords a deep red precipitate that dissolves upon gentle heating. Cooling to ambient temperature yields a crop of red/purple crystals which, following analysis ultimately by a single crystal XRD study, were shown to be **25**.

In the solid-state (**Fig. 5.5**) **25** is dimeric with each lithium atom coordinated by one phosphonium ylide Lewis base. Dibenzylamidolithium itself is well-characterised in the solid-state,[2] being trimeric and thus susceptible to deaggregation by a suitable neutral Lewis base donor such as **2**. The Li_2N_2 core in **25** is unremarkable [Li(1)-N(1) 2.046(3) Å, Li(1)-N(1a) 2.001(3) Å; Li(1)-N(1)-Li(1a) 76.80(14)°, N(1)-Li(1)-N(1a) 103.20(14)°] and of similar symmetry to those found in **A** (the analogous dibenzylamidolithium complex with **1**),[12] $[(PhCH_2)_2NLi.OEt_2]_2$ and $[(PhCH_2)_2NLi.hmpa]_2$.[3] A similar transoid arrangement of the neutral ylide donors across the Li_2N_2 core, such as seen for **25**, was also a feature of **A**.

---

[12] M. G. Davidson, D. R. Armstrong and D. Moncrieff, *Angew. Chem., Int. Ed. Engl.*, **34**, 478 (1995).

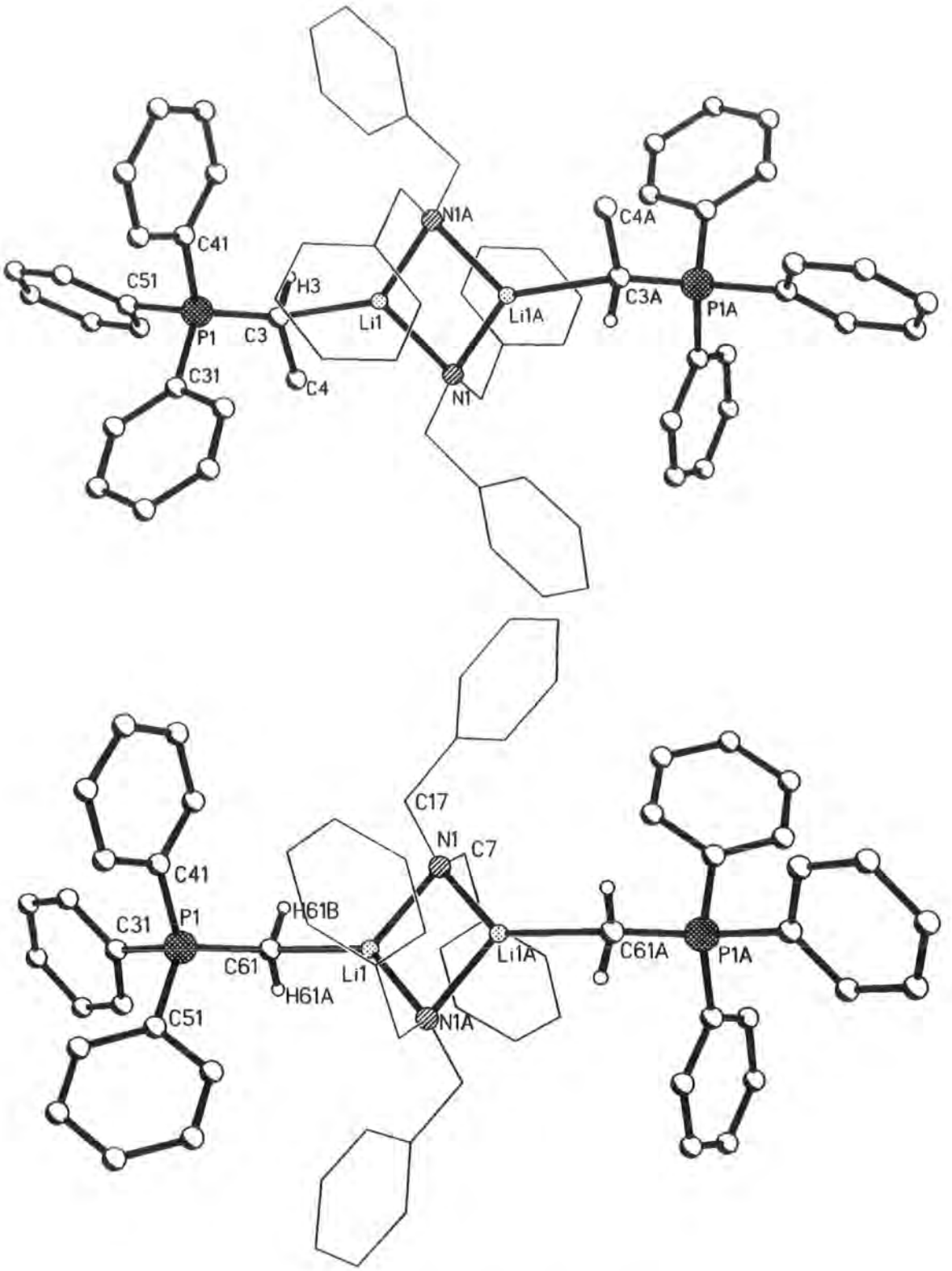

Figure 5.5 Single crystal XRD structures of 25 (top) and A (bottom) (dibenzylamido groups in outline)

The Li-C_{ylide} distance in **25** [2.321(3) Å] is in the expected range for lithium alkyls [2.1-2.4 Å],[13] but slightly more elongated than for **A** [2.207(4) Å]. This effect may be caused by an increased steric crowding, but is more likely to be an electronic effect. However, the Li-C distance is indicative of a strong and essentially ionic interaction.

The ylidic carbon atom is more pyramidalised [sum of angles around C(3) excluding Li(1) = 343°] than in the structure of the parent ylide **2** (sum of angles = 354°), but less so than in **A** (sum of angles = 334°). The P-C_{ylidic} bond length [1.707(2) Å] is slightly elongated with respect to **2** [1.661(6) Å] and more so than was found for **A** [1.702(2) Å][12] and **1** [1.693 (ave.) Å].[14]

There is also a unique P-C_{ipso} bond that is both elongated and has a wider C_{ipso}-P-C_{ylidic} angle than the other two bonds [P-C(51) 1.845(2), P-C(41) 1.811(2), P-C(31) 1.817(2) Å; C(3)-P-C(51) 119.28(8), C(3)-P-C(41) 112.23(8), C(3)-P-C(31) 109.90(8) °]. This is not a feature of **2**, which has a C_1 symmetry with three unique P-C_{ipso} bonds, but was observed in the structures of **A** and **1**.[12,14] The ylidic carbon atom of **25** is also, to the author's knowledge, the first chiral Li-C to be structurally characterised using XRD, crystallised as a racemate. Fraenkel et al.[15] investigated the solution behaviour of *sec*-butyllithium and other chiral alkyllithiums, but have not characterised any in the solid-state.

Addition of toluene to sodium bis(trimethylsilyl)amide and **2** yields a yellow/orange precipitate which dissolves upon heating and on cooling affords a crop of orange crystals. Analysis, ultimately by a single crystal XRD study, revealed the product to be **27**.

Complex **27** is also dimeric in the solid-state with a Na_2N_2 core (**Fig. 5.6**). The structure of sodium bis(trimethylsilyl)amide is polymeric (or trimeric),[7] but this is deaggregated upon complexation by **2**. There is a transoid arrangement of the neutral ylide fragments across the Na_2N_2 core, which was also a feature of **25** and **A**. However, the analogous complex

---

[13] W. Setzer and P. v. R. Schleyer, *Adv. Organomet. Chem.*, **24**, 253 (1985).
[14] H. Schmidbaur, J. Jeong, A. Schier, W. Graf, D. L. Wilkinson, G. Müller and C. Krüger, *New. J. Chem.*, **13**, 341 (1989).
[15] G. Fraenkel, M. Henrichs, M. Hewitt and B. M. Su, *J. Am. Chem. Soc.*, **106**, 255 (1984); G. Fraenkel, *Abstracts of Papers of the ACS*, **191**, 20 (1986).

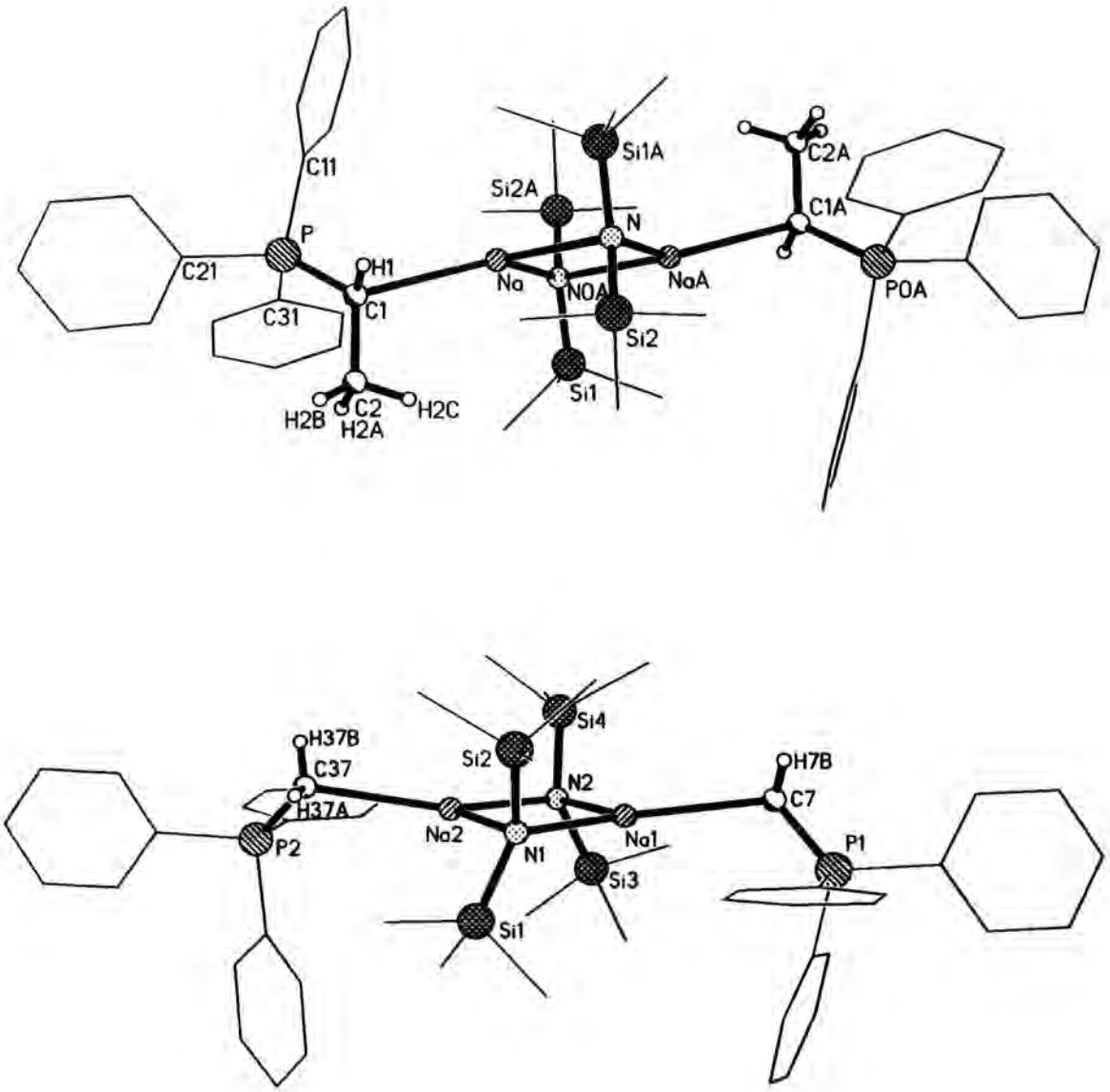

Figure 5.6 Single crystal XRD structures of 27 (top) and B (bottom) (organic periphery in outline)

of **1** with sodium bis(trimethylsilyl)amide[16] **B** contains a cisoid arrangement of ylide fragments (**Fig. 5.6**) thus displaying that the interaction is essentially ionic and unrestricted in its directionality. A comparison of the two cores (**27** and **B**) reveals few differences in the parameters, **27** being slightly more compressed than **B** (simply a manifestation of the increased steric crowding).

The Na-C_{ylidic} distance in **27** [2.645(3)Å] is marginally longer than that seen in the sodium aryloxide-phosphonium ylide structure **10** [2.489(2)Å], but still indicative of a strong bonding interaction.[17] In comparison, the Na-C_{ylidic} distance in **B** is little different [2.629Å (ave.)].

Similarly to **25**, the ylidic carbon becomes more pyramidalised upon complexation (sum of angles excluding sodium = 342°, c.f. 354° for **2**). However, the ylidic carbon is again more pyramidalised for the methylide complex **B** (ave. sum of angles = 337°). The P-C_{ylidic} bond length [1.710(2)Å] is of the same order as found in **25** and, therefore, similarly elongated with respect to **2**. For **B** there is virtually no elongation [1.696Å].

The structure of **27** displays the same general feature of a unique P-C_{ipso} bond [P-C(21) 1.833(2), P-C(11) 1.812(2), P-C(31) 1.820(2) Å; C(1)-P-C(21) 121.98(11), C(1)-P-C(11) 108.19(11), C(1)-P-C(31) 109.68(11) °] that is both elongated and has a wider angle than the other two bonds. This is also a feature of **B**.

Similarly to **25**, there is a chiral ylidic carbon in **27**. Again, to the author's knowledge, this is the first chiral sodium bound carbon atom to be structurally characterised using XRD. Another interesting feature of **27** is the close approach by a carbon atom of the trimethylsilyl group to sodium [Na-C(4a) 3.03(3) Å; Na(a)-Na-C(4a) 93.7(3) °]. Often, an agostic interaction between a hydrogen atom and alkali metal can be seen in the structures of alkali metal amides, but it is clear (**Fig. 5.7**) in this case that the hydrogens are pointing away from the sodium atom and that the carbon atom is ideally aligned to form such a

---

[16] M. G. Davidson, *Unpublished results*.
[17] See for example: R. den Besten, M. T. Lakin, N. Veldman, A. L. Spek and L. Brandsma, *J. Organomet. Chem.*, **514**, 191 (1996); V. Jordan, U. Behrens, F. Olbrich and E. Weiss, *J. Organomet. Chem.*, **517**, 81 (1996); H. Viebrock, U. Behrens and E. Weiss, *Chem. Ber.*, **127**, 1399 (1994).

bond. This feature was reported in the solid-state structures of a range of alkali metal tris(trimethylsilyl)silanides[18] [$(Me_3Si)_3SiM$ (M = alkali metal)] and is also likely to be a feature of **26** in the solid-state. The solid-state structure of **B** also contains short Na-C contacts of a similar magnitude to **27** [3.05(5) and 2.95(6) Å].

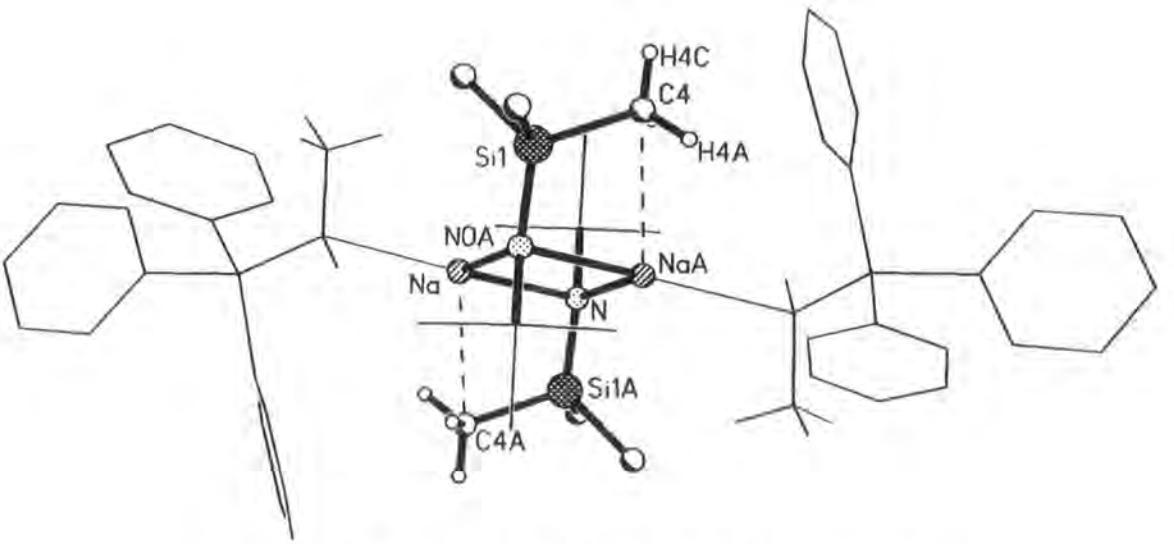

Figure 5.7 Na-C interactions observed in the solid-state for 27 (phosphonium ylide and non-participating groups in outline)

[18] K. W. Klinkhammer and W. Schwarz, *Z. Anorg. Allg. Chem.*, **619**, 1777 (1993); K. W. Klinkhammer, *Eur. J. Chem.*, **3**, 1418 (1997).

5.3 Solution-state studies of complexes 25-28

Complex	δ_{CHR}/ppm	$^2J_{PH}$/Hz	δ_{Me}/ppm	$^3J_{PH}$/Hz	Ref
1	0.9	7.6	-	-	this work
A	0.5	4.7	-	-	16
B	0.4	6.2	-	-	15
2	1.2	17.5	2.2	19.0	this work
25	1.0	12.4	2.1	19.6	this work
26	1.0	4.1	2.1	21.4	this work
27	0.95	13.1	2.3	19.6	this work

Table 5.2 Summary of ^{1}H NMR data for $Ph_3PCHR.MNR_2$ complexes

A consideration of the ylidic carbon chemical shift (δ_{CHR}) and the corresponding $^2J_{PH}$ coupling constant reveals several interesting points. Firstly, upon complexation δ_{CHR} moves to a higher frequency and the magnitude of $^2J_{PH}$ is reduced. Secondly and, more significantly, δ_{CHR} and $^2J_{PH}$ are concentration dependent.[12] The data given above (**Table 5.2**) are for 0.04M solutions. However, in more dilute solution (0.0006M) **A** gave values of 0.73ppm (δ_{CHR}) and 3.3Hz ($^2J_{PH}$), respectively. A similar reduction was also observed for **B** (0.41ppm and 3.0Hz). This finding is consistent with a monomer-dimer (or higher oligomer) equilibrium in solution for **A** and **B**. A monomer, in which lithium/sodium would be only two coordinate, would exert a greater influence on the electronic structure and, hence, on the coupling constant than a dimer (or higher oligomer) in which the metal would be three coordinate.

Ligand dissociation can be discounted since in a more dilute solution the coupling constant would *increase* for such a dynamic process, due to the higher $^2J_{PH}$ coupling constant observed for the free (uncomplexed) ligand **2**. Cryoscopy results for **A** and **B** (degree of association *n* increases with increasing concentration) also suggest a monomer-dimer equilibrium in solution for these related complexes.[12]

Multi-nuclear variable-temperature and -concentration NMR experiments on **27** give some clear indications that monomer-dimer equilibria are an inherent solution-state behaviour of this family of complexes. This can be seen clearly from the variable-concentration ^{31}P NMR spectra (**Fig. 5.8**). As the sample becomes more dilute the amount of monomer in solution increases with a concomitant decrease in the amount of dimer. In the most dilute solution there is only monomer present. The existence of a higher oligomer in solution cannot be completely discounted, but is highly unlikely since in the solid-state **27** is dimeric and the complex remains intact in solution.

Complex **26** is produced by the co-crystallisation of **2** and lithium bis(trimethylsilyl)amide from hexane. It is possible to separate a colourless and a red crystalline product. Analysis of the red crystalline product reveals it to be **2**, whilst analysis of the colourless product **26** indicates the presence of a complexed lithium amide (evident from both ^{31}P and ^{1}H NMR spectroscopy - **Chapter 3**). Its solution and solid-state behaviour is (presumably) similar to the other species in this series. **28**, also characterised by NMR spectroscopy, is an example of a complexed lithium amide with **3**, and should, similarly, be dimeric in the solid-state.

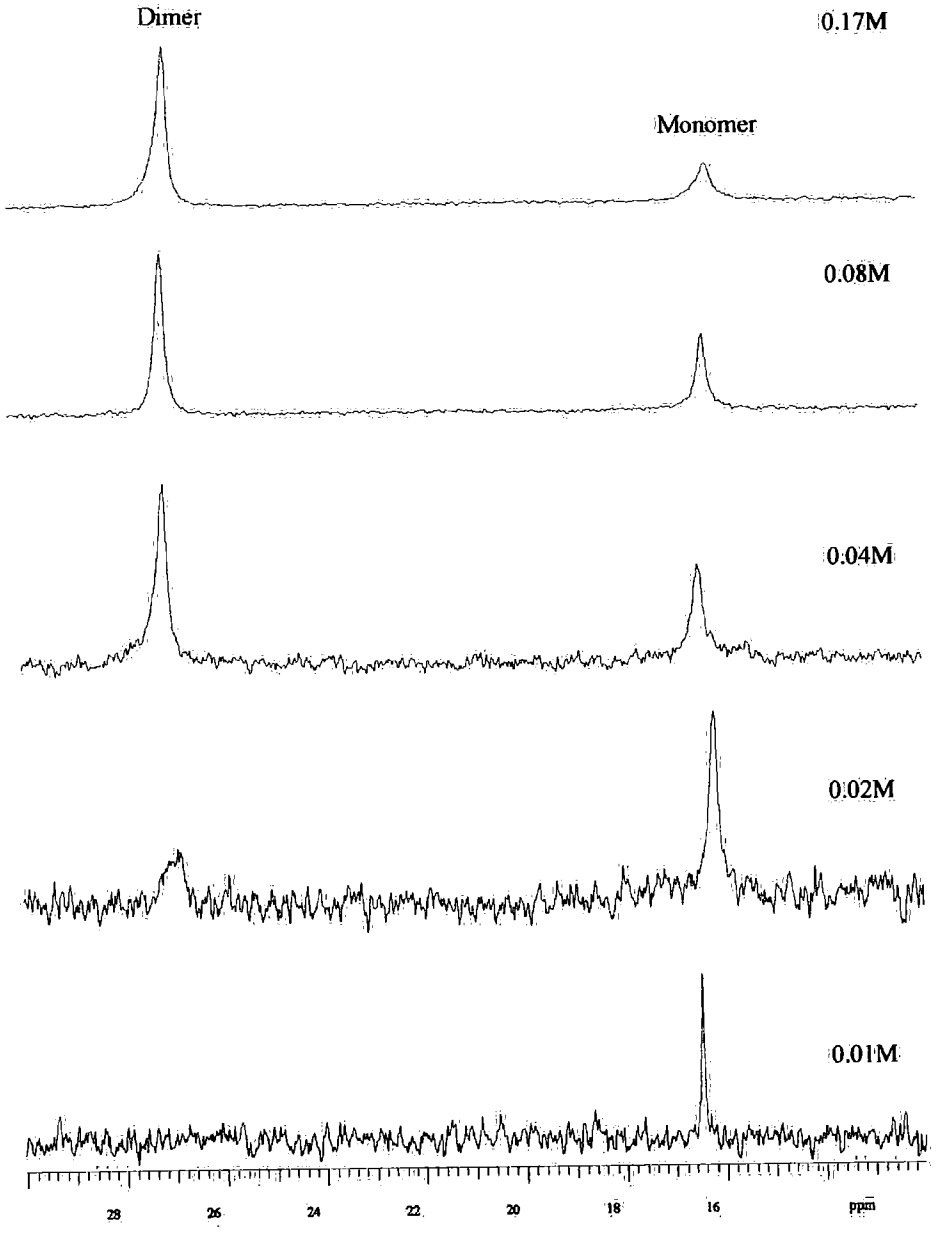

Figure 5.8 Variable-concentration ^{31}P NMR spectra for 27 @ 193K

5.4 Studies of the Wittig reaction

Since Georg Wittig's nobel-prize winning discovery in 1953 of the reaction that now bears his name, the mechanism of the Wittig reaction has been extensively studied.[19] An important method for studying the mechanism is to monitor the stereochemical outcome of reactions. Recently, the effects on stereochemistry and reactivity of alkali metals, in particular lithium salts[20] and lithiated Wittig reagents,[21] have been of considerable interest.

The classical Wittig mechanism (**Scheme 1.4**) involves reaction between a phosphonium ylide and aldehyde or ketone with the formation of two betaine intermediates, which collapse to alkenes (*Z*/*E*) via very transient oxaphosphetane species.[22] However, the questions of what intermediate predominates and what mechanistic factors govern the stereochemical outcome are still unresolved. Oxaphosphetanes are now known to be rather longer-lived intermediates than previously thought and can be readily observed at low temperature by NMR spectroscopy.[23] Maryanoff et al.[19,24] have detected a stereochemical drift from *Z* to *E* oxaphosphetanes, prior to complete conversion to alkene and phosphine oxide, for Wittig reactions involving non-stabilised phosphonium ylides in the presence of lithium and sodium species. McEwen et al.[25] reported the effects of lithium, sodium and potassium bases on the *E*/*Z* ratio for a stabilised phosphonium ylide. Verkade et al.[26] detailed a stabilised phosphonium ylide capable of producing solely *E* olefins in the presence of NaHMDS.

---

[19] For reviews, see: A. W. Johnson with special contributions by W. C. Kaska, K. A. O. Starzewski and D. A. Dixon, *'Ylides and Imines of Phosphorus'*, John Wiley & Sons Inc., New York (1993), Chp. 9; E. Vedejs and M. J. Peterson, *Top. Stereochem.*, **21**, 1 (1994); B. E. Maryanoff and A. B. Reitz, *Chem. Rev.*, **89**, 863 (1989); H. J. Cristau, *Chem. Rev.*, **94**, 1299 (1994).

[20] B. E. Maryanoff, A. B. Reitz, M. S. Mutter, R. R. Inners, H. R. Almond, R. R. Whittle and R. A. Olofson, *J. Am. Chem. Soc.*, **108**, 7664 (1986).

[21] E. J. Corey and J. Kang, *J. Am. Chem. Soc.*, **104**, 4724 (1982); E. J. Corey, J. Kang and K. Kyler, *Tet. Lett.*, **26**, 555 (1985); B. Schaub, T. Jenny and M. Schlosser, *Tet. Lett.*, **25**, 4097 (1984); B. Schaub and M. Schlosser, *Tet. Lett.*, **26**, 1623 (1985).

[22] M. Schlosser, *Top. Stereochem.*, **5**, 1 (1970).

[23] E. Vedejs and K. A. J. Snoble, *J. Am. Chem. Soc.*, **95**, 5778 (1973).

[24] B. E. Maryanoff, A. B. Reitz and B. A. Duhl-Emswiler, *J. Am. Chem. Soc.*, **107**, 217 (1985); A. B. Reitz, S. O. Nortey, A. D. Jordan, Jnr., M. S. Mutter and B. E. Maryanoff, *J. Org. Chem.*, **51**, 3302 (1986).

[25] W. J. Ward, Jnr. and W. E. McEwen, *J. Org. Chem.*, **55**, 493 (1990).

[26] Z. Wang and J. G. Verkade, *Tet. Lett.*, **39**, 9331 (1998).

Phosphonium ylide **2** is non-stabilised with a methyl substituent on the ylidic carbon. Its alkali metal complexes, therefore, have potential for studying the effects of metals on the stereochemical outcome of Wittig reactions. The procedure undertaken in this work was as follows. Ylide **2** was synthesised via the 'lithium salt-free' method[27] and stored in a dry, argon-filled glove-box. Complexes of **2** were prepared as described in the experimental section (**Chapter 3**) and also stored in a dry, argon-filled glove-box.

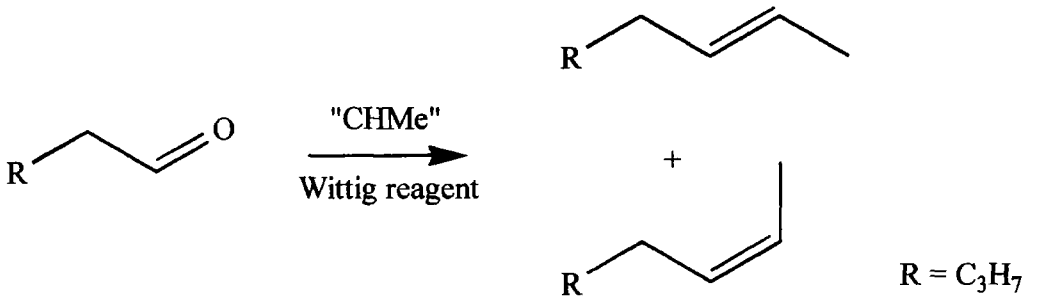

Scheme 5.1

Wittig reactions (**Scheme 5.1**) were performed using the previously isolated crystalline solids, i.e. stoichiometric complexes of **2** with an alkali-metal amide, and valeraldehyde [$CH_3(CH_2)_3CHO$]. Following agitation for 12 hours the reaction mixture was neutralised with saturated ammonium chloride solution and the organic layer dried with magnesium sulfate. The relative amounts of *Z* and *E* isomers could then be determined by gas chromatography.

Wittig reagent	Solvent	*Z*/*E* ratio	Graph ref.
Ph_3PCHMe **2**	thf	>9.5:1	1
Ph_3PCHMe **2**	tol	>9/5:1	2
$(PhCH_2)_2NLi.CHMePPh_3$ **25**	thf	4:1	3
$(PhCH_2)_2NLi.CHMePPh_3$ **25**	tol	2:1	4
$(Me_3Si)_2NNa.CHMePPh_3$ **27**	tol	4:1	5
$(^tBu)_2C_6H_2MeOLi.CHMePPh_3$ **11**	tol	4.5:1	6

Table 5.3 G.C. results for Wittig reactions (-78°C)

[27] R. Koster, D. Simic and M. Grassberger, *Liebigs Ann. Chem.*, **739**, 281 (1970); H. Schmidbaur, H. Stühler and W. Vornberger, *Chem. Ber.*, **105**, 1084 (1972).

As can be seen from the data (**Table 5.3/Graph 5.1**), there is a slight increase in the amount of *E* isomer produced for both lithium and sodium complexes of **2**. There is also an increase for the reaction of **25** in thf solution (Graph ref. 3), where deaggregation to a monomeric species is likely or break-up of the complex may occur.

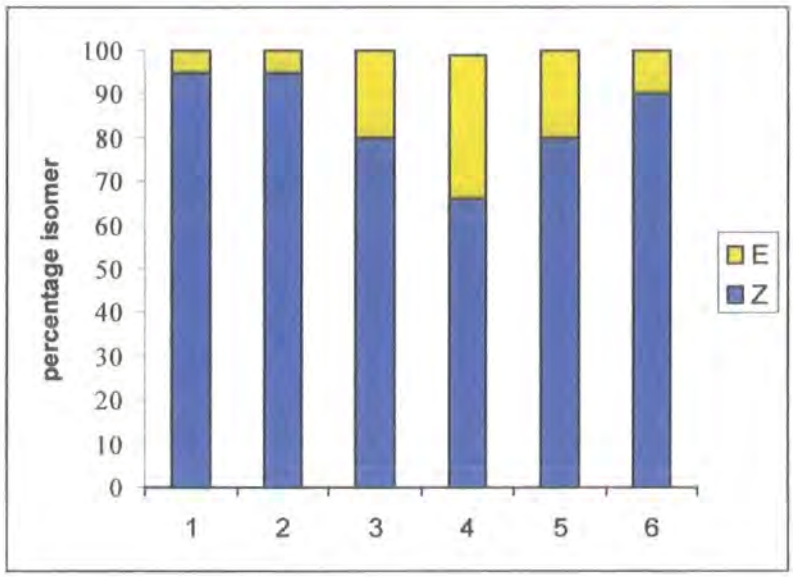

Graph 5.1

These initial results suggest that the alkali metal is intimately involved in the course of the reaction. Further studies must be undertaken to elucidate this behaviour more completely, including *ab initio* MO studies, variable-temperature and -concentration Wittig reaction studies.

This evidence, however, allows us to draw some general conclusions regarding a proposed mechanism (**Scheme 5.2**). Firstly, we know from solution-state studies (and can elucidate from solid-state data) that there is a monomer-dimer [(II)-(I)] solution equilibrium in operation for these systems. In the first step, therefore, it is reasonable to postulate that a monomeric lithium (or sodium) amide-phosphonium ylide complex [(II)] can complex to the aldehyde generating a lithium-carbonyl/ylide complex [(III)], prior to P-O or C-C bond formation, which cannot happen with salt-free conditions.

Enolisation [(III)-(V)], if it occurs, must be reversible since no aldehyde was recovered, i.e. no G.C. peak corresponding to starting material. Some *ab initio* evidence[28] for the intermediate shown [(IV)] has been obtained from *ab initio* MO calculations. The Li-C and C-C bond-formation shown can lead to the Wittig products, and presumably it is this interaction that results in the change of stereochemistry. Under 'salt-free' Wittig reactions, the intermediate is a transient species in which the carbonyl group and phosphonium ylide overlap. It is now widely considered[25] that P-O bond formation precedes C-C formation under such conditions. The role of lithium in this case may be to obstruct the P-O bond formation until the C-C bond has formed, thus enabling some alteration of olefin stereochemistry.

[28] D. R. Armstrong and M. G. Davidson, *Unpublished results.*

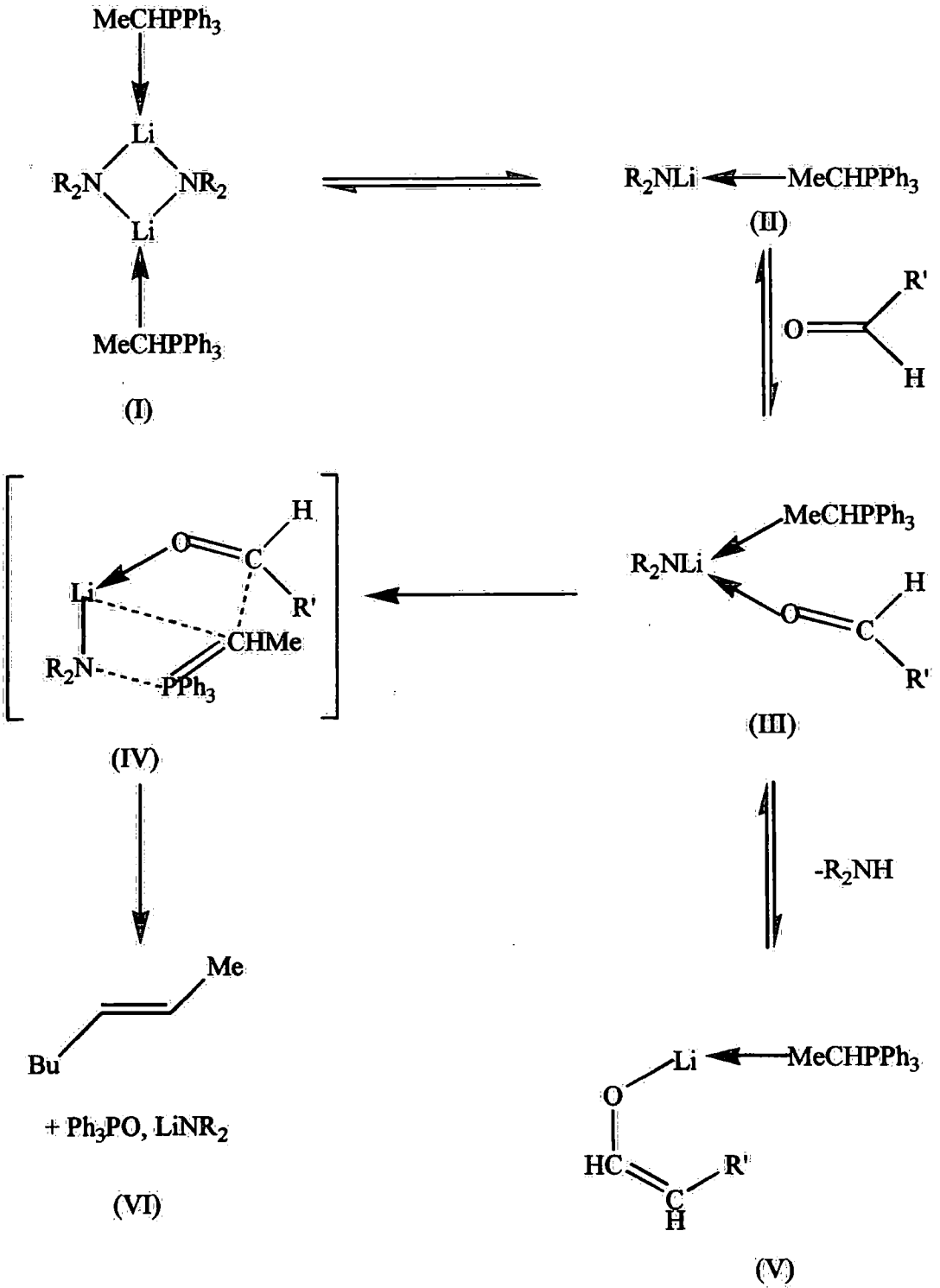
MeCHPPh3
Li
R2N
NR2
Li
MeCHPPh3
(I)
R2NLi
MeCHPPh3
(II)
R'
O
H
MeCHPPh3
R2NLi
H
O
C
R'
(III)
-R2NH
Li
MeCHPPh3
O
HC
R'
C
H
(V)
H
O
C
Li
R'
CHMe
R2N
PPh3
(IV)
Me
Bu
+ Ph3PO, LiNR2
(VI)

Scheme 5.2

5.5 Conclusions

(i) **25** and **27** are chiral triphenylphosphonium ethylide **2** complexed-alkali metal amides and form dimers in the solid-state.

(ii) **27** exhibits a monomer-dimer equilibrium in solution and this should be true of all these related complexes **25-28**.

(iii) Alkali metal complexes of **2** can be used directly in Wittig reactions as stoichiometric reagents. Alkali metal amides appear to work better than aryloxides in achieving higher *E* alkene stereoselectivity.

(iv) Further work in this area must concentrate on the effects on the stereochemistry of variable-temperature and -concentration studies.

(v) The use of other metal amides may further reduce the *Z*/*E* ratio.

6. Discussion: *N*-metallated iminophosphoranes

The complexes (**Table 6.1**) discussed in this chapter were all prepared as described in the experimental section. The chapter will begin with a brief overview of some of the applications of *N*-metallated iminophosphoranes, before a discussion of their solid-state structures both from a single crystal XRD, theoretical and NMR perspective. The solution behaviour of **29** will also be discussed.

Complex	Empirical Formula
29	$Ph_3PNLi{\cdot}LiX{\cdot}2thf$
30	$(Me_2N)_3PNLi$
31	Ph_3PNCu
32	$(Me_2N)_3PNCu$
33	$Ph_3PNMgCl{\cdot}OP(NMe_2)_3$
34	$(Me_2N)_3PNMgBr{\cdot}HNP(NMe_2)_3$
35	$[(Me_2N)_3PNH]_2MgBr_2$

Table 6.1 Complexes discussed in this chapter

6.1 Background

N-lithio(triphenyl)iminophosphorane ($LiNPPh_3$) has been known for nearly thirty years,[1] although it has generally not been isolated, but generated and used *in situ*. Indeed, it is only very recently that the isolation and structural characterisation of simple *N*-(s-block-metallated) iminophosphoranes has been reported.[2,3,4]

---

[1] H. Schmidbaur and G. Jonas, *Chem. Ber.*, **100**, 1120 (1967).
[2] A. S. Batsanov, M. G. Davidson, J. A. K. Howard, S. Lamb, C. Lustig and R. D. Price, *J. Chem. Soc., Chem. Commun.*, 1211 (1997).
[3] S. Anfang, G. Seybert, K. Harms, G. Geisler, W. Massa and K. Dehnicke, *Z. Anorg. Allg. Chem.*, **624**, 1187 (1998).
[4] A. S. Batsanov, P.D. Bolton, R. C. B. Copley, M. G. Davidson, J. A. K. Howard, C. Lustig and R. D. Price, *J. Organomet. Chem.*, **550**, 445 (1998).

N-lithioiminophosphoranes find utility in organic and inorganic syntheses as synthons for RN^{2-} and as precursors for *N*-substituted iminophosphoranes containing either inorganic, organometallic or organic fragments.[5,6] Recent *ab initio* MO calculations[7] suggest that iminophosphoranes are able to form strong complexes with lithium, maybe even stronger than those with phosphine oxides, a common Lewis base for s-block metals.[8]

N-lithioiminophosphoranes provide a facile route (**Scheme 6.1**) to primary or secondary amines via the hydrolysis of monoalkylated-iminophosphoranes or dialkylated-aminophosphonium salts.[9] It is possible to prepare amino acids by extending this to α-bromo esters.

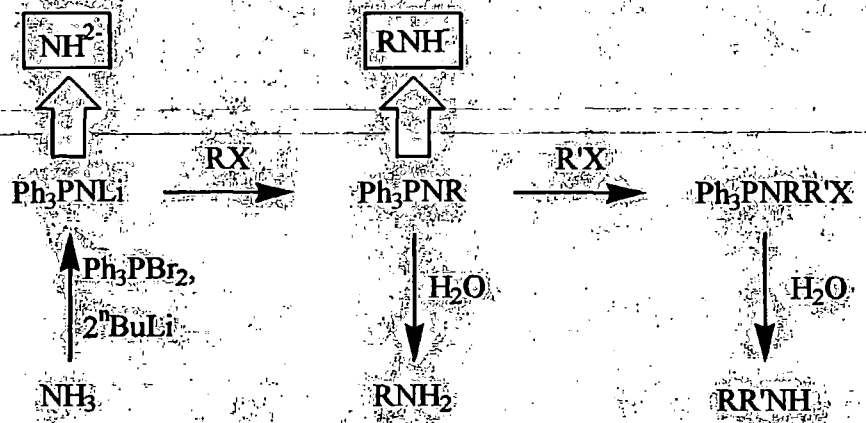

Scheme 6.1

Acylation of *N*-lithioiminophosphoranes is possible without the use of an activated acylating agent, e.g. at 40°C $LiNPPh_3$ reacts with esters, whereas there is no reaction with Ph_3PNH **4** at the same temperature. There are many other reactions that are possible using an *N*-lithiated derivative, including tosylation and bromination (**Scheme 6.2**), making them useful and versatile intermediates for organic synthesis.

[5] A. W. Johnson with special contributions by W. C. Kaska, K. A. O. Starzewski and D. A. Dixon, *'Ylides and Imines of Phosphorus'*, John Wiley & Sons Inc., New York (1993).
[6] H-J. Cristau, J. Kadoura, L. Chiche and E. Toreilles, *Bull. Chim. Soc. Fr.*, **4**, 515 (1989).
[7] D. R. Armstrong, M. G. Davidson and D. Moncrieff, *Angew. Chem., Int. Ed. Engl.*, **34**, 478 (1995).
[8] W. Setzer and P. von R. Schleyer, *Adv. Organomet. Chem.*, **24**, 353 (1985); C. Shade and P. von R. Schleyer, *Adv. Organomet. Chem.*, **27**, 169 (1987); R. Snaith and D. S. Wright, *'Lithium Chemistry- A Theoretical and Experimental Overview'*, ed. A. M. Sapse, P. von R. Schleyer, Wiley, New York (1995).
[9] H-J. Cristau, *Chem. Rev.*, **94**, 1299 (1994).

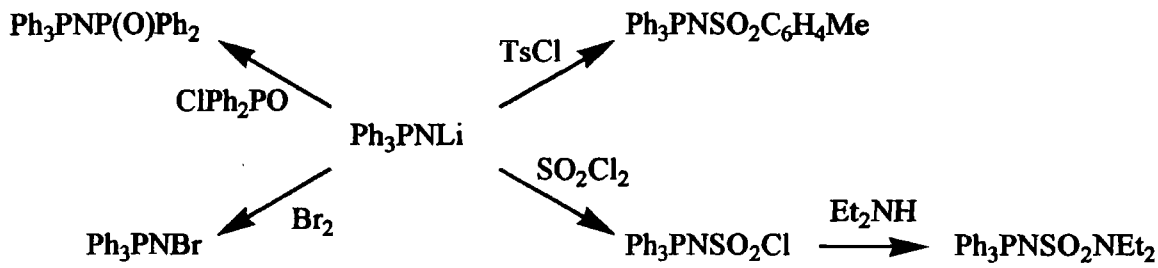

Scheme 6.2

N-acyliminophosphoranes are thermally unstable at approx. 200°C and decompose to give nitriles.[10] Application of *N*-lithioiminophosphoranes in acylation permits new *N*-(α,β-unsaturated)iminophosphoranes to be accessed. These are able to achieve intramolecular aza-Wittig reactions at lower temperatures (65-110°C) to yield the corresponding nitriles. Dilithiation of the aminophosphonium salt, followed by acylation, allows a one-pot synthesis of the cyclic product (**Scheme 6.3**).

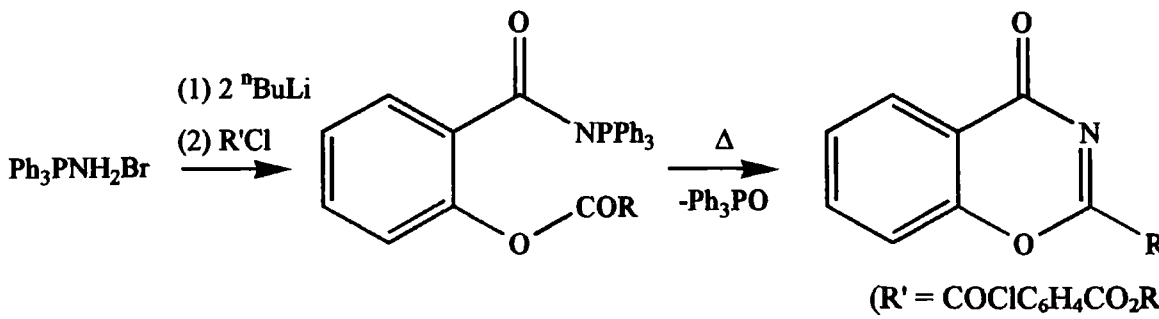

Scheme 6.3

Use of a chiral phosphine group in the generation of *N*-lithioiminophosphoranes may produce chiral aminating agents, particularly useful in the generation of amino acids. Their use as transmetallation reagents (*vide infra*), especially for transition metals, is likely to increase dramatically in the future. There is already an example of a phosphonium ylide-transition metal complex that can be applied to stereospecific syntheses (**Scheme 6.4**).[11]

---

[10] H-J. Cristau, A. Hammami and E. Torreilles, *Heteroatom Chem.*, **10**, 49 (1999).

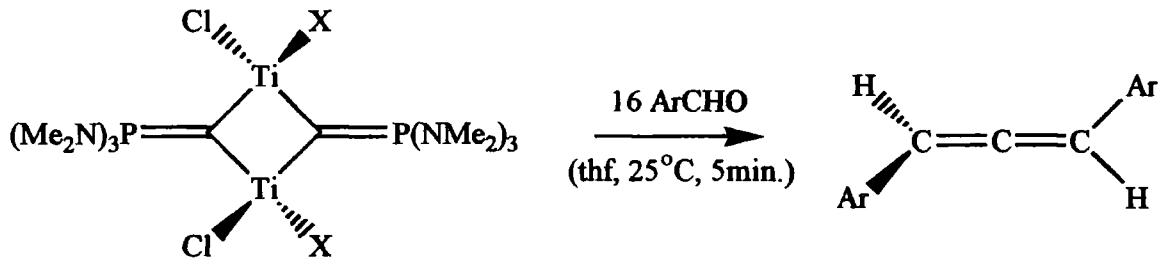

Scheme 6.4

N-substitution by an inorganic fragment has been known since the first reported synthesis of Ph_3PNLi.[1] Simple examples include substitution by a trialkylsilyl, germyl or stannyl group (**Scheme 6.5**).[1]

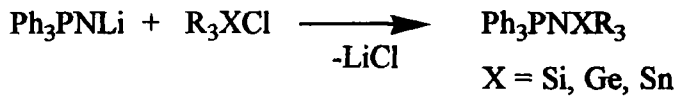

Scheme 6.5

6.2 Solid and solution-state studies of 29

6.2.1 Solid-state study of 29

As described in chapter 4, examples of fully structurally characterised s-block metal iminophosphorane complexes are very scarce.[2,3,4] The majority of reported structures involve the imino nitrogen only as an intramolecular stabilising group (**Fig. 4.21**).[12]

Reaction of amino(triphenyl)phosphonium halide† with two equivalents of ^{n}BuLi in arene solution yields a white precipitate, which dissolves upon the addition of a small excess of

---

[11] K. A. Hughes, P. G. Dopico, M. Sabat and M. G. Finn, *Angew. Chem., Int. Ed. Engl.*, **32**, 554 (1993).
[12] A. Muller, B. Neumuller and K. Dehnicke, *Chem. Ber.*, 253 (1996); F. Lopez-Ortiz, E. Pelaez-Arango, B. Tejerina, E. Perez-Carreno and S. Garcia-Granda, *J. Am. Chem. Soc.*, **117**, 9972 (1995); A. Steiner and D. Stalke, *Inorg. Chem.*, **32**, 1977 (1993); *Angew. Chem., Int. Ed. Engl.*, **34**, 1752 (1995).
† either chloride or bromide.

thf with gentle heating. Upon cooling to ambient temperature, a crop of transparent blocks of **29** was isolated. Following single crystal XRD studies on both benzene (**29b**) and toluene (**29a**) solvated crystals (**Fig. 6.1**) obtained using the bromide salt, the solid-state structure was shown to be a tetramer.[2] Moreover, the tetramer can be considered to be constituted of one lithium bromide dimer and one dimer of *N*-lithio(triphenyl) iminophosphorane. There is also a cisoid arrangement of phosphorane iminato ligands ($Ph_3P{=}N^-$) across the $Li_4N_2Br_2$ core.

The synthesis and isolation of **29** by the dilithiation of an amino(triphenyl)phosphonium halide represents a significant result. The ability to solubilise lithium halides, and thus prevent association into an infinite $(LiX)_\infty$ lattice (c.f. NaCl lattice), demonstrates the powerful Lewis basicity of *N*-lithioiminophosphoranes. There are several other mixed-anion pseudo-cubane structures known, but these complexes all contain C-Li[13] and O-Li[14] fragments. The family of complexes **29**, are unique as mixed-anion tetramers containing N-Li fragments.

The structure‡ within the tetramer consists of a cubanoid $Li_4N_2Br_2$ core (**Fig. 6.2**), in which each lithium is four coordinate via association with three μ_3 bridging anionic centres and one terminal thf molecule. One face of the cubanoid is distorted (Li_2Br_2) by a fold along the Li··Li axis (angle of fold = 30°). This distortion may not be entirely due to steric effects (anion-anion repulsions), although it is something that has been noted in other structures containing a $Li_4R_2X_2$ core.[13a,14]

---

[13] *(a)* H. Schmidbaur, A. Schier and U. Schubert, *Chem. Ber.*, **116**, 1938 (1983); *(b)* H. Hope and P. Power, *J. Am. Chem. Soc.*, **105**, 5320 (1983).

[14] P. A. van der Schaaf, M. P. Hogerheide, D. M. Grove, A. L. Spek and G. van Koten, *J. Chem. Soc., Chem. Commun.*, 1703 (1992).

‡ all crystallographic data given for **29** is for the benzene-solvated complex **29b**.

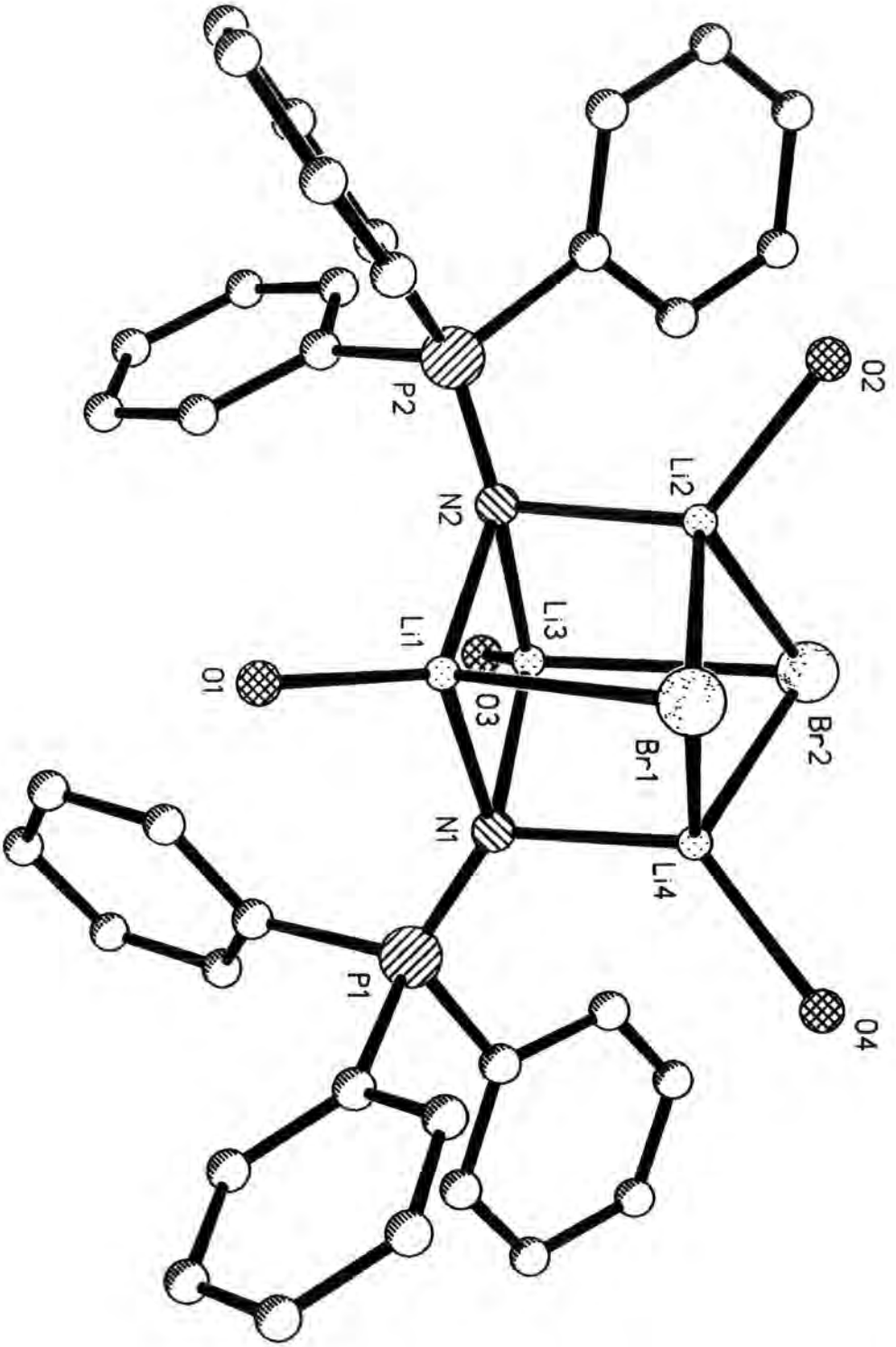

Figure 6.1 Single crystal XRD structure of 29 (thf carbon atoms omitted for clarity)

If one considers the tetramer as composed of two separate dimeric ring systems (Li_2N_2 and Li_2Br_2) then a comparison of the inter- and intra-molecular N-Li and Br-Li distances reveals another possible explanation for the ring puckering. As regards the N-Li distances, the average intermolecular separation is 1.971 Å [e.g. Li(2)-N(2)], whereas the analogous intramolecular distance averages 2.005 Å [e.g. Li(1)-N(1)]. The average intermolecular Br-Li distance [e.g. Li(1)-Br(1)], however, is 2.738 Å, whilst the corresponding intramolecular separation is 2.603 Å [e.g. Li(2)-Br(2)]. This may be a simple coordination phenomenon or perhaps the lithium cations exhibit a preference for interactions with the phosphorane iminato ligand over the bromide anion. These results alone, do not resolve the question as to whether the core originates from Li_2Br_2 and Li_2N_2 or two LiN.LiBr moieities. The phosphonium centres are essentially identical and pyramidalised [ave. sum of angles = 348°].

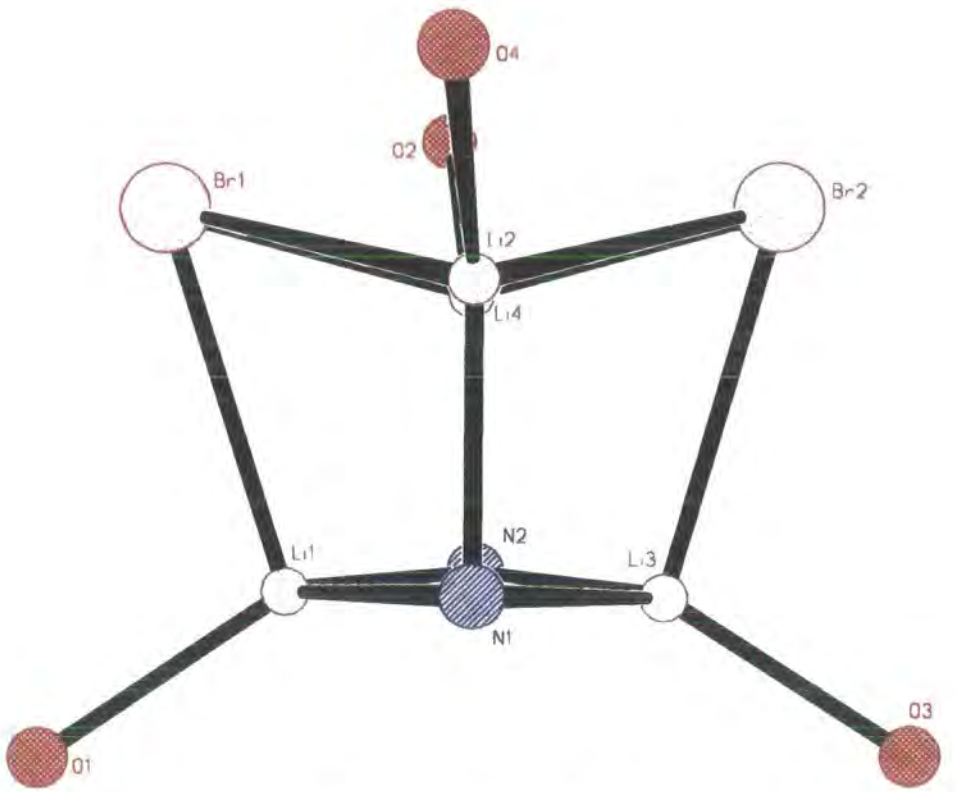

Figure 6.2 Core of 29

In the most similar known structure, a lithium phenolate-lithium iodide aggregate,[14] the same preference for the phenolate over iodide anion is not observed, i.e. phosphorane iminato ligands appear to be more strongly Lewis basic than phenolate anions.

Complex **29** provides structural information for the phosphorane iminato ligand, a useful ligand in organic synthesis[6,9,10] and transition metal chemistry.[15] The P-N bond length in **29** [1.541 Å (ave.)] is short, in comparison to the recognised P=N double bond range [1.55 to 1.64 Å].[16] This shortening of the P-N bond in comparison to the parent ligand **4** [1.582(2) Å][17] and neutral, but complexed ligands **13** [1.578(2) Å] and **14** [1.581(2) Å], is a feature manifested in all *N*-s-block-metallated iminophosphorane complexes. This is due mainly to electrostatic shortening upon deprotonation (*vide infra*) and the μ_3 capping of each Li_3 face.

Very recently, the structure of $[(LiNPPh_3)_6 \cdot 5thf]$ has been reported.[3] The structural parameters obtained are in good agreement with **29**. The thf molecules are not complexed to lithium. The intermolecular N-Li bond lengths average 2.031 Å and the intramolecular N-Li bond lengths average 1.989 Å, which are similar in magnitude to those found in **29**. Another feature of $[(LiNPPh_3)_6.5thf]$ is a short P-N bond length [1.538 Å (ave.)]

Another alkali metal *N*-metallated iminophosphorane complex has also been reported recently, namely $[(KNPPh_3)_6 \cdot 4C_7H_8]$.[18] This complex, a hexamer, is derived from the stacking of two K_3N_3 units to form a ladder-type structure. The structure also contains long-range π-K interactions and a short average P-N separation [1.532 Å].

---

[15] *(a)* K. Dehnicke and J. Stahle, *Polyhedron*, **8**, 707 (1989); *(b)* K. Dehnicke and F. Weller, *Coord. Chem. Rev.*, **158**, 103 (1997); *(c)* K. Dehnicke, M. Krieger and W. Massa, *ibid.*, **182**, 19 (1999).
[16] P. Rademacher, *'Strukturen organischer Molekule'*, Bd. 2, Verlag Chemie, Weinheim (1987).
[17] M. G. Davidson, A. E. Goeta, J. A. K. Howard, C. W. Lehmann, G. M. McIntyre and R. D. Price, *J. Organomet. Chem.*, **550**, 449 (1998).
[18] S. Chitsaz, B. Neumuller and K. Dehnicke, *Z. Anorg. Allg. Chem.*, **625**, 9 (1999).

6.2.2 Solution-state studies of 29[§]

The solution-state structure of **29** is important since dilithiation of aminophosphonium salts is a widely used method of generating *N*-lithioiminophosphoranes *in situ*. A greater understanding of the solution behaviour may explain and allow us to predict some of the properties of these species during organic transformations. Variable-concentration and multi-nuclear NMR experiments were performed on a sample of **29**, together with some cryoscopic studies.

6.2.2.1 Cryoscopy (C_6H_6)[19]

Concentration	ΔT/K	M_r	Degree of association n*
0.003M	0.042	394±42	n = 0.77
0.008M	0.103	494±20	n = 0.96
0.014M	0.151	549±15	n = 1.07

Table 6.2 Cryoscopy results for 29

Cryoscopic studies yield a concentration dependent relative molecular mass. As the amount of solute (**29b**) increases so does the degree of association, n. The values of n calculated indicate deaggregation of the tetramer in solution. There are many possible homo- and heteroanion oligomers that may be present in an arene solution of **29** (**Scheme 6.6**).

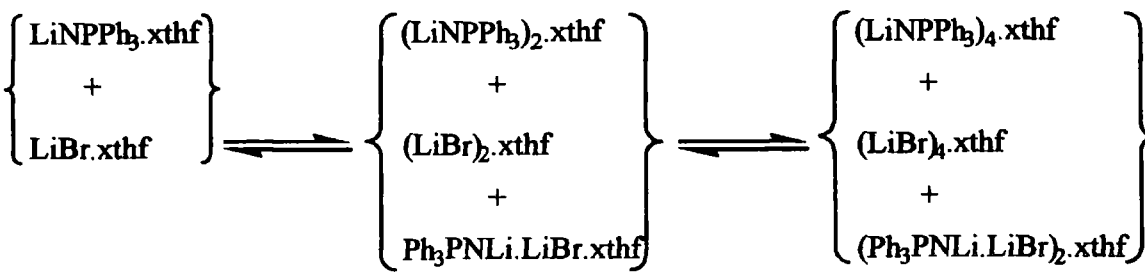

Scheme 6.6 Some possible oligomers in an arene solution of 29

[§] Solution state studies were performed on a benzene-solvated sample of **29b**.

[19] M. G. Davidson, R. Snaith, D. Stalke, D. S. Wright, *J. Org. Chem.*, **58**, 2810 (1993).

* The degree of association n, was calculated by reference to one unit of ($Ph_3PNLi{\cdot}LiBr{\cdot}2thf$).

6.2.2.2 Variable concentration NMR studies @ 293K, solvent C_6D_6.

0.01M solution		0.05M solution		0.09M solution	
δ/ppm	Integral	δ/ppm	Integral	δ/ppm	Integral
2.0	1 (s)	1.8	1 (s)	1.8	1 (s)
-1.2	3.4 (s)	-1.3	3.5 (s)	-1.3	4.5 (s)
-3.9	1.9 (s)	-4.5	4.7 (s)	-4.5	7.8 (s)
-5.5	0.4 (s)	-5.5	0.3 (s)	-5.5	1.5 (s)

Table 6.3 VC ^{31}P NMR studies of 29

The variable concentration ^{31}P NMR studies were performed at ambient temperature. As the concentration increases, there are marked changes in the relative intensities of the peaks. Relative to the peak at approximately 2ppm, the other peaks all increase in intensity. As was the case with the cryoscopy results, these alone do not indicate which species are present in solution, but suggest that there are several species involved in complex solution equilibria.

6.2.2.3 Other multi-nuclear NMR studies @ 293K

^{31}P and ^{7}Li NMR studies were also performed in both benzene and toluene solutions at ambient temperature. When a previously isolated sample of **29** is re-dissolved in toluene, lithium bromide is precipitated from the solution upon heating. This finding can, presumably, be related to the difference in boiling points between toluene and benzene (110-1 and 80 °C) respectively.[20] In the absence of an excess (6-8 fold) of thf, such as is the case during the preparation of **29**, heating of **29** between 80 and 111 °C converts the lithium bromide adduct (kinetic product) into an *N*-lithioiminophosphorane (thermodynamic product), without any complexed lithium bromide.

[20] D. R. Line, Ed., *'Handbook of Chemistry and Physics'*, 73rd ed., 8-49 (1992-3).

C_6D_6 solution		C_7D_8 solution	
δ /ppm	Multiplicity	δ/ppm	Multiplicity
-0.52	Singlet	-0.82	Singlet
2.49	Singlet	2.48	Singlet
4.26	Singlet	-	-
4.94	Singlet	-	-
5.64	Singlet	5.50	Singlet

Table 6.4 ^{31}P NMR data for 29 in C_6D_6 and C_7D_8

C_6D_6 solution		C_7D_8 solution	
δ /ppm	Multiplicity	δ/ppm	Multiplicity
1.5-1.8	Multiplet	1.88	Singlet
1.8-2.1	Multiplet	2.12	Singlet
3.13	Singlet	3.32	Singlet

Table 6.5 ^{7}Li NMR data for 29 in C_6D_6 and C_7D_8

The existence of only $(LiNPPh_3)_n$ oligomers in a C_7D_8 solution in the case of these NMR studies (^{31}P and ^{7}Li) allows us to tentatively identify some species. The presence of three signals in the ^{31}P NMR in C_7D_8 solution can be assigned to monomer, dimer and either tetramer or hexamer (n = 1, 2, 4 or 6). The latter cannot be satisfactorily resolved since in the solid-state, thf plays no bonding role to lithium for $(LiNPPh_3)_6$[3] and this may be similarly true in solution. Therefore, a tetrameric species involving thf complexation may be formed, or a hexamer (hexagonal prism in the solid state) without thf-solvation.

This assignment suggests that the remaining two peaks, i.e. the two present in C_6D_6 solution, but not in C_7D_8 solution, contain lithium bromide. There are still several possibilities and it is not yet possible to assign these to either $(LiBr)_n$.xthf or $(Ph_3PNLi{\cdot}LiBr)_n$.xthf species. The overlap of signals due to the narrow spectral width of ^{7}Li NMR allows little further information as regards the solution behaviour to be gleaned.

Notwithstanding the above ambiguities with regards to the solution behaviour, this result has shown that dilithiation of aminophosphonium halides does not lead to a solution of lithium halide free *N*-lithioiminophosphoranes, as had been previously described.[6] This is important since this is a common method for generating the reactive species in solution, and also since the solution structure is relevant to the nature of the reactive species and lithium bromide is known to have an effect on the reactivity and selectivity of a reagent.[5]

6.3 Solid-state studies of complexes 30-35

Complex **30** is also an *N*-lithioiminophosphorane, $[(Me_2N)_3PNLi]$. Despite attempts to study the solid-state structure through XRD techniques, it has yet to be satisfactorily resolved. (A unit-cell was calculated, but the resulting final data set could not be solved). However, extrapolating from the information for **29** and also that for $[(LiNPPh_3)_6{\cdot}5thf]$,[3] we can draw some assumptions with regards to the solid-state structure.

It is generated by reaction of **5** with ^{n}BuLi in toluene, can be isolated as a crystalline solid and stored in a dry, glove box. Its NMR data (**Chapter 3**) and the full characterisation of its derivatives (*vide infra*), identify it as an *N*-lithiated iminophosphorane. The solid-state structure is most likely to be based on a hexamer, since there is no coordinating solvent present in the lattice to deaggregate the ideal hexameric structure. We may also infer that the average P-N separation will be shortened in comparison to the parent ligand **5**.

Transmetallation reactions are well known in chemistry, often in the synthesis of organometallic compounds from their salts.[21] The transmetallation of *N*-lithioiminophosphoranes is a simple way of producing novel *N*-metallated iminophosphoranes. The syntheses of **31** and **32** are two such examples of this type of reaction.

---

[21] Ch. Elschenbroich and A. Salzer, *'Organometallics - A Concise Introduction'*, VCH, 2nd Edn. (1992).

Reaction of **29** (or $LiNPPh_3$ generated *in situ*) with Cu^ICl results in a transmetallation reaction (**Scheme 6.7**). The resulting complex **31** was identified by NMR spectroscopy and a single crystal XRD study.

$$2(Ph_3P{=}NLi.LiBr.2thf)_2 \xrightarrow[-2\ LiCl,\ 2\ LiBr]{+\ 4\ Cu^ICl} (Ph_3P{=}NCu)_4$$

Scheme 6.7 Transmetallation reaction of 29

In the solid-state **31** adopts a Cu_4N_4 square core with μ_2-bridging nitrogen atoms at the corners and linear Cu^I atoms (**Fig. 6.3a**). Close inspection reveals two distinct types of phosphorane iminato ligands, viz. P(1)/P(4) and P(2)/P(3). The two types of ligand adopt a transoid arrangement across the bridging Cu_4N_4 core with respect to each other, but have a cisoid relationship with the other ligand of their type (**Fig. 6.3b**), i.e. P(1) and P(3) are situated transoid with respect to each other, but P(1) and P(4) have a cisoid relationship.

Consider the two distinct type of ligands (**Table 6.6**), the phosphorus environments are fairly similar, both are pyramidalised and both contain a unique C_{ipso}-P-N bond vector. The two corresponding nitrogen environments, e.g. N(1) and N(2), are markedly different. This is clearly seen in **Fig. 6.4**, which reveals that at N(1) the copper atoms are situated 37.5° below the P-N bond, whereas at N(2) the copper atoms lie only 23° below the P-N bond. Thus, N(1) is more pyramidalised than N(2).

Bond vector	P-N bond length/Å	$\Sigma\angle_{phosphorus}$ / °	$\Sigma\angle_{nitrogen}$ / °
P(1)-N(1)	1.558(8)	341	341
P(2)-N(2)	1.555(7)	343	352
P(3)-N(3)	1.551(7)	342	352
P(4)-N(4)	1.561(7)	344	342

Table 6.6 Summary of structural parameters for 31

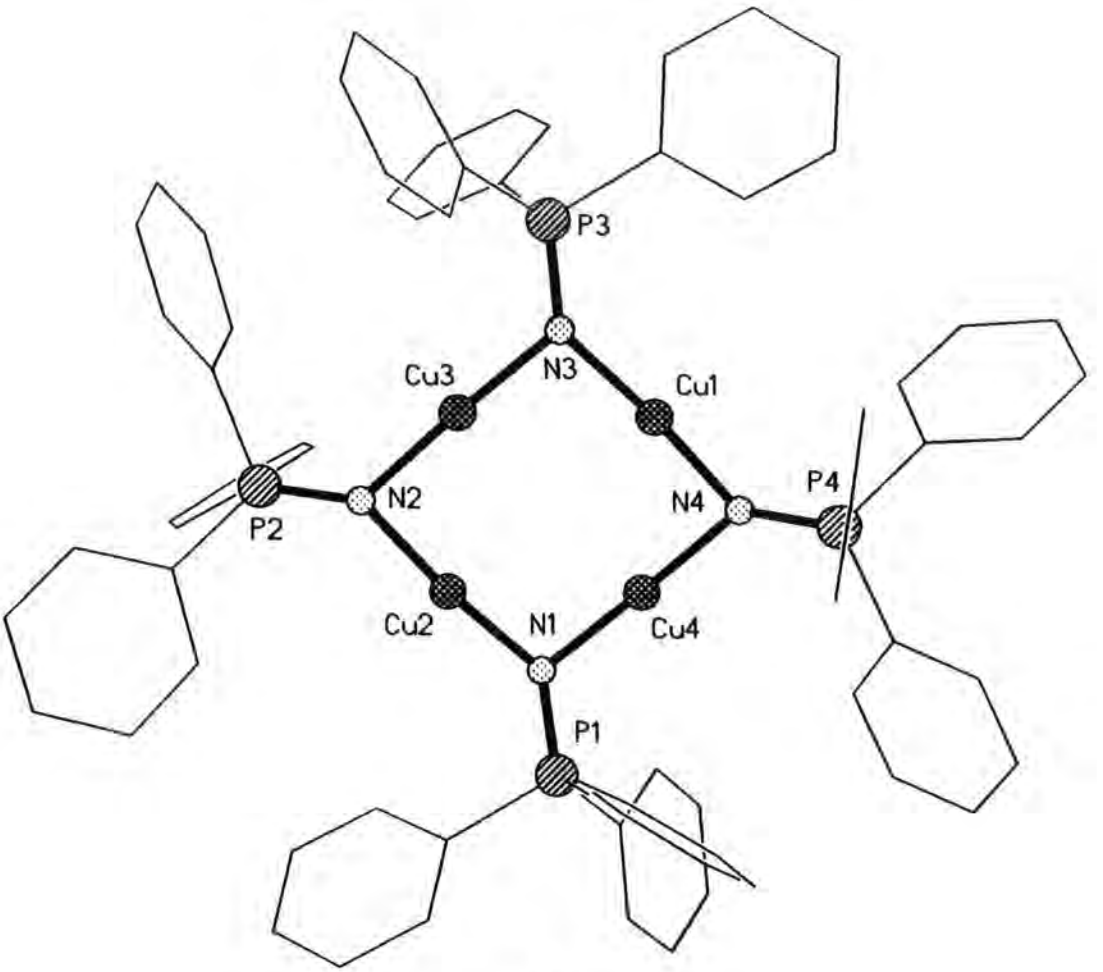

(a)

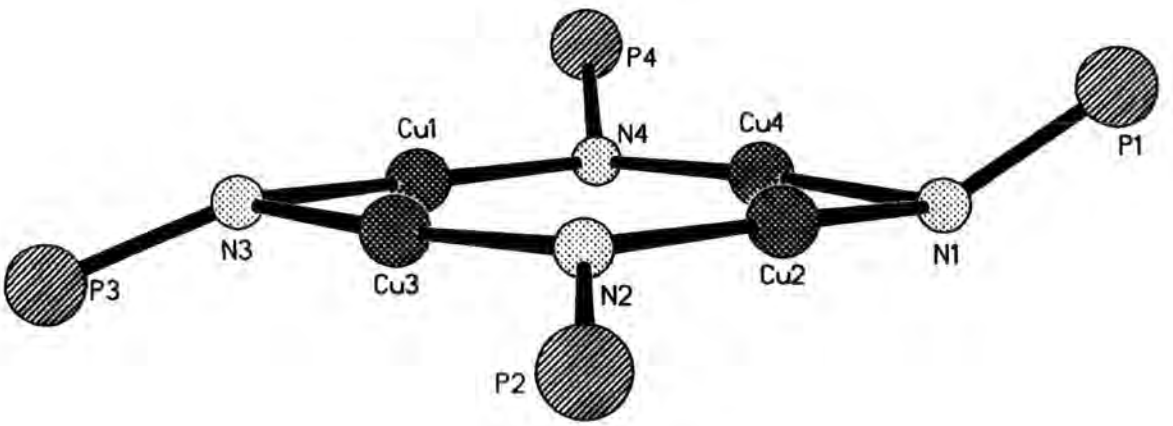

(b)

Figure 6.3 (a) Single crystal XRD structure of 31 (phenyl groups in outline); (b) Core atoms of 31 showing transoid and cisoid relationships

The average P-N bond length [1.556 Å] is shorter than that seen for the parent iminophosphorane ligand **4** [1.582(2) Å],[17] a feature that was also noted for **29** and $[(LiNPPh_3)_6 \cdot 5thf]$.[3]

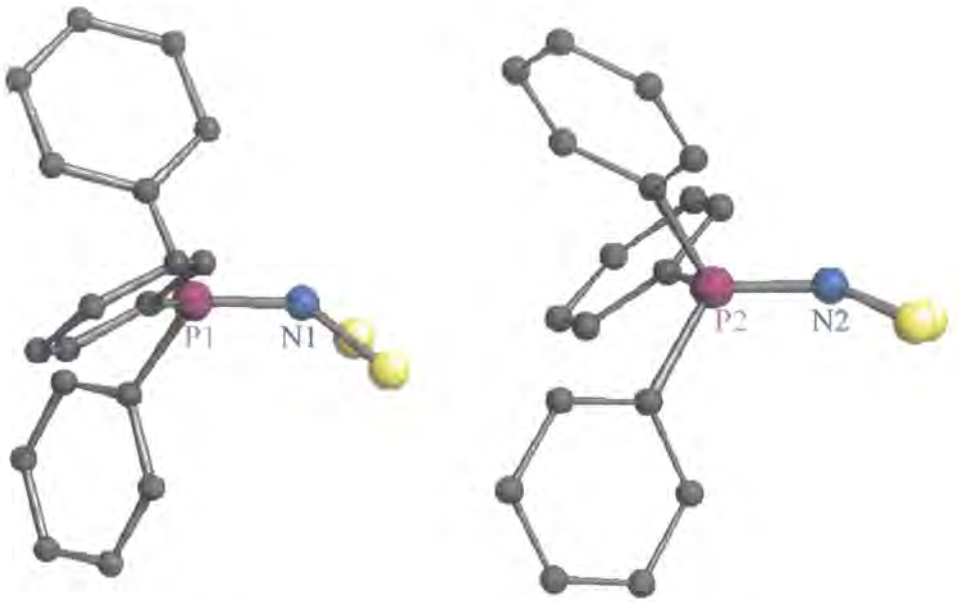

Figure 6.2 Two distinct ligands of 31

The Cu-N bond lengths range from 1.855 to 1.880 Å, with a Cu_4N_4 core that is approximately square [ave. N-Cu-N angle = 176 °; ave. Cu-N-Cu angle = 93 °]. The Cu-N distances here are much shorter than those previously reported for copper-iminophosphorane complexes, which range from 1.96- 2.03Å.[22,23,24] More significantly, the Cu-N distances are shorter even than for simple Cu^I amides with similar Cu_4N_4 square cores [1.92 Å (ave). for CuHMDS[25]].

Previously reported copper-iminophosphorane complexes have generally contained Cu^{II} centres and have tended to form clusters, but very recently [15c] a Cu^I-iminophosphorane complex was described showing a similar Cu_4N_4 square core and μ_2 bridging nitrogen

---

[22] R. M. zu Kocker, A. Behrendt, K. Dehnicke and D. Fenske, *Z. Natursforsch*, **49b**, 301 (1994); R. M. zu Kocker, A. Behrendt, K. Dehnicke and D. Fenske, *ibid.*, **49b**, 987 (1994).
[23] T. Miekisch, H. J. Mai, R. M. zu Kocker, K. Dehnicke, J. Nagull and H. Goesmann, *Z. Anorg. Allg. Chem.*, **622**, 583 (1996).
[24] R. M. zu Kocker, J. Pebler, C. Friebel, K. Dehnicke and D. Fenske, *Z. Anorg. Allg. Chem.*, **621**, 1311 (1995).
[25] A. M. James, R. K. Laxman, F. R. Fronczek and A. W. Maverick, *Inorg. Chem.*, **37**, 3785 (1998).

atoms. This example, however, contained neutral iminophosphorane donors and $SO_3CF_3^-$ counter-anions.

Reaction of **30** with Cu^ICl gives a transmetallation reaction, exactly analogous to that between **29** and Cu^ICl (**Scheme 6.7**), produces complex **32**. **32** is the dimethylamino analogue of **31**, and displays many of the same structural features (**Fig. 6.5**). The basis of the structure is, similarly to **31**, a Cu_4N_4 square core with a transoid arrangement of directly opposite phosphorane iminato ligands.

The solid-state structure of **32** also contains two distinct phosphorus environments (**Table 6.7**). Both phosphonium centres are pyramidalised, with similar P-N bond lengths that are notably shortened with respect to **5**,[26] P(1)-N(1) being slightly more abbreviated.

Bond vector	P-N bond length/Å	$\Sigma\angle_{phosphorus}$ / °	$\Sigma\angle_{nitrogen}$ / °
P(1)-N(1)	1.533(2)	345	355
P(2)-N(2)	1.550(2)	344	344

Table 6.7 Summary of structural parameters for 32

As with **31**, the two different phosphorane iminato sites show a marked difference in the degree of pyramidalisation of their iminic nitrogen centres [N(2) is more pyramidal by 11° - **Fig. 6.6**]. This difference is manifested in the orientation of the copper atoms attached to each iminic centre. The two copper atoms [Cu(1) and Cu(2a)] bonded to N(1) lie 17.5° above the P(1)-N(1) bond, whilst the two copper atoms [Cu(1) and Cu(2)] bonded to N(2) are situated 32.5° above the P(2)-N(2) bond.

[26] N. W. Mitzel, *Personal Communication*.

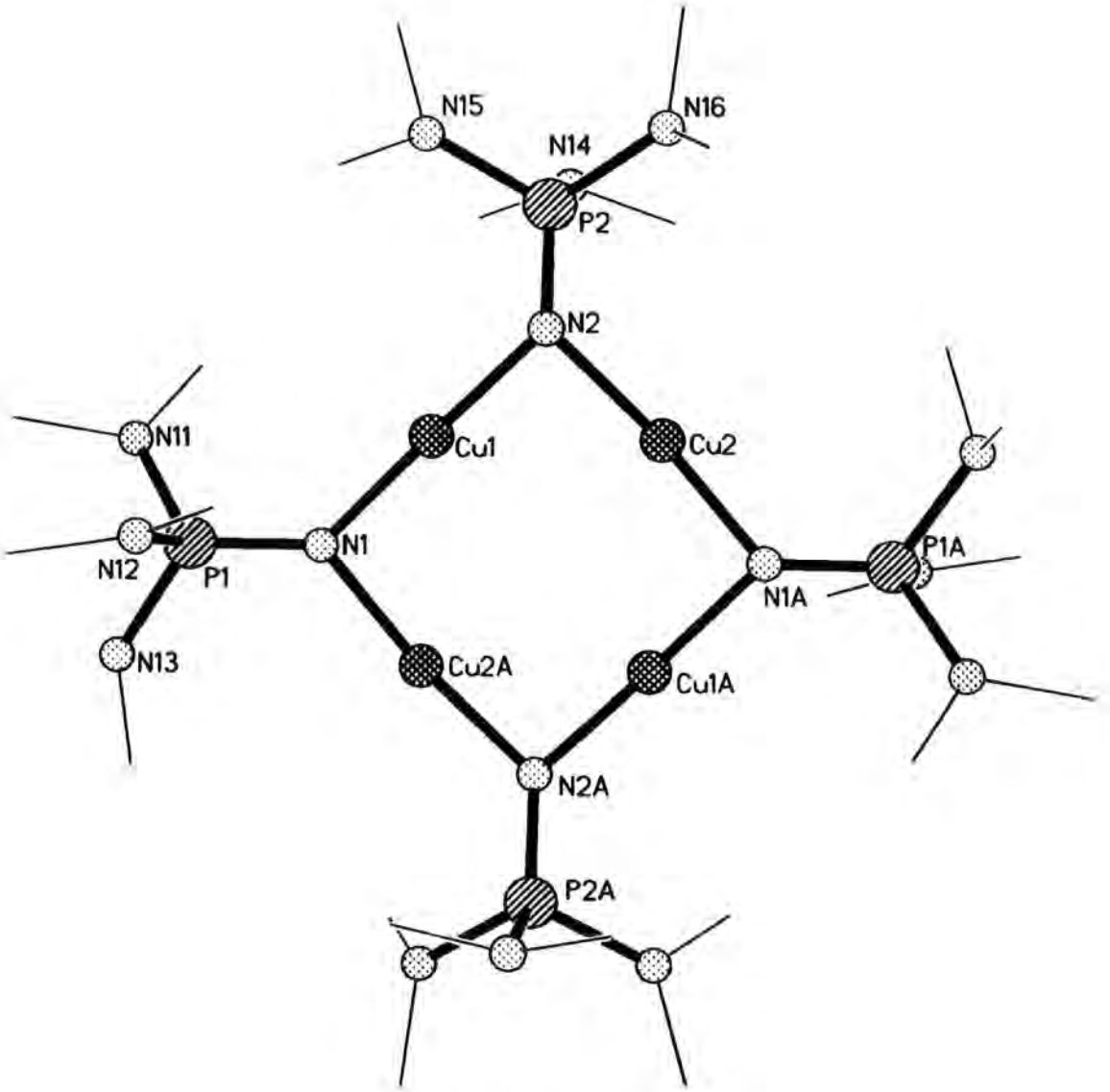

Figure 6.5 Single crystal XRD structure of 32 (methyl groups in outline)

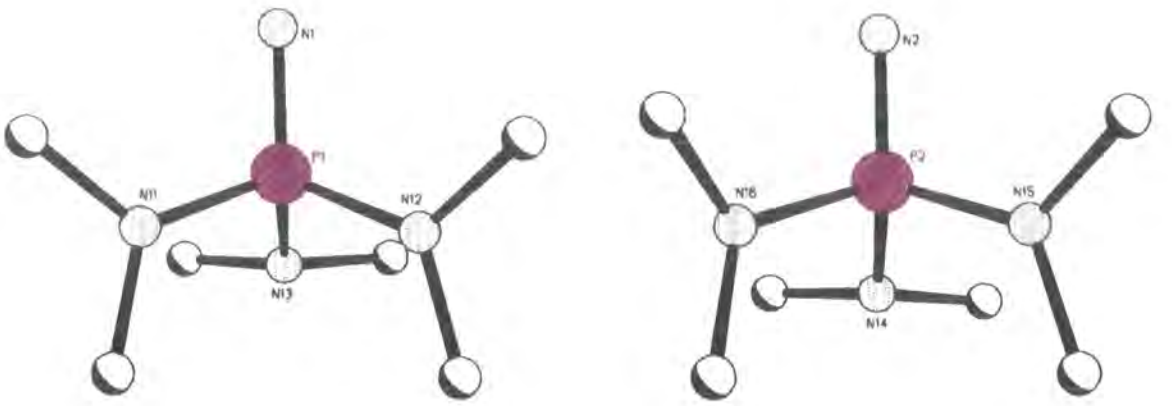

(a) (b)

Figure 6.4 Local phosphorus environment around P(1) and P(2)

At a first glance the two fragments appear very similar. However, upon closer inspection they differ quite dramatically and, in particular, the geometry of the dimethylamino groups.

Bond vector	P-N bond length/Å	$\Sigma\angle_{nitrogen}$ / °
P(1)-N(11)	1.663(2)	360
P(1)-N(12)	1.670(2)	360
P(1)-N(13)	1.682(2)	343
P(2)-N(14)	1.682(2)	344
P(2)-N(15)	1.653(2)	359
P(2)-N(16)	1.684(2)	350

Table 6.3 Structural parameters for dimethylamino groups of 32

For the case of P(1), there is a classic C_s symmetry with one unique dimethylamino substituent on phosphorus that is both pyramidalised and has an elongated P-N distance [P(1)-N(13)]. The other two substituents are planar and vertical (**Fig. 6.6a**).

Considering P(2), there are now two pyramidalised dimethylamino groups, both having elongated P-N distances, one of which is vertical [P(2)-N(16)] and the other horizontal [P(2)-N(14)] (**Fig. 6.6b**). The symmetry is almost C_s, but is slightly distorted due to the non-planar vertical dimethylamino group.

The basis of this distortion and the existence of two slightly different symmetries within the same molecule is not yet fully understood.

As was the case for **31**, the Cu_4N_4 core in **32** is approximately square, [ave. N-Cu-N 175°, ave. Cu-N-Cu 93°]. The Cu-N distances range from 1.852 to 1.864 Å and are also short in comparison to previously reported Cu-N distances for iminophosphoranes,[22,23,24] but are in good agreement with those found for **31**.

Transmetallation using $LiNPPh_3$ was also been recently reported using some lanthanide elements.[3] By reacting cyclooctatetraenide lanthanide complexes, $[Ln(C_8H_8)Cl(thf)_2]$ with *N*-lithioimino(triphenyl)phosphorane in thf, however, the product isolated contains both lithium and the lanthanide element (cerium or samarium) and has the general formula, $[Ln(C_8H_8)Li_3Cl_2(NPPh_3)_2(thf)_3]$.

The incorporation of lithium chloride into the $LiNPPh_3$ lattice is similar to **29**, but the completion of the tetrameric core by a lanthanide element may lead to further fascinating and novel complexes, based on **29** and **30**. The transmetallation reaction (**Scheme 6.7**) applied here in the syntheses of **31** and **32** should, however, be applicable to other metal systems.

Reaction of **4**, in the presence of **7**, with ethylmagnesium chloride yields a white precipitate, which dissolves upon heating. Cooling affords crystals of **33**, which following NMR spectroscopy and a single crystal XRD study were shown to be an *N*-magnesio iminophosphorane complex.[4] The iminophosphorane **4** reacts as a protic acid, whilst **7** completes the tetrahedral coordination sphere of magnesium through its Lewis base type ligation.

In the solid state **33** dimerises through μ_2-bridging ligands (**Fig. 6.8**), to give an almost perfectly square Mg_2N_2 ring. The chlorine atoms sit trans to one another with respect to the Mg_2N_2 ring, the hmpa (**7**) ligands are situated likewise. That the complex bridges through nitrogen and not chlorine is perhaps at first surprising. However, recent calculations on similar systems for Me_2N^-, $(H_3Si)_2N^-$ and $(Me_3Si)_2N^-$ revealed a general

preference over chloride bridging. The enolate anion $H(CH_2{=})CO^-$ was calculated to be favoured over halide bridging in model complexes and this is manifested in $[\{Bu^tC(=CH_2)OMgBr{\cdot}hmpa\}_2]$, which has an analogous structure to **33** (**Fig. 6.7**).[27c]

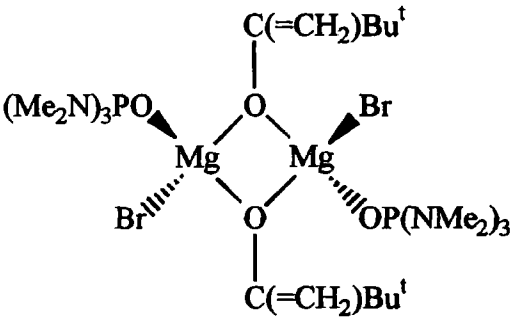

Figure 6.7 Bridging enolate anion in $[\{Bu^tC(=CH_2)OMgBr.hmpa\}_2]$

The structure of **33** allows us to compare two different phosphorane iminato ligand sites, i.e. a μ_3-Li site **29** and a μ_2-Mg site **33**. The phosphonium centre of the phosphorane iminato ligand in **33** is pyramidalised (sum of angles = 345°), with a P-N bond length of 1.555(1) Å. In **29** the phosphonium centre was similarly pyramidalised (sum of angles = 348°), but the P-N bond length was shorter (ave. 1.541 Å). Thus, it appears that the μ_3-Li site is better able to stabilise (shorten) the P-N bond. This argument reinforces the electrostatic arguments given above.

As regards the magnesium geometry: the Mg-N distances [ave. 2.039 Å] are at the short end of the range of previously reported complexed (tetracoordinate) magnesium amides[27] and also those for other Mg-iminophosphorane complexes;[28] the Mg-O distances are in the range of previously reported $X_2Mg(hmpa)_2$ complexes.[27a,29]

---

[27] *(a)* W. Clegg, F. J. Craig, K. W. Henderson, A. R. Kennedy, R. E. Mulvey, P. A. O'Neill and D. Reed, *Inorg. Chem.*, **36**, 6238 (1997); *(b)* K. W. Henderson, R. E. Mulvey, W. Clegg and P. A. O'Neil, *J. Organomet. Chem.*, **439**, 237 (1992); *(c)* I. Schranz, L. Stahl and R. J. Staples, *Inorg. Chem.*, **37**, 1493 (1998).

[28] A. Muller, M. Krieger, B. Neumuller, K. Dehnicke and J. Magull, *Z. Anorg. Allg. Chem.*, **623**, 1081 (1997).

[29] J. F. Allan, W. Clegg, K. W. Henderson, L. Horsburgh and A. R. Kennedy, *J. Organomet. Chem.*, **559**, 173 (1998).

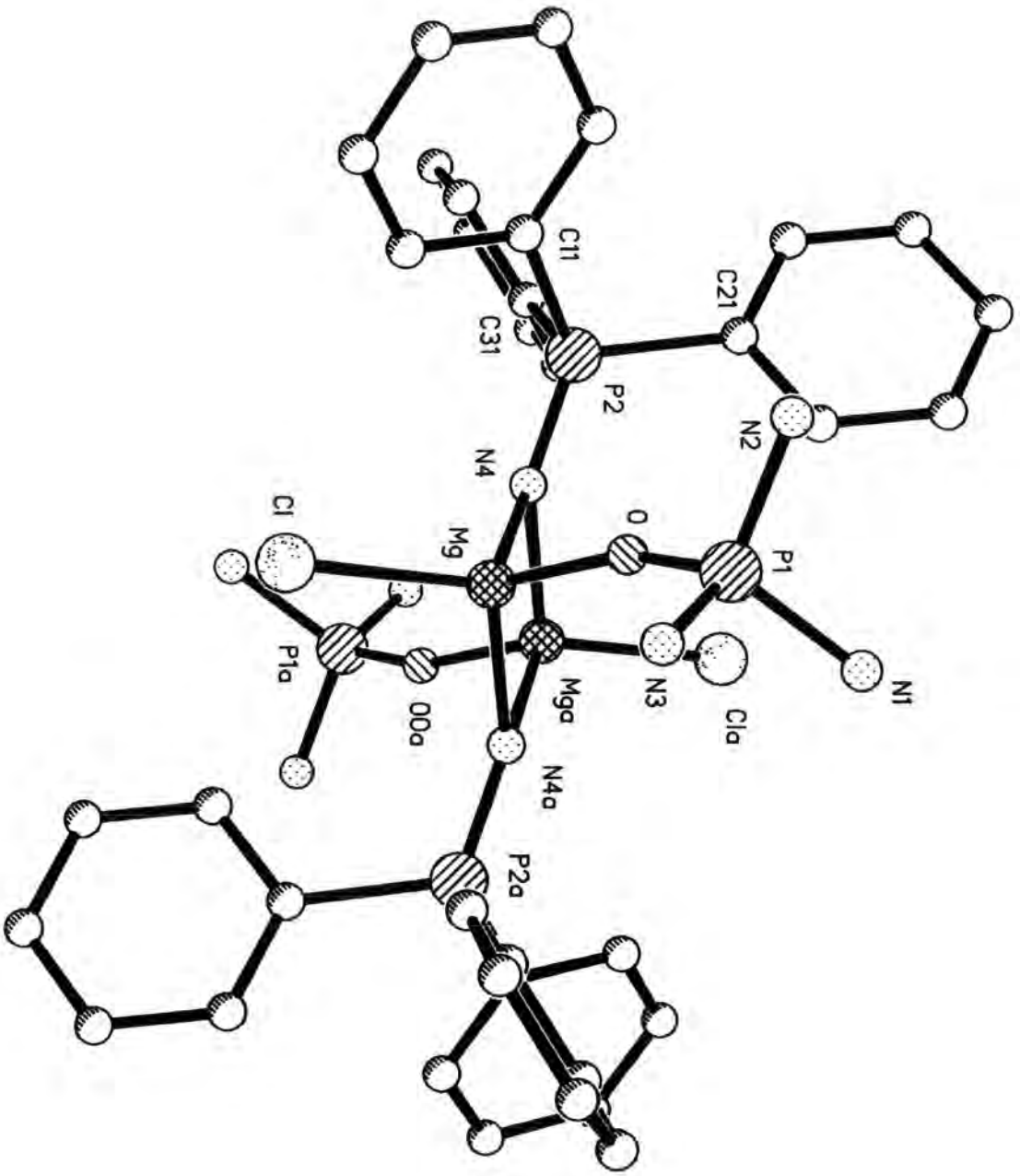

Figure 6.8 Single crystal XRD structure of 33 (methyl groups of hmpa omitted)

A comparison of the geometry of 7 with that of the complexed ligand in **33** highlights some interesting differences. The unique dimethylamino groups are similarly pyramidalised [sum of angles in 7 = 347°; sum of angles in **33** = 350°] and the P-O distance is little changed [**7**: 1.477(1) Å; **33**: 1.497(1) Å]. A closer inspection of the phosphonium centres, however, show a marked difference in the degree of pyramidalisation [**7**: sum of angles = 350°; **33**: sum of angles = 332°]. The P-O-Mg angle [163.7°] is in a range of parameters for Mg-7 complexes described by Clegg et al.[27a] They argue that the magnitude of this angle could be purely a steric effect, based on an ionic representation (**Fig. 6.9**) of 7. The latter allows 7 to solvate a metal centre without a tendency for a particular angle. The differing degrees of pyramidalisation of the phosphonium centres in 7 and **33** may be, similarly, due to steric factors.

$$(Me_2N)_3\overset{+}{P}\text{——}\overset{-}{O}$$

Figure 6.9 Ionic representation of 7

The geometry of the Ph_3PNMg_2 moiety is very similar to that found in **1**.[30] In the latter structure, the Ph_3P group is distorted from idealised C_{3v} symmetry such that the Ph-P bond perpendicular to the methylene plane is unique and elongated with respect to the other two Ph-P bonds, a feature much discussed in **Chapter 4**. The plane of the ylidic methylene group is also tilted towards the unique phenyl group. In the case of Ph_3PNMg_2, the same features persist - the iminic nitrogen is pyramidalised such that the NMg_2 plane is tilted towards the unique P-Ph vector, which is also elongated relative to the other two Ph-P bonds (**Fig. 6.10**).

[30] H. Schmidbaur, J. Jeong, A. Schier, W. Graf, D. L. Wilkinson, G. Muller and C. Kruger, *New. J. Chem.*, **13**, 341 (1989).

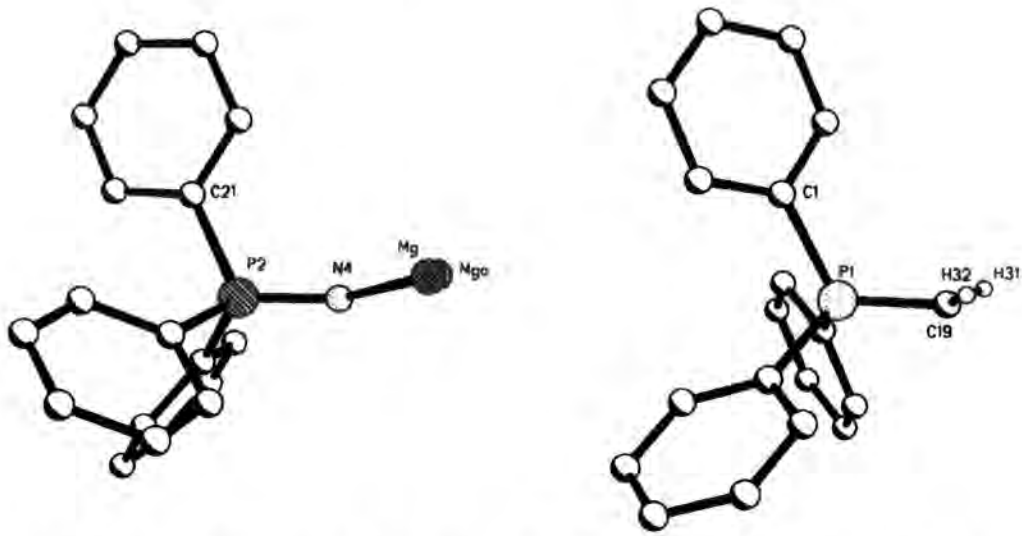

Figure 6.10 Geometry of Ph_3PNMg_2 unit in 33 and Ph_3PCH_2 unit in 1

The rationale for these structural features in **1** is that the ylidic character of the methylene bond causes the distortion. For Ph_3PNMg_2, this can be accounted for by considering the isoelectronic relationship between Ph_3PCH_2 and Ph_3PN^-. Both species have a lone pair of electrons (either in a π-orbital or a N/C p-orbital) which can participate in ylidic P-C or P-N bonding. It is reasonable to assume that the iminic P-N bonding is causing the deviation from ideality.

33 is one of the first simple *N*-magnesioiminophosphorane complexes to be described (one other example of a *N*-metallated complex has been recently reported[28]) and also one of only a few Mg-hmpa complexes to be described.[27,29] There are also two known imido-alkaline earth metal complexes known, viz. $[(Bu^t_2C{=}N)_2Be]_2$ and $[(Ph_2C{=}N)MgBr]_2{\cdot}3thf$.[31,32]

---

[31] B. Hall, J. B. Farmer, H. M. M. Shearer, J. D. Sowerby and K. Wade, *J. Chem. Soc., Dalton*, 102 (1979).
[32] K. Manning, E. A. Petch, H. M. M. Shearer and K. Wade, *J. Chem. Soc., Chem. Commun.*, 107 (1976).

Reaction of two equivalents of **5** with methylmagnesium bromide, with heating, affords a colourless solution. Analysis of crystals (grown at -40°C), initially by NMR spectroscopy and ultimately by a single crystal XRD study (**Fig. 6.12**), reveal the product to be **34**, which is analogous to **33**, i.e. an *N*-magnesioiminophosphorane complex. The difference in **34** is that the ligand **5** acts as both a protic acid and Lewis base donor. This allows us to make a direct comparison between ligated $(Me_2N)_3PN^-$ and $(Me_2N)_3PNH$ (**Fig. 6.11**) within the same molecule.

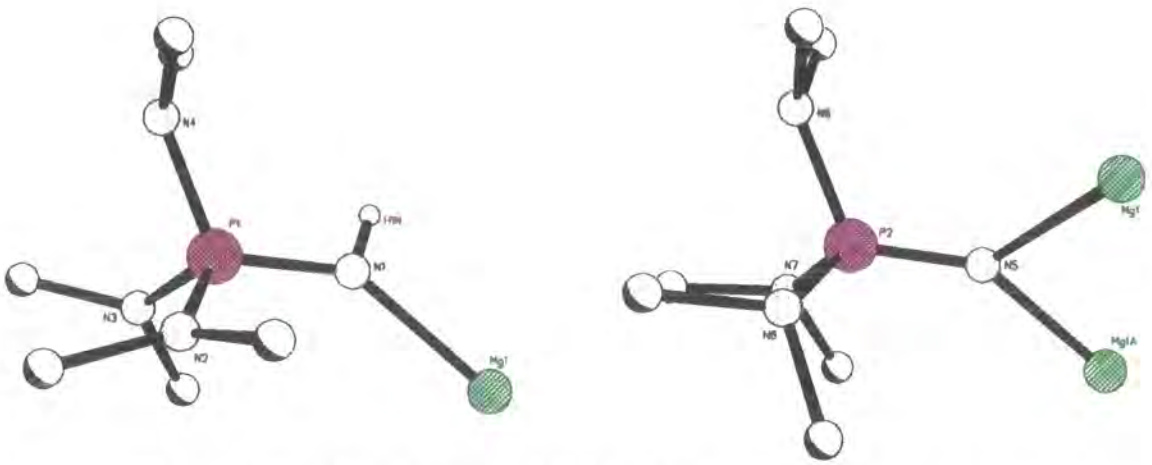

Figure 6.11 $(Me_2N)_3PNH$ and $(Me_2N)_3PN^-$ moieties present in 34

Bond vector	P-N bond length/Å	$\Sigma\angle_{phosphorus}$ / °	$\Sigma\angle_{nitrogen}$ / °
P(1)-N(1)	1.576(5)	337	355[¶]
P(1)-N(2)	1.643(5)	337	358
P(1)-N(3)	1.644(5)	337	360
P(1)-N(4)	1.653(5)	337	349
P(2)-N(5)	1.531(4)	346	358
P(2)-N(6)	1.685(5)	346	349
P(2)-N(7)	1.681(5)	346	356
P(2)-N(8)	1.683(5)	346	347

Table 6.9 Summary of structural parameters for 34

[¶] Based on a fixed hydrogen position.

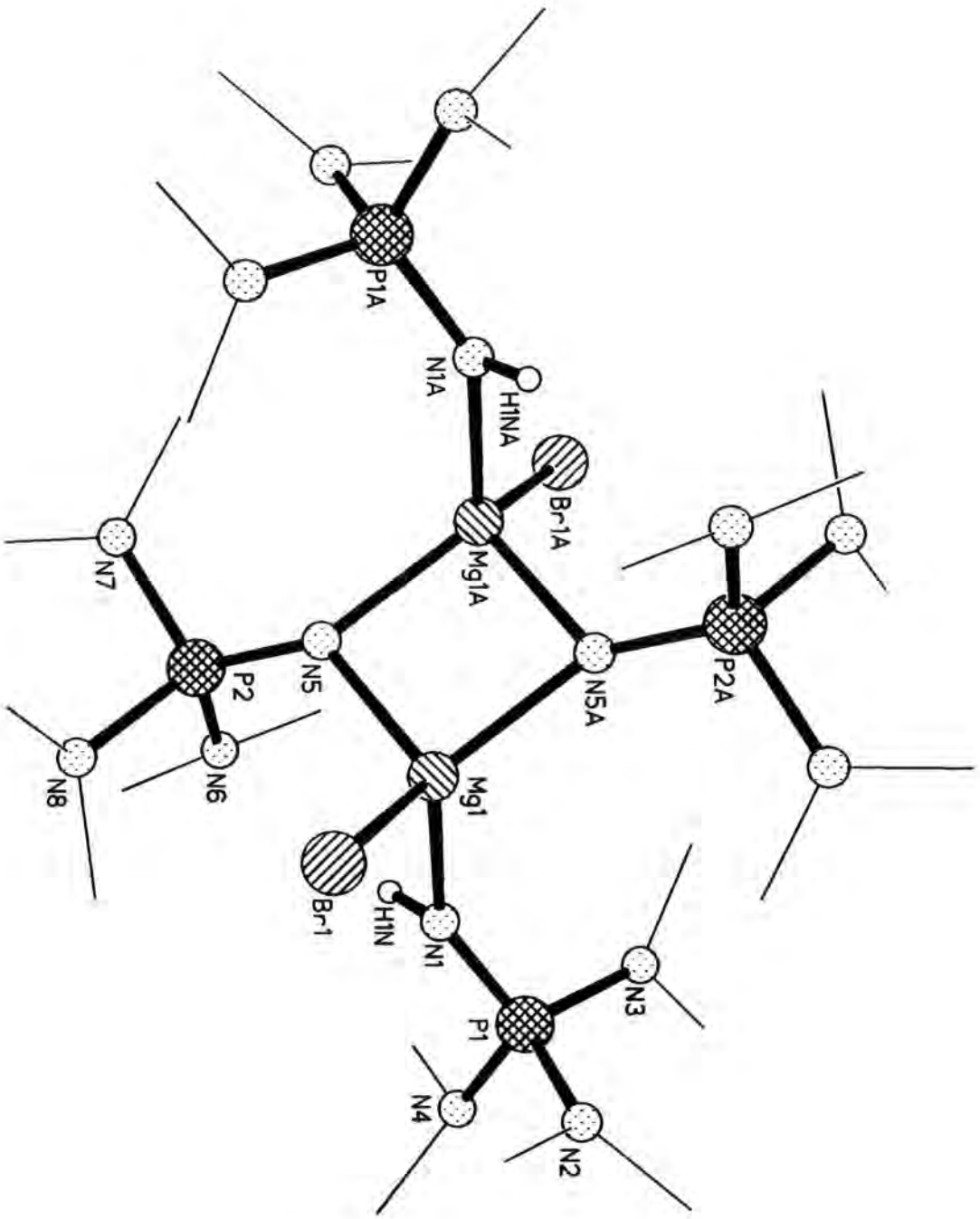

Figure 6.12 Single crystal XRD structure of 34 (methyl groups in outline)

There are some marked differences between the anionic donor $(Me_2N)_3PN^-$ and neutral Lewis base donor $(Me_2N)_3PNH$ (**5**). Firstly, as we have seen for the other *N*-metallated iminophosphorane complexes, the P-N bond length [P(1)-N(1)] for the *N*-metallated species is shorter than that of the neutral donor. Secondly, the phosphonium centre is marginally more pyramidalised in the case of the *N*-metallated species. Perhaps most striking, however, is the large difference in the geometries at the two phosphonium centres.

For the anionic ligand, a pseudo C_s symmetry is adopted [although one of the vertical ligands (N6) is also pyramidalised], but for the case of the neutral Lewis base donor there is now more of a tendency to C_1 symmetry (i.e. the three dimethylamino groups are inequivalent). This result is quite significant since within the same molecule two subtly different chemical environments can be switched from one symmetry to another through changes in their electronic environment. Steric effects can be almost discounted, although the neutral donor does come into close contact with a bromide ion. Crystal packing is also unlikely to have such dramatic effects on the symmetry within the same molecule.

The other parameters of interest in the molecule are largely unremarkable: the Mg-N distances show a similar trend to **33**, with the shorter distances being between magnesium and the anionic nitrogen centre. The P-N-Mg angles [144.8(3) and 146.0(3)°] are more acute than the P-O-Mg range [151.2 to 174.8°] reported for Mg-hmpa complexes.[27a]

The P-N-M angle for similar dimeric structures of iminophosphoranes appears to be in the range 133.0 to 148.2°. For $R_3PNH{\cdot}Li$ complexes this range is 143.6 (**15**) to 148.2° (**13**), whilst the $R_3PNH{\cdot}Na$ complexes discussed have values of 137.9 (**17**) and 138.0° (**14**). Complex **33** has a P-N-Mg angle of 133.0°. [This suggests that the iminophosphorane ligand has more directionality in its bonding to metal centres than **7**, although the small differences in steric demands between all these complexes may not make this a fair comparison to the hmpa (**7**) complexes].

Complex **35** was originally prepared from the reaction of methylmagnesium bromide (in diethylether) and **5**. Following analysis of the starting materials it was discovered that the methylmagnesium bromide was more accurately described as a magnesium bromide-etherate [$MgBr_2(OEt_2)_2$]. Reaction of anhydrous magnesium bromide with **5**, in diethylether, also yields **35**.

35 shows an analogous Lewis base ligation of magnesium to that in **33**. Inorganic complexes of the type $MgBr_2 \cdot xL$ are well known, for example L = thf, C_5H_5N (x = 4 in both cases).[33,34] The analogous magnesium complex of **7** has also been recently reported,[29] viz. $MgBr_2 \cdot (7)_2$.

In the solid state **35** forms a monomer with a transoid arrangement of iminophosphorane (**5**) ligands across the N-Mg-N bridge (**Fig. 6.13**). The Mg-N distance [2.032(3) Å] is comparable to those for **33** and **34**, and similarly close to those for other magnesium complexes of this type.[29] The P-N-Mg angle [140.1°] is close to that for **34**, whilst the P-N separation [1.580(3) Å] is little changed upon coordination, as one would expect. Across the N-Mg-N bridge the angle is 118.6(2)°, but the N-Mg-Br angle [112.5(1)°] is more indicative of a tetrahedral geometry around magnesium.

The phosphonium centre is pyramidalised [sum of angles = 335°], whilst the local symmetry at phosphorus is tending towards C_1. The unique dimethylamino group [at N(4)] is slightly pyramidalised [sum of angles = 353°], but does not have an elongated P-N bond. N(3)-P(1) is elongated and also marginally pyramidalised [sum of angles = 356°].

---

[33] N. Metzler, H. Noth, M. Schmidt and A. Treirl, *Z. Natursforsch*, **49b**, 1448 (1994).
[34] S. Halut-Deportes, *Acta Cryst.*, **B33**, 599 (1977).

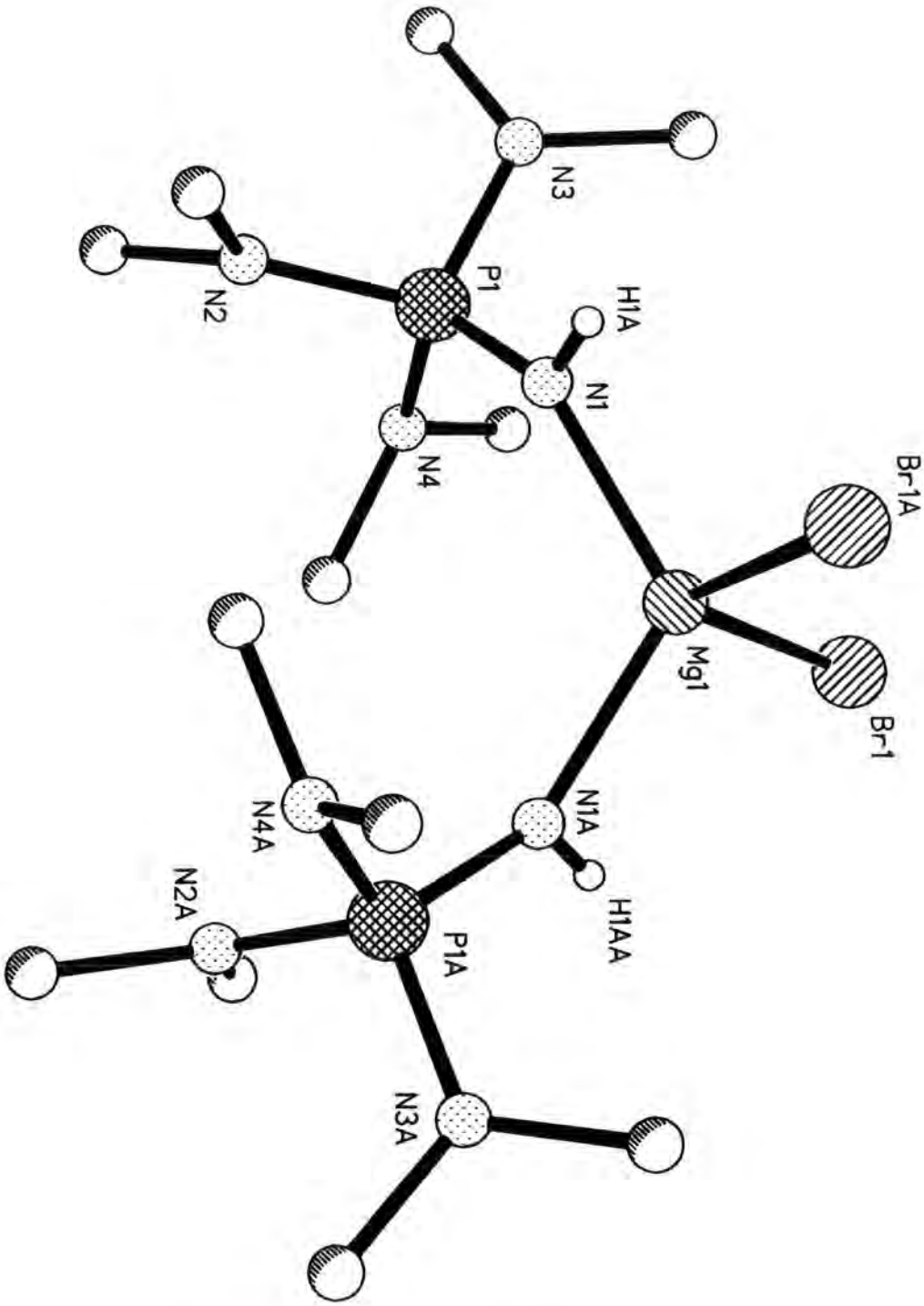

Figure 6.13 Single crystal XRD structure of 35

Comparing the three $(Me_2N)_3PNXMg$ environments discussed so far, there is a pattern of changing symmetry across the series. $(Me_2N)_3PNMg_2$ **[34]** adopts a C_s symmetry (**Fig. 6.14a**), whereas $(Me_2N)_3PNHMg$ **[34]** lies somewhere between C_s and C_1 (**Fig. 6.14b**). Finally, $(Me_2N)_3PNHMg$ **[35]** has a C_1 symmetry (**Fig. 6.14c**).

(a) **(b)** **(c)**

Figure 6.14 Symmetry of $P(NMe_2)_3$ groups in 34 and 35

Across the series (**a**)-(**c**) there are several factors in operation. Firstly, there is a change from an anionic nitrogen centre (**a**) to a neutral nitrogen donor ligand [(**b**) and (**c**)]. Secondly the magnesium environment is changing: in (**a**) and (**b**), magnesium is bonded to three anionic (two nitrogen and one bromide) centres and one neutral (nitrogen) centre; in (**c**) it is bonded to two anionic (bromide) and two neutral (nitrogen) centres.

These results suggest that by making small changes to the phosphorus-nitrogen environment, it is possible to alter the symmetry of the substituent groups on phosphorus. This evidence is perhaps the strongest indication so far that the local symmetry is being affected by electronic, as well as steric, effects.

If one considers a series of related structures of general formula R_3PNR', there is an interesting trend that develops (**Table 6.10**).

Compound/Complex	P-N bond length/Å
Ph_3PNH_2Br	1.615(3)
$Ph_3PNH{\cdot}LiOC_6H_2(^tBu)_2Me$ (**13**)	1.578(2)
$Ph_3PNH{\cdot}NaOC_6H_2(^tBu)_2Me$ (**14**)	1.581(2)
Ph_3PNH (**4**)[¥]	1.562(3)
$Ph_3PNMgCl{\cdot}OP(NMe_2)_3$ (**33**)	1.555(1)
$Ph_3PNLi{\cdot}LiBr{\cdot}2thf$ (**29**)	1.541(3)
$(LiNPPh_3)_6{\cdot}5thf$	1.538(ave.)
$(KNPPh_3)_6{\cdot}4C_7H_8$	1.532(ave.)

Table 6.10 Summary of P-N distances for various structures related to 4

As the phosphorus environment is altered from a phosphonium salt [Ph_3PNH_2Br][35] to an *N*-metallated species [$(KNPPh_3)_6{\cdot}4C_7H_8$],[18] there is a concomitant shortening of the P-N distance. The phosphonium salt has the longest separation (although this is short in comparison to a typical P-N single bond), which is not unexpected. If we consider the two canonical forms described earlier for iminophosphoranes then the cause of this trend becomes clearer (**Fig. 6.15**).

$$R_3P{=\!=}NR' \longleftrightarrow R_3\overset{+}{P}{-}\overset{-}{N}R'$$

Figure 6.15 Two resonance canonical forms of an iminophosphorane

Considering the phosphonium salt [R' = H_2Br], either the phosphorus or nitrogen environment is neutral, depending upon which resonance form we choose (**Fig. 6.16**). Thus, there is little electrostatic shortening of the P-N bond possible. The short distance, however, suggests that there is a large degree of contribution from the imine [P=N] canonical form.

[¥] For continuity the XRD determined P-N distance is given here.

[35] E. Pohl, H. J. Gosink, R. Herbst-Irmer, M. Noltemeyer, H. W. Roesky and G. M. Sheldrick, *Acta Cryst.*, **C49**, 1280 (1993).

Figure 6.16 Canonical forms for Ph_3PNH_2Br

For complexes **13** and **14** and the parent ligand **4**, the representation in **Fig. 6.15** holds true. The parent iminophosphorane is a hybrid of the two canonical forms and whilst **13** and **14** are both complexes of **4**, the nitrogen-metal interaction is essentially ionic (between anionic nitrogen centre and cationic metal centre). Consequently, there is only a small degree of disruption to the P-N bonding and the difference in bond lengths in comparison to the parent ligand **4** is small.

All the *N*-metallated complexes given above (**Table 6.10**), have abbreviated P-N bond lengths in comparison to **4**. One conclusion that can be drawn from this is that metallation of an *N*-(unsubstituted)iminophosphorane stabilises (shortens) the P-N bond. This can, likewise, be explained in terms of the ionic nature of the interaction (**Fig. 6.17**). Upon metallation the nitrogen centre becomes anionic. This allows electrostatic shortening of the P-N bond through an interaction between the cationic phosphonium and the anionic iminic nitrogen centres.

Figure 6.17 Canonical forms for *N*-metallated iminophosphoranes

It is worthy of note that the same feature is observed in *N*-metallated iminophosphorane complexes in which the metal is a lanthanide.[36] Three complexes of the general formula $M_2Cp_3(NPPh_3)_3$ have been synthesised (M = Y, Dy, Er) and subjected to a single crystal XRD study (**Fig. 6.18**).

[36] S. Anfang, K. Harms, F. Weller, O. Borgmeier, H. Lueken, H. Schilder and K. Dehnicke, *Z. Anorg. Allg. Chem.*, **624**, 159 (1998).

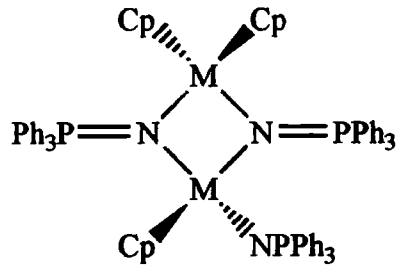

Figure 6.18 Solid-state structure of $M_2Cp_3(NPPh_3)_3$

The P-N distance for the bridging (μ_2) phosphorane iminato ligand is longer than that of the terminal ligand, but both are shorter than that for **4**. For the bridging ligand the P-N bond lengths range from 1.566 (M = Dy) to 1.577 (M = Er, Y) Å, whilst for the terminal ligand the range is 1.512 (M = Er) to 1.547 (M = Y) Å. This further vindicates the electrostatic shortening model proposed for the s-block metallated iminophosphoranes.

6.4 Solid-state NMR studies

Solid-state NMR experiments[37] were performed on five structurally related compounds (**Table 6.11**). All five compounds are based on imino(triphenyl)phosphorane **4**. The aim of the solid-state NMR work was to further investigate the nature and electronic structure of the P-N bond in species whose single crystal XRD structures had already been determined.

Complex	Structure	Reference
-	$Ph_3P{=}NH_2Br$	35
13	$[ArOLi{\cdot}HNP{=}PPh_3]$	This work
4	Ph_3PNH	17
33	$[Ph_3PNMgCl{\cdot}OP(NMe_2)_3]_2$	4
29	$[(Ph_3PNLi{\cdot}LiBr{\cdot}2thf)_2]$	2

Table 6.11 Complexes studied by solid-state NMR

[37] J. C. Cherryman, R. K. Harris, M. G. Davidson and R. D. Price, *J. Braz. Chem. Soc.*, **in press**.

As with the majority of the work in this thesis, the compounds in question are, with one exception, air- and moisture-sensitive. Thus, for the purposes of solid-state NMR it was necessary in each case to prepare sealed glass inserts in a glove box. In some instances samples were packed into a plastic rotor to facilitate fast collection of data.

The XRD data was used to calculate information on the dipolar tensors. It was also used in *ab initio* calculations of the shielding anisotropy and quadrupolar tensors using the Gaussian 94 molecular modelling package.[$]

A full explanation of the theoretical and technical details of solid-state NMR and *ab initio* calculations is far beyond the scope of this work. A brief summary of the results will be given here.

The air-stable sample, Ph_3PNH_2Br, was extensively studied as a model compound, since it could be easily prepared in a plastic rotor insert, thus allowing more versatility to its experiments. As a result of this, its signal/noise ratio is also lower than the other samples studied. A representation of its ^{31}P spectrum is given below (**Fig. 6.19**).

The ^{13}C NMR isotropic shifts reflect the existence of reduced symmetry in the solid-state that was also observed in XRD data (the data for **4** and **33** is uncertain and hence in parentheses).

Compound	δ_{iso}/ppm	$^1J_{PC}$/Hz	δ_{iso}/ppm	$^1J_{PC}$/Hz	δ_{iso}/ppm	$^1J_{PC}$/Hz
Ph_3PNH_2Br	121.4	108	121.4	108	128.7	72
13	130.3	80	132.1	95	134.2	60
4	(128.3)	-	(130.6)	-	(135.6)	-
33	(137.8)	-	(139.7)	-	(145.9)	-
29	140.9	34	143.4	70	143.4	70

Table 6.12 Quaternary ^{13}C chemical shifts and coupling constants

[$] The calculations and solid-state NMR experiments were undertaken by Dr J. C. Cherryman of the solid-state NMR research group (Prof. R. K. Harris) in Durham to whom I am gratefully indebted.

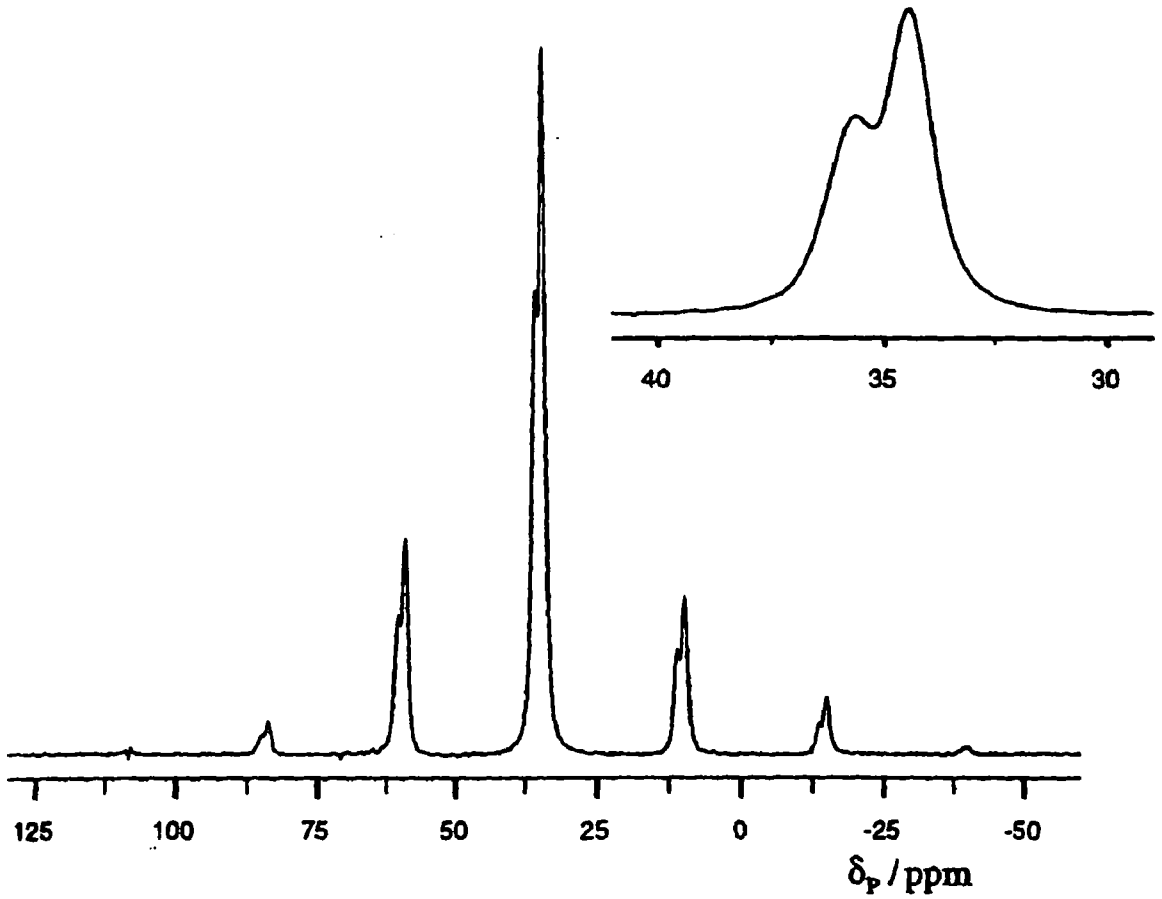

Figure 6.19 ^{31}P CPMAS NMR spectrum of Ph_3PNH_2Br

The existence of at least one unique ipso carbon atom in each case is further indication of the reduction in symmetry (i.e. not C_{3v}) that is observed in the solid-state. For Ph_3PNH_2Br there are two peaks in a 2:1 ratio. This correlates with the observed XRD structure in which there is one unique phenyl group with an elongated P-C_{ipso} bond and wider N-P-C_{ipso} angle.[35] The average C_{ipso} chemical shift increases as the corresponding average P-N bond length decreases, with a concomitant increase in the P-C_{ipso} bond length. As the P-N bond distance shortens, due to increased electrostatic interaction, the ipso carbon atoms become more deshielded.

Residual dipolar information obtained from ^{31}P MAS spectra indirectly yields information on the ^{14}N atom. Using XRD data to calculate the dipolar coupling constant it was possible to calculate information about the quadrupolar tensor and its orientation using *ab initio* MO calculations. The best information obtained was for Ph_3PNH_2Br, whose tensor

(χ_{zz}) was predicted to lie at 95° to the P-N bond, roughly where a lone pair may reside (**Fig. 6.20**).

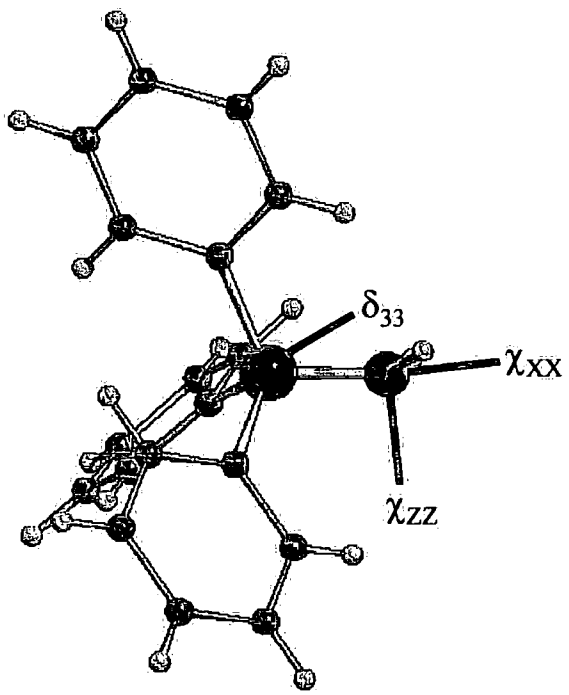

Figure 6.20 XRD structure of Ph_3PNH_2Br
(directions of shielding and quadrupolar tensors superimposed)

6.5 Conclusions

This work, along with some very recent papers,[3,18] has demonstrated that it is possible to synthesise and isolate simple s-block metal complexes of *N*-unsubstituted iminophosphoranes. A number of conclusions can be drawn from the results.

(i) **29** highlights the strong Lewis basicity of *N*-lithiated iminophosphoranes through the incorporation of lithium bromide into the structure. The possibility of other similar complexes being prepared cannot be discounted and it is evident that the dilithiation of aminophosphonium salts (a common route to *N*-lithioiminophosphoranes) does not produce lithium halide-free samples of the desired reagent. This is certain to influence the reactivity and selectivity of such species in synthetic applications.

(ii) The solution-state behaviour of **29** remains unclear. However, it is evident that there are several oligomers in solution and that they are involved in complex equilibria.

(iii) **31** and **32** reveal the utility of transmetallation reactions using *N*-lithioiminophosphorane complexes, such as **29** and **30**. This strategy should be applicable to a wide range of metal compounds and provides an alternative route to the deprotonation of neutral species.

(iv) **33-35** are examples of novel magnesium iminophosphorane complexes. They illustrate the versatility of the iminophosphorane ligand, which can act as either a protic acid or a neutral Lewis base donor. It should be possible to prepare a range of complexes of the type $R_3PNMX{\cdot}L$ for a variety of different Lewis bases, L.

(v) Small changes to the P-N chemical environment has produced subtle alterations to the symmetry of the PR_3 backbone. This is most easily seen in the complexes involving **5** as the parent ligand. As reported in the literature,[26,38] the symmetry of the parent

---

[38] N. W. Mitzel, B. A. Smart, K-H. Dreihaupl, D. W. H. Rankin and H. Schmidbaur, *J. Am. Chem. Soc.*, **118**, 12673 (1996).

phosphine and ligand **5** is C_s, but through altering the substituents attached to the iminic nitrogen it has been possible to force the symmetry towards C_1.

(vi) Shortening of the P-N bond length (and a concomitant lengthening of the skeletal P-distance) upon *N*-metallation has been shown to be an inherent feature of all these complexes and also others, in which there is no M-N back-bonding. Electrostatic shortening of the bond is the most likely explanation of this trend.

(vii) Solid-state NMR spectroscopy has confirmed the XRD local structures at phosphorus and indirectly yielded some information about the electronic environment of the ^{14}N atom.

7. Discussion: Alkyldiphenylphosphonium ylides and imines

This chapter will commence with a brief outline of the synthetic applications of alkyldiphenylphosphonium ylides and imines. It will then go on to discuss the solid-state structures of complexes **36-38**. Finally, the synthesis of compound **39** and solid-state structure of salt **40** is described.

Complex	Empirical Formula
A	$MePh_2PNPh$
36	$[Ph_2P(=NPh)CH_2Li]_4$
37	$\{[Ph_2P(=NPh)CH_2(Me)_2PNLi]_3[Ph_2P(=NPh)CH_2Li]\}$
38	$[Ph_2P(=NPh)CH_2Li.LiOC_6H_2(Me)^tBu_2]_2$
39	$Ph_2MePCHPh$
40	$[Ph_2MePCH_2Ph]^+[C_6H_2(Me)^tBu_2O]^-$

Table 7.1

7.1 Introduction

Examples of simple *N*-s-block-metallated iminophosphoranes are still rare (**Chapter 6**). However, phosphazenes containing an α-proton are readily metallated and have wide-ranging utility in organic synthesis, particularly in the construction of C-C and C=C bonds.[1] Historically, it has been α-lithiated organophosphorus species that have been most useful for this purpose, notably Horner (α-lithiated phosphine oxides)[2] and Wadsworth-Emmons (α-lithiated phosphonic acid esters)[3] reagents.

---

[1] F. López-Ortiz, E. Peláez-Arango, B. Tejerina, E. Pérez-Carreño and S. García-Granda, *J. Am. Chem. Soc.*, **117**, 9972 (1995) and references cited therein.

[2] *(a)* L. Horner, H. Hoffmann and H. G. Wippel, *Chem. Ber.*, **91**, 61 (1958); *(b)* A. W. Johnson with special contributions by W. C. Kaska, K. A. O. Starzewski and D. A. Dixon, *'Ylides and Imines of Phosphorus'*, John Wiley & Sons Inc., New York, (1993), Chp 11.

Alkyldiphenylphosphonium imines can be easily metallated and selectively added to a range of electrophiles.[1] This allows the synthesis of phosphorus substituted heterocycles[4] or olefins[5] to be undertaken via functionalisation of the phosphine backbone (**Scheme 7.1**). The olefin may be further functionalised at the α-position (if R' = H) or the amino group.

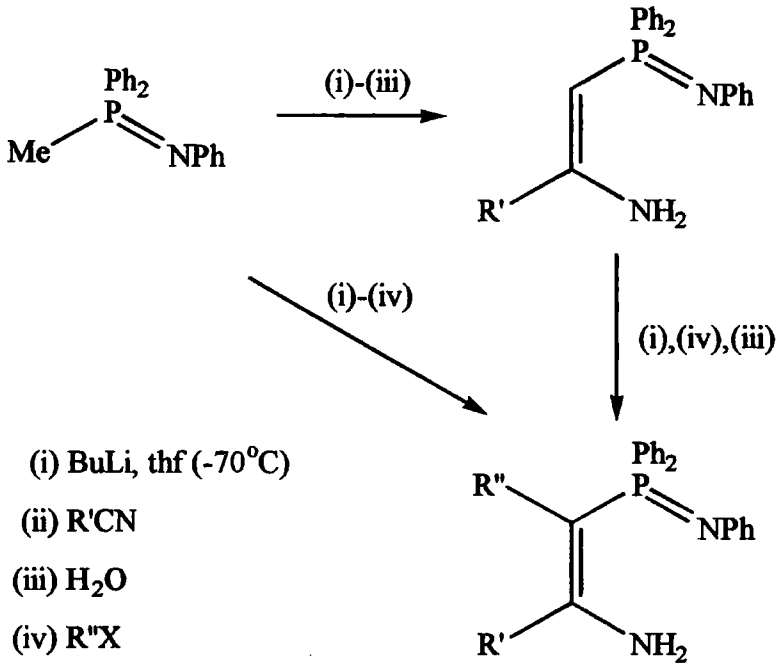

Scheme 7.1

Alkyldiphenylphosphonium ylides also offer the possibility of α-metallation. This has been widely applied to Wittig reactions (**Scheme 7.2**),[6] particularly with hindered, i.e. less reactive, ketones.[7] A crystal structure of an α-lithiated phosphonium ylide has also been reported (**Chapter 1**).[8]

---

[3] W. S. Wadsworth and W. D. Emmons, *J. Am. Chem. Soc.*, **83**, 2733 (1961); ref. 3*(b)* Chp 10.
[4] J. Barluenga, F. López and F. Palacios, *J. Chem. Soc., Chem. Commun.*, 1681 (1985).
[5] J. Barluenga, F. López, F. Palacios, F. H. Cano and M. de la C. Foces-Foces, *J. Chem. Soc., Perkin Trans. I.*, 1681 (1985).
[6] H-J. Cristau, *Chem. Rev.*, **94**, 1299 (1994).
[7] H-J. Cristau, Y. Ribeill, L. Chiche and F. Plenat, *J. Organomet. Chem.*, **C47**, 352 (1988).
[8] R. E. Cramer, M. A. Bruck and J. W. Gilje, *Organometallics*, **5**, 1497 (1986).

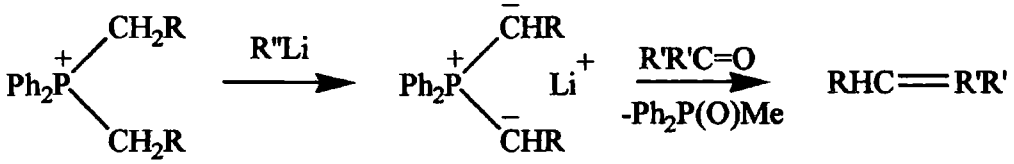

Scheme 7.2

7.2 Solid-state structures of complexes 36-38†

Reaction of *N*-phenylmethyldiphenylphosphazene **A** with *n*-butyllithium yields **36**. In the presence of thf, **36** forms a monomer in the solid-state, in which two molecules of thf complete the lithium coordination sphere (**Fig. 7.1**). The latter structure was recently reported by López-Ortiz et al.[1]

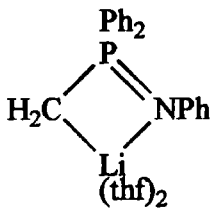

Figure 7.1 Monomer of 36 in thf

Due to the reported difference in stereoselectivity between the unsolvated and thf-solvated complexes, we have now undertaken a structural investigation of the unsolvated complex. In the absence of thf, **36** is able to aggregate and forms a tetramer (**Fig. 7.2**) with a mirror plane through Li(1) and Li(3). The structure contains three distinct lithium centres. Li(1) and Li(2) are bonded to two formally neutral nitrogen and two carbanionic centres, whereas the third, Li(3), is bonded to solely carbanionic centres. The most likely reason for this unusual structural motif, rather than a simpler ladder structure, may be unfavourable steric interactions that such a structure would invoke. The unique lithium atom is able to sit between all four carbanionic centres, thereby satisfying its electronic demands and enabling the highest possible oligomer to be formed.

The structural parameters of the anion of **36** are very similar to those of its thf complexed analogue.[1] For P(1), the P-N distance is 1.613(6)Å, which is little changed from the thf monomer [1.614(6)].[‡] There are three Li-C contacts[9] for C(3): C(3)-Li(1) 2.254(11), C(3)-Li(2a) 2.415(13), C(3)-Li(3) 2.518(14) Å, c.f. [2.23(1) Å]. Li(3) has two very short (and two longer) Li-C contacts: [Li(3)-C(13) 2.142(10) Å - Li(3)-C(3) *vide supra*], as a result of its positioning between four carbanionic centres. The Li-N distances are, however, similarly short: N(1)-Li(1) 2.043(6), N(1)-Li(2) 2.162(13) Å,[10] c.f. [2.00(1) Å] - this is again due to the ionic nature of the N-Li bond.

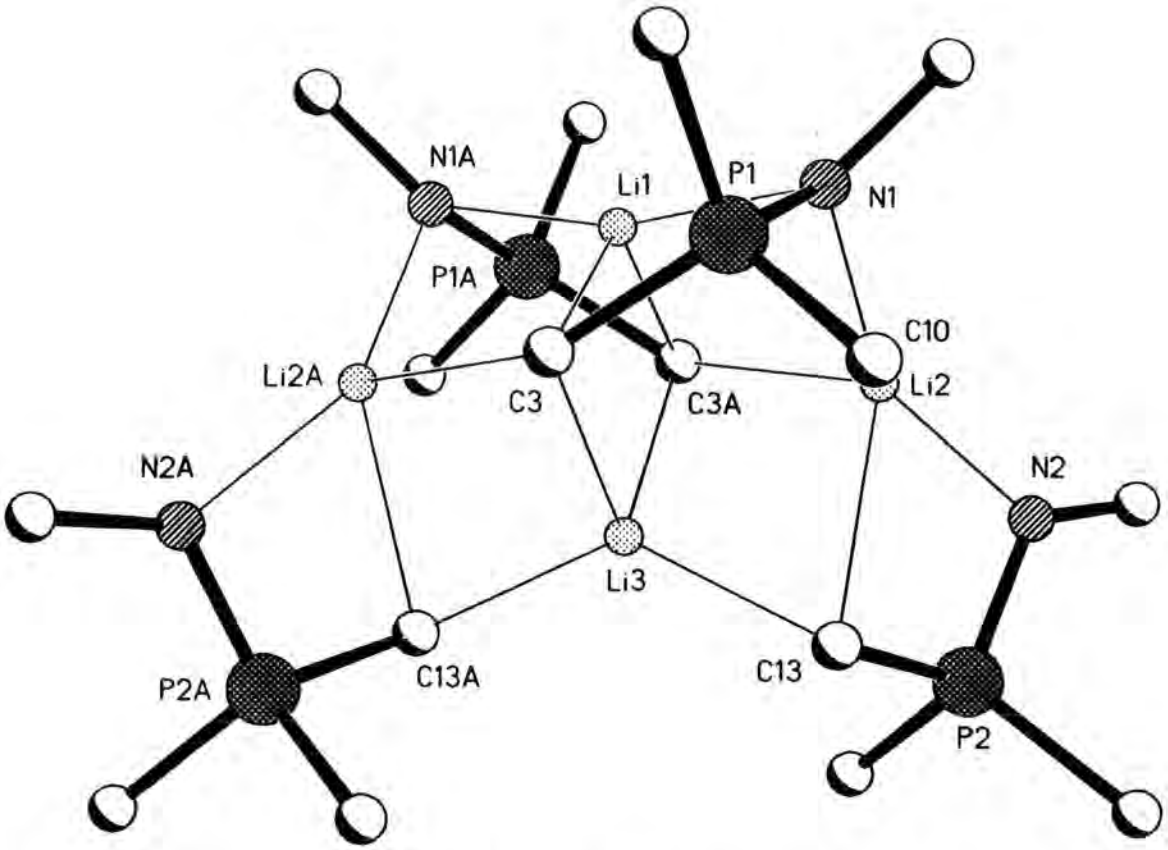

Figure 7.2 Single crystal XRD structure of 36 (phosphorus and nitrogen bound phenyl groups omitted for clarity, except for ipso carbon atoms)

---

[1] This work was carried out in collaboration with Prof. López-Ortiz (University of Almeria).
[‡] Values in parentheses for the X-ray structure of $Ph_2P(CH_2Li)NPh.2thf$.[1]
[9] W. Setzer and P. von R. Schleyer, *Adv. Organomet. Chem.*, **24**, 353 (1985).
[10] M. F. Lappert, P. P. Power, A. R. Sanger and R. C. Sryvastava, *'Metal and Metalloid Amines'*, Ellis Horwood-John Wiley: Chichester (1980).

In comparison to the thf-complexed monomer, **36** has a slightly elongated P-C separation {P(1)-C(3) 1.746(7) Å [1.707(7) Å]}, but a similar angle {C(3)-P(1)-N(1) 106.1(3) ° [105.6(3) °]}.[1] The phosphorus environment at P(2) differs from P(1) in that it has a marginally elongated P-N separation [P(2)-N(2) 1.622(6) Å] reflecting its terminal nitrogen [N(2)] as opposed to a bridging nitrogen [N(1)], but a smaller P-C distance [P(2)-C(13) 1.729(8) Å] since C(13) is a μ_2-carbanion and C(3) is μ_3.

Complex **37** was synthesised in an analogous fashion to **36** (lithiation of **A**), but in a different solvent system (hexane:benzene). In the solid-state (**Fig. 7.3**), it forms a pseudo-cubane Li_4N_3C core. The structure consists of two types of phosphorus ligand. One [P(4)] is an α-lithiated derivative of **A**, as was seen for **36**. The other three ligands have NPCPN backbones, i.e. $[Ph_2P(=NPh)CH_2(Me)_2PN]^-$ anions, with one phosphorus [e.g. P(1)] attached to two phenyl groups, having a phosphazene bond to NPh and attached to the other phosphorus centre [P(5)] via a methylene bridge [C(1)]. P(5) is also bonded to two methyl groups and N(5).

The pseudo-cubane core is strained insomuchas C(4) is puckered out of the cube with a concomitant lengthening of its Li-C bond distances [Li(1)-C(4) 2.519(7), Li(3)-C(4) 2.485(7), Li(4)-C(4) 2.398(7) Å]. For the "normal" anionic ligand the remaining parameters are similar to both **36** and its thf monomer [P(4)-N(4) 1.610(3), P(4)-C(4) 1.754(4) Å; N(4)-P(4)-C(4) 107.90(18) °].[1]

The most interesting structural feature of **37** is the unusual NPCPN anion (**Fig. 7.4**). The structural parameters for the NPC portion do not differ greatly from those of **36** [P(1)-N(1) 1.598(3), P(1)-C(1) 1.787(3) Å; N(1)-P(1)-C(1)107.51(17) °]. However, the CPN section of the ligand is fairly unusual. The P-C distance [P(5)-C(1) 1.918(3) Å] is elongated with respect to P(1)-C(1), its P-Me bonds [P(5)-C(51) 1.865(4), P(5)-C(52) 1.876(3) Å] and a classical P-C single bond (1.87 Å),[11] although the P-N distance [1.598(2) Å] is shorter than for the neutral donor. This shortened P-N distance in comparison to the formally neutral donor nitrogen atoms is something observed in all *N*-

[11] F. H. Allen, O. Kennard, D. G. Watson, L. Brammer, A. G. Orpen and R. Taylor, *J. Chem. Soc. Perkin Trans. II*, S1-S19 (1987).

metallated iminophosphoranes (**Chapter 6**). Unsurprisingly, the N-Li distances are marginally longer for the formally neutral donors [2.07 Å (ave.) and N(4)-Li(4) 2.013(6) Å] than for the anionic interactions [1.94 Å (ave.)].[10]

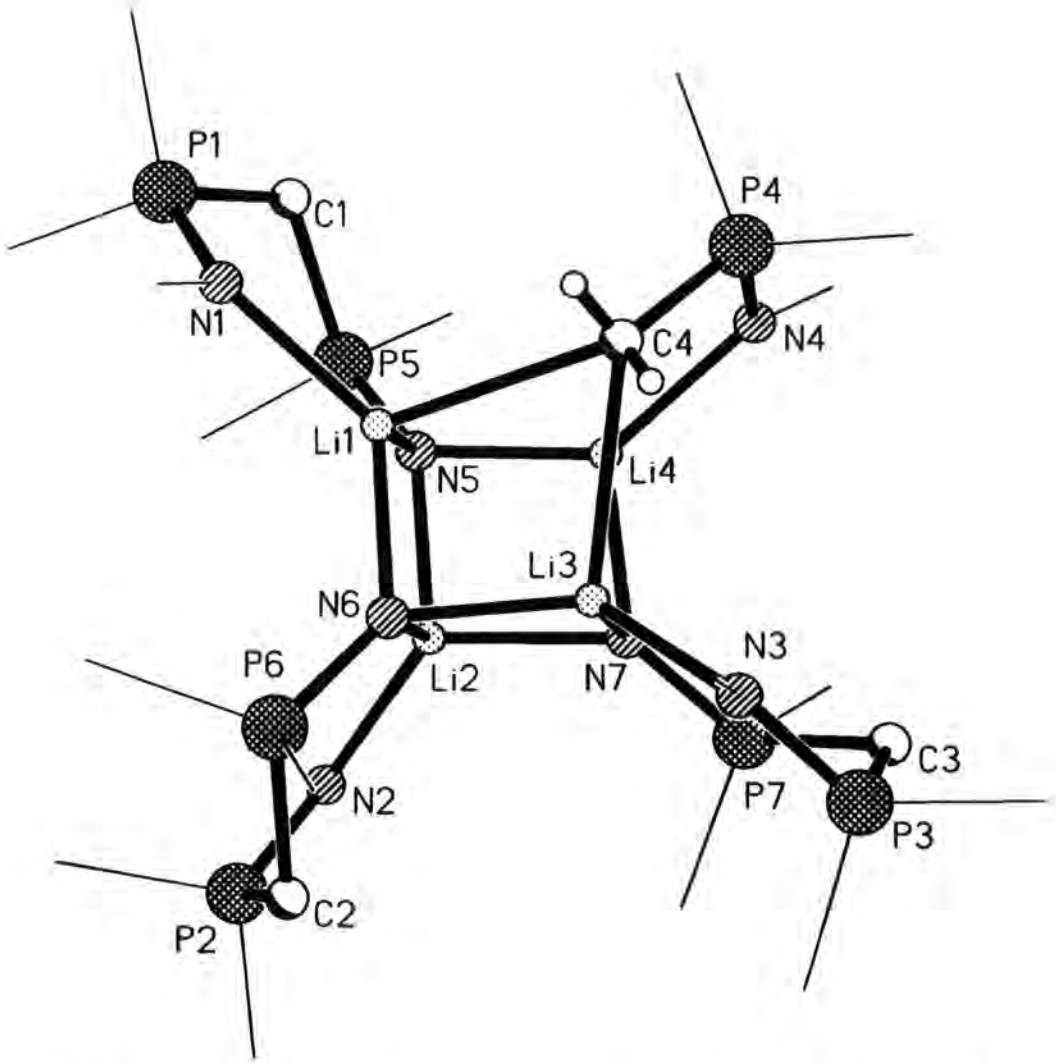

Figure 7.3 Single crystal XRD structure of 37 (phenyl groups omitted for clarity except for ipso carbon atoms in outline; methyl groups in outline)

The mechanism of formation for **37** is not yet clear (nor is the reproducibility of its synthesis), but there is clearly some coupling of a $Ph_2P(=NPh)CH_2$ anion with another phosphorus centre. It is interesting to note that the same anion is observed in the ^{31}P NMR spectra of **36** in solution after storage for some time. Whether **37** is a hydrolysis product (unlikely considering the lack of oxygen) or the result of a slow coupling reaction is unclear to date.

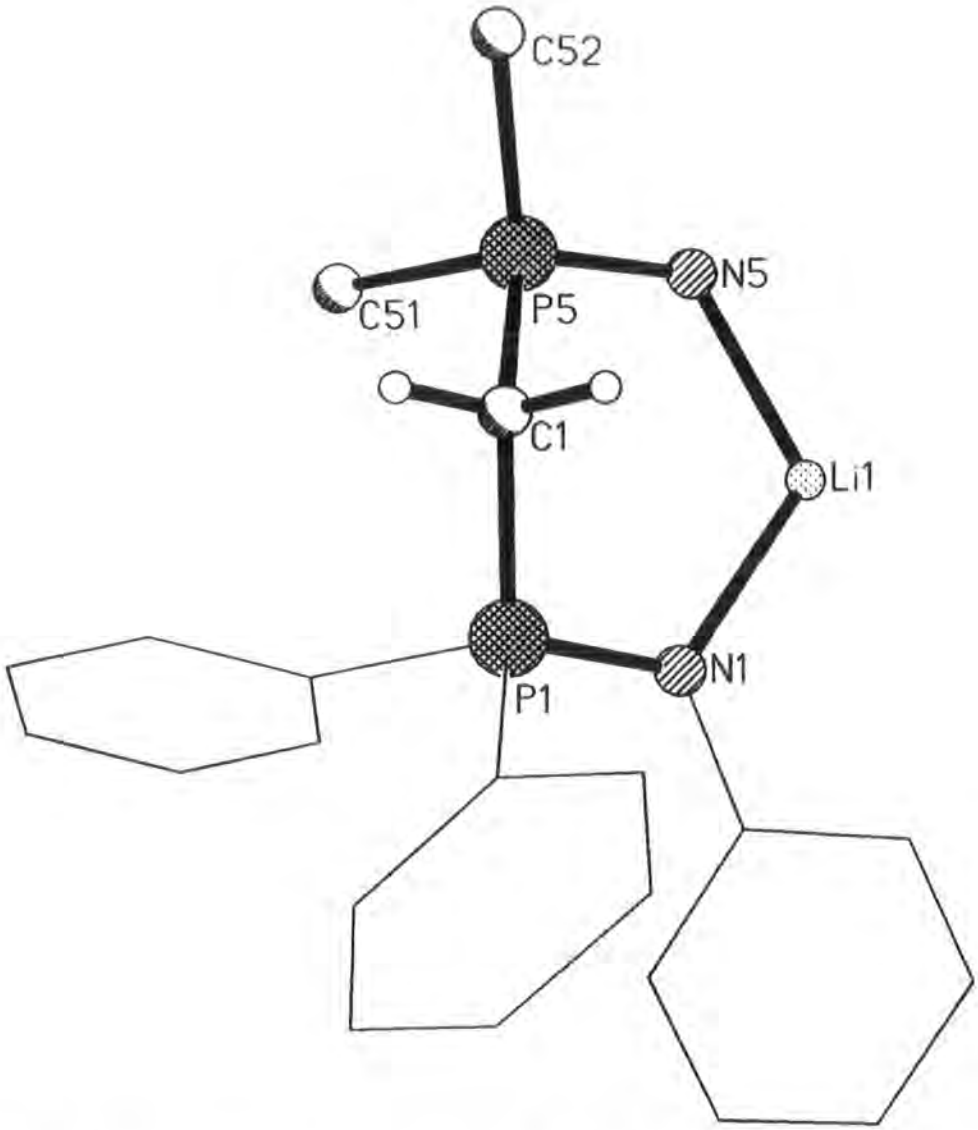

Figure 7.4 One of three PNCPN ligands in the single-crystal XRD structure of 37 (hydrogens omitted for clarity)

Reaction of **A** with 2,6-di-tert-butyl-4-methylphenol in the presence of two equivalents of *n*-butyllithium yields a white precipitate, which dissolves in toluene upon gentle heating. Analysis, ultimately by a single crystal XRD study, revealed the product to be **38**.

Mixed-anion complex **38** forms a dimeric ladder-type structure in the solid-state, with a lithium aryloxide core surrounded by two α-lithiated-*N*-phenylmethyldiphenylphosphazene ligands (**Fig. 7.5**). The inner Li_2O_2 core differs from those of lithium aryloxide structures discussed earlier (**Chapter 4**) [Li(2)-O(1) 1.911(8), Li(2a)-O(1)1.989(9) Å; Li(2)-O(1)-Li(2a) 79.6(4), O(1)-Li(2)-O(1a) 100.4(4) °]. The core is distorted further from a square arrangement due to the steric demands of the ladder structure.

Each lithium is three co-ordinate, either through association with a carbanionic and two aryloxide centres [Li(2)] or one neutral phosphazene, one carbanionic and one aryloxide centre [Li(1)]. Li(1) displays a Li-O distance of 1.933(8) Å and a particularly short Li-N distance [1.941(9) Å], with a Li-C bond towards the upper limit of the expected range[10] [2.407(11)].[§] Li(2), however, has a much shorter organometallic bond [Li(2)-C(1) 2.169(9) Å].

The P-N separation [1.669(4) Å] is marginally longer than seen in the previous two examples, but the P(1)-C(1) distance is of a similar magnitude [1.746(4) Å]. The other rings of the ladder (two symmetry equivalent PCNLi and two symmetry equivalent CLiOLi) are also distorted from square. For the PCNLi rings: P(1)-C(1)-Li(1) is 80.0(3)° and P(1)-N(1)-Li(1) is 97.4(3)°, whilst for the CLiOLi rings: O(1)-Li(2)-C(1) is 109.8° and C(1)-Li(1)-O(1) is 102.8(4)°.

In Chapter 4, lithium aryloxide dimers were utilised as stable acceptors of electron density from Lewis bases in order to investigate the effect of complexation on structure and reactivity. It is interesting to note that here the Li_2O_2 dimer can be considered as a Lewis acid acceptor as well as a Lewis base donor.

[§] Li-H agostic interactions with the tert-butyl groups of the phenol may also exist, but the refinement of these groups is too poor to draw any such conclusions.

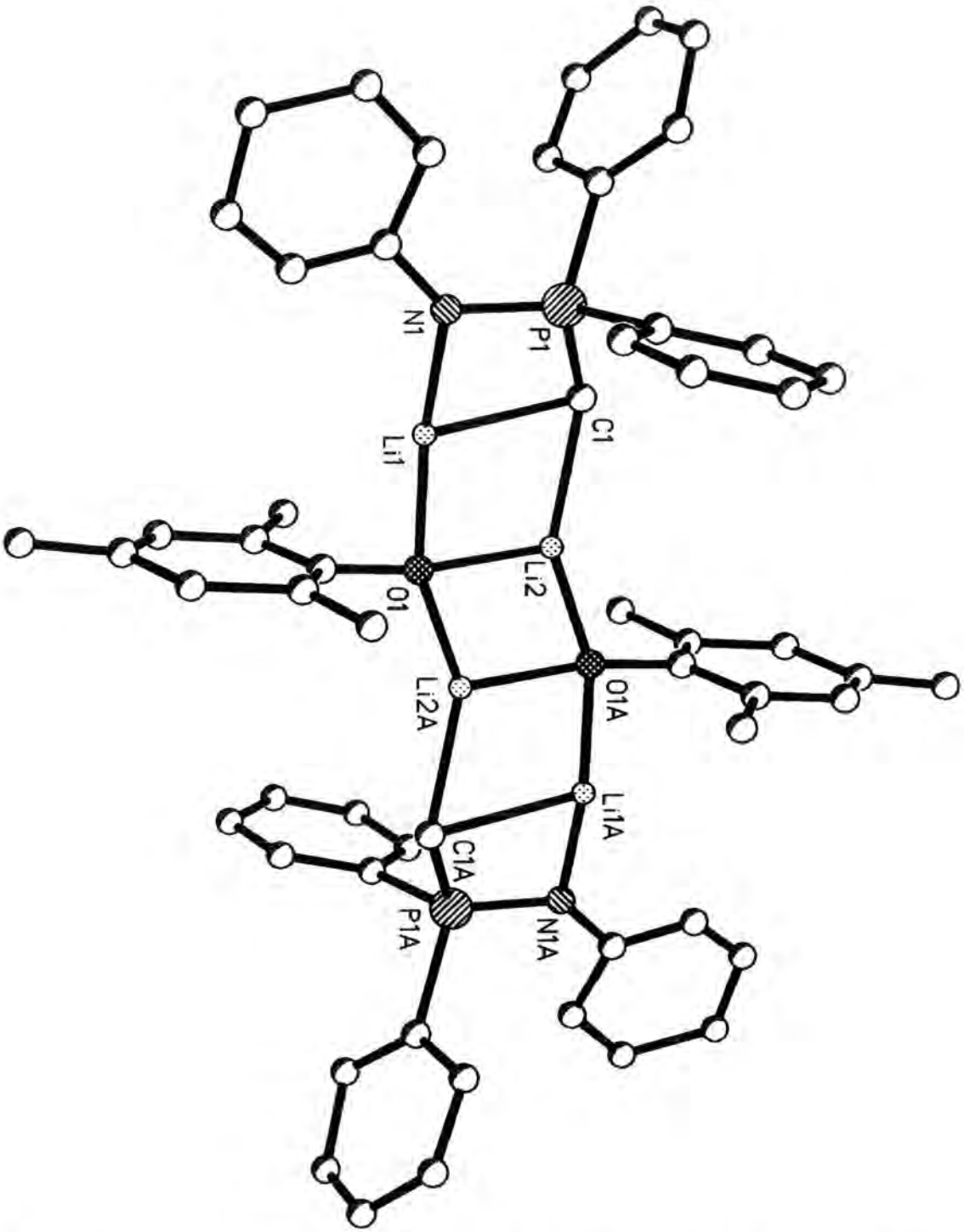

Figure 7.5 Single-crystal XRD structure of 38 (methyl group of tert-butyl groups omitted for clarity)

The solution-state behaviour is currently under investigation using multi-nuclear variable temperature NMR techniques. A monomer-dimer equilibrium is thought to be in operation, but a variable concentration study will be necessary in order to confirm this.

Complex **38** may have some interesting synthetic organic applications. An analogue of **38** is already under investigation in collaboration with Prof. López-Ortiz. Early results showing some promising indications.

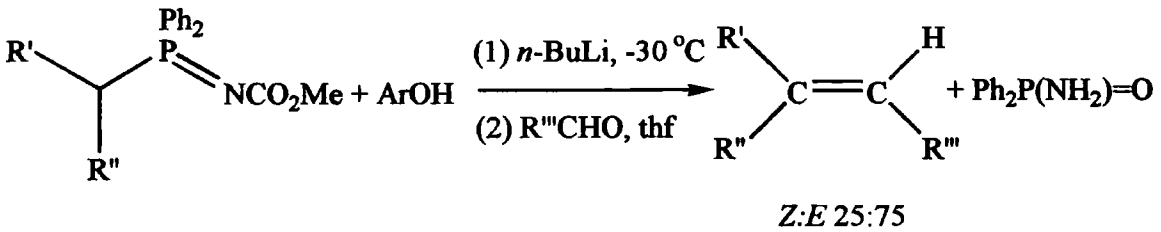

Scheme 7.3

In situ lithiation of the functionalised *P*-alkyl-*N*-(methylcarboxyl)diphenylphosphazene (**Scheme 7.3**) affords an intermediate analogous to **38**. Further reaction with a carbonyl compound, such as an aldehyde, generates an olefin enriched in *E* isomer. In the absence of the lithium aryloxide, no stereoselectivity is observed.

Analogues of **38** with mixed-metal structures (Li/other s-block metal) may have super-basic properties. [12] Traditional super-bases have employed an organolithium/heavier Group I metal alkoxide mixture.[13,14] It is not a huge conceptual step to the use of s-block metal aryloxide/α-lithiated *N*-diarylphosphazene mixtures.

---

[12] M. Schlosser, *J. Organomet. Chem.*, **8**, 9 (1967).
[13] M. Schlosser and S. Strunk, *Tet. Lett.*, **25**, 741 (1984).
[14] See also for example: S. Harder and A. Streitweiser, *Angew. Chem., Int. Ed. Engl.*, **32**, 1066 (1993); W. Bauer and L. Lochmann, *J. Am. Chem. Soc.*, **114**, 7482 (1992).

7.3 Solid-state structures of A, 39 and 40

For completeness, the following structures, carried out as part of the work described above, are included in this section.

The structure of ligand **A** is fairly unremarkable, the P-N bond length [1.578 Å (ave.)] is in the known range for iminophosphoranes[15] and is shorter than for the α-lithiated derivatives discussed earlier (*vide supra*). The P-C distances [1.796 Å (ave.)] are longer than in the metallated derivatives. There are two different molecules in the asymmetric unit (**Fig. 7.6**), which differ markedly in their C_{methyl}-P-N angles [(**a**) 107.80(8), (**b**) 116.35 °] and the orientation of the P=NPh fragment with respect to the methyl substituent. This again highlights the directionality of any π-σ^* back-bonding and the low barrier to rotation around the P-N bond.

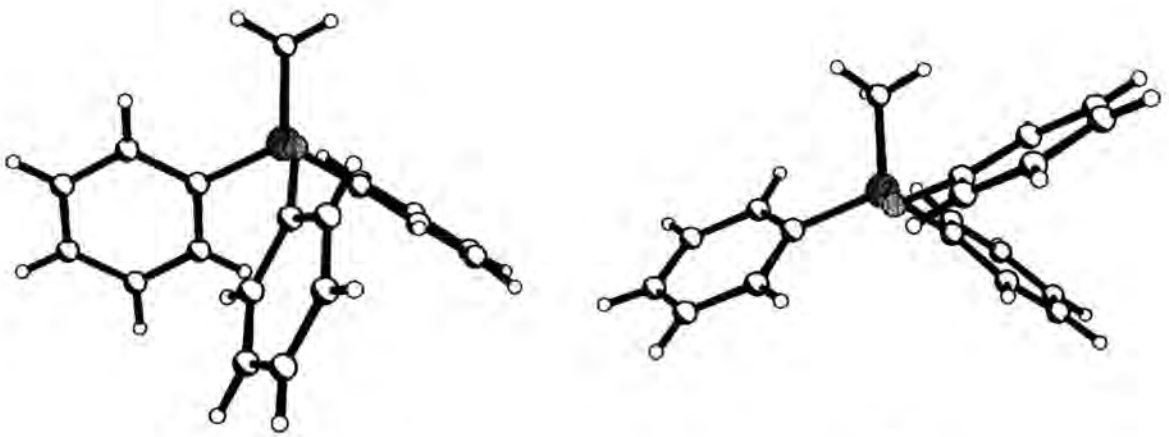

(a) **(b)**

Figure 7.6 Two molecules in the asymmetric unit of ligand A

[15] M. G. Davidson, A. E. Goeta, J. A. K. Howard, C. W. Lehmann, G. M. McIntyre and R. D. Price, *J. Organomet. Chem.*, **550**, 449 (1998).

Ligand **39** is another example of an isolable phosphonium ylide (albeit semi-stabilised), viz. methyldiphenylphosphonium benzylide. It has yet to be characterised in the solid-state, but should be of a similar nature to triphenylphosphonium benzylide and triphenylarsonium benzylide, the single crystal XRD structures of which are both known.[16,17] The latter two compounds aggregate into dimers via C-H...C hydrogen bonding interactions in the solid-state (**Fig. 7.7**).

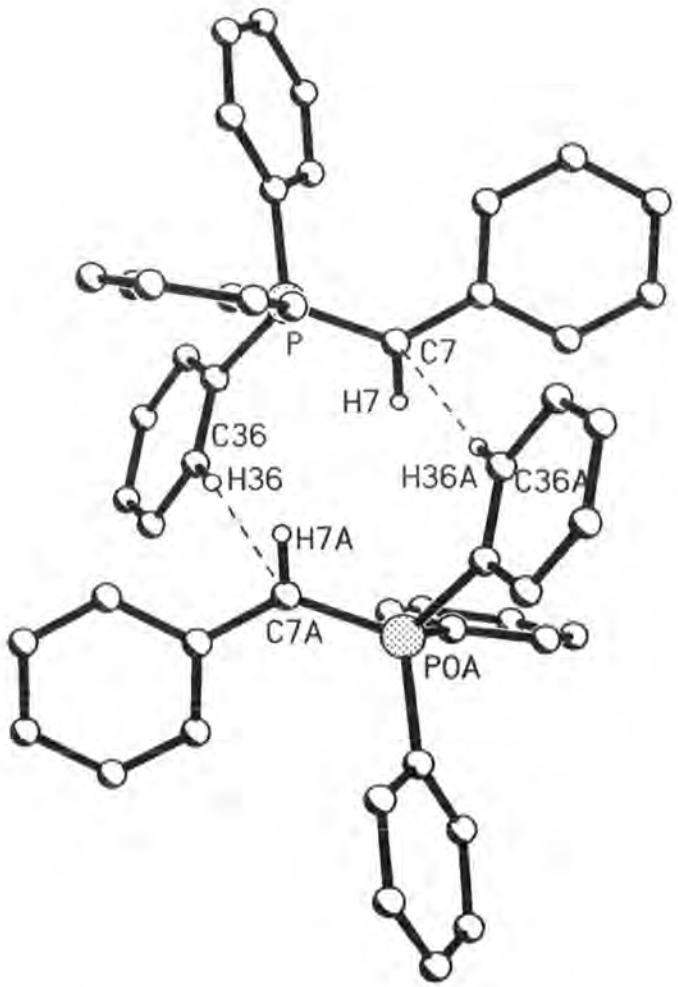

Figure 7.7 Dimeric aggregation of Ph_3PCHPh in the solid-state

[16] A. S. Batsanov, M. G. Davidson, J. A. K. Howard, S. Lamb and C. Lustig, *J. Chem. Soc., Chem. Commun.*, 1791 (1996).
[17] M. G. Davidson, *Unpublished results.*

The methyl substituent on **39** offers it some versatility in comparison to many other phosphonium benzylides. The latter are generally inert to simple protonation or complexation reactions under ambient conditions. However, **39** can be α-lithiated (in a similar fashion to $Ph_2MePNPh$ - *vide supra*), although a completely unambiguous characterisation of the product has not yet been possible. Deprotonation of 2,6-di-tert-butyl-4-methylphenol with **39** in toluene affords a red precipitate, which dissolves upon heating. Analysis of the product, ultimately by a single-crystal XRD study, revealed it to be **40**.

Complex **40** is a hydrogen-bonded donor-acceptor complex. Historically there has been some debate over the existence of C-H...O hydrogen bonds. Taylor and Kennard[18] studied over 100 organic compounds from the CSD that had been structurally characterised by neutron diffraction. Their conclusion was that C-H...O contacts were found to occur frequently and they were able to preclude steric factors and van der Waals interactions as explanations due to the short nature of the interactions. Desiraju,[19] in another series of CSD studies, has further strengthened this argument. There are increasingly fewer people who have still to be convinced as to their existence.[20] In the solid-state (**Fig. 7.9**), **40** is monomeric and analogous to the donor-acceptor complexes of **1** or **2** and this phenol (**Fig. 7.8**). Aggregation to higher oligomers is prohibited by the bulky phenol substituents. However, there is no evidence for longer-range C-H...π interactions in **40**, such as are seen in the complex shown below (**Fig. 7.8**).[21]

---

[18] R. Taylor and O. Kennard, *J. Am. Chem. Soc.*, **104**, 5063 (1982).
[19] G. R. Desiraju, *J. Chem. Soc., Chem. Commun.*, 179 (1989); *ibid.*, 454 (1990); T. Steiner and G. R. Desiraju, *J. Chem. Soc., Chem. Commun.*, 891 (1998).
[20] F. A. Cotton, L. M. Daniels, G. T. Jordan IV and C. A. Murillo, *J. Chem. Soc., Chem. Commun.*, 1673 (1997).
[21] S. Lamb, *PhD Thesis*, University of Durham, 1998.

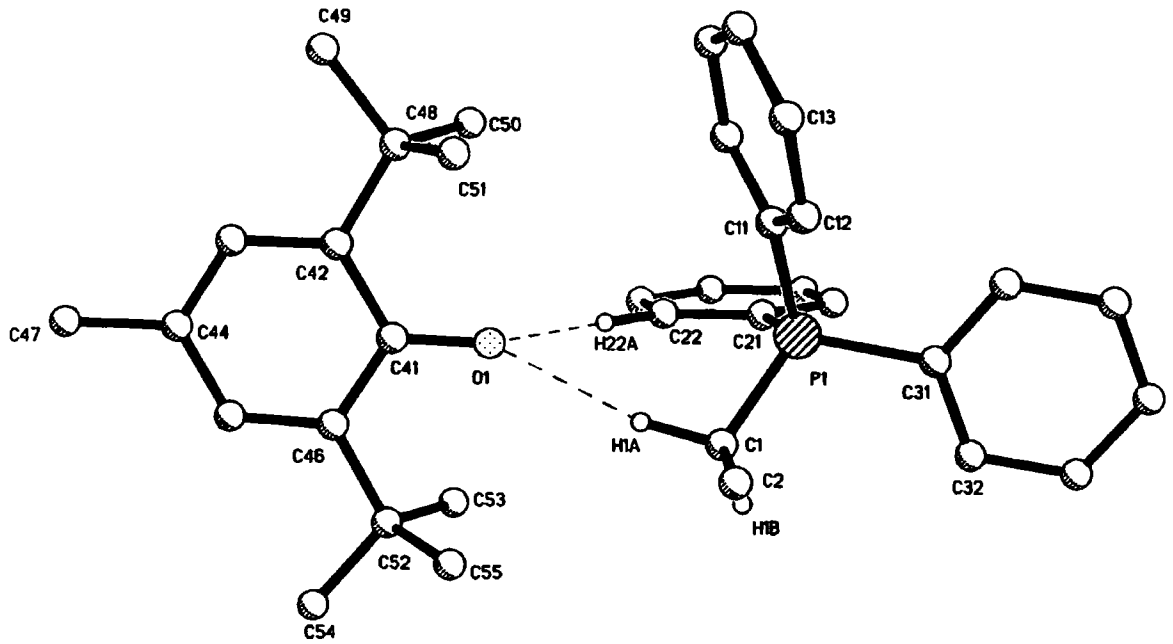

Figure 7.8 Monomeric aggregate of 2 with 2-6-di-tert-butyl-4-methylphenol

The solid-state structure of **40** contains two C-H...O hydrogen bonds, one of which is a C(alkyl)-H...O, the other a C(aryl)-H...O interaction. Perhaps surprisingly, the benzyl group is not involved in the hydrogen bonding interactions. The parameters are summarised below (**Table 7.2**).

Interaction[¶]	r(X-H)/Å	r(H...O)/Å	∠X-H...O/°	r(X...O)/Å
C1-H1a...O1	0.93	2.29	168	3.202(3)
C20-H20...O1	1.02	2.30	171	3.306(3)

Table 7.2 Summary of hydrogen bond parameters for 40

C-O separations for this type of interaction are generally in the range 3.5-4.0Å.[22] In **40**, the two C-O separations are short in comparison to this range [C(1)-O(1) 3.20Å; C(20)-O(1) 3.31Å]. This reflects the strong interaction between the phosphonium cation and aryloxide anion. The C-H...O parameters for the analogous complex of **2** agree well, though in the latter case the C(aryl)-H...O distance is shorter [H...O 1.998(3)Å].[3]

[¶] Refined using a fixed hydrogen position.

[22] G. R. Desiraju, *Angew. Chem. Int. Ed. Engl.*, **34**, 2311 (1995).

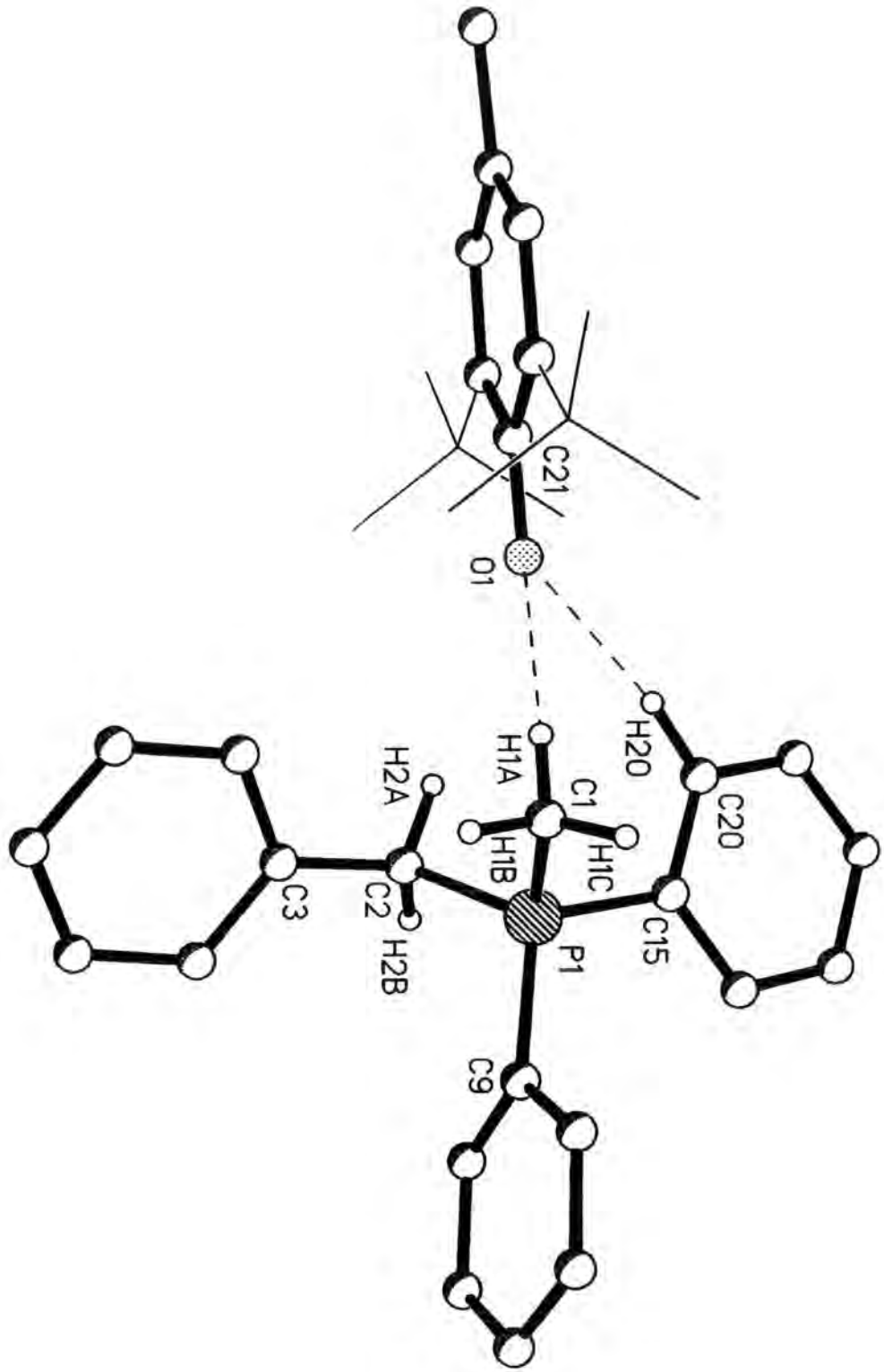

Figure 7.9 Single crystal XRD structure of 40 (tert-butyl groups in outline)

7.4 Conclusions

(i) Complex **36** has been analysed in the solid-state and shown to be a tetramer, with an unusual coordination of one lithium. The structural parameters are in good agreement with the thf-complexed monomer that has been previously reported in the literature.

(ii) Complex **37** was serendipitously prepared during the attempted synthesis of **36** in benzene. It contains an unusual NPCPN ligand in the solid-state. Its solution behaviour is complex and currently under investigation.

(iii) Complex **38** has a ladder-type structure containing a lithium aryloxide core. An analogue of **38** has been applied to olefin synthesis with some enrichment of the *E* isomer being observed.

(iv) Super-base type complexes may be accessible by the introduction of heavier s-block metal aryloxides/alkoxides into the structure. It may be possible to introduce some chirality to these potential reagents by utilising a phenol possessing chiral substituents.

(v) $Ph_2MePCHPh$, benzylide **39** shows an unusual level of reactivity for a semi-stabilised phosphonium ylide, undergoing α-lithiation and protonation reactions.

(vi) Protonation of **39** with 2,6-di-tert-butyl-4-methylphenol yields a monomeric donor-acceptor complex, which associates via C(aryl)-H...O and C(alkyl)-H...O hydrogen bonds in the solid-state.

(vii) Salt **39** provides an alternative route to phosphonium ylide-complexed s-block metal aryloxide structures through metallation of the salt.

8. Discussion: Miscellaneous reactions

During the course of these studies, a number of results were obtained either unexpectedly, or in order to provide background for the main body of the thesis. Since such results do not conveniently fit into the previous chapters they are discussed in detail below, due to their general relevance to the work described above.

The compounds discussed in this section were prepared as described in the experimental section. The chapter will commence with a discussion of complexes **41** and **42**. **43** will be discussed firstly in terms of its solid-state structure and then the mechanism of its formation will be explored. This will be followed by a brief discussion of the solid-state structures of complex **44**.

Complex	Empirical Formula
41	$[Ph_3PNH_2]^+[Ph_2C_6H_2O]^-$
42	$[(Me_2N)_3PNH_2]^+[Ph_2C_6H_2O]^-$
43	$Ph_2(C_3H_4Ph)PNP(C_3H_5)Ph$
44	$(Ph_2PS)_2NLi{\cdot}OPMePh_2$

Table 8.1 Complexes discussed in this chapter

8.1 Solid-state structure of complexes 41 and 42

Reaction of **4** with 2,6-diphenylphenol in toluene/thf yields a yellow precipitate, which dissolves upon gentle warming. On cooling to ambient temperature, a crystalline product could be isolated which, following analysis ultimately by a single-crystal XRD study, was revealed to be **41**.

41 is a typical donor-acceptor complex containing N-H...O hydrogen bonds. Hydrogen bonds can be most simply represented as D-H...A, in which D-H is the donor and A the acceptor. The attraction is predominantly electrostatic (A being a centre of high electron density; D-H the positive or dipolar counterpart).[1] Hydrogen bonding is generally viewed as a weak association, but has marked effects on the supramolecular structure and is undoubtedly the most extensive mode of intermolecular interaction found in organic solids.[2] There has been much recent interest in further rationalising the role of hydrogen bonding in fields such as crystal engineering, which has lead to the synthesis of novel materials and extended aggregates.[3]

In the solid-state (**Fig. 8.1**), **41** contains two crystallographically independent dimeric aggregates in the asymmetric unit. They differ slightly in the degree of pyramidalisation of the nitrogen atom, i.e. the extent to which the amino group is directed out of a planar P-NH_2 arrangement. Considering P(1), the amino plane lies at an approximate angle of 22° to the P-N bond, whilst for P(2) this angle is 23°. (This difference is insignificant, since these angles are based on XRD determined proton positions).

Both aggregates display the same structural motif: an eight-membered $(...H\text{-}N\text{-}H...O)_2$ ring, two N-H...O hydrogen bonds and one C-H...O bond through association with an aryl proton. The hydrogen bond parameters are shown below (**Table 8.2**).

---

[1] L. Pauling, 'The Nature of the Chemical Bond and the Structure of Molecules and Crystals – An Introduction to Modern Structural Chemistry.', 2nd Edn., OUP, London (1940).
[2] G. R. Desiraju, *Angew. Chem., Int. Ed. Engl.*, **34**, 2328 (1995) and references cited therein.
[3] See for example: C. B. Ankeroy and K. R. Seddon, *Chem. Soc. Rev.*, **22**, 397 (1993).

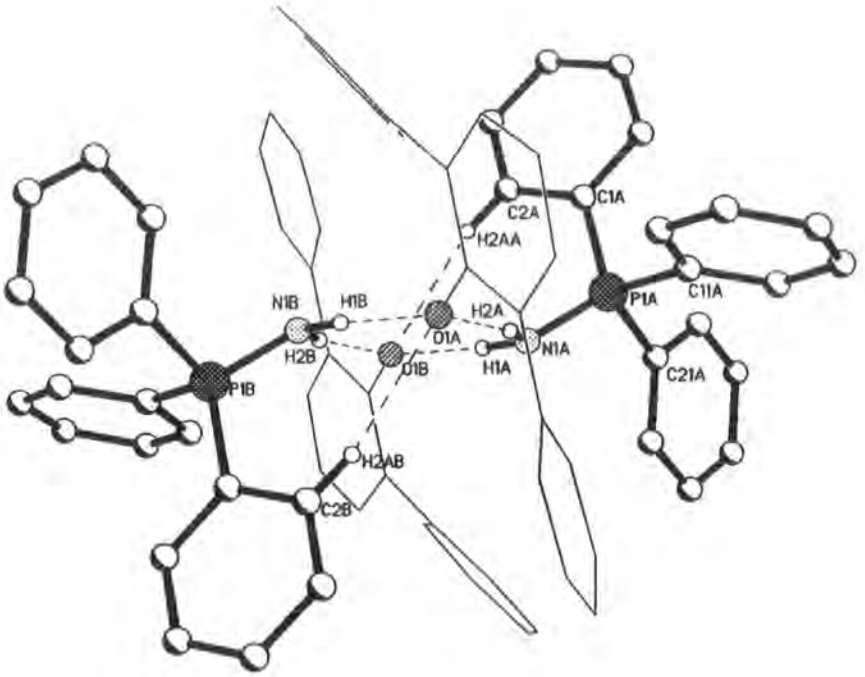

Figure 8.1 One dimer in the solid-state structure of 41
(all hydrogens omitted except those involved in hydrogen bonding; organic anion in outline)

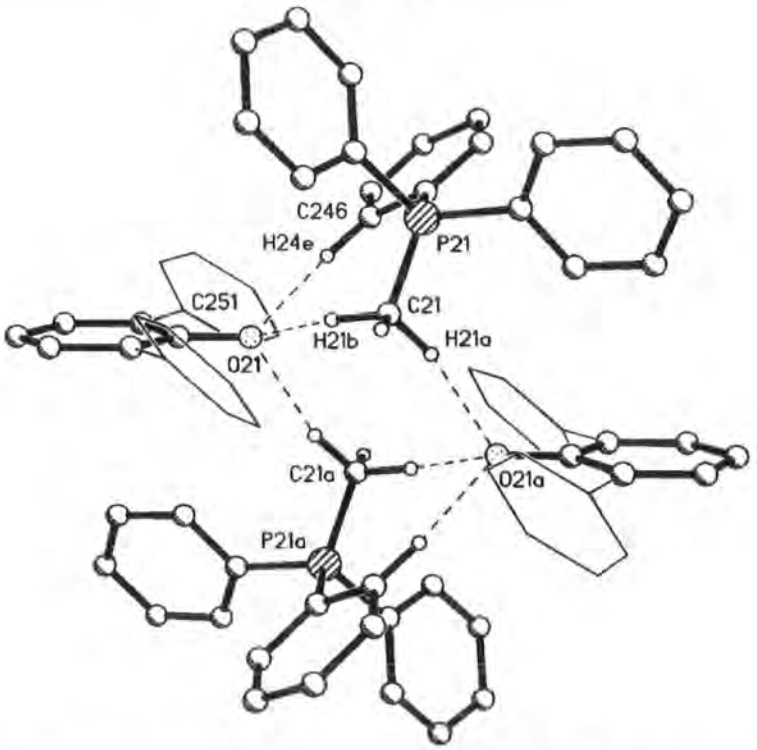

Figure 8.2 Neutron diffraction structure of 1 and 2,6-diphenylphenol
(all hydrogens omitted except those involved in hydrogen bonding; organic anion in outline)

Interaction	r(X-H)/Å	r(H...O)/Å	∠X-H...O/°	r(X...O)/Å
N1a-H2a...O1a	0.90(3)	1.96(3)	165(3)	2.840(3)
N1a-H1a...O1b	0.95(3)	1.82(3)	170(3)	2.760(3)
C2a-H2aa...O1b†	0.95	2.42	167	3.351(3)
N2a-H3a...O2a	0.93(3)	1.95(3)	162(3)	2.852(3)
N2a-H4a...O2b	0.93(3)	1.88(3)	166(3)	2.790(3)
C66a-H66a...O2b†	0.95	2.43	159	3.331(3)

Table 8.2 Summary of hydrogen bond parameters for 41

The structure is said to be trifurcated, in that the oxygen anion experiences three hydrogen bonding interactions. In the presence of the stronger N-H...O interactions, the interaction with the *ortho*-proton of the aryl ring is arguably negligible, but does fall within the range of recognised distances for C-H...O hydrogen bonds. C...O separations for such interactions are generally in the range[4] 3.50-4.0 Å - in this case the C...O separations are 3.331 and 3.352 Å.

An exactly analogous and isoelectronic structure is formed between **1** and 2,6-diphenylphenol[5] (**Fig. 8.2**) which is also trifurcated. The latter aggregates via three C-H...O bonds in the absence of any stronger interactions. This factor necessitates a closer contact between the aryl proton and anionic oxygen, with a concomitant shortening of the hydrogen bond distances (2.12 and 2.17 Å, c.f. 2.42 and 2.43 Å in **41**). Taken together, the alkyltriphenylphosphonium salt and the aminophosphonium salt constitute a rare example of C-H...O and N-H...O analogues that form isomorphous supramolecular structures.

The N-H...O parameters in **41** are within the recognised range for such interactions (1.80 to 2.0 Å for H...O separations)[2] - they range from 1.82 to 1.96 Å (**Table 8.2**). In a

† Refined using a fixed hydrogen position.

[4] G. R. Desiraju, *Acc. Chem. Res.*, **29**, 441 (1996).

[5] Reproduced with permission: S. Lamb, *PhD Thesis*, University of Durham, 1998.

calix[4]arene complex of $[Ph_3PNH_2]^+$ there is also an N-H...O interaction - in this case the H...O separation is 1.86(5)Å.[6]

There have been several other recent structures reported of amino(triphenyl)phosphonium salts.[7,8,9,10,11] All of these exhibit some form of N-H...X hydrogen bonding, including N-H...Br,[7,10] N-H...Cl[8,9] and N-H...N interactions.[11] A summary of some of their bond parameters is given below.

Compound	P-N distance/Å	ΣN_{iminic}/°	$\Sigma C_{ipso}PN$/°	Ref
35	1.618 (ave.)	349	333	This work
Ph_3PNH_2Br	1.615(2)	352	331	7
$Ph_3PNH_2Cl.CH_2Cl_2$	1.616(3)	357	332	8
$Ph_3PNH_2Cl.CH_2Cl_2$	1.615(6)	351	331	9
Ph_3PNHBu^tBr	1.628(7)	-	329	10
Ph_3PNHPr^iBr	1.621(3)	-	328	10
$[Ph_3PNH_2]^+[(CN)_2\ CPh]^-$	1.622(2)	-	-	11

Table 8.3 Structural parameters of various aminophosphonium salts

As can be seen from the table, the structures have parameters of a similar magnitude. In each structure, however, there is a unique C_{ipso}-P-N bond that is both wider and elongated with respect to the other two. This was an inherent feature of most of the parent ligands discussed in **Chapter 4** and appears also to be an inherent feature in these aminophosphonium salts. This is understandable since the aminophosphonium cation $(R_3PNH_2)^+$ is isoelectronic with phosphonium ylides (R_3PCH_2), which implies that similar considerations should hold for both moieties (**Chapter 1**). It is also interesting to note that

---

[6] M. G. Davidson and S. Lamb, *Unpublished results.*

[7] E. Pohl, H. J. Gosink, R. Herbst-Irmer, M. Noltemeyer, H. W. Roesky and G. M. Sheldrick, *Acta Cryst.*, **C49**, 1280 (1993).

[8] F. Weller, D. Nuszhar, K. Dehnicke, F. Gingl and J. Strahle, *Z. Anorg. Allg. Chem.*, **602**, 7 (1991).

[9] M. B. Hursthouse, N. P. C. Walker, C. P. Warrens and J. D. Woolins, *J. Chem. Soc. Dalton Trans.*, 1043 (1985).

[10] C. Imrie, T. A. Modro, P. H. van Rooyen, C. C. P. Wagener, K. Wallace, H. R. Hudson, M. McPartlin, J. B. Nasirun and L. Powroznyk, *J. Phys. Org. Chem.*, **8**, 41 (1995).

[11] P. Molina, C. Lopez-Leonardo, J. Llamas-Botia, C. Foces-Foces and C. Fernandez-Castano, *J. Chem. Soc. Chem. Commun.*, 1387 (1995).

changing the counter-ion or the substituents on nitrogen has little effect on the phosphorus environment and causes only small perturbations to the amino group.

Reaction of **5** with 2,6-diphenylphenol in toluene yields a yellow precipitate, which dissolves upon gentle heating. Cooling to ambient temperature affords a crop of yellow blocks **42**, which following a single crystal XRD study were shown to be analogous to **41**.

Aminophosphonium salt **42** is also a donor-acceptor complex, associated into dimers (**Fig. 8.3**) via two N-H...O hydrogen bonds. As was the case for **41**, there are two discrete cations in the asymmetric unit. In this case there is a more marked difference between the two aminophosphonium salts (**Fig. 8.4**). One molecule (**I**) contains an almost planar amino group [angle between the amino (NH_2) plane and P-N bond vector is 8°], whilst the other molecule (**II**) is more pyramidalised (same angle 28°).

The table below (**Table 8.4**) highlights the differing degrees of pyramidalisation of the two nitrogen centres, one is planar (sum of angles around nitrogen = 360°) and the other pyramidal (sum of angles = 352°). There is no unique amino group for the planar structure (**I**), all three amino groups are different and the local symmetry around phosphorus is C_1. For the pyramidal case (**II**), there is a unique P-NMe_2 bond that is elongated, although it is not particularly pyramidalised (sum of angles around unique group = 356°).

Compound	P-N distance/Å	ΣN_{iminio}/°	ΣNPN_{iminio}/°
42 (planar)	1.590(2)	360	331
42 (pyramidal)	1.596(3)	352	332
16	1.574(2)	356	339
5	1.557(1)	-	341

Table 8.4 Summary of bond parameters for compounds 5, 16 and 42

It is unusual to observe two significantly different conformations in the solid-state of the same moiety within one crystal. However, in this case the observation of both a planar and a pyramidal amino group highlights the very low energy barrier to inversion at the nitrogen

of aminophosphonium cations. This is directly analogous to low energy barriers that have been calculated for phosphonium ylides[12] and silylamines.[13]

Considering the aminophosphonium skeletons, it is possible to compare the structural parameters of **42** with those of its parent ligand **5** and lithium salt **16** (**Table 8.4**).

Down the series from NH_2^+ **42** to $NHLi^+$ **16** to NH **5**, there is a decrease in the P-N bond length. This observation can be rationalised in the following way. The neutral ligand **5** has two lone pairs of electrons and is able to use both of these to delocalise electron density through negative hyperconjugation. For the complex **16**, the lithium cation partially localises one of these lone pairs, thus its capacity for delocalisation is reduced, with a concomitant increase in the P-N bond length. Finally, for the aminophosphonium salt **42**, the additional hydrogen atom causes a complete localisation of one orbital (a formal covalent bond) leaving only one available lone-pair orbital, thus it has the longest P-N distance. There is also a decrease in the degree of pyramidalisation of the phosphonium centre across the series.

Interaction	r(X-H)/Å	r(H...O)/Å	∠X-H...O/°
N11a-H11b...O1a	0.92(4)	1.86(4)	163(3)
N11a-H11a...O2a	0.83(4)	1.95(4)	165(4)
N21a-H21b...O1a	0.84(4)	1.93(4)	163(3)
N21a-H21a...O2a	0.92(4)	1.82(4)	166(3)
N31a-H31b...O3a	0.85(4)	1.94(4)	164(3)
N31a-H31a...O3b	0.96(4)	1.86(4)	170(3)

Table 8.5 Summary of hydrogen bonding parameters for 42

The N-H...O parameters (**Table 8.5**) in the structure of **42** agree closely with those of **41**.

[12] A. W. Johnson with special contributions by W. C. Kaska, K. A. O. Starzewski and D. A. Dixon, *'Ylides and Imines of Phosphorus'*, John Wiley & Sons Inc., New York, (1993), Chp. 2.
[13] K. Ruhlandt-Senge, R. A. Bartlett, M. M. Olmstead and P. P. Power, *Angew. Chem., Int. Ed. Engl.*, **32**, 425 (1993).

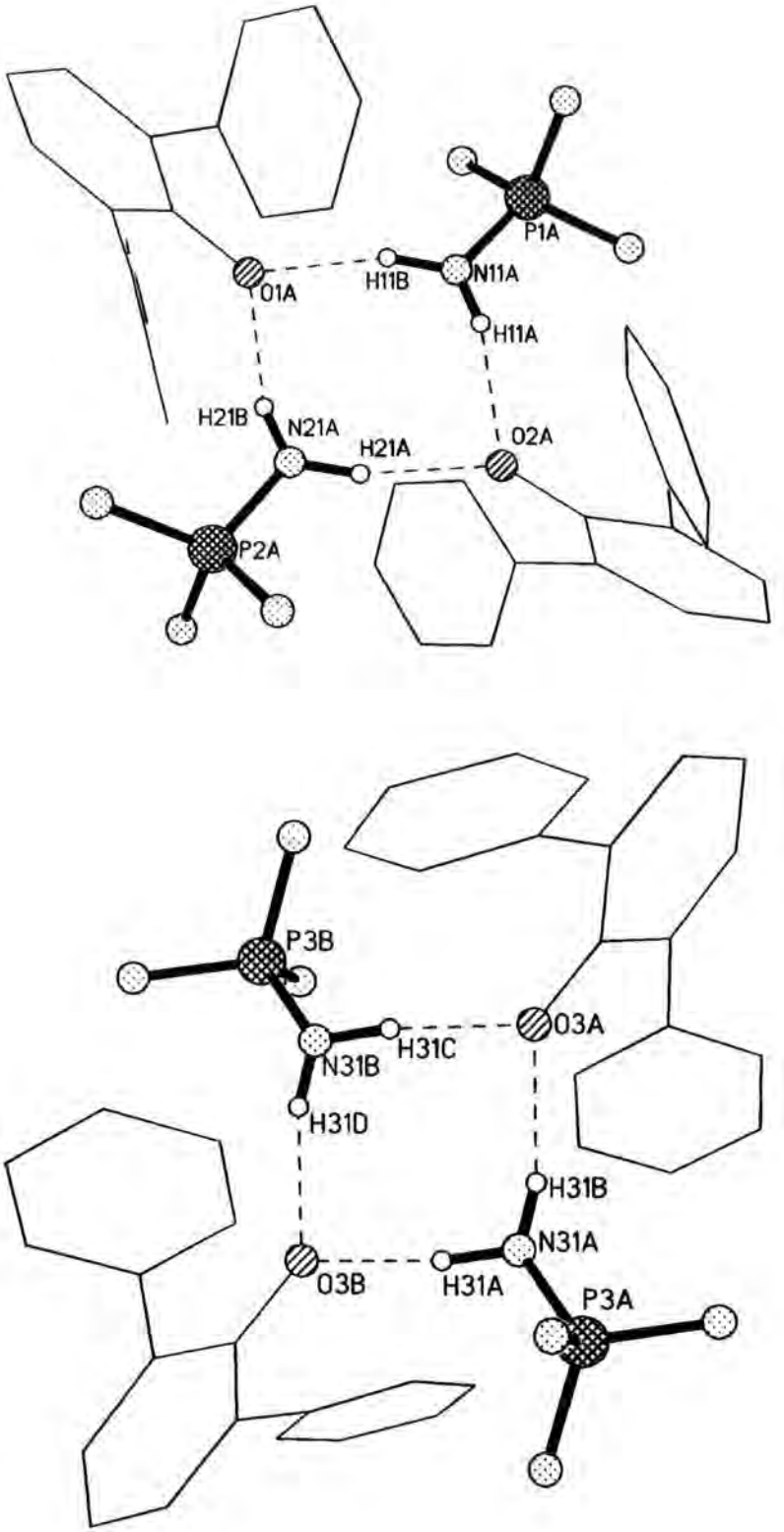

Figure 8.3 Two dimeric units of 42 (all hydrogens except those involved in hydrogen bonding omitted; organic anion in outline)

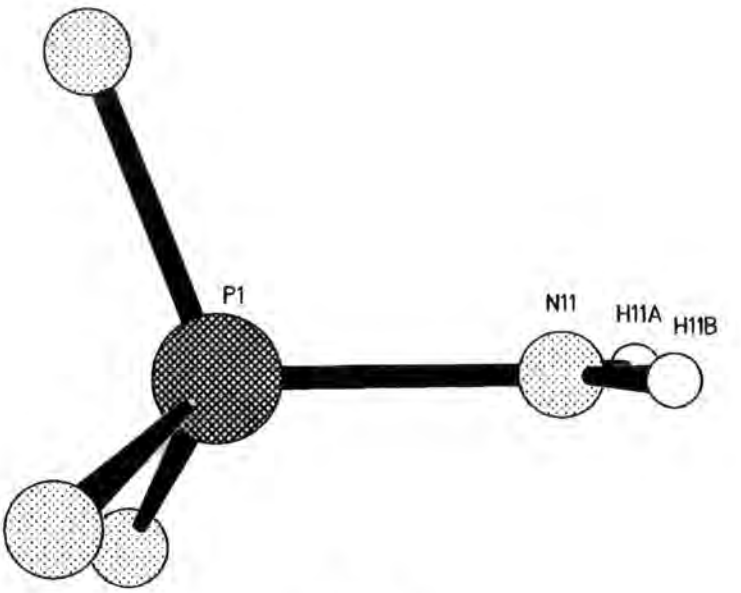

(I)

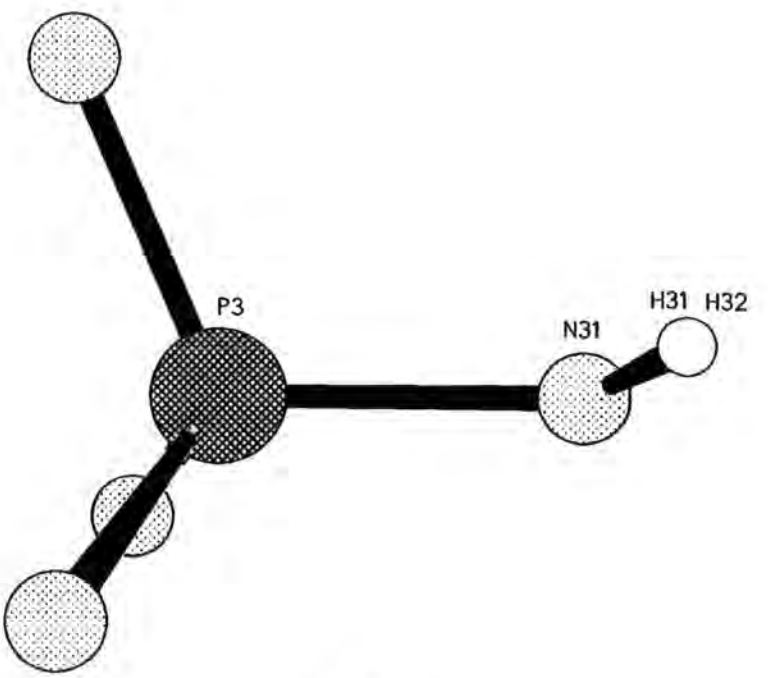

(II)

Figure 8.4 Two different aminophosphonium cations of 42

8.2 Solid-state structure and *in situ* NMR studies of 43

During the attempted synthesis (**Scheme 8.1**) of triphenylphosphonium cyclopropylide **L** using **A** and sodium amide as base in thf (a standard method of ylide formation but not one that has been previously reported),[14,15] a crystalline compound was isolated whose ^{31}P NMR spectrum precluded the simple cyclopropylide **L** as the product. Instead the isolation of a compound containing two phosphorus centres was inferred.

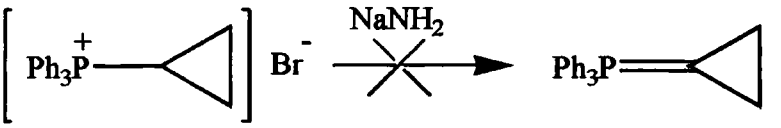

A **L**

Scheme 8.1 Standard ylide formation from phosphonium salt

A single crystal XRD study revealed the product to be a chiral *N*-phosphine substituted iminophosphorane **43**. Further NMR,‡ including *in situ* studies of the reaction mechanism, and chemical analysis confirm **43** as the bulk product.

Whilst **43** is not the first example of an *N*-phosphine-substituted iminophosphorane,[16,17,18,19] previous examples have been synthesised via markedly different routes, often involving coupling reactions using reagents such as $Li[N(PPh_2)_2]$.[17] The serendipitous synthesis here poses several interesting mechanistic questions which have been addressed by *in situ* variable temperature NMR studies. **Scheme 8.2** represents one possible mechanism that is consistent both with the NMR results presented here and with previous work.

---

[14] Ref 12, Ch. 4.
[15] H. Schmidbaur, A. Schier, B. Milewski-Mahrla and U. Schubert, *Chem. Ber.*, **115**, 722 (1982).
‡ Professor Lopez-Ortiz is gratefully acknowledged for his inexhaustible efforts.
[16] H.G. Ang, Y.M. Yai, L.L. Koh and W.L. Kwik, *J. Chem. Soc., Chem. Commun.*, 850 (1991).
[17] P. Braunstein, R. Hasselbring, A. Tiripicchio and F. Ugozzoli, *J. Chem. Soc., Chem. Commun.*, 37 (1995).
[18] A. Schmidpeter, K-H Zirzow, G. Burget, G. Huttner and I. Jibril, *Chem. Ber.*, **117**, 1695 (1984).
[19] K.V. Katti, B. D. Santarsiero, A.A. Pinkerton and R.G. Cavell, *Inorg. Chem.*, 1993, **32**, 5919.

Initially, nucleophilic attack at phosphorus of **A** [$\delta(^{31}P)$ 31.22] by nitrogen gives the aminophosphonium salt **B** and PhNa. **B** and the PhNa thus formed react rapidly, eliminating benzene (analogous to loss of hydrocarbon which occurs during the hydrolysis of phosphorus ylides)[20] to yield the cyclopropyl(diphenyl)iminophosphorane **C** as a first identifiable intermediate [$\delta(^{31}P)$ 27.84].[§] The transformation is very slow below 0 °C, but is completed after 30 min at ambient temperature. The presence of the cyclopropyl moiety is deduced from the ^{13}C NMR data: δ 9.09 (CH, $^{1}J_{PC}$ 103.8 Hz), 4.3 (CH_2, $^{2}J_{PC}$ 3.6 Hz). By allowing the sample to stand at 25 °C the iminophosphorane **C** equilibrates with the aminophosphonium cyclopropylide **D** [characterised through the ^{1}H, ^{13}C, and ^{31}P NMR spectra: δ (^{1}H) 0.88 (CH_2, $^{3}J_{PH}$ 27.2 Hz), δ (^{13}C) 8.72 (CH_2, $^{2}J_{PC}$ 8.3 Hz), δ (^{31}P) 16.7 ppm]. After approx. 2 h at 25 °C a 1:1 equilibrium is established between both species. At –20 °C, the iminophosphorane **C** predominates over the aminoylide tautomer (60:40), whereas this ratio is reversed at 60°C. The iminophosphorane aminoylide tautomerism has precedent.[21] Recently it has been claimed to be involved in the synthesis of enaminecyclopentenones mediated by alkyldiphenyliminophosphoranes.[22]

During the equilibration process between **C** and **D** (at ambient temperature) the ^{31}P spectrum shows the appearance of two phosphorus doublets, corresponding to the final product **43** (δ 23.2 and 55.7, $^{2}J_{PP}$ 94 Hz) together with a broad signal at 38.7 ppm. The intensity of both groups of signals increases with the concomitant decrease in the intensity of the signals of **C/D**. On heating the sample at 60 °C for 5 hours **C** completely disappears. Further reaction at room temperature is slow in a sealed NMR tube, but the aminoylide **D** completely transforms to **43** after five days.

Deprotonation of **C/D** by a second equivalent of sodium amide affords the *N*-sodiated iminophosphorane **E** and aminoylide **F**. The existence of **E** (analogous to R_3PNLi)[23] has previously been proposed by Schmidbaur et al., as an intermediate in the formation of a

---

[20] Ref. 3, Ch. 5 and references therein.
[§] NMR data quoted for experiments on a Bruker DPX 300 spectrometer (unless otherwise stated).
[21] T. A. Mastryukova and M. Y. Kabachnik, *Russ. Chem. Rev.*, **52**, 1012 (1983).
[22] J. M. Álvarez-Gutiérrez and F. López-Ortiz, *Chem. Commun.*, 1583 (1996).
[23] H. Schmidbaur and H. Jonas, *Chem. Ber.*, **100**, 1120 (1967).

phosphonium ylide-substituted iminophosphorane.[24] In the absence of any starting material available, the formation of **43** may then proceed by nucleophilic attack of **E/F** on the neutral intermediates **C/D**, yielding the metallated iminophosphorane **G**. Intramolecular abstraction of the methine proton of **G** affords the iminophosphorane-substituted ylide **H**, which is deprotonated to give the anion **J**. This can rearrange to **K** via a process resembling the Sommelet-Hauser rearrangement.[25] Subsequent neutralisation of **K** leads to the final *N*-phosphino iminophosphorane **43**. Alternatively, a direct route from **H** to **43** could be achieved by invoking a Stevens' rearrangement. The thermal phospha-Stevens' rearrangements of phosphonium ylides is known to proceed under forcing conditions.[26] However, the conjugation of the P=C linkage in **H** with the iminophosphorane moiety may allow the rearrangement to occur at ambient temperature.[27]

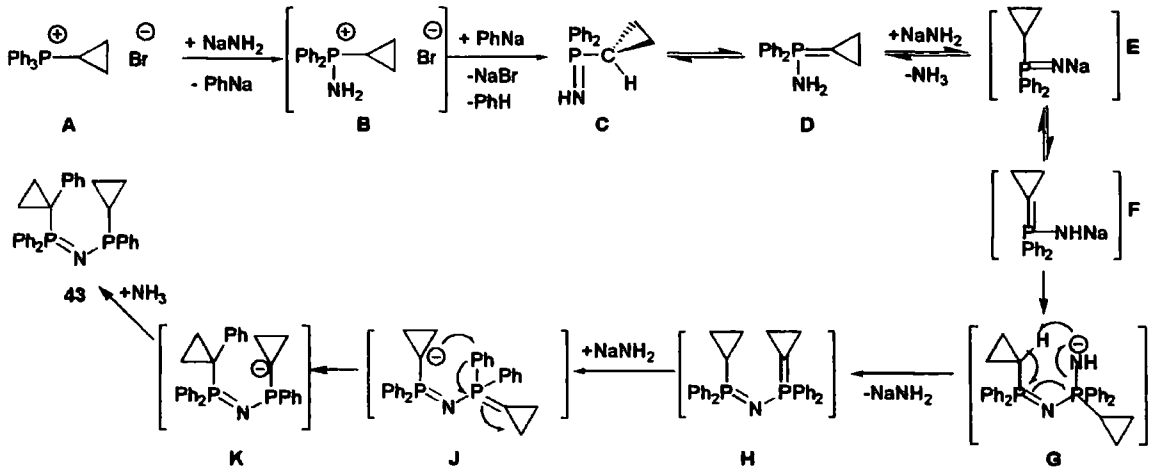

Scheme 8.2

Although the mechanism described above is speculative, the first intermediates involved have been identified by NMR and overall this route emphasises the strong involvement of metallic base interactions in organic/inorganic transformations involving organophosphorus species, even under such mild conditions as these. This is, for example,

---

[24] H. Schmidbaur and H-J. Fuller, *Angew. Chem.*, **15**, 501 (1976).
[25] G. M. Brooke and J. A. K. J. Ferguson, J. Chem. Soc. Perkin Trans. 1, 2023 (1988).
[26] *(a)* D. G. Gilheany, D. A. Kennedy, J. F. Malone and J. B. Walker, *J. Chem. Soc., Chem. Commun.*, 1217 (1984); *(b)* A. Maercker, A. Bsata and R. Jung, *Main Group Met. Chem.*, **10**, 11 (1987).
[27] K. Makita, J. Koketsu, F. Ando, Y. Ninomiya and N. Koga, *J. Am. Chem. Soc.*, **120**, 5764 (1998).

known to be a factor in the stereochemical outcome of Wittig reactions, but is still little understood.[28]

Unambiguous characterisation of **43** was achieved by a single crystal XRD study and then verified by COSY NMR experiments. Below is shown the ^{31}P and $^{1}H\{^{31}P\}$ NMR spectra (**Fig. 8.7**).*

The molecular geometry of **43** is unremarkable (**Fig. 8.5**): the P-N distances [P(1)-N 1.572(3) Å; P(2)-N 1.689(3) Å] and the P-N-P angle [123.4(2)°] are similar to those found in other substituted iminophosphoranes,[16-19] and the conformations of the cyclopropyl groups are usual (**Fig. 8.6**).[29]

The crystal packing of **43** is characterised by H...P(III) contacts between inversion-related molecules (**Fig. 8.8**). The P...H distance, 3.13 Å for the observed H position [C-H 0.98(4) Å] or 3.01 Å for the idealised one, is longer than in $(Ph_3PMe)^+ \{[C_6H_2(CF_3)_3\text{-}2,4,6]_2P\}^-$ (2.79 Å)[30] and close to the sum of the van der Waals radii (3.07 Å from crystallographic data,[31] 3.24 Å from *ab initio* calculations[32]). Thus the contact cannot be regarded as a hydrogen bond proper, as in $Ph_2PC(Ph)=CBu^nB(OH)CBu^n{}_2NBu^tCMe$ (with an OH...P distance of 2.30 Å),[33] but neither is it likely to be merely incidental, given the acidity of the cyclopropyl hydrogen atom and its pointing almost exactly towards the lone electron pair of the P(2) atom. The existence of an H...P contact, rather than an H...N interaction, such as was previously found[34] in $Ph_3P=NH$ **4**, can be explained by steric overcrowding of **43**, wherein the N atom lone pair is almost entirely masked by the H atoms at C(2) and C(42), which lie at 2.69 and 2.57 Å from the N atom and close to its sp^2 plane. This is a feature of **43** that should be significant in its coordination chemistry.

---

[28] B. E. Maryanoff and A. B. Reitz, *Chem. Rev.*, **89**, 863 (1989).

* 400MHz NMR data - selective ^{31}P decoupling @ δ = 24.3 and 57.8 ppm.

[29] F. H. Allen, J. P. M. Lommerse, V. J. Hoy, J. A. K. Howard and G. R. Desiraju, *Acta Crystallogr.*, **B52**, 734 (1996).

[30] M. G. Davidson, K. B. Dillon, J. A. K. Howard, S. Lamb and M. D. Roden, *J. Organomet. Chem.*, **550**, 481 (1998).

[31] M. Yu. V. Zefirov, P. M. Zorkii, *Russ. Chem. Rev.*, 1989, **58**, 421.

[32] M. Francl, R. F. Hout Jnr. and W. J. Hehre, *J. Am. Chem. Soc.*, 1984, **106**, 563.

[33] I. A. Litvinov and V. A. Naumov, *Zh. Strukt. Khim.*, 1993, **34**(3), 91; M. Yu. V. Zefirov, P. M. Zorkii, *Russ. Chem. Rev.*, 1995, **64**, 415.

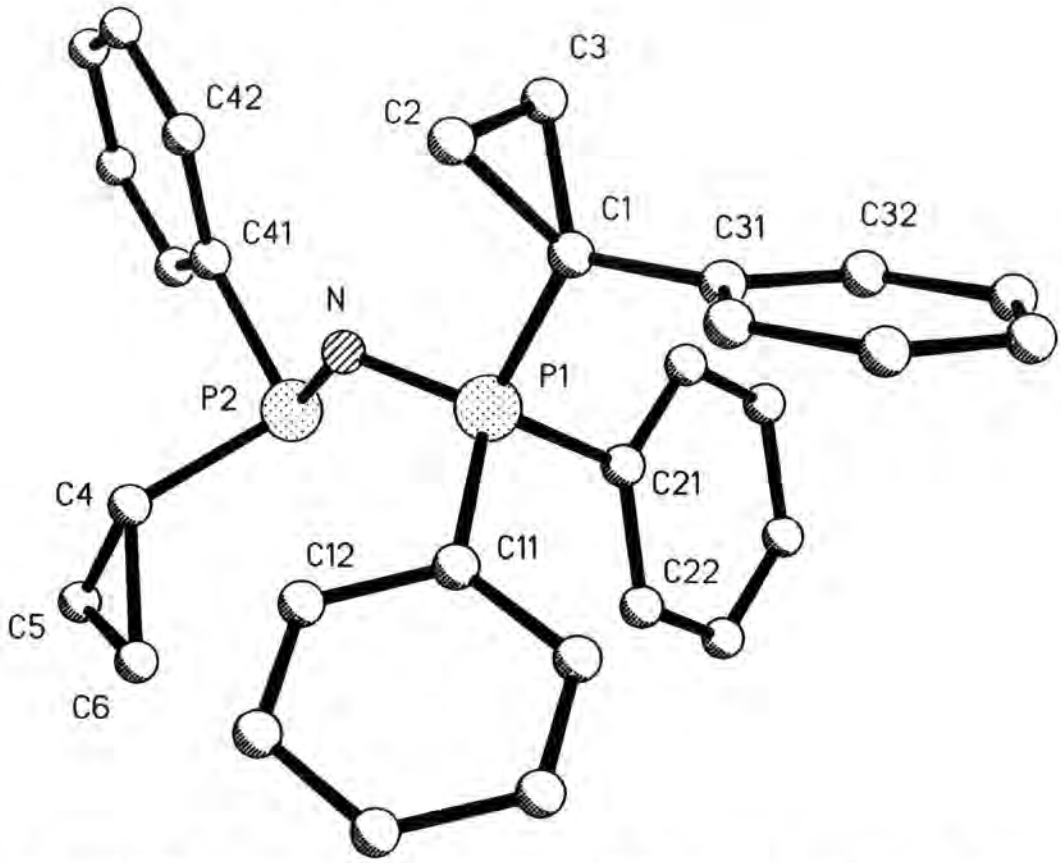

Figure 8.5 Single crystal XRD structure of 43 (hydrogens omitted for clarity)

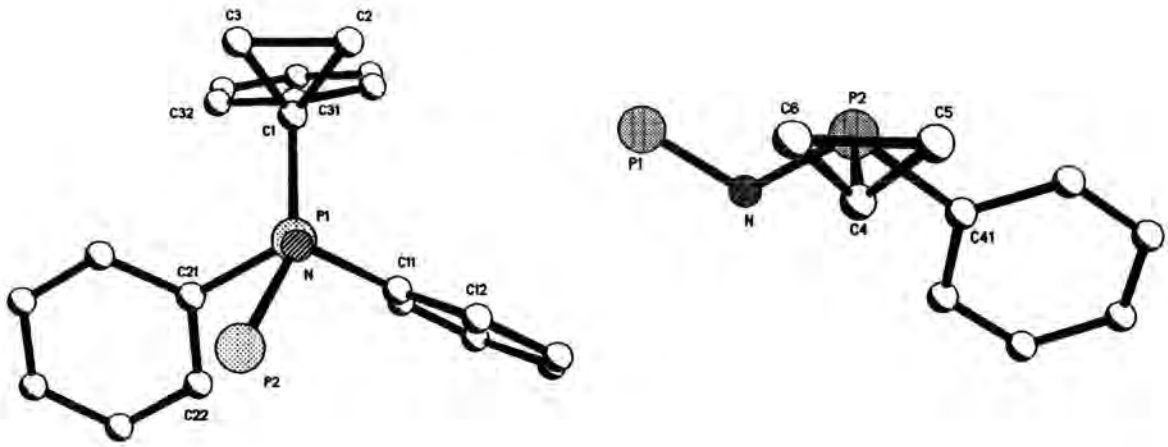

Figure 8.6 Conformations of the cyclopropyl groups in 43 (organic periphery omitted)

---

[34] M. G. Davidson, A. E. Goeta, J. A. K. Howard, C. W. Lehmann, G. M. McIntyre and R. D. Price, *J. Organomet. Chem.*, **550**, 449 (1998).

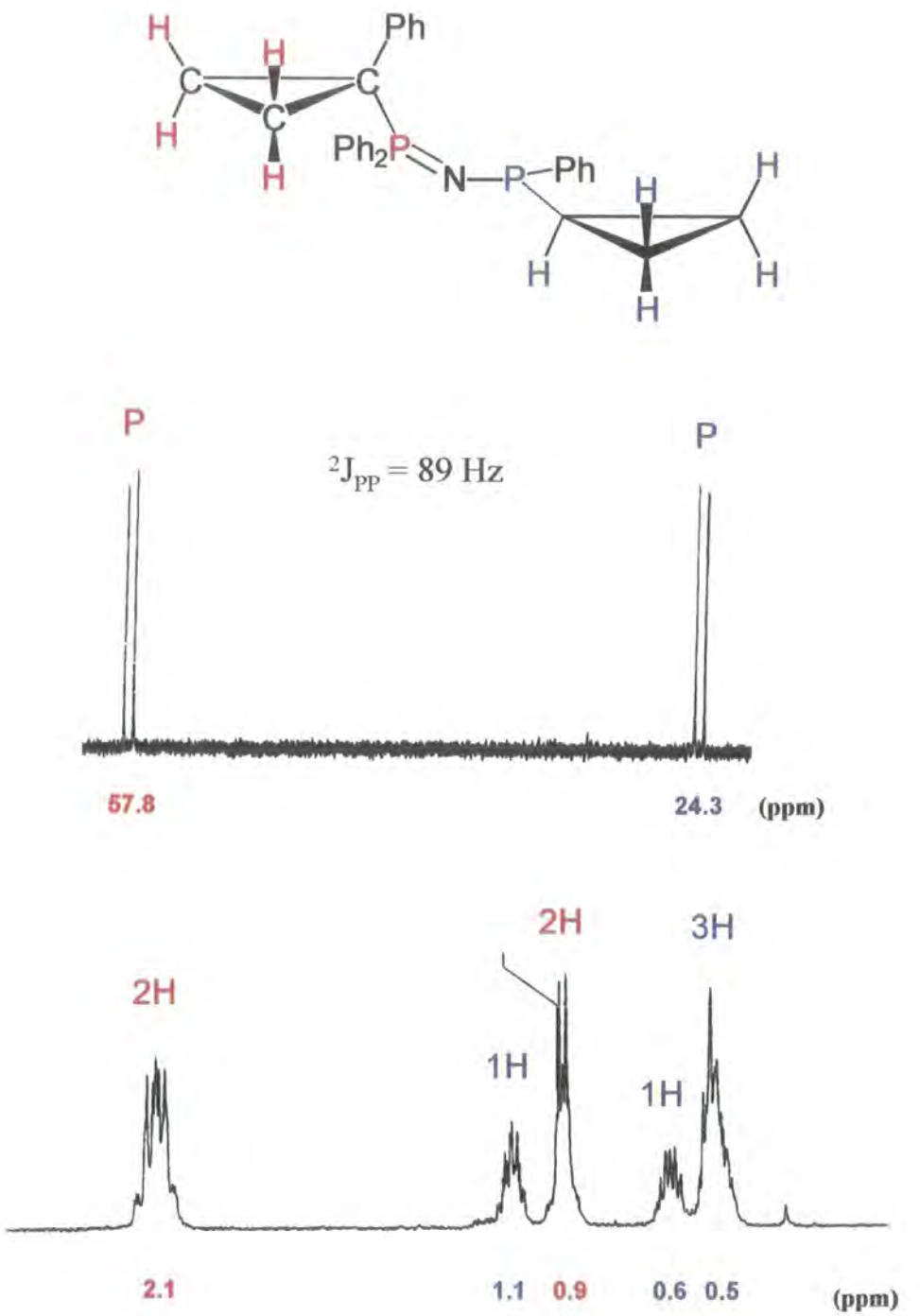

Figure 8.3 ^{31}P and ^{1}H (cyclopropyl region only) NMR spectra of 43

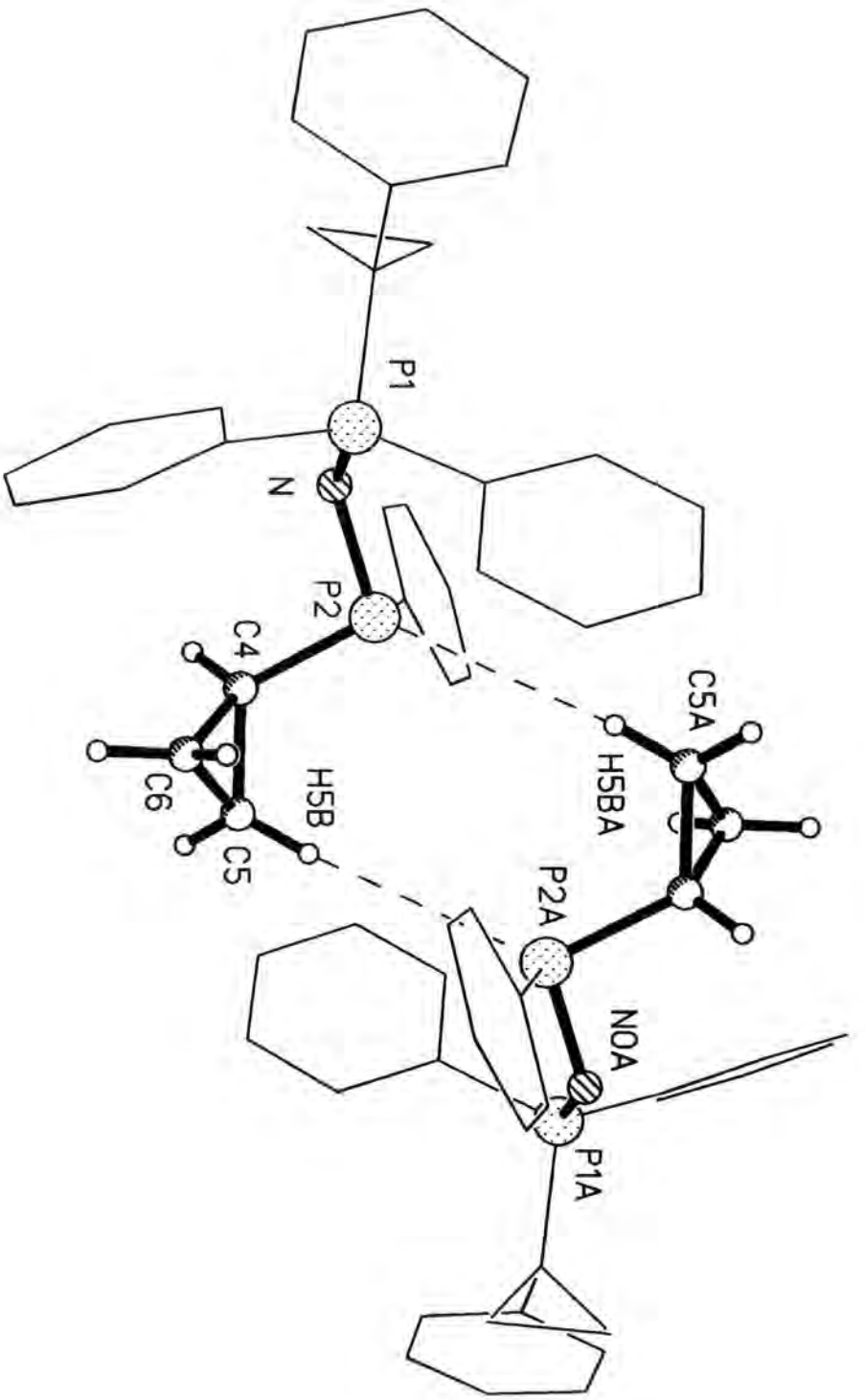

Figure 8.8 Dimeric aggregation via C-H...P interactions in 43 (organic periphery not involved in hydrogen bonding in outline)

8.3 Solid-state structure of complex 44

Complex **44** is an example of a phosphine oxide-lithium amide complex. It was formed originally by the reaction of **1**, tetraphenyldithioimidodiphosphinate $[(Ph_2PS)_2NH]$[35] in the presence of a small amount of atmospheric moisture and ^{n}BuLi (the synthesis is reproducible using methyldiphenylphosphine oxide directly). $MePh_2PO$ is the hydrolysis decomposition product of **1**. It is formed in preference to Ph_3PO, since protonation of **1** by water, to give $Ph_3PMe(OH)$, is followed by elimination of the most stable anion, i.e. $C_6H_5^-$ and not CH_3^-. Its characterisation was ultimately achieved via a single crystal XRD study (**Fig. 8.9**), which revealed the structure to be dimeric containing both Li-O and Li-S interactions.

The P-S bond lengths [ave. P-S distance = 1.991Å] are little changed upon coordination to those found in the parent ligand $(Ph_2PS)_2NH$ [1.916Å (ave.)].[36] Similarly, the P-O distance is within the expected range [1.507(2)Å].[37] The Li-S bond lengths [2.420Å (ave.)] are short in comparison to previously reported lengths[38] and shorter than that in **22**. The basis for this is presumably since for this structure there is a degree of delocalisation of the negative charge through the tetraphenyl-dithioimidodiphosphinate ligand and, therefore, a greater electrostatic shortening of the Li-S bond length. The Li-O bond lengths [1.93Å (ave.)] are in the expected range (1.85-2.0Å)[39] for lithium-phosphine oxide structures.

---

[35] F. T. Wang, *Synth. React. Inorg. Met. Chem.*, **8**, 120 (1978).

[36] H. Noth, *Z. Natursforsch*, **B37**, 1491 (1982); S. Husebye and K. Maartmann-Moe, *Acta Chem. Scand. Ser. A*, **37**, 439 (1983); P. B. Hitchcock, J. F. Nixon, I. Silaghi-Dumitrescu and I. Haiduc, *Inorg. Chim. Acta*, **96**, 77 (1985).

[37] G. Bandoli, G. Bartolozzo, D. A. Clemente, U. Croatto and C. Panattoni, *J. Chem. Soc. A*, 2778 (1970); G. Ruban and V. Zabel, *Cryst. Struct. Commun.*, **5**, 671 (1976); A. L. Spek, *Acta Crsyt.*, **C43**, 1233 (1987); N. W. Mitzel, *Personal Communication.*

[38] See for example: J. J. Ellison and P. P. Power, *Inorg. Chem.*, **33**, 4231 (1994); A. J. Banister, D. Barr, A. T. Brooker, W Clegg, M. J. Cunnington, M. J. Doyle, S. Drake, W. R. Gill, K. Manning, P. R. Raithby, R. Snaith, K. Wade and D. S. Wright, *J. Chem. Soc., Chem. Commun.*, 105 (1990); G. A. Sigel and P. P. Power, *Inorg. Chem.*, **26**, 2819 (1987).

[39] See for example: D. R. Armstrong, R. E. Mulvey, G. T. Walker, D. Barr, R. Snaith and D. Reed, *J. Chem. Soc. Dalton Trans.*, 617 (1988); F. S. Mair, D. Scully, A. J. Edwards, P. R. Raithby and R. Snaith, *Polyhedron*, **14**, 2397 (1995); C. J. Cramer, S. E. Denmark, P. C. Miller, R. L. Dorow, K. A. Swiss and S. R. Wilson, *J. Am. Chem. Soc.*, **116**, 2437 (1994); M. G. Davidson, J. A. K. Howard, S. Lamb and C. W. Lehmann, *J. Chem. Soc., Chem. Commun.*, 1607 (1997).

The use of $(Ph_2PS)_2NH$ and closely related ligands has recently attracted widespread interest in coordination chemistry.[40] There are several examples of s-block metal complexes,[40] including sodium,[40c] potassium[40b,e] and barium.[40d]

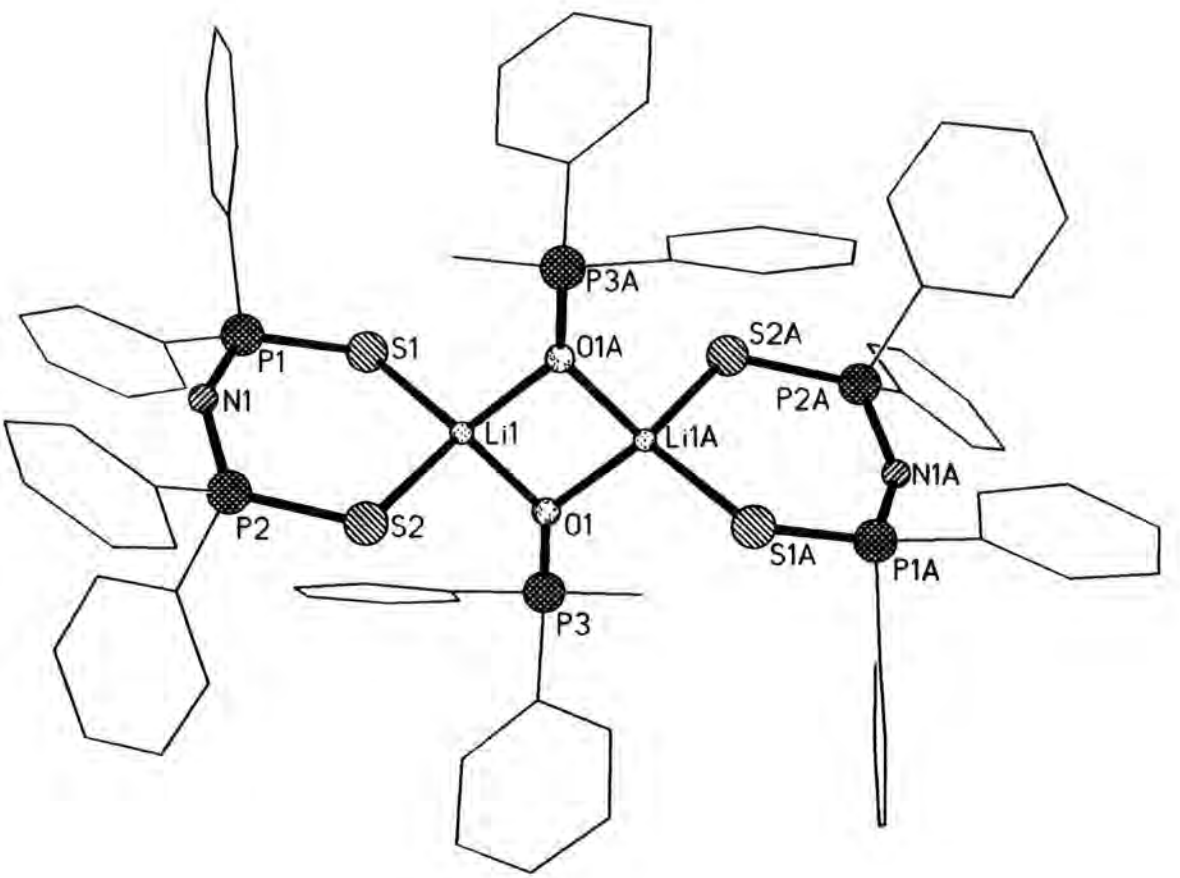

Figure 8.9 Single crystal XRD structure of 44 (organic groups in outline;hydrogens omitted for clarity)

[40] See for example: *(a)* P. Bhattacharyya, A. M. Z. Slawin and M. B. Smith, *J. Chem. Soc., Dalton Trans.*, 2467 (1998); *(b)* A. M. Z. Slawin, J. Ward, D. J. Williams and J. D. Woollins, *J. Chem. Soc., Chem. Commun.*, 421 (1994); *(c)* J. Yang, J. E. Drake, S. Hernandez-Ortega, R. Rösler and C. Silvestru, *Polyhedron*, **16**, 4061 (1997); *(d)* G. Kräuter, S. K. Sunny and W. S. Rees, Jnr., *Polyhedron*, **17**, 391 (1997); *(e)* R. Cea-Olivares and H. Noth, *Z. Natursforsch*, **B42**, 1507 (1987).

8.4 Conclusions

(i) Aminophosphonium salts have been shown to assemble via N-H...O and, in some instances, C-H...O hydrogen bonds at the supramolecular level. The analogous alkylphosphonium salt is isomorphous with **41**. This is an unusual case where C-H...O hydrogen bonding can directly replace stronger N-H...O interactions.

(ii) The isoelectronic relationship of $Ph_3PNH_2^+$ and Ph_3PCH_2 is also highlighted by **41**, which has the same structural motif of a unique P-C_{ipso} bond observed in the structures of many non-stabilised phosphonium ylides.

(iii) In the solid-state, **42** highlights the low energy-barrier between pyramidal and planar amino group arrangements. This low energy barrier has been observed previously for phosphonium ylides[12] and silylamines.[13]

(iv) Standard ylide formation in the reaction of cyclopropyltriphenylphosphonium bromide and sodium amide is not observed. Instead the reaction yields an *N*-phosphinoiminophosphorane **43**, whose nitrogen originates from sodium amide.

(v) *In situ* VT NMR studies on the formation of **43** have identified two intermediates, revealing the initial step to be nucleophilic displacement of a phenyl ring, i.e. not phosphonium ylide formation by deprotonation of the acidic α-proton.

(vi) The reaction highlights the inherent problems caused by the presence of metals/metal bases in Wittig reactions.

(vii) Compound **43** should act as a multifunctional ligand in coordination chemistry. The latter is currently under investigation, although the high degree of organic periphery surrounding the bridging nitrogen atom is likely to have a profound effect on its behaviour.

Appendix A

Supplementary Crystallographic Data

Supplementary Crystallographic Data

Number used in text	Table Number
(9)	A.1a/b
(10)	A.2a/b
(11)	A.3a/b
(12)	A.4a/b
(13)	A.5a/b
(14)	A.6a/b
(15)	A.7a/b
(16)	A.8a/b
(17)	A.9a/b
(22)	A.10a/b
(25)	A.11a/b
(27)	A.12a/b
(29a)	A.13a/b
(29b)	A.14a/b
(31)	A.15a/b
(32)	A.16a/b
(33)	A.17a/b
(34)	A.18a/b
(35)	A.19a/b
(36)	A.20a/b
(37)	A.21a/b
(38)	A.22a/b
(40)	A.23a/b
(41)	A.24a/b
(42)	A.25a/b
(43)	A.26a/b
(44)	A.27a/b
$MeC_6H_2(^tBu)_2OLi.thf$	A.28a/b
$Ph_2MePNPh$	A.29a/b

'It is best to do things systematically, since we are only human, and disorder is our worst enemy' (HESIOD 8th century B.C.).

Table A.1a Crystal data and structure refinement for (9).

Identification code	(9)
Empirical formula	C86 H98 Li2 O2 P2
Formula weight	1239.46
Temperature	150(2) K
Wavelength	0.71073 A
Crystal system	Triclinic
Space group	P-1
Unit cell dimensions	a = 11.0300(10) A alpha = 74.260(10) deg. b = 13.0630(10) A beta = 78.060(10) deg. c = 13.6090(10) A gamma = 76.860(10) deg.
Volume	1815.7(3) A^3
Z	1
Density (calculated)	1.134 Mg/m^3
Absorption coefficient	0.107 mm^-1
F(000)	666
Crystal size	0.40 x 0.25 x 0.20 mm
Theta range for data collection	1.65 to 26.00 deg.
Index ranges	-13<=h<=11, -16<=k<=16, -16<=l<=15
Reflections collected	11661
Independent reflections	7063 [R(int) = 0.0340]
Max. and min. transmission	0.9789 and 0.9585
Refinement method	Full-matrix least-squares on F^2
Data / restraints / parameters	7063 / 0 / 611
Goodness-of-fit on F^2	1.080
Final R indices [I>2sigma(I)]	R1 = 0.0557, wR2 = 0.1066
R indices (all data)	R1 = 0.0918, wR2 = 0.1262
Largest diff. peak and hole	0.309 and -0.306 e.A^-3

Table A.1b Atomic coordinates (x 10^4) and equivalent isotropic displacement parameters (A^2 x 10^3) for (9). U(eq) is defined as one third of the trace of the orthogonalized Uij tensor.

	x	y	z	U(eq)
P	5677(1)	2786(1)	2534(1)	25(1)
Li	5186(4)	4490(3)	4292(3)	26(1)
O(1)	4405(1)	5923(1)	4341(1)	21(1)
C(1)	6251(2)	7357(2)	3347(2)	25(1)
C(2)	6913(3)	8344(2)	2938(3)	45(1)
C(3)	6847(3)	6550(2)	2665(2)	36(1)
C(4)	6552(3)	6846(3)	4450(2)	35(1)
C(5)	2616(3)	10152(2)	2005(2)	35(1)
C(6)	1730(2)	6454(2)	4072(2)	25(1)
C(7)	2148(2)	5485(2)	3568(2)	30(1)
C(8)	395(2)	6984(2)	3825(3)	38(1)
C(9)	1604(3)	6062(2)	5260(2)	31(1)
C(10)	5631(3)	4004(2)	2803(2)	27(1)
C(11)	3982(2)	6908(2)	3786(2)	20(1)
C(12)	4814(2)	7667(2)	3315(2)	23(1)
C(13)	4328(2)	8699(2)	2768(2)	25(1)
C(14)	3075(2)	9032(2)	2631(2)	25(1)
C(15)	2280(2)	8285(2)	3067(2)	25(1)
C(16)	2680(2)	7240(2)	3644(2)	21(1)
C(21)	5721(2)	2757(2)	1192(2)	27(1)
C(22)	6091(3)	3610(2)	417(2)	38(1)
C(23)	6111(3)	3630(3)	-616(2)	45(1)
C(24)	5773(3)	2803(2)	-877(2)	42(1)
C(25)	5390(3)	1953(3)	-112(2)	42(1)
C(26)	5356(3)	1923(2)	926(2)	36(1)
C(31)	4291(2)	2219(2)	3190(2)	28(1)
C(32)	4376(3)	1188(2)	3815(2)	37(1)
C(33)	3275(3)	788(2)	4328(2)	44(1)
C(34)	2116(3)	1442(2)	4194(2)	41(1)
C(35)	2014(3)	2466(2)	3564(2)	42(1)
C(36)	3106(2)	2853(2)	3053(2)	35(1)
C(41)	7065(2)	1857(2)	2954(2)	27(1)
C(42)	7810(2)	1142(2)	2380(2)	33(1)
C(43)	8887(3)	466(2)	2711(2)	38(1)
C(44)	9243(3)	505(2)	3612(2)	39(1)
C(45)	8508(3)	1211(2)	4194(2)	39(1)
C(46)	7414(3)	1874(2)	3879(2)	34(1)
C(51)	104(4)	4605(4)	1516(3)	81(1)
C(52)	-278(4)	3615(5)	1632(4)	85(2)
C(53)	481(4)	2853(4)	1166(3)	74(1)
C(54)	1607(4)	3029(3)	601(3)	65(1)
C(55)	1991(4)	3977(3)	479(3)	62(1)
C(56)	1253(4)	4774(3)	915(3)	67(1)
C(61)	9042(5)	815(5)	-307(3)	83(2)
C(62)	8785(4)	-178(5)	206(3)	82(1)
C(63)	9731(6)	-1009(5)	524(4)	88(1)

Table A.2a Crystal data and structure refinement for (10).

Identification code	(10)
Empirical formula	C44.50 H48 Na O P
Formula weight	652.79
Temperature	150(2) K
Wavelength	0.71073 A
Crystal system	Triclinic
Space group	P -1
Unit cell dimensions	a = 11.1382(7) A alpha = 72.634(3) deg. b = 13.2408(1) A beta = 79.720(1) deg. c = 13.8945(8) A gamma = 77.256(3) deg.
Volume	1893.5(2) A^3
Z	2
Density (calculated)	1.145 Mg/m^3
Absorption coefficient	0.116 mm^-1
F(000)	698
Crystal size	0.54 x 0.50 x 0.40 mm
Theta range for data collection	1.55 to 27.48 deg.
Index ranges	-14<=h<=14, -16<=k<=17, -18<=l<=18
Reflections collected	19914
Independent reflections	8588 [R(int) = 0.0144]
Absorption correction	Multi-scan
Max. and min. transmission	0.962305 and 0.862564
Refinement method	Full-matrix least-squares on F^2
Data / restraints / parameters	8580 / 0 / 458
Goodness-of-fit on F^2	1.038
Final R indices [I>2sigma(I)]	R1 = 0.0399, wR2 = 0.1098
R indices (all data)	R1 = 0.0481, wR2 = 0.1199
Largest diff. peak and hole	0.391 and -0.300 e.A^-3

Table A.2b Atomic coordinates (x 10^4) and equivalent isotropic displacement parameters (A^2 x 10^3) for (10). U(eq) is defined as one third of the trace of the orthogonalized Uij tensor.

	x	y	z	U(eq)
P(1)	9283(1)	2235(1)	2643(1)	20(1)
Na(1)	9670(1)	532(1)	10888(1)	28(1)
O(1)	9319(1)	1053(1)	9256(1)	23(1)
C(1)	3893(2)	73(2)	4008(2)	46(1)
C(2)	4932(2)	-180(2)	3344(2)	48(1)
C(3)	5708(2)	538(2)	2904(1)	46(1)
C(4)	5458(2)	1514(2)	3119(2)	50(1)
C(5)	4427(2)	1774(2)	3776(2)	47(1)
C(6)	3622(2)	1048(2)	4234(1)	40(1)
C(7)	2501(2)	1319(2)	4942(2)	71(1)
C(8)	9257(2)	990(1)	2542(1)	27(1)
C(10)	9251(1)	2398(1)	3907(1)	23(1)
C(11)	8893(2)	1589(1)	4742(1)	32(1)
C(12)	8838(2)	1680(2)	5721(1)	40(1)
C(13)	9147(2)	2567(2)	5876(1)	39(1)
C(14)	9523(2)	3368(2)	5050(1)	38(1)
C(15)	9576(1)	3287(1)	4067(1)	31(1)
C(20)	7953(1)	3168(1)	2128(1)	22(1)
C(21)	7693(1)	3193(1)	1169(1)	26(1)
C(22)	6635(1)	3852(1)	783(1)	32(1)
C(23)	5839(1)	4496(1)	1340(1)	34(1)
C(24)	6101(1)	4492(1)	2279(1)	35(1)
C(25)	7154(1)	3828(1)	2673(1)	28(1)
C(30)	10668(1)	2712(1)	1939(1)	23(1)
C(31)	10628(1)	3740(1)	1286(1)	28(1)
C(32)	11711(2)	4075(1)	745(1)	35(1)
C(33)	12837(2)	3382(1)	862(1)	37(1)
C(34)	12894(1)	2357(1)	1515(1)	36(1)
C(35)	11814(1)	2021(1)	2056(1)	30(1)
C(40)	8877(1)	2048(1)	8761(1)	19(1)
C(41)	7588(1)	2373(1)	8611(1)	20(1)
C(42)	7164(1)	3432(1)	8069(1)	23(1)
C(43)	7928(1)	4197(1)	7679(1)	25(1)
C(44)	9168(1)	3876(1)	7838(1)	24(1)
C(45)	9673(1)	2832(1)	8351(1)	20(1)
C(46)	7444(2)	5330(1)	7077(1)	35(1)
C(50)	6685(1)	1568(1)	9009(1)	24(1)
C(51)	7090(1)	641(1)	8497(1)	30(1)
C(52)	6623(2)	1109(1)	10169(1)	32(1)
C(53)	5351(1)	2083(1)	8781(1)	38(1)
C(60)	11088(1)	2526(1)	8397(1)	24(1)
C(61)	11723(2)	3517(1)	8062(1)	37(1)
C(62)	11662(1)	1821(1)	7668(1)	33(1)
C(63)	11428(1)	1916(1)	9471(1)	30(1)
C(70)	4415(5)	3505(3)	5735(3)	110(1)
C(71)	5594(6)	3545(6)	5639(4)	88(2)
C(72)	3559(5)	4441(6)	5380(4)	73(1)
C(73)	4923(6)	4466(5)	5216(3)	73(2)
C(74)	6064(2)	4602(3)	5114(2)	75(1)

Table A.3a Crystal data and structure refinement for (11)

Identification code	(11)
Empirical formula	C42 H50 Li O P
Formula weight	608.73
Temperature	150(2) K
Wavelength	0.71073 A
Crystal system	Triclinic
Space group	P-1
Unit cell dimensions	a = 10.6007(2) A alpha = 72.9160(10) deg. b = 12.7385(2) A beta = 85.4710(10) deg. c = 14.4390(2) A gamma = 78.4990(10) deg.
Volume, Z	1825.91(5) A^3, 2
Density (calculated)	1.107 Mg/m^3
Absorption coefficient	0.105 mm^-1
F(000)	656
Crystal size	0.38 x 0.34 x 0.25 mm
Theta range for data collection	1.48 to 27.52 deg.
Limiting indices	-13<=h<=13, -16<=k<=16, -18<=l<=18
Reflections collected	17348
Independent reflections	8339 [R(int) = 0.0294]
Absorption correction	None
Max. and min. transmission	0.83 and 0.92
Refinement method	Full-matrix least-squares on F^2
Data / restraints / parameters	8302 / 0 / 606
Goodness-of-fit on F^2	1.093
Final R indices [I>2sigma(I)]	R1 = 0.0511, wR2 = 0.1030
R indices (all data)	R1 = 0.0788, wR2 = 0.1259
Largest diff. peak and hole	0.268 and -0.307 e.A^-3

Table A.3b Atomic coordinates (x 10^4) and equivalent isotropic displacement parameters (A^2 x 10^3) for (11). U(eq) is defined as one third of the trace of the orthogonalized Uij tensor.

	x	y	z	U(eq)
Li	9826(3)	4506(2)	882(2)	23(1)
P(1)	9845(1)	2622(1)	3270(1)	23(1)
O(1)	10615(1)	3969(1)	-133(1)	20(1)
C(1)	9875(2)	3932(2)	2495(1)	26(1)
C(2)	9064(2)	4905(2)	2830(2)	34(1)
C(11)	8368(2)	954(2)	3569(2)	37(1)
C(12)	7250(2)	562(2)	3526(2)	45(1)
C(13)	6163(2)	1287(2)	3115(2)	48(1)
C(14)	6185(2)	2410(2)	2741(2)	47(1)
C(15)	7300(2)	2816(2)	2782(2)	37(1)
C(16)	8394(2)	2094(2)	3204(1)	26(1)
C(21)	12005(2)	891(2)	3730(2)	33(1)
C(22)	12954(2)	72(2)	3514(2)	39(1)
C(23)	13077(2)	-61(2)	2590(2)	37(1)
C(24)	12249(2)	634(2)	1874(2)	35(1)
C(25)	11296(2)	1456(2)	2084(1)	30(1)
C(26)	11159(2)	1589(2)	3013(1)	25(1)
C(31)	9980(2)	2508(2)	4552(1)	25(1)
C(32)	10842(2)	3096(2)	4770(2)	33(1)
C(33)	11031(2)	3044(2)	5722(2)	36(1)
C(34)	10362(2)	2414(2)	6469(2)	37(1)
C(35)	9488(2)	1843(2)	6262(2)	38(1)
C(36)	9288(2)	1893(2)	5309(1)	30(1)
C(40)	7132(4)	4608(4)	5727(5)	120(2)
C(41)	6135(3)	3859(2)	5914(2)	63(1)
C(42)	5961(4)	3345(3)	5244(3)	80(1)
C(43)	5094(5)	2665(4)	5375(4)	99(2)
C(44)	4348(4)	2474(3)	6215(5)	98(2)
C(45)	4490(3)	3005(3)	6899(3)	84(1)
C(46)	5380(3)	3693(3)	6745(2)	69(1)
C(51)	11238(2)	3057(1)	-362(1)	18(1)
C(52)	10552(2)	2321(1)	-620(1)	18(1)
C(53)	11256(2)	1399(1)	-887(1)	22(1)
C(54)	12592(2)	1147(2)	-908(1)	24(1)
C(55)	13242(2)	1849(2)	-631(1)	24(1)
C(56)	12620(2)	2786(1)	-361(1)	20(1)
C(57)	9064(2)	2512(1)	-592(1)	21(1)
C(58)	8544(2)	1633(2)	-916(2)	28(1)
C(59)	8552(2)	2422(2)	450(1)	26(1)
C(60)	8485(2)	3656(2)	-1274(2)	30(1)
C(61)	13438(2)	3512(2)	-69(1)	25(1)
C(62)	14893(2)	3059(2)	-125(2)	39(1)
C(63)	13214(2)	4700(2)	-764(2)	37(1)
C(64)	13138(2)	3536(2)	982(2)	36(1)
C(65)	13317(3)	153(2)	-1212(2)	39(1)

Table A.4a Crystal data and structure refinement for (12).

Identification code	(12)
Empirical formula	C44 H86 Li2 N6 O2 P2
Formula weight	807.01
Temperature	150(2) K
Wavelength	0.71073 A
Crystal system	Triclinic
Space group	P-1
Unit cell dimensions	a = 11.542(3) A alpha = 101.601(4) deg. b = 13.639(3) A beta = 105.363(3) deg. c = 17.598(4) A gamma = 104.788(3) deg.
Volume	2473.3(11) A^3
Z	2
Density (calculated)	1.084 Mg/m^3
Absorption coefficient	0.127 mm^-1
F(000)	888
Crystal size	? x ? x ? mm
Theta range for data collection	1.25 to 30.32 deg.
Index ranges	-16<=h<=15, -18<=k<=19, -22<=l<=23
Reflections collected	30250
Independent reflections	13342 [R(int) = 0.0312]
Refinement method	Full-matrix least-squares on F^2
Data / restraints / parameters	13286 / 0 / 849
Goodness-of-fit on F^2	1.098
Final R indices [I>2sigma(I)]	R1 = 0.0537, wR2 = 0.1162
R indices (all data)	R1 = 0.0837, wR2 = 0.1415
Largest diff. peak and hole	0.586 and -0.386 e.A^-3

Table A.4b Atomic coordinates (x 10^4) and equivalent isotropic displacement parameters (A^2 x 10^3) for (12). U(eq) is defined as one third of the trace of the orthogonalized Uij tensor.

	x	y	z	U(eq)
P(1)	2815(1)	5500(1)	2884(1)	22(1)
O(1)	-997(1)	6507(1)	2570(1)	19(1)
C(1)	-1673(2)	5693(1)	2756(1)	18(1)
N(1)	-3202(2)	9726(1)	3210(1)	29(1)
Li(1)	-1120(3)	7776(2)	2334(2)	24(1)
P(2)	-3187(1)	9414(1)	2253(1)	22(1)
O(2)	453(1)	8195(1)	2164(1)	18(1)
C(2)	-1517(2)	5721(1)	3600(1)	21(1)
N(2)	-4651(2)	9406(1)	1739(1)	30(1)
Li(2)	598(3)	6942(2)	2432(2)	24(1)
N(3)	-2212(2)	10379(1)	2071(1)	36(1)
C(3)	-575(2)	6681(2)	4322(1)	27(1)
N(4)	3525(2)	6135(1)	3881(1)	34(1)
C(4)	-898(3)	7686(2)	4249(2)	44(1)
N(5)	3959(2)	5123(1)	2601(1)	28(1)
C(5)	-612(3)	6554(2)	5164(1)	43(1)
N(6)	1775(2)	4341(1)	2736(1)	28(1)
C(6)	799(2)	6813(2)	4346(2)	41(1)
C(7)	-2247(2)	4860(2)	3770(1)	25(1)
C(8)	-3128(2)	3972(1)	3161(1)	26(1)
C(9)	-3952(2)	3090(2)	3379(2)	39(1)
C(10)	-3253(2)	3937(1)	2350(1)	24(1)
C(11)	-2564(2)	4764(1)	2122(1)	20(1)
C(12)	-2824(2)	4672(1)	1196(1)	23(1)
C(13)	-3769(3)	3588(2)	634(1)	39(1)
C(14)	-1603(2)	4806(2)	974(1)	35(1)
C(15)	-3420(2)	5505(2)	973(1)	29(1)
C(16)	1116(2)	8971(1)	1935(1)	18(1)
C(17)	994(2)	8856(1)	1086(1)	20(1)
C(18)	141(2)	7829(1)	400(1)	22(1)
C(19)	671(2)	6927(2)	523(1)	33(1)
C(20)	96(2)	7911(2)	-466(1)	35(1)
C(21)	-1240(2)	7534(2)	395(1)	34(1)
C(22)	1721(2)	9687(2)	878(1)	23(1)
C(23)	2569(2)	10621(2)	1456(1)	26(1)
C(24)	3385(2)	11470(2)	1206(2)	40(1)
C(25)	2663(2)	10729(1)	2275(1)	23(1)
C(26)	1961(2)	9949(1)	2534(1)	19(1)
C(27)	2120(2)	10154(1)	3456(1)	22(1)
C(28)	3112(2)	11233(2)	3985(1)	34(1)
C(29)	2570(2)	9311(2)	3792(1)	33(1)
C(30)	858(2)	10161(2)	3590(1)	34(1)
C(31)	-2217(3)	9636(3)	3875(2)	49(1)
C(32)	-3876(3)	10403(2)	3515(2)	50(1)
C(33)	-5713(2)	8615(2)	1817(2)	43(1)
C(34)	-4877(3)	9406(3)	877(2)	50(1)
C(35)	-1298(2)	10244(2)	1666(2)	37(1)
C(36)	-2334(4)	11437(2)	2217(3)	69(1)
C(37)	-2785(2)	8299(2)	2053(1)	26(1)
C(38)	4185(3)	5631(3)	4430(2)	57(1)
C(39)	3858(2)	7270(2)	4211(2)	45(1)
C(40)	5174(2)	5985(2)	2837(2)	42(1)
C(41)	3574(2)	4517(2)	1733(2)	39(1)
C(42)	2101(3)	3399(2)	2853(2)	41(1)
C(43)	493(2)	4262(2)	2752(2)	33(1)
C(44)	2095(2)	6254(2)	2399(1)	27(1)

Table A.5a Crystal data and structure refinement for (13).

Identification code	(13)
Empirical formula	C33 H39 Li N O P
Formula weight	503.56
Temperature	150(2) K
Wavelength	0.71073 A
Crystal system	Monoclinic
Space group	P2(1)/c
Unit cell dimensions	a = 12.035(1) A alpha = 90 deg. b = 25.572(2) A beta = 104.91(1) deg. c = 9.807(1) A gamma = 90 deg.
Volume	2916.6(4) A^3
Z	4
Density (calculated)	1.147 g/cm^3
Absorption coefficient	0.119 mm^-1
F(000)	1080
Crystal size	0.4 x 0.25 x 0.2 mm
Theta range for data collection	1.6 to 26.0 deg.
Index ranges	-17<=h<=16, -35<=k<=31, -13<=l<=14
Reflections collected	18754
Independent reflections	5727 [R(int) = 0.0573]
Observed reflections, I>2sigma(I)	4241
Absorption correction	Semiempirical on Laue equivalents
Max. and min. transmission	0.9951 and 0.8382
Refinement method	Full-matrix least-squares on F^2
Data / restraints / parameters	5617 / 0 / 491
Goodness-of-fit on F^2	1.128
Final R indices [I>2sigma(I)]	R1 = 0.0532, wR2 = 0.0939
R indices (all data)	R1 = 0.0855, wR2 = 0.1133
Extinction coefficient	0.0018(3)
Largest diff. peak and hole	0.319 and -0.251 e.A^-3

Table A.5b Atomic coordinates (x 10^4) and equivalent isotropic displacement parameters (A^2 x 10^3) for (13). U(eq) is defined as one third of the trace of the orthogonalized Uij tensor.

	x	y	z	U(eq)
P	2085.3(5)	1052.9(2)	2306.0(6)	26.6(2)
O	5710(1)	444.1(5)	5331(1)	23.8(3)
N	2793(2)	549.9(8)	2933(2)	31.8(5)
Li	4240(3)	273(1)	4176(4)	26(1)
C(1)	6235(2)	909(1)	5568(2)	22(1)
C(2)	6933(2)	1095(1)	4684(2)	24(1)
C(3)	7411(2)	1597(1)	4920(2)	27(1)
C(4)	7262(2)	1921(1)	5989(2)	28(1)
C(5)	6619(2)	1729(1)	6872(2)	27(1)
C(6)	6102(2)	1236(1)	6704(2)	24(1)
C(7)	7192(2)	753(1)	3505(2)	27(1)
C(8)	7758(2)	2469(1)	6187(3)	42(1)
C(9)	5404(2)	1054(1)	7740(2)	29(1)
C(11)	1439(2)	1390(1)	3547(2)	30(1)
C(12)	1280(2)	1112(1)	4703(3)	41(1)
C(13)	806(2)	1356(2)	5688(3)	54(1)
C(14)	472(2)	1868(1)	5521(3)	56(1)
C(15)	622(3)	2150(1)	4380(4)	56(1)
C(16)	1113(2)	1914(1)	3398(3)	43(1)
C(21)	935(2)	929(1)	738(2)	29(1)
C(22)	-87(2)	1217(1)	409(3)	39(1)
C(23)	-922(2)	1118(1)	-834(3)	51(1)
C(24)	-759(2)	740(1)	-1753(3)	55(1)
C(25)	242(3)	447(1)	-1437(3)	52(1)
C(26)	1090(2)	543(1)	-193(3)	41(1)
C(31)	3002(2)	1540(1)	1826(2)	26(1)
C(32)	4029(2)	1677(1)	2797(3)	32(1)
C(33)	4730(2)	2063(1)	2469(3)	36(1)
C(34)	4407(2)	2319(1)	1188(3)	37(1)
C(35)	3396(2)	2187(1)	220(3)	43(1)
C(36)	2697(2)	1797(1)	528(3)	39(1)
C(71)	6077(2)	571(1)	2450(3)	37(1)
C(72)	7899(2)	273(1)	4176(3)	35(1)
C(73)	7903(2)	1037(1)	2642(3)	37(1)
C(91)	5931(2)	555(1)	8515(3)	33(1)
C(92)	5405(3)	1460(1)	8892(3)	40(1)
C(93)	4133(2)	964(1)	6950(3)	40(1)

Table A.6a Crystal data and structure refinement for (14).

Identification code	(14)
Empirical formula	C78 H90 N2 Na2 O2 P2
Formula weight	1195.44
Temperature	423(2) K
Wavelength	0.71073 A
Crystal system, space group	Triclinic, P-1
Unit cell dimensions	a = 10.53170(10) A alpha = 115.52 deg. b = 13.6970(2) A beta = 100.59 deg. c = 14.2771(2) A gamma = 103.00 deg.
Volume	1716.07(4) A^3
Z, Calculated density	1, 1.157 Mg/m^3
Absorption coefficient	0.123 mm^-1
F(000)	640
Crystal size	0.50 x 0.25 x 0.10 mm
Theta range for data collection	1.67 to 27.47 deg.
Limiting indices	-13<=h<=13, -17<=k<=17, -18<=l<=18
Reflections collected / unique	19368 / 7807 [R(int) = 0.0377]
Completeness to theta = 27.47	99.3 %
Absorption correction	Multiscan
Max. and min. transmission	1.000000 and 0.878357
Refinement method	Full-matrix least-squares on F^2
Data / restraints / parameters	7807 / 0 / 568
Goodness-of-fit on F^2	1.042
Final R indices [I>2sigma(I)]	R1 = 0.0452, wR2 = 0.0890
R indices (all data)	R1 = 0.0731, wR2 = 0.1023
Extinction coefficient	not refined
Largest diff. peak and hole	0.288 and -0.319 e.A^-3

Table A.6b Atomic coordinates (x 10^4) and equivalent isotropic displacement parameters (A^2 x 10^3) for (14). U(eq) is defined as one third of the trace of the orthogonalized Uij tensor.

	x	y	z	U(eq)
Na(1)	843(1)	5179(1)	1118(1)	27(1)
O(1)	151(1)	6344(1)	607(1)	22(1)
C(1)	26(2)	7368(1)	902(1)	20(1)
C(2)	-1152(2)	7597(1)	1199(1)	20(1)
C(3)	-1264(2)	8679(2)	1476(1)	22(1)
C(4)	-293(2)	9557(1)	1479(1)	23(1)
C(5)	861(2)	9338(2)	1212(1)	23(1)
C(6)	1059(2)	8284(1)	935(1)	21(1)
C(7)	2394(2)	8119(2)	692(1)	26(1)
C(8)	3359(2)	9197(2)	760(2)	40(1)
C(9)	2068(2)	7117(2)	-471(2)	36(1)
C(10)	3203(2)	7898(2)	1551(2)	35(1)
C(11)	-2290(2)	6671(2)	1213(1)	23(1)
C(12)	-3507(2)	7067(2)	1452(2)	33(1)
C(13)	-2897(2)	5541(2)	103(2)	30(1)
C(14)	-1714(2)	6404(2)	2115(2)	31(1)
C(0)	-488(2)	10701(2)	1741(2)	33(1)
N(1)	1946(2)	5939(1)	2960(1)	26(1)
P(1)	2968(1)	5684(1)	3711(1)	20(1)
C(21)	2339(2)	5421(2)	4717(1)	22(1)
C(22)	2216(2)	4415(2)	4773(2)	27(1)
C(23)	1700(2)	4263(2)	5553(2)	35(1)
C(24)	1320(2)	5115(2)	6280(2)	36(1)
C(25)	1449(2)	6122(2)	6234(2)	35(1)
C(26)	1947(2)	6275(2)	5457(2)	30(1)
C(31)	3265(2)	4408(1)	2805(1)	22(1)
C(32)	4585(2)	4386(2)	2816(1)	27(1)
C(33)	4758(2)	3405(2)	2051(2)	34(1)
C(34)	3620(2)	2452(2)	1277(2)	35(1)
C(35)	2304(2)	2467(2)	1262(2)	31(1)
C(36)	2118(2)	3437(2)	2021(1)	27(1)
C(41)	4654(2)	6796(1)	4514(1)	21(1)
C(42)	5340(2)	7332(2)	4016(2)	27(1)
C(43)	6620(2)	8195(2)	4606(2)	31(1)
C(44)	7223(2)	8541(2)	5705(2)	32(1)
C(45)	6557(2)	8016(2)	6202(2)	29(1)
C(46)	5275(2)	7142(2)	5611(1)	25(1)
C(1X)	9101(2)	1026(2)	5230(2)	39(1)
C(2X)	8558(2)	644(2)	4121(2)	41(1)
C(3X)	7191(2)	482(2)	3680(2)	38(1)
C(4X)	6361(2)	699(2)	4343(2)	35(1)
C(5X)	6906(2)	1071(2)	5447(2)	35(1)
C(6X)	8277(2)	1239(2)	5897(2)	36(1)

Table A.7a Crystal data and structure refinement for (15).

Identification code	(15)
Empirical formula	C42 H84 Li2 N8 O2 P2
Formula weight	809.0
Temperature	220(2) K
Wavelength	0.71073 A
Crystal system	Triclinic
Space group	P-1
Unit cell dimensions	a = 10.500(1) A alpha = 85.65(1) deg. b = 11.639(1) A beta = 72.56(1) deg. c = 11.787(1) A gamma = 66.25(1) deg.
Volume	1256.2(2) A^3
Z	1
Density (calculated)	1.069 Mg/m^3
Absorption coefficient	0.126 mm^-1
F(000)	444
Crystal size	0.40 x 0.27 x 0.13 mm
Theta range for data collection	1.8 to 27.5 deg.
Index ranges	-13<=h<=13, -10<=k<=15, -15<=l<=15
Reflections collected	10127
Independent reflections	5690 [R(int) = 0.0397]
Absorption correction	None
Refinement method	Full-matrix least-squares on F^2
Data / restraints / parameters	5598 / 16 / 266
Goodness-of-fit on F^2	1.119
Final R indices [I>2sigma(I)]	R1 = 0.0979, wR2 = 0.1965
R indices (all data)	R1 = 0.1469, wR2 = 0.2697
Largest diff. peak and hole	.431 and -.557 e.A^-3

Table A.7b Atomic coordinates (x 10^4) and equivalent isotropic displacement parameters (A^2 x 10^3) for (15). U(eq) is defined as one third of the trace of the orthogonalized Uij tensor.

	x	y	z	U(eq)
P	6599(1)	7860(1)	2767(1)	46(1)
O	5739(3)	4147(2)	3997(2)	37(1)
N(1)	5662(4)	7293(4)	3740(4)	52(1)
N(2A)	5611(9)	9244(8)	2468(8)	67(2)
N(2B)	5615(8)	8929(7)	1955(7)	57(2)
N(3)	7700(7)	8364(6)	3119(5)	100(2)
N(4)	7729(5)	6753(4)	1754(4)	70(1)
Li	5391(7)	5805(6)	4429(6)	42(1)
C(1)	6396(4)	3473(3)	2957(3)	36(1)
C(2)	5587(4)	3555(4)	2148(3)	43(1)
C(3)	6345(5)	2912(4)	1033(3)	47(1)
C(4)	7817(5)	2175(4)	683(4)	49(1)
C(5)	8575(4)	2065(4)	1491(3)	46(1)
C(6)	7919(4)	2685(3)	2626(3)	39(1)
C(7)	3917(5)	4313(4)	2469(4)	53(1)
C(8)	3505(6)	5702(5)	2725(6)	80(2)
C(9)	3307(6)	4255(6)	1451(5)	76(2)
C(10)	3152(5)	3747(6)	3537(4)	75(2)
C(11)	8562(6)	1484(5)	-544(4)	65(1)
C(12)	8854(4)	2511(4)	3468(4)	48(1)
C(13)	10446(5)	1586(6)	2932(5)	80(2)
C(14)	8906(5)	3759(5)	3737(5)	66(1)
C(15)	8261(5)	1970(5)	4637(4)	58(1)
C(16A)	4185(12)	9529(11)	2427(11)	77(3)
C(16B)	4233(13)	9045(13)	1891(12)	87(4)
C(17A)	6201(19)	10126(16)	1766(16)	133(6)
C(17B)	6328(17)	9502(15)	942(13)	113(5)
C(18A)	7349(19)	9083(16)	4217(14)	127(6)
C(19A)	9093(15)	7089(14)	3327(14)	99(4)
C(18B)	6888(17)	9789(13)	3490(15)	120(5)
C(19B)	8718(18)	7754(17)	3666(15)	115(5)
C(20)	7402(8)	5766(6)	1437(5)	93(2)
C(21A)	9164(12)	6675(12)	949(11)	80(3)
C(21B)	8483(15)	7217(13)	598(11)	93(4)

Table A.8a Crystal data and structure refinement for (16).

Identification code	(16)
Empirical formula	C24 H32 Li N4 O P
Formula weight	430.45
Temperature	150(2) K
Wavelength	0.71073 A
Crystal system	Triclinic
Space group	P -1
Unit cell dimensions	a = 10.5364(2) A alpha = 65.027(1) deg. b = 11.4243(2) A beta = 64.915(1) deg. c = 12.2900(1) A gamma = 67.513(1) deg.
Volume, Z	1176.67(3) A^3, 2
Density (calculated)	1.215 Mg/m^3
Absorption coefficient	0.139 mm^-1
F(000)	460
Crystal size	0.48 x 0.15 x 0.14 mm
Theta range for data collection	1.92 to 27.48 deg.
Limiting indices	-13<=h<=13, -14<=k<=14, -15<=l<=15
Reflections collected	13270
Independent reflections	5354 [R(int) = 0.0515]
Absorption correction	None
Refinement method	Full-matrix least-squares on F^2
Data / restraints / parameters	5322 / 0 / 408
Goodness-of-fit on F^2	1.148
Final R indices [I>2sigma(I)]	R1 = 0.0565, wR2 = 0.1042
R indices (all data)	R1 = 0.0879, wR2 = 0.1327
Largest diff. peak and hole	0.307 and -0.420 e.A^-3

Table A.8b Atomic coordinates (x 10^4) and equivalent isotropic displacement parameters (A^2 x 10^3) for (16). U(eq) is defined as one third of the trace of the orthogonalized Uij tensor.

	x	y	z	U(eq)
Li(1)	-1067(4)	10874(4)	-393(4)	23(1)
O(1)	-986(2)	9654(2)	1182(1)	19(1)
C(1)	-1633(2)	9137(2)	2401(2)	18(1)
C(2)	-2586(2)	9974(2)	3166(2)	20(1)
C(3)	-3205(3)	9413(3)	4467(2)	24(1)
C(4)	-2956(3)	8048(3)	5044(2)	27(1)
C(5)	-2053(3)	7223(3)	4307(2)	24(1)
C(6)	-1361(2)	7720(2)	3007(2)	20(1)
C(11)	-398(2)	6755(2)	2296(2)	21(1)
C(12)	-312(3)	6980(3)	1057(2)	26(1)
C(13)	575(3)	6045(3)	430(3)	36(1)
C(14)	1393(4)	4847(3)	1029(3)	42(1)
C(15)	1313(3)	4597(3)	2259(3)	39(1)
C(16)	436(3)	5541(3)	2880(3)	29(1)
C(21)	-3055(2)	11447(2)	2627(2)	22(1)
C(22)	-3075(3)	12297(3)	3193(3)	30(1)
C(23)	-3685(3)	13663(3)	2793(3)	38(1)
C(24)	-4289(3)	14211(3)	1825(3)	41(1)
C(25)	-4251(3)	13380(3)	1240(3)	37(1)
C(26)	-3640(3)	12026(3)	1629(2)	26(1)
N(1)	-2371(2)	11759(2)	-1466(2)	23(1)
P(1)	-2901(1)	11552(1)	-2378(1)	18(1)
N(2)	-4672(2)	12069(2)	-2095(2)	26(1)
N(3)	-2339(2)	12352(2)	-3930(2)	24(1)
N(4)	-2365(2)	9937(2)	-2203(2)	22(1)
C(31)	-5622(3)	11887(3)	-789(3)	39(1)
C(32)	-5433(3)	12369(3)	-2980(3)	37(1)
C(33)	-2740(4)	13818(3)	-4301(3)	39(1)
C(34)	-834(3)	11829(4)	-4620(3)	36(1)
C(35)	-2960(3)	9369(3)	-2691(3)	34(1)
C(36)	-978(3)	9094(3)	-2007(3)	31(1)

Table A.9a Crystal data and structure refinement for (17).

Identification code	(17)
Empirical formula	C21 H42 N4 Na O P
Formula weight	420.55
Temperature	150(2) K
Wavelength	0.71073 A
Crystal system	Monoclinic
Space group	P2(1)/n
Unit cell dimensions	a = 11.70660(10) A alpha = 90 deg. b = 13.3919(2) A beta = 102.4930(10) deg. c = 16.2803(2) A gamma = 90 deg.
Volume, Z	2491.89(5) A^3, 4
Density (calculated)	1.121 Mg/m^3
Absorption coefficient	0.145 mm^-1
F(000)	920
Crystal size	0.22 x 0.36 x 0.40 mm
Theta range for data collection	1.96 to 30.37 deg.
Limiting indices	-16<=h<=11, -17<=k<=18, -22<=l<=21
Reflections collected	16639
Independent reflections	6456 [R(int) = 0.0515]
Absorption correction	Multiscan
Max. and min. transmission	0.956250 and 0.819878
Refinement method	Full-matrix least-squares on F^2
Data / restraints / parameters	6359 / 0 / 270
Goodness-of-fit on F^2	1.193
Final R indices [I>2sigma(I)]	R1 = 0.0584, wR2 = 0.1155
R indices (all data)	R1 = 0.0931, wR2 = 0.1585
Largest diff. peak and hole	0.280 and -0.328 e.A^-3

Table A.9b Atomic coordinates (x 10^4) and equivalent isotropic displacement parameters (A^2 x 10^3) for (17). U(eq) is defined as one third of the trace of the orthogonalized Uij tensor.

	x	y	z	U(eq)
P(1)	3953(1)	7071(1)	2439(1)	27(1)
Na(1)	4686(1)	5505(1)	805(1)	30(1)
N(1)	3746(2)	6198(2)	1781(1)	36(1)
N(2)	4274(2)	6703(2)	3432(1)	37(1)
N(3)	5118(2)	7750(2)	2383(1)	30(1)
N(4)	2805(2)	7831(2)	2318(1)	37(1)
O(1)	5870(1)	5877(1)	-99(1)	24(1)
C(1)	4966(3)	7257(2)	4142(2)	54(1)
C(2)	3585(3)	5891(2)	3683(2)	54(1)
C(3)	2053(3)	8015(3)	1487(2)	55(1)
C(4)	2735(3)	8595(2)	2949(2)	49(1)
C(5)	6240(2)	7235(2)	2450(2)	41(1)
C(6)	5000(2)	8624(2)	1832(2)	35(1)
C(11)	6503(2)	6694(2)	119(1)	20(1)
C(12)	7665(2)	6638(2)	642(1)	22(1)
C(13)	8244(2)	7522(2)	942(1)	25(1)
C(14)	7763(2)	8464(2)	740(1)	28(1)
C(15)	6681(2)	8511(2)	181(1)	26(1)
C(16)	6041(2)	7667(2)	-148(1)	22(1)
C(17)	8402(3)	9403(2)	1109(2)	45(1)
C(20)	4858(2)	7777(2)	-782(1)	26(1)
C(21)	4569(3)	8879(2)	-1016(2)	45(1)
C(22)	3840(2)	7358(2)	-424(2)	35(1)
C(23)	4905(2)	7232(2)	-1609(1)	33(1)
C(30)	8268(2)	5620(2)	875(1)	25(1)
C(33)	7599(2)	5003(2)	1421(2)	34(1)
C(32)	8326(2)	5039(2)	65(1)	30(1)
C(31)	9537(2)	5726(2)	1382(2)	36(1)

Table A.10a Crystal data and structure refinement for (22).

Identification code	(22)
Empirical formula	C43.50 H46 Li O P S
Formula weight	654.77
Temperature	150(2) K
Wavelength	0.71073 A
Crystal system	Triclinic
Space group	'P-1'
Unit cell dimensions	a = 10.943 A alpha = 73.5440(10) deg. b = 13.31780(10) A beta = 78.91 deg. c = 13.64850(10) A gamma = 79.14 deg.
Volume	1853.05(2) A^3
Z	2
Density (calculated)	1.174 Mg/m^3
Absorption coefficient	0.163 mm^-1
F(000)	698
Crystal size	? x ? x ? mm
Theta range for data collection	1.57 to 30.43 deg.
Index ranges	-15<=h<=15, -18<=k<=18, -19<=l<=19
Reflections collected	23127
Independent reflections	9992 [R(int) = 0.0366]
Refinement method	Full-matrix least-squares on F^2
Data / restraints / parameters	9906 / 0 / 462
Goodness-of-fit on F^2	1.058
Final R indices [I>2sigma(I)]	R1 = 0.0501, wR2 = 0.1280
R indices (all data)	R1 = 0.0670, wR2 = 0.1672
Largest diff. peak and hole	0.432 and -0.530 e.A^-3

Table A.10b Atomic coordinates (x 10^4) and equivalent isotropic displacement parameters (A^2 x 10^3) for (22). U(eq) is defined as one third of the trace of the orthogonalized Uij tensor.

	x	y	z	U(eq)
P(1)	4293(1)	2220(1)	2571(1)	17(1)
O(1)	5604(1)	-924(1)	619(1)	17(1)
Li(1)	4922(3)	444(2)	691(2)	23(1)
S(1)	4293(1)	778(1)	2447(1)	23(1)
C(11)	4273(2)	2233(1)	3900(1)	19(1)
C(12)	4625(2)	3088(2)	4127(1)	24(1)
C(13)	4601(2)	3089(2)	5155(2)	28(1)
C(14)	4241(2)	2234(2)	5953(1)	28(1)
C(15)	3915(2)	1375(2)	5727(1)	29(1)
C(16)	3922(2)	1374(2)	4704(1)	24(1)
C(21)	2934(2)	3127(1)	2115(1)	19(1)
C(22)	2573(2)	3087(1)	1196(1)	23(1)
C(23)	1505(2)	3733(2)	847(2)	26(1)
C(24)	792(2)	4423(2)	1411(2)	26(1)
C(25)	1153(2)	4479(2)	2313(2)	26(1)
C(26)	2223(2)	3830(2)	2670(1)	24(1)
C(31)	5680(2)	2797(1)	1874(1)	19(1)
C(32)	5610(2)	3824(1)	1226(1)	23(1)
C(33)	6709(2)	4224(2)	696(2)	27(1)
C(34)	7875(2)	3606(2)	818(2)	27(1)
C(35)	7950(2)	2595(2)	1476(2)	27(1)
C(36)	6855(2)	2184(1)	2004(1)	22(1)
C(51)	9634(2)	678(2)	3682(2)	28(1)
C(52)	8448(2)	490(2)	4228(2)	32(1)
C(53)	7641(2)	1264(2)	4635(2)	34(1)
C(54)	8015(2)	2238(2)	4503(2)	33(1)
C(55)	9194(2)	2431(2)	3969(2)	34(1)
C(56)	9994(2)	1660(2)	3561(2)	32(1)
C(57)	10494(2)	-160(2)	3242(2)	38(1)
C(71)	6041(2)	-1899(1)	1138(1)	16(1)
C(72)	7345(2)	-2186(1)	1271(1)	17(1)
C(73)	7751(2)	-3210(1)	1837(1)	19(1)
C(74)	6954(2)	-3974(1)	2278(1)	20(1)
C(75)	5701(2)	-3692(1)	2128(1)	19(1)
C(76)	5215(2)	-2683(1)	1581(1)	17(1)
C(77)	3787(2)	-2429(1)	1530(1)	19(1)
C(78)	8289(2)	-1379(1)	842(1)	20(1)
C(79)	7414(2)	-5062(1)	2915(2)	27(1)
C(81)	3152(2)	-3435(2)	1865(2)	29(1)
C(82)	3499(2)	-1856(2)	427(2)	24(1)
C(83)	3162(2)	-1732(2)	2269(2)	26(1)
C(84)	9644(2)	-1876(2)	1027(2)	29(1)
C(85)	7917(2)	-488(1)	1405(1)	23(1)
C(86)	8351(2)	-930(2)	-336(1)	24(1)
C(91)	-1280(6)	5748(7)	4704(5)	63(2)
C(92)	-629(7)	6642(6)	4241(4)	123(2)
C(93)	830(12)	6104(8)	4285(6)	102(4)
C(94)	1061(4)	5175(4)	4793(3)	73(1)
C(95)	-336(6)	5694(5)	4744(4)	50(1)

Table A.11a Crystal data and structure refinement for (25).

Identification code	(25)
Empirical formula	C34 H33 Li N P
Formula weight	493.52
Temperature	150(2) K
Wavelength	0.71073 A
Crystal system	Monoclinic
Space group	P(2)1/n
Unit cell dimensions	a = 13.0780(10) A alpha = 90 deg. b = 10.6250(10) A beta = 105.370(10) deg. c = 20.2180(10) A gamma = 90 deg.
Volume	2708.9(4) A^3
Z	4
Density (calculated)	1.210 Mg/m^3
Absorption coefficient	0.125 mm^-1
F(000)	1048
Crystal size	? x ? x ? mm
Theta range for data collection	1.67 to 25.00 deg.
Index ranges	-17<=h<=15, -13<=k<=13, -20<=l<=26
Reflections collected	15934
Independent reflections	4763 [R(int) = 0.0392]
Refinement method	Full-matrix least-squares on F^2
Data / restraints / parameters	4686 / 0 / 466
Goodness-of-fit on F^2	1.074
Final R indices [I>2sigma(I)]	R1 = 0.0384, wR2 = 0.0762
R indices (all data)	R1 = 0.0564, wR2 = 0.0885
Largest diff. peak and hole	0.249 and -0.278 e.A^-3

Table A.11b Atomic coordinates (x 10^4) and equivalent isotropic displacement parameters (A^2 x 10^3) for (25). U(eq) is defined as one third of the trace of the orthogonalized Uij tensor.

	x	y	z	U(eq)
P	3747(1)	3629(1)	1930(1)	20(1)
N	4324(1)	6257(1)	-83(1)	26(1)
Li	4733(2)	4710(3)	533(2)	28(1)
C(1)	3164(2)	6203(2)	-278(1)	30(1)
C(2)	4647(2)	7566(2)	54(1)	29(1)
C(3)	4402(1)	4764(2)	1606(1)	23(1)
C(4)	4012(2)	6123(2)	1612(1)	28(1)
C(11)	2618(1)	6868(2)	-948(1)	28(1)
C(12)	2564(1)	6310(2)	-1583(1)	31(1)
C(13)	2103(2)	6929(2)	-2195(1)	36(1)
C(14)	1677(2)	8124(2)	-2183(1)	42(1)
C(15)	1719(2)	8690(2)	-1563(1)	44(1)
C(16)	2187(2)	8070(2)	-951(1)	38(1)
C(21)	5841(2)	7710(2)	340(1)	27(1)
C(22)	6403(2)	8571(2)	60(1)	40(1)
C(23)	7493(2)	8705(2)	311(1)	48(1)
C(24)	8047(2)	7987(2)	860(1)	42(1)
C(25)	7504(2)	7136(2)	1153(1)	39(1)
C(26)	6411(2)	6994(2)	893(1)	35(1)
C(31)	2335(1)	3708(2)	1512(1)	23(1)
C(32)	2015(1)	3723(2)	795(1)	30(1)
C(33)	946(2)	3746(2)	453(1)	35(1)
C(34)	184(2)	3761(2)	815(1)	36(1)
C(35)	490(2)	3746(2)	1524(1)	39(1)
C(36)	1561(1)	3716(2)	1872(1)	32(1)
C(41)	4178(1)	2059(2)	1783(1)	22(1)
C(42)	3459(1)	1062(2)	1628(1)	26(1)
C(43)	3812(2)	-148(2)	1549(1)	28(1)
C(44)	4877(2)	-373(2)	1627(1)	31(1)
C(45)	5592(2)	614(2)	1775(1)	38(1)
C(46)	5250(2)	1827(2)	1853(1)	32(1)
C(51)	3840(1)	3618(2)	2856(1)	24(1)
C(52)	4100(1)	4741(2)	3222(1)	28(1)
C(53)	4209(2)	4773(2)	3928(1)	34(1)
C(54)	4069(1)	3689(2)	4272(1)	36(1)
C(55)	3821(2)	2571(2)	3918(1)	35(1)
C(56)	3707(2)	2529(2)	3214(1)	30(1)

Table A.12a Crystal data and structure refinement for (27).

Identification code	(27)
Empirical formula	C26 H37 N Na P Si2
Formula weight	473.71
Temperature	150(2) K
Wavelength	0.71073 A
Crystal system	Triclinic
Space group	P -1
Unit cell dimensions	a = 10.0623(8) A alpha = 105.774(4) deg. b = 10.3932(10) A beta = 99.236(4) deg. c = 14.2947(13) A gamma = 102.193(5) deg.
Volume, Z	1367.9(2) A^3, 2
Density (calculated)	1.150 Mg/m^3
Absorption coefficient	0.218 mm^-1
F(000)	508
Crystal size	1.00 x 0.95 x 0.25 mm
Theta range for data collection	1.52 to 30.32 deg.
Limiting indices	-10<=h<=13, -14<=k<=14, -20<=l<=19
Reflections collected	12314
Independent reflections	7130 [R(int) = 0.0334]
Absorption correction	Multiscan
Max. and min. transmission	1.0000 and 0.7896
Refinement method	Full-matrix least-squares on F^2
Data / restraints / parameters	7092 / 0 / 428
Goodness-of-fit on F^2	1.117
Final R indices [I>2sigma(I)]	R1 = 0.0535, wR2 = 0.1131
R indices (all data)	R1 = 0.0887, wR2 = 0.1453
Largest diff. peak and hole	0.466 and -0.408 e.A^-3

Table A.12b Atomic coordinates (x 10^4) and equivalent isotropic displacement parameters (A^2 x 10^3) for (27). U(eq) is defined as one third of the trace of the orthogonalized Uij tensor.

	x	y	z	U(eq)
P(1)	2820(1)	5639(1)	1733(1)	18(1)
Si(1)	5870(1)	11709(1)	3694(1)	23(1)
Si(2)	7044(1)	8622(1)	6010(1)	24(1)
N(1)	5520(2)	9080(2)	5938(2)	23(1)
Na(1)	4471(1)	8614(1)	4102(1)	25(1)
C(11)	6720(3)	10462(3)	2948(2)	36(1)
C(12)	7307(3)	12905(3)	4800(2)	35(1)
C(13)	5530(4)	12837(3)	2896(2)	37(1)
C(21)	8265(4)	9602(4)	5423(3)	47(1)
C(22)	8098(3)	8965(4)	7319(2)	38(1)
C(23)	6835(3)	6725(3)	5337(2)	34(1)
C(30)	4293(2)	6299(2)	2681(2)	20(1)
C(31)	5724(3)	6462(3)	2428(2)	27(1)
C(41)	1317(2)	5675(2)	2278(2)	21(1)
C(42)	971(3)	4750(3)	2809(2)	28(1)
C(43)	-105(3)	4816(3)	3305(2)	36(1)
C(44)	-852(3)	5785(3)	3269(2)	39(1)
C(45)	-537(3)	6690(3)	2737(2)	38(1)
C(46)	547(3)	6638(3)	2234(2)	30(1)
C(51)	2375(2)	3866(2)	868(2)	20(1)
C(52)	3448(3)	3344(3)	532(2)	26(1)
C(53)	3139(3)	2049(3)	-186(2)	33(1)
C(54)	1759(3)	1246(3)	-574(2)	33(1)
C(55)	688(3)	1732(3)	-232(2)	31(1)
C(56)	986(3)	3039(3)	479(2)	26(1)
C(62)	2563(3)	6064(3)	-149(2)	25(1)
C(65)	3407(3)	8948(3)	660(2)	29(1)
C(63)	2684(3)	6888(3)	-768(2)	28(1)
C(66)	3301(3)	8131(3)	1289(2)	24(1)
C(64)	3108(3)	8320(3)	-367(2)	28(1)
C(61)	2879(2)	6677(2)	892(2)	20(1)

Table A.13a Crystal data and structure refinement for (29a)

Identification code	(29a)
Empirical formula	C62.50 H74 Br2 Li4 N2 O4 P2
Formula weight	1166.76
Temperature	150(2) K
Wavelength	0.71073 A
Crystal system	Triclinic
Space group	P-1
Unit cell dimensions	a = 10.575(1) A alpha = 100.61(1) deg. b = 13.882(1) A beta = 91.33(1) deg. c = 22.398(1) A gamma = 109.81(1) deg.
Volume	3027.5(4) A^3
Z	2
Density (calculated)	1.280 Mg/m^3
Absorption coefficient	1.438 mm^-1
F(000)	1214
Crystal size	0.50 x 0.32 x 0.20 mm
Theta range for data collection	1.67 to 27.77 deg.
Index ranges	-12<=h<=13, -16<=k<=13, -26<=l<=27
Reflections collected	14163
Independent reflections	9818 [R(int) = 0.0416]
Absorption correction	Semi-empirical
Max. and min. transmission	0.8986 and 0.6176
Refinement method	Full-matrix least-squares on F^2
Data / restraints / parameters	9428 / 16 / 663
Goodness-of-fit on F^2	1.301
Final R indices [I>2sigma(I)]	R1 = 0.0795, wR2 = 0.1550
R indices (all data)	R1 = 0.1108, wR2 = 0.2706
Largest diff. peak and hole	0.936 and -0.595 e.A^-3

Table A.13b Atomic coordinates (x 10^4) and equivalent isotropic displacement parameters (A^2 x 10^3) for (29a). U(eq) is defined as one third of the trace of the orthogonalized Uij tensor.

	x	y	z	U(eq)
Br(1)	2974(1)	6881(1)	4155(1)	44(1)
Br(2)	1345(1)	6216(1)	2394(1)	46(1)
P(1)	5867(2)	8698(1)	2781(1)	33(1)
P(2)	3965(2)	4186(1)	2698(1)	31(1)
Li(1)	3044(12)	7704(9)	3197(6)	41(3)
Li(2)	2220(11)	5386(10)	3191(6)	45(3)
Li(3)	3972(11)	6314(10)	2342(5)	42(3)
Li(4)	4927(12)	6693(10)	3437(6)	42(3)
O(1)	2366(5)	8855(4)	3441(3)	51(1)
O(2)	779(6)	4242(5)	3437(3)	72(2)
O(3)	4272(6)	6101(5)	1480(2)	66(2)
O(4)	6577(5)	6981(4)	3987(2)	54(2)
N(1)	4794(5)	7708(4)	2915(3)	35(1)
N(2)	3955(5)	5306(4)	2891(2)	33(1)
C(1)	2533(10)	9785(8)	3218(5)	77(3)
C(2A)	2014(19)	10494(14)	3723(9)	56(5)
C(3A)	916(22)	9605(16)	3946(10)	69(6)
C(2B)	1594(21)	10233(17)	3469(10)	65(5)
C(3B)	1454(18)	9858(13)	4153(8)	48(4)
C(4)	1271(10)	8712(8)	3827(4)	67(3)
C(5)	-534(10)	3928(11)	3148(5)	107(4)
C(6A)	-1141(19)	4463(16)	3588(8)	88(5)
C(6B)	-1497(32)	3753(28)	3592(14)	81(9)
C(7)	-666(13)	4263(12)	4196(6)	119(5)
C(8)	665(10)	4158(7)	4059(4)	69(3)
C(9)	5450(9)	6021(7)	1221(4)	61(2)
C(10A)	5260(26)	5798(22)	539(9)	111(9)
C(11A)	4021(21)	6092(20)	425(9)	81(7)
C(12A)	3777(20)	6638(15)	1042(8)	69(5)
C(10B)	5440(19)	6555(17)	693(9)	77(6)
C(11B)	4013(20)	6508(20)	580(12)	92(8)
C(12B)	3197(17)	5773(15)	992(8)	68(5)
C(13)	7480(8)	6397(7)	3948(4)	56(2)
C(14)	8165(10)	6636(8)	4573(4)	71(3)
C(15)	8146(8)	7718(7)	4856(4)	59(2)
C(16)	7134(8)	7899(6)	4446(4)	53(2)
C(17)	7288(6)	8490(5)	2386(3)	38(2)
C(18)	7765(9)	8864(6)	1880(4)	62(3)
C(19)	8822(11)	8632(8)	1605(6)	93(4)
C(20)	9417(8)	8028(8)	1845(5)	76(3)
C(21)	8938(9)	7631(8)	2345(5)	75(3)
C(22)	7883(8)	7855(8)	2617(4)	63(3)
C(23)	6721(7)	9729(5)	3447(3)	34(2)
C(24)	5989(8)	9868(6)	3950(3)	41(2)
C(25)	6561(8)	10657(6)	4456(3)	49(2)
C(26)	7871(9)	11323(6)	4479(3)	49(2)
C(27)	8632(8)	11181(6)	3993(4)	50(2)
C(28)	8060(7)	10401(5)	3483(3)	42(2)
C(29)	5273(7)	9434(6)	2305(3)	37(2)
C(30)	4036(8)	8923(8)	1957(4)	66(3)
C(31)	3535(9)	9426(9)	1584(5)	84(4)
C(32)	4250(10)	10443(9)	1557(4)	74(3)
C(33)	5474(9)	10961(7)	1891(4)	52(2)
C(34)	5984(8)	10461(6)	2269(3)	43(2)
C(35)	4475(7)	3637(5)	3309(3)	35(2)
C(36)	4916(8)	2783(6)	3194(3)	45(2)
C(37)	5340(9)	2417(7)	3664(4)	56(2)
C(38)	5343(8)	2886(6)	4259(4)	53(2)
C(39)	4917(8)	3729(6)	4387(3)	49(2)
C(40)	4473(7)	4101(6)	3911(3)	45(2)
C(41)	2341(6)	3173(6)	2347(3)	39(2)
C(42)	1562(8)	3459(7)	1956(4)	59(2)
C(43)	303(9)	2741(8)	1694(5)	78(3)
C(44)	-152(9)	1742(9)	1797(5)	79(3)
C(45)	622(10)	1474(9)	2183(5)	93(4)
C(46)	1858(8)	2174(7)	2459(4)	64(3)
C(47)	5132(6)	4001(5)	2128(3)	31(2)
C(48)	6499(7)	4617(6)	2253(3)	47(2)
C(49)	7427(8)	4524(7)	1838(4)	53(2)
C(50)	7018(8)	3824(6)	1298(4)	47(2)

C(51)	5665(8)	3205(6)	1158(3)	51(2)
C(52)	4741(7)	3294(6)	1577(3)	40(2)
C(53)	62(25)	5134(15)	271(7)	79(12)
C(54)	74(33)	4955(19)	-360(7)	71(11)
C(55)	497(27)	4163(17)	-659(6)	84(14)
C(56)	908(15)	3551(12)	-327(7)	95(9)
C(57)	896(15)	3730(12)	304(7)	106(8)
C(58)	472(15)	4521(13)	602(6)	81(6)
C(59)	-395(34)	5988(20)	593(10)	101(17)
C(60A)	2344(10)	9377(7)	-18(5)	83(4)
C(61A)	3245(12)	10013(10)	-347(5)	116(7)
C(62A)	3366(14)	11057(10)	-285(7)	135(8)
C(63A)	2586(14)	11464(8)	106(7)	117(7)
C(64A)	1685(13)	10827(9)	435(6)	108(6)
C(65A)	1564(11)	9784(9)	373(5)	85(5)
C(66A)	2312(18)	8284(8)	-120(8)	200(13)
C(60B)	1824(19)	10320(13)	270(9)	62(8)
C(61B)	1477(18)	9249(13)	232(9)	35(5)
C(62B)	2159(23)	8701(13)	-130(10)	115(15)
C(63B)	3189(23)	9222(18)	-454(11)	72(9)
C(64B)	3536(22)	10293(18)	-416(11)	86(12)
C(65B)	2854(23)	10842(13)	-54(11)	90(11)
C(66B)	1124(32)	10895(20)	697(15)	231(36)

Table A.14a Crystal data and structure refinement for (29b).

Identification code	(29b)
Empirical formula	C61 H71 Br2 Li4 N2 O4 P2
Formula weight	1145.72
Temperature	150(2) K
Wavelength	0.71073 A
Crystal system	Triclinic
Space group	P-1
Unit cell dimensions	a = 10.682(1) A alpha = 102.91(1) deg. b = 13.758(1) A beta = 90.85(1) deg. c = 22.280(1) A gamma = 109.74(1) deg.
Volume	2989.4(4) A^3
Z	2
Density (calculated)	1.273 Mg/m^3
Absorption coefficient	1.455 mm^-1
F(000)	1190
Crystal size	0.48 x 0.44 x 0.36 mm
Theta range for data collection	1.88 to 27.91 deg.
Index ranges	-12<=h<=11, -16<=k<=16, -28<=l<=26
Reflections collected	18255
Independent reflections	10556 [R(int) = 0.0339]
Absorption correction	Semi-empirical
Max. and min. transmission	0.6379 and 0.5249
Refinement method	Full-matrix least-squares on F^2
Data / restraints / parameters	10463 / 21 / 673
Goodness-of-fit on F^2	1.094
Final R indices [I>2sigma(I)]	R1 = 0.0450, wR2 = 0.1032
R indices (all data)	R1 = 0.0582, wR2 = 0.1268
Largest diff. peak and hole	0.853 and -0.536 e.A^-3

Table A.14b Atomic coordinates (x 10^4) and equivalent isotropic displacement parameters (A^2 x 10^3) for (29b). U(eq) is defined as one third of the trace of the orthogonalized Uij tensor.

	x	y	z	U(eq)
Br(1)	3013(1)	6827(1)	4145(1)	40(1)
Br(2)	1350(1)	6045(1)	2369(1)	39(1)
P(1)	5869(1)	8546(1)	2748(1)	28(1)
P(2)	3954(1)	4008(1)	2652(1)	26(1)
Li(1)	3086(6)	7599(5)	3174(3)	38(1)
Li(2)	2237(6)	5247(5)	3167(3)	40(1)
Li(3)	3985(6)	6127(4)	2313(2)	34(1)
Li(4)	4929(6)	6582(4)	3418(3)	35(1)
O(1)	2411(3)	8776(2)	3418(1)	51(1)
O(2)	812(3)	4117(2)	3406(1)	59(1)
O(3)	4277(3)	5836(2)	1433(1)	52(1)
O(4)	6563(3)	6891(2)	3976(1)	49(1)
N(1)	4804(3)	7567(2)	2889(1)	30(1)
N(2)	3926(3)	5147(2)	2857(1)	29(1)
C(1)	2505(5)	9649(4)	3162(3)	73(2)
C(2A)	2014(9)	10391(6)	3658(4)	49(2)
C(3A)	907(10)	9568(6)	3918(5)	66(3)
C(2B)	1529(10)	10137(9)	3473(4)	64(3)
C(3B)	1464(10)	9786(5)	4098(4)	50(2)
C(4)	1320(6)	8625(4)	3812(2)	72(1)
C(5)	-486(5)	3722(5)	3097(2)	85(2)
C(6A)	-1152(9)	4316(7)	3549(3)	77(2)
C(6B)	-1495(11)	3588(13)	3555(4)	83(5)
C(7)	-663(7)	4201(6)	4157(3)	110(2)
C(8)	663(5)	4092(4)	4038(2)	70(1)
C(9)	5460(4)	5839(3)	1141(2)	50(1)
C(10)	5429(6)	6368(4)	617(2)	79(2)
C(11)	3963(7)	6203(6)	483(2)	94(2)
C(12)	3287(6)	5604(6)	942(2)	96(2)
C(13)	7474(4)	6315(3)	3943(2)	52(1)
C(14)	8148(6)	6601(4)	4572(2)	72(1)
C(15)	8150(5)	7715(4)	4852(2)	59(1)
C(16)	7118(4)	7861(3)	4445(2)	53(1)
C(17)	7266(3)	8297(3)	2352(2)	34(1)
C(18)	7727(4)	8634(3)	1829(2)	48(1)
C(19)	8769(5)	8365(4)	1550(3)	68(1)
C(20)	9368(4)	7777(4)	1802(3)	66(1)
C(21)	8912(4)	7428(4)	2312(2)	63(1)
C(22)	7862(4)	7679(3)	2592(2)	50(1)
C(23)	6732(3)	9641(3)	3422(2)	31(1)
C(24)	6009(4)	9808(3)	3929(2)	37(1)
C(25)	6607(4)	10643(3)	4449(2)	43(1)
C(26)	7914(4)	11300(3)	4471(2)	48(1)
C(27)	8646(4)	11127(3)	3979(2)	48(1)
C(28)	8059(4)	10303(3)	3456(2)	40(1)
C(29)	5263(3)	9232(3)	2254(2)	32(1)
C(30)	4051(4)	8663(3)	1890(2)	47(1)
C(31)	3531(4)	9133(4)	1505(2)	58(1)
C(32)	4212(5)	10177(4)	1484(2)	53(1)
C(33)	5425(4)	10751(3)	1840(2)	44(1)
C(34)	5945(4)	10282(3)	2222(2)	37(1)
C(35)	4475(3)	3492(3)	3270(1)	30(1)
C(36)	4933(4)	2638(3)	3153(2)	42(1)
C(37)	5364(4)	2301(3)	3636(2)	50(1)
C(38)	5343(4)	2814(3)	4239(2)	49(1)
C(39)	4889(4)	3663(3)	4365(2)	47(1)
C(40)	4454(4)	4002(3)	3883(2)	38(1)
C(41)	2359(3)	2967(3)	2288(2)	32(1)
C(42)	1578(4)	3222(3)	1889(2)	48(1)
C(43)	350(4)	2475(3)	1603(2)	60(1)
C(44)	-102(4)	1475(4)	1713(2)	58(1)
C(45)	665(5)	1219(4)	2105(2)	64(1)
C(46)	1885(4)	1952(3)	2392(2)	52(1)
C(47)	5110(3)	3797(2)	2073(1)	29(1)
C(48)	6460(4)	4426(3)	2206(2)	41(1)
C(49)	7387(4)	4321(3)	1794(2)	48(1)
C(50)	6975(4)	3589(3)	1225(2)	44(1)
C(51)	5638(4)	2965(3)	1080(2)	40(1)
C(52)	4713(4)	3063(3)	1501(2)	33(1)
C(53)	1435(5)	-515(7)	294(3)	91(2)

C(54)	1723(6)	561(6)	324(2)	82(2)
C(55)	2703(5)	1050(4)	-4(2)	67(1)
C(56)	3370(5)	484(4)	-360(2)	68(1)
C(57)	3088(5)	-559(4)	-381(2)	66(1)
C(58)	2126(6)	-1071(4)	-64(2)	72(1)
C(59)	-213(6)	5383(6)	586(3)	89(2)
C(60)	95(7)	4489(8)	453(4)	120(3)
C(61)	304(8)	4067(7)	-179(5)	137(3)

Table A.15a Crystal data and structure refinement for (31).

Identification code	(31)
Empirical formula	C18 H15 Cu N P
Formula weight	339.82
Temperature	150(2) K
Wavelength	0.71073 A
Crystal system	Monoclinic
Space group	P(2)1/c
Unit cell dimensions	a = 9.1614(7) A alpha = 90 deg. b = 24.476(2) A beta = 98.478(4) deg. c = 29.530(2) A gamma = 90 deg.
Volume	6549.3(7) A^3
Z	16
Density (calculated)	1.379 Mg/m^3
Absorption coefficient	1.423 mm^-1
F(000)	2784
Crystal size	? x ? x ? mm
Theta range for data collection	1.09 to 24.00 deg.
Index ranges	-11<=h<=11, -30<=k<=31, -30<=l<=38
Reflections collected	35843
Independent reflections	10275 [R(int) = 0.1774]
Refinement method	Full-matrix least-squares on F^2
Data / restraints / parameters	9861 / 0 / 802
Goodness-of-fit on F^2	1.160
Final R indices [I>2sigma(I)]	R1 = 0.0842, wR2 = 0.1275
R indices (all data)	R1 = 0.1798, wR2 = 0.1780
Largest diff. peak and hole	0.651 and -0.603 e.A^-3

Table A.15b Atomic coordinates (x 10^4) and equivalent isotropic displacement parameters (A^2 x 10^3) for (31). U(eq) is defined as one third of the trace of the orthogonalized Uij tensor.

	x	y	z	U(eq)
Cu(1)	1733(1)	3001(1)	1620(1)	21(1)
P(1)	3418(3)	2550(1)	3414(1)	21(1)
N(1)	3831(9)	2556(3)	2921(2)	22(2)
C(1)	1465(11)	2603(4)	3469(3)	28(3)
Cu(2)	3838(1)	1990(1)	2503(1)	21(1)
P(2)	4939(3)	1010(1)	1993(1)	18(1)
N(2)	3814(8)	1475(3)	2039(2)	21(2)
C(2)	524(12)	2206(4)	3238(4)	40(3)
Cu(3)	2839(1)	1954(1)	1601(1)	21(1)
P(3)	1860(3)	2422(1)	672(1)	20(1)
N(3)	1776(9)	2445(3)	1193(2)	25(2)
C(3)	-974(12)	2222(5)	3240(4)	47(3)
Cu(4)	2733(1)	3040(1)	2509(1)	22(1)
P(4)	388(3)	3891(1)	2126(1)	20(1)
N(4)	1753(8)	3522(3)	2086(2)	21(2)
C(4)	-1591(12)	2636(5)	3469(4)	42(3)
C(5)	-688(11)	3025(5)	3700(3)	37(3)
C(6)	832(11)	3005(4)	3702(3)	34(3)
C(7)	4063(10)	1939(4)	3730(3)	23(2)
C(8)	5348(11)	1694(4)	3636(3)	32(3)
C(9)	5905(12)	1226(4)	3855(4)	41(3)
C(10)	5144(15)	985(4)	4176(4)	48(4)
C(11)	3841(16)	1207(5)	4269(4)	48(3)
C(12)	3300(13)	1687(4)	4043(3)	33(3)
C(13)	4339(10)	3104(4)	3760(3)	20(2)
C(14)	5086(9)	3496(4)	3547(3)	24(2)
C(15)	5830(12)	3913(4)	3811(4)	39(3)
C(16)	5818(12)	3937(4)	4275(4)	48(3)
C(17)	5094(13)	3536(5)	4491(4)	49(3)
C(18)	4361(11)	3127(4)	4233(3)	34(3)
C(19)	6907(10)	1182(4)	2085(3)	23(2)
C(20)	7321(12)	1673(4)	1902(3)	32(3)
C(21)	8812(13)	1813(5)	1933(4)	45(3)
C(22)	9843(12)	1467(5)	2156(4)	43(3)
C(23)	9483(12)	975(5)	2346(4)	41(3)
C(24)	7974(11)	841(4)	2311(3)	33(3)
C(25)	4785(10)	432(4)	2366(3)	18(2)
C(26)	4494(10)	526(4)	2810(3)	29(3)
C(27)	4447(11)	104(4)	3123(3)	31(3)
C(28)	4705(10)	-425(4)	2995(3)	32(3)
C(29)	5037(11)	-532(4)	2563(3)	28(2)
C(30)	5069(10)	-105(4)	2253(3)	24(2)
C(31)	4658(10)	725(4)	1411(3)	19(2)
C(32)	3219(11)	679(4)	1183(3)	24(2)
C(33)	2962(11)	511(4)	732(3)	29(3)
C(34)	4144(13)	379(4)	509(4)	36(3)
C(35)	5577(12)	410(4)	731(4)	38(3)
C(36)	5825(12)	582(4)	1181(3)	34(3)
C(37)	3693(10)	2440(4)	508(3)	20(2)
C(38)	4173(11)	2852(4)	234(3)	29(3)
C(39)	5648(11)	2880(5)	159(3)	37(3)
C(40)	6633(11)	2493(4)	353(4)	35(3)
C(41)	6180(11)	2083(4)	624(3)	33(3)
C(42)	4728(11)	2053(4)	699(3)	30(3)
C(43)	809(10)	2965(4)	341(3)	20(2)
C(44)	168(10)	2904(4)	-113(3)	30(3)
C(45)	-647(12)	3323(5)	-339(4)	38(3)
C(46)	-882(11)	3792(4)	-113(4)	34(3)
C(47)	-245(14)	3867(5)	330(4)	50(3)
C(48)	591(12)	3444(4)	562(3)	37(3)
C(49)	1040(10)	1795(4)	410(3)	20(2)
C(50)	1350(13)	1583(4)	-4(4)	42(3)
C(51)	621(14)	1127(5)	-203(4)	50(3)
C(52)	-446(13)	884(5)	15(5)	50(4)
C(53)	-758(12)	1072(5)	422(5)	54(4)
C(54)	-34(11)	1530(4)	626(4)	34(3)
C(55)	-1446(10)	3586(4)	1984(3)	23(2)
C(56)	-2082(11)	3335(4)	2337(3)	28(3)
C(57)	-3429(11)	3064(4)	2234(4)	38(3)

C(58)	-4141(11)	3036(4)	1787(4)	36(3)
C(59)	-3487(11)	3273(4)	1432(4)	31(3)
C(60)	-2144(10)	3545(4)	1542(3)	26(2)
C(61)	315(11)	4473(4)	1740(3)	23(2)
C(62)	1495(11)	4571(4)	1492(3)	35(3)
C(63)	1458(13)	5020(5)	1211(4)	43(3)
C(64)	307(14)	5390(5)	1163(4)	48(3)
C(65)	-839(13)	5294(5)	1404(4)	52(4)
C(66)	-848(13)	4844(4)	1694(4)	45(3)
C(67)	398(10)	4207(4)	2690(3)	17(2)
C(68)	1669(11)	4188(4)	3009(3)	25(2)
C(69)	1695(12)	4427(4)	3438(3)	34(3)
C(70)	487(12)	4693(4)	3554(4)	35(3)
C(71)	-786(12)	4707(4)	3241(4)	35(3)
C(72)	-846(10)	4472(4)	2816(3)	26(2)
C(90)	3696(35)	-38(13)	4842(12)	113(12)
C(91)	4193(46)	-471(14)	4492(14)	75(11)
C(92)	5534(42)	-572(8)	4502(8)	126(9)
C(93)	3271(43)	277(27)	5132(21)	119(23)
C(94)	4871(86)	-212(15)	4832(13)	96(19)

Table A.16a Crystal data and structure refinement for (32).

Identification code	(32)
Empirical formula	C6 H18 Cu N4 P
Formula weight	240.75
Temperature	150(2) K
Wavelength	0.71073 A
Crystal system	Monoclinic
Space group	P2(1)/n
Unit cell dimensions	a = 13.253(3) A alpha = 90 deg. b = 14.007(3) A beta = 117.24(3) deg. c = 13.319(3) A gamma = 90 deg.
Volume	2198.3(8) A^3
Z	8
Density (calculated)	1.455 Mg/m^3
Absorption coefficient	2.092 mm^-1
F(000)	1008
Crystal size	0.2 x 0.3 x 0.4 mm
Theta range for data collection	2.31 to 30.55 deg.
Index ranges	-9<=h<=9, -19<=k<=19, -15<=l<=18
Reflections collected	12738
Independent reflections	4170 [R(int) = 0.0300]
Refinement method	Full-matrix least-squares on F^2
Data / restraints / parameters	4154 / 0 / 229
Goodness-of-fit on F^2	1.095
Final R indices [I>2sigma(I)]	R1 = 0.0237, wR2 = 0.0620
R indices (all data)	R1 = 0.0265, wR2 = 0.0717
Largest diff. peak and hole	0.334 and -0.340 e.A^-3

Table A.16b Atomic coordinates (x 10^4) and equivalent isotropic displacement parameters (A^2 x 10^3) for (32). U(eq) is defined as one third of the trace of the orthogonalized Uij tensor.

	x	y	z	U(eq)
Cu(1)	1436(1)	4441(1)	531(1)	22(1)
Cu(2)	249(1)	5049(1)	1563(1)	20(1)
P(1)	2024(1)	4326(1)	-1448(1)	19(1)
P(2)	2333(1)	3815(1)	2961(1)	18(1)
N(1)	1174(2)	4390(1)	-967(1)	25(1)
N(2)	1696(2)	4561(1)	2022(1)	22(1)
N(11)	2777(2)	3323(1)	-1052(2)	40(1)
N(12)	2915(2)	5248(1)	-1146(2)	35(1)
N(13)	1507(2)	4295(1)	-2861(1)	28(1)
N(14)	1802(2)	2716(1)	2920(1)	24(1)
N(15)	3596(2)	3561(1)	3065(1)	29(1)
N(16)	2434(2)	4194(1)	4204(1)	26(1)
C(1)	3637(3)	3079(2)	-1385(3)	60(1)
C(2)	2638(3)	2635(2)	-351(3)	60(1)
C(3)	3658(3)	5430(2)	-1653(3)	53(1)
C(4)	3032(3)	5935(2)	-303(3)	56(1)
C(5)	960(3)	5175(2)	-3457(2)	49(1)
C(6)	838(3)	3461(2)	-3427(2)	57(1)
C(7)	735(3)	2671(2)	2971(2)	37(1)
C(8)	1803(3)	2070(2)	2056(2)	45(1)
C(9)	4336(3)	2786(2)	3754(2)	53(1)
C(10)	4172(2)	4194(2)	2632(2)	44(1)
C(11)	2550(2)	5218(1)	4428(2)	36(1)
C(12)	3061(2)	3636(2)	5229(2)	42(1)

Table A.17a Crystal data and structure refinement for (33)

Identification code	(33)
Empirical formula	C48 H66 Cl2 Mg2 N8 O2 P4
Formula weight	1030.49
Temperature	150(2) K
Wavelength	0.71073 A
Crystal system	Triclinic
Space group	P-1
Unit cell dimensions	a = 10.249(1) A alpha = 114.45(1) deg. b = 11.313(1) A beta = 94.32(1) deg. c = 13.050(1) A gamma = 96.34(1) deg.
Volume	1356.7(2) A^3
Z	1
Density (calculated)	1.261 Mg/m^3
Absorption coefficient	0.305 mm^-1
F(000)	544
Crystal size	0.4 x 0.3 x 0.3 mm
Theta range for data collection	1.73 to 30.33 deg.
Index ranges	-14<=h<=12, -15<=k<=15, -12<=l<=18
Reflections collected	11101
Independent reflections	7148 [R(int) = 0.0251]
Absorption correction	None
Refinement method	Full-matrix least-squares on F^2
Data / restraints / parameters	7081 / 0 / 430
Goodness-of-fit on F^2	1.143
Final R indices [I>2sigma(I)]	R1 = 0.0384, wR2 = 0.0971
R indices (all data)	R1 = 0.0455, wR2 = 0.1168
Largest diff. peak and hole	0.553 and -0.351 e.A^-3

Table A.17b Atomic coordinates (x 10^4) and equivalent isotropic displacement parameters (A^2 x 10^3) for (33). U(eq) is defined as one third of the trace of the orthogonalized Uij tensor.

	x	y	z	U(eq)
Mg	4937(1)	3606(1)	4472(1)	17(1)
Cl	6607(1)	2324(1)	4439(1)	28(1)
P(1)	2081(1)	1389(1)	3305(1)	21(1)
P(2)	5083(1)	5093(1)	2751(1)	16(1)
O	3328(1)	2360(1)	3632(1)	26(1)
N(1)	780(1)	1974(2)	3897(1)	30(1)
N(2)	1706(1)	778(1)	1909(1)	27(1)
N(3)	2275(1)	200(1)	3683(1)	25(1)
N(4)	5222(1)	5055(1)	3931(1)	19(1)
C(1)	-73(2)	2582(3)	3377(2)	48(1)
C(2)	921(2)	2630(2)	5152(2)	39(1)
C(3)	699(2)	-381(2)	1301(2)	44(1)
C(4)	2027(2)	1552(2)	1277(2)	32(1)
C(5)	3505(2)	-372(2)	3485(2)	32(1)
C(6)	1217(2)	-625(2)	3891(2)	33(1)
C(11)	5459(2)	3614(2)	1596(1)	20(1)
C(12)	6405(2)	2952(2)	1868(2)	34(1)
C(13)	6720(3)	1807(2)	1031(2)	48(1)
C(14)	6097(2)	1313(2)	-79(2)	40(1)
C(15)	5159(2)	1957(2)	-357(1)	30(1)
C(16)	4833(2)	3098(2)	476(1)	25(1)
C(21)	3437(2)	5309(1)	2240(1)	21(1)
C(22)	2343(2)	5049(2)	2734(2)	27(1)
C(23)	1078(2)	5198(2)	2360(2)	35(1)
C(24)	909(2)	5610(2)	1500(2)	36(1)
C(25)	2000(2)	5901(2)	1020(2)	32(1)
C(26)	3258(2)	5753(2)	1392(1)	26(1)
C(31)	6135(1)	6452(1)	2657(1)	19(1)
C(32)	7070(2)	6286(2)	1893(1)	25(1)
C(33)	7812(2)	7381(2)	1859(2)	31(1)
C(34)	7630(2)	8642(2)	2585(2)	30(1)
C(35)	6710(2)	8821(2)	3350(2)	27(1)
C(36)	5969(2)	7730(2)	3388(1)	23(1)

Table A.18a Crystal data and structure refinement for (34).

Identification code	(34)
Empirical formula	C16 H37 Br Mg N8 P2
Formula weight	513.70
Temperature	150.0(5). K
Wavelength	0.71073 A
Crystal system	Triclinic
Space group	P-1
Unit cell dimensions	a = 9.645(2) A alpha = 92.647(5) deg. b = 11.048(2) A beta = 91.030(5) deg. c = 11.997(2) A gamma = 95.216(3) deg.
Volume	1271.4(4) A^3
Z	2
Density (calculated)	1.342 Mg/m^3
Absorption coefficient	1.786 mm^-1
F(000)	538
Crystal size	0.3 x 0.2 x 0.1 mm
Theta range for data collection	1.70 to 27.50 deg.
Index ranges	-11<=h<=13, -15<=k<=15, -16<=l<=16
Reflections collected	9271
Independent reflections	5795 [R(int) = 0.0505]
Absorption correction	Multi-scan
Refinement method	Full-matrix least-squares on F^2
Data / restraints / parameters	5631 / 3 / 237
Goodness-of-fit on F^2	1.069
Final R indices [I>2sigma(I)]	R1 = 0.0717, wR2 = 0.1359
R indices (all data)	R1 = 0.1333, wR2 = 0.1842
Largest diff. peak and hole	1.263 and -0.662 e.A^-3

Table A.18b Atomic coordinates (x 10^4) and equivalent isotropic displacement parameters (A^2 x 10^3) for (34). U(eq) is defined as one third of the trace of the orthogonalized Uij tensor.

	x	y	z	U(eq)
Br(1)	2699(1)	637(1)	2800(1)	31(1)
Mg(1)	4718(2)	-92(2)	3846(1)	19(1)
P(1)	6817(2)	-1689(1)	2072(1)	20(1)
P(2)	6772(2)	2271(1)	4510(1)	19(1)
N(1)	6258(5)	-597(4)	2767(4)	20(1)
N(2)	5498(5)	-2312(4)	1296(4)	25(1)
N(3)	7433(5)	-2709(4)	2853(4)	26(1)
N(4)	8135(5)	-1363(5)	1241(4)	26(1)
N(5)	5802(5)	1198(4)	4887(3)	19(1)
N(6)	8277(5)	1849(4)	3993(4)	26(1)
N(7)	7096(5)	3360(4)	5529(4)	27(1)
N(8)	6285(5)	3110(4)	3461(4)	23(1)
C(1)	4455(7)	-1602(6)	816(5)	36(2)
C(2)	5526(7)	-3518(6)	759(6)	41(2)
C(3)	6994(7)	-2849(6)	4000(5)	31(1)
C(4)	8361(7)	-3609(6)	2471(6)	38(2)
C(5)	7869(7)	-846(7)	163(5)	42(2)
C(6)	9457(7)	-868(7)	1762(6)	40(2)
C(7)	8956(6)	975(6)	4642(5)	31(1)
C(8)	9322(7)	2695(6)	3503(6)	39(2)
C(9)	8036(7)	4440(5)	5391(5)	31(1)
C(10)	6925(7)	3084(6)	6697(5)	35(2)
C(11)	6251(7)	2590(6)	2313(4)	30(1)
C(12)	5067(6)	3785(6)	3646(5)	30(1)
C(1S)	11133(11)	-4350(9)	343(8)	77(3)
C(3S)	9171(12)	-4509(11)	-717(10)	94(3)
C(2S)	10358(12)	-3721(10)	-386(10)	102(4)
C(4S)	8345(20)	-3915(18)	-1470(15)	83(6)

Table A.19a Crystal data and structure refinement for (35).

Identification code	(35)
Empirical formula	C6 H19 Br Mg0.50 N4 P
Formula weight	270.29
Temperature	150(2) K
Wavelength	0.71073 A
Crystal system	Monoclinic
Space group	I2/a
Unit cell dimensions	a = 16.1780(3) A alpha = 90 deg. b = 8.1692(2) A beta = 95.8300(10) deg. c = 18.6067(5) A gamma = 90 deg.
Volume	2446.37(10) A^3
Z	8
Density (calculated)	1.468 Mg/m^3
Absorption coefficient	3.483 mm^-1
F(000)	1112
Crystal size	0.2 x 0.2 x 0.1 mm
Theta range for data collection	2.20 to 27.48 deg.
Index ranges	-21<=h<=19, -10<=k<=10, -24<=l<=24
Reflections collected	8611
Independent reflections	2802 [R(int) = 0.0525]
Refinement method	Full-matrix least-squares on F^2
Data / restraints / parameters	2801 / 0 / 190
Goodness-of-fit on F^2	0.942
Final R indices [I>2sigma(I)]	R1 = 0.0433, wR2 = 0.0946
R indices (all data)	R1 = 0.0697, wR2 = 0.1111
Largest diff. peak and hole	2.064 and -0.564 e.A^-3

Table A.19b Atomic coordinates (x 10^4) and equivalent isotropic displacement parameters (A^2 x 10^3) for (35). U(eq) is defined as one third of the trace of the orthogonalized Uij tensor.

	x	y	z	U(eq)
Br(1)	1689(1)	1531(1)	4018(1)	33(1)
P(1)	3623(1)	5683(1)	4020(1)	20(1)
Mg(1)	2500	3156(2)	5000	20(1)
N(1)	3453(2)	4423(4)	4633(2)	23(1)
N(4)	2778(2)	6171(4)	3504(2)	26(1)
N(3)	4303(2)	4899(4)	3513(2)	26(1)
N(2)	3969(2)	7453(4)	4343(2)	28(1)
C(22)	4517(2)	7588(5)	5013(2)	29(1)
C(42)	2510(3)	5240(6)	2846(2)	38(1)
C(41)	2079(3)	6908(6)	3840(3)	37(1)
C(32)	4272(3)	3160(6)	3314(3)	41(1)
C(31)	4753(3)	5917(7)	3032(3)	47(1)
C(21)	3892(4)	9030(6)	3966(3)	53(1)

Table A.20a Crystal data and structure refinement for (36).

Identification code	(36)
Empirical formula	C19 H17 Li N P
Formula weight	297.25
Temperature	293(2) K
Wavelength	0.71073 A
Crystal system	Monoclinic
Space group	C2/c
Unit cell dimensions	a = 18.763(4) A alpha = 90 deg. b = 20.181(4) A beta = 104.52(3) deg. c = 25.127(5) A gamma = 90 deg.
Volume	9210.7(32) A^3
Z	22
Density (calculated)	1.179 Mg/m^3
Absorption coefficient	0.158 mm^-1
F(000)	3432
Crystal size	? x ? x ? mm
Theta range for data collection	1.51 to 22.50 deg.
Index ranges	-24<=h<=24, -26<=k<=26, -32<=l<=32
Reflections collected	25486
Independent reflections	6017 [R(int) = 0.0827]
Refinement method	Full-matrix least-squares on F^2
Data / restraints / parameters	5863 / 0 / 502
Goodness-of-fit on F^2	1.904
Final R indices [I>2sigma(I)]	R1 = 0.1093, wR2 = 0.2962
R indices (all data)	R1 = 0.1545, wR2 = 0.3152
Largest diff. peak and hole	1.085 and -0.338 e.A^-3

Table A.20b Atomic coordinates (x 10^4) and equivalent isotropic displacement parameters (A^2 x 10^3) for (36). U(eq) is defined as one third of the trace of the orthogonalized Uij tensor.

	x	y	z	U(eq)
P(1)	6411(1)	938(1)	2553(1)	36(1)
N(1)	6018(3)	695(3)	3021(2)	35(1)
Li(1)	5000	822(8)	2500	37(4)
C(1)	5742(4)	1372(4)	2071(3)	35(2)
P(2)	5668(1)	2788(1)	3719(1)	32(1)
N(2)	5583(3)	2090(3)	4018(2)	33(1)
Li(2)	5544(6)	1491(6)	3395(5)	41(3)
C(2)	5890(4)	2570(4)	3115(3)	40(2)
Li(3)	5000	2154(10)	2500	65(6)
C(11)	7220(4)	1437(4)	2833(3)	41(2)
C(12)	7523(4)	1834(4)	2483(3)	53(2)
C(13)	8122(5)	2234(4)	2698(4)	61(2)
C(14)	8438(5)	2256(5)	3253(4)	67(3)
C(15)	8150(4)	1867(5)	3606(4)	65(3)
C(16)	7536(4)	1473(4)	3398(3)	50(2)
C(21)	6723(4)	228(4)	2225(3)	47(2)
C(22)	7396(5)	200(4)	2082(3)	60(2)
C(23)	7589(7)	-349(6)	1826(4)	83(3)
C(24)	7124(9)	-877(7)	1705(4)	106(5)
C(25)	6439(7)	-868(5)	1842(4)	91(4)
C(26)	6263(5)	-319(4)	2098(4)	67(3)
C(31)	6286(4)	203(3)	3425(3)	39(2)
C(32)	6985(4)	-96(4)	3523(3)	46(2)
C(33)	7200(5)	-569(4)	3932(3)	61(3)
C(34)	6742(6)	-761(4)	4258(3)	60(2)
C(35)	6048(5)	-470(4)	4165(3)	55(2)
C(36)	5824(4)	4(3)	3757(3)	41(2)
C(41)	6330(4)	3325(4)	4187(3)	37(2)
C(42)	6193(5)	3950(4)	4364(4)	58(2)
C(43)	6749(6)	4308(4)	4726(4)	75(3)
C(44)	7437(5)	4031(5)	4910(4)	65(3)
C(45)	7565(5)	3425(5)	4743(4)	68(3)
C(46)	7037(4)	3073(4)	4381(3)	52(2)
C(51)	4811(4)	3252(4)	3510(3)	41(2)
C(52)	4178(4)	2984(4)	3589(3)	42(2)
C(53)	3491(5)	3294(5)	3370(3)	63(3)
C(54)	3469(6)	3868(6)	3072(4)	86(4)
C(55)	4105(6)	4153(5)	2984(4)	84(3)
C(56)	4779(5)	3842(4)	3207(3)	59(2)
C(61)	5469(3)	2027(3)	4551(3)	31(2)
C(62)	5549(4)	1396(4)	4787(3)	44(2)
C(63)	5428(4)	1290(5)	5305(3)	54(2)
C(64)	5235(5)	1792(5)	5595(4)	62(3)
C(65)	5169(4)	2424(4)	5378(3)	54(2)
C(66)	5285(4)	2547(4)	4861(3)	39(2)
C(71)	3124(6)	1077(6)	4306(3)	70(3)
C(72)	2377(8)	990(8)	4198(4)	104(4)
C(73)	1919(8)	1533(11)	4182(6)	130(6)
C(74)	2208(8)	2133(8)	4297(5)	120(5)
C(75)	2986(9)	2234(8)	4417(5)	121(5)
C(76)	3433(7)	1689(7)	4416(4)	88(3)
C(77)	3622(6)	517(6)	4331(4)	91(4)
C(81)	-272(5)	-248(7)	-393(6)	128(18)
C(82)	-574(5)	376(7)	-363(6)	20(6)
C(83)	-322(4)	765(7)	103(6)	44(8)
C(84)	234(5)	531(6)	538(6)	59(9)
C(85)	536(5)	-93(6)	507(6)	88(13)
C(86)	284(5)	-482(6)	42(6)	29(6)
C(91)	10589(4)	767(4)	2277(5)	105(7)
C(92)	9960(4)	758(4)	1931(5)	95(7)
C(93)	9928(5)	655(5)	1402(5)	63(10)
C(97)	9247(4)	746(4)	2113(4)	110(8)
C(101)	9376(5)	3066(4)	1864(5)	121(9)
C(102)	9632(5)	2425(4)	1997(4)	97(7)
C(103)	10106(4)	2294(4)	2507(4)	41(6)
C(104)	10325(5)	2804(5)	2884(4)	87(6)
C(105)	10070(5)	3445(4)	2752(6)	94(7)
C(106)	9596(5)	3576(4)	2242(6)	112(8)

Table A.21a Crystal data and structure refinement for (37).

Identification code	(37)
Empirical formula	C24 H27 Li2 N P2
Formula weight	405.29
Temperature	293(2) K
Wavelength	0.71073 A
Crystal system	Triclinic
Space group	P-1
Unit cell dimensions	a = 13.327(3) A alpha = 90.03(3) deg. b = 14.467(3) A beta = 98.86(3) deg. c = 26.915(5) A gamma = 114.51(3) deg.
Volume	4653.2(16) A^3
Z	8
Density (calculated)	1.157 Mg/m^3
Absorption coefficient	0.195 mm^-1
F(000)	1712
Crystal size	? x ? x ? mm
Theta range for data collection	1.54 to 27.48 deg.
Index ranges	-17<=h<=16, -18<=k<=18, -34<=l<=34
Reflections collected	51139
Independent reflections	21247 [R(int) = 0.0321]
Refinement method	Full-matrix least-squares on F^2
Data / restraints / parameters	21247 / 0 / 1013
Goodness-of-fit on F^2	1.534
Final R indices [I>2sigma(I)]	R1 = 0.0749, wR2 = 0.2174
R indices (all data)	R1 = 0.1107, wR2 = 0.2363
Largest diff. peak and hole	1.426 and -1.077 e.A^-3

A.21b Atomic coordinates (x 10^4) and equivalent isotropic displacement parameters (A^2 x 10^3) for (37). U(eq) is defined as one third of the trace of the orthogonalized Uij tensor.

	x	y	z	U(eq)
P(1)	431(1)	938(1)	6611(1)	28(1)
N(5)	1331(2)	-539(2)	7568(1)	15(1)
Li(1)	2121(5)	-43(4)	7021(2)	35(1)
N(1)	1566(2)	845(2)	6564(1)	29(1)
C(1)	-375(3)	-118(3)	6938(1)	33(1)
N(6)	3636(2)	310(2)	7363(1)	14(1)
P(2)	4752(1)	1651(1)	8655(1)	27(1)
C(2)	5429(3)	1467(2)	8168(1)	29(1)
Li(2)	2840(4)	-206(4)	7940(2)	30(1)
N(2)	3542(2)	708(2)	8606(1)	28(1)
N(3)	4537(2)	-1633(2)	7086(1)	32(1)
N(7)	2753(2)	-1591(2)	7853(1)	16(1)
Li(3)	3404(5)	-1088(4)	7255(2)	33(1)
P(3)	4868(1)	-2344(1)	7473(1)	33(1)
C(3)	3715(3)	-3021(2)	7794(1)	35(1)
N(4)	241(2)	-3198(2)	7108(1)	31(1)
Li(4)	1349(4)	-1846(4)	7454(2)	31(1)
P(4)	514(1)	-2927(1)	6550(1)	31(1)
C(4)	1689(3)	-1754(3)	6602(2)	42(1)
P(5)	262(1)	-317(1)	7596(1)	32(1)
P(6)	4743(1)	1348(1)	7470(1)	30(1)
P(7)	3172(1)	-2306(1)	8194(1)	34(1)
C(51)	570(3)	812(3)	8028(1)	37(1)
C(52)	-909(3)	-1449(3)	7790(2)	41(1)
C(61)	4468(3)	2490(2)	7334(1)	34(1)
C(62)	5872(3)	1399(3)	7115(1)	35(1)
C(71)	2043(3)	-3348(3)	8455(2)	43(1)
C(72)	4291(3)	-1575(3)	8734(1)	41(1)
C(111)	570(3)	2072(3)	6959(1)	41(1)
C(112)	1610(4)	2840(3)	7126(1)	51(1)
C(113)	1734(7)	3723(4)	7388(2)	89(2)
C(114)	777(9)	3807(5)	7492(2)	112(3)
C(115)	-241(7)	3046(5)	7338(2)	90(2)
C(116)	-380(5)	2168(4)	7063(2)	63(1)
C(121)	-373(3)	919(3)	5998(1)	35(1)
C(122)	-670(3)	1716(3)	5844(1)	44(1)
C(123)	-1250(3)	1671(4)	5362(2)	53(1)
C(124)	-1543(3)	855(4)	5032(2)	54(1)
C(125)	-1244(3)	68(4)	5174(2)	53(1)
C(126)	-658(3)	112(3)	5653(1)	43(1)
C(131)	2315(3)	1413(2)	6249(1)	29(1)
C(132)	3091(3)	1063(3)	6133(1)	34(1)
C(133)	3913(3)	1616(3)	5860(1)	43(1)
C(134)	3973(3)	2543(3)	5675(2)	48(1)
C(135)	3197(3)	2872(3)	5773(1)	44(1)
C(136)	2377(3)	2336(2)	6053(1)	35(1)
C(211)	5655(3)	1794(3)	9260(1)	34(1)
C(212)	5827(3)	943(3)	9414(1)	45(1)
C(213)	6514(4)	1006(3)	9876(2)	55(1)
C(214)	7011(3)	1900(3)	10172(2)	52(1)
C(215)	6843(4)	2731(4)	10026(2)	57(1)
C(216)	6162(4)	2675(3)	9571(1)	47(1)
C(221)	4732(3)	2891(2)	8577(1)	31(1)
C(222)	3713(3)	2957(3)	8533(1)	41(1)
C(223)	3662(4)	3884(3)	8441(2)	61(1)
C(224)	4623(4)	4726(3)	8386(2)	73(2)
C(225)	5638(4)	4668(3)	8433(2)	57(1)
C(226)	5697(3)	3756(3)	8534(1)	39(1)
C(231)	2861(3)	505(2)	8975(1)	32(1)
C(232)	1919(3)	-433(3)	8923(1)	40(1)
C(233)	1165(3)	-689(3)	9255(2)	54(1)
C(234)	1343(4)	-1(4)	9659(2)	64(1)
C(235)	2266(4)	906(4)	9722(2)	59(1)
C(236)	3017(3)	1172(3)	9389(1)	42(1)
C(311)	5123(3)	-3329(3)	7176(2)	40(1)
C(312)	4278(4)	-3980(3)	6806(2)	59(1)
C(313)	4382(5)	-4795(4)	6589(2)	72(1)
C(314)	5333(5)	-4958(3)	6732(2)	65(1)
C(315)	6184(4)	-4304(3)	7094(2)	55(1)
C(316)	6092(3)	-3492(3)	7314(2)	46(1)

C(321)	6075(3)	-1658(3)	7959(1)	37(1)
C(322)	6390(3)	-2137(3)	8365(2)	49(1)
C(323)	7260(4)	-1579(4)	8749(2)	59(1)
C(324)	7809(4)	-538(4)	8736(2)	64(1)
C(325)	7508(3)	-44(3)	8341(2)	54(1)
C(326)	6641(3)	-607(3)	7953(2)	42(1)
C(331)	5091(3)	-1242(2)	6673(1)	33(1)
C(332)	6155(3)	-1165(3)	6632(1)	37(1)
C(333)	6644(3)	-760(3)	6213(2)	43(1)
C(334)	6105(3)	-413(3)	5836(2)	50(1)
C(335)	5056(3)	-465(3)	5877(2)	48(1)
C(336)	4574(3)	-870(3)	6289(1)	39(1)
C(401)	8836(6)	2734(8)	9051(4)	129(4)
C(402)	9210(7)	2144(6)	9350(4)	118(3)
C(403)	10180(6)	2143(5)	9368(3)	102(2)
C(404)	10912(6)	2757(6)	9101(3)	100(2)
C(405)	10622(8)	3357(9)	8801(3)	162(5)
C(406)	9625(10)	3398(9)	8759(3)	151(4)
C(411)	853(1)	-3869(1)	6243(1)	52(1)
C(412)	1125(1)	-3724(1)	5762(1)	294(11)
C(413)	1406(1)	-4420(1)	5529(1)	352(13)
C(414)	1414(2)	-5260(1)	5776(1)	81(2)
C(415)	1142(1)	-5405(1)	6257(1)	85(2)
C(416)	861(1)	-4709(1)	6491(1)	76(2)
C(421)	-672(1)	-2835(1)	6154(1)	32(1)
C(422)	-1604(1)	-2928(1)	6358(1)	36(1)
C(423)	-2504(1)	-2804(1)	6067(1)	40(1)
C(424)	-2455(1)	-2577(1)	5567(1)	48(1)
C(425)	-1533(1)	-2479(1)	5358(1)	57(1)
C(426)	-642(1)	-2598(1)	5649(1)	51(1)
C(431)	-607(1)	-4065(1)	7244(1)	29(1)
C(432)	-1353(1)	-4902(1)	6910(1)	33(1)
C(433)	-2181(1)	-5755(1)	7087(1)	38(1)
C(434)	-2270(1)	-5775(1)	7597(1)	41(1)
C(435)	-1572(1)	-4945(1)	7924(1)	42(1)
C(436)	-755(1)	-4100(1)	7750(1)	37(1)
C(501)	5777(2)	3079(1)	4656(1)	93(2)
C(502)	6369(1)	2758(1)	5067(1)	111(2)
C(503)	6945(1)	3452(1)	5496(1)	114(3)
C(504)	6895(2)	4395(1)	5507(1)	80(2)
C(505)	6289(2)	4639(1)	5121(1)	77(2)
C(506)	5715(2)	4003(1)	4691(1)	77(2)
C(801)	3690(30)	4010(30)	9950(15)	224(15)
C(802)	4800(20)	3796(15)	10331(7)	121(5)
C(803)	6050(20)	5150(20)	10144(9)	143(7)
C(811)	-431(12)	-4870(10)	9920(5)	83(3)
C(812)	-231(11)	-4044(10)	9449(5)	77(3)
C(813)	-1139(15)	-3795(13)	9330(6)	95(4)
C(818)	-50(30)	-4450(30)	9664(15)	243(16)
C(817)	-480(30)	-3440(30)	9181(15)	252(16)
C(816)	-1010(30)	-4660(20)	9676(10)	172(9)
C(806)	4740(30)	4486(18)	9900(10)	176(9)
C(815)	-1400(30)	-3400(20)	9165(12)	204(12)
C(814)	-1800(40)	-4320(30)	9531(17)	284(18)
C(805)	5610(30)	4590(30)	10307(10)	173(10)
C(804)	4020(30)	3800(20)	10220(12)	169(9)

Table A.22a Crystal data and structure refinement for (38)

Identification code	(38)
Empirical formula	C40 H20 Li4 N4 O4 P4
Formula weight	772.24
Temperature	293(2) K
Wavelength	0.71073 A
Crystal system	Triclinic
Space group	P-1
Unit cell dimensions	a = 13.561(3) A alpha = 105.27(3) deg. b = 14.211(3) A beta = 90.02(3) deg. c = 24.345(5) A gamma = 118.38(3) deg.
Volume	3938.3(14) A^3
Z	4
Density (calculated)	1.302 Mg/m^3
Absorption coefficient	0.237 mm^-1
F(000)	1568
Crystal size	? x ? x ? mm
Theta range for data collection	3.26 to 27.39 deg.
Index ranges	-11<=h<=17, -17<=k<=16, -29<=l<=31
Reflections collected	29038
Independent reflections	14411 [R(int) = 0.0605]
Refinement method	Full-matrix least-squares on F^2
Data / restraints / parameters	14392 / 0 / 925
Goodness-of-fit on F^2	2.859
Final R indices [I>2sigma(I)]	R1 = 0.1191, wR2 = 0.3686
R indices (all data)	R1 = 0.1393, wR2 = 0.3833
Largest diff. peak and hole	1.920 and -0.772 e.A^-3

Table A.22b Atomic coordinates (x 10^4) and equivalent isotropic displacement parameters (A^2 x 10^3) for (38). U(eq) is defined as one third of the trace of the orthogonalized Uij tensor.

	x	y	z	U(eq)
P(1)	7341(1)	4782(1)	6290(1)	31(1)
O(1)	5681(2)	6089(2)	5465(1)	29(1)
N(1)	7645(3)	6107(3)	6587(2)	35(1)
C(26)	4381(3)	6345(4)	6410(2)	27(1)
C(16)	5383(3)	7375(3)	6252(2)	26(1)
C(11)	5975(3)	7191(4)	5783(2)	30(1)
C(29)	3419(3)	5541(4)	5898(2)	30(1)
C(15)	5752(4)	8523(4)	6572(2)	34(1)
C(42)	8570(4)	3810(4)	6639(2)	37(1)
C(28)	4823(4)	5658(4)	6628(2)	32(1)
C(31)	6201(4)	3714(4)	6564(2)	36(1)
C(36)	5752(4)	4078(5)	7037(2)	39(1)
C(41)	8568(4)	4593(4)	6378(2)	37(1)
C(1)	6834(4)	4463(5)	5568(2)	38(1)
C(27)	3842(4)	6778(4)	6903(2)	35(1)
C(51)	8152(3)	6810(4)	7149(2)	34(1)
C(43)	9513(4)	3671(5)	6668(2)	46(1)
C(14)	6674(4)	9479(4)	6473(2)	42(1)
C(56)	8256(4)	7917(4)	7322(2)	40(1)
C(35)	4802(5)	3264(6)	7205(2)	53(2)
C(52)	8575(4)	6505(4)	7565(2)	40(1)
C(12)	6897(4)	8162(4)	5661(2)	46(1)
C(53)	9063(4)	7269(5)	8113(2)	48(1)
C(54)	9156(5)	8352(5)	8269(2)	53(1)
C(46)	9527(5)	5255(7)	6151(3)	70(2)
C(32)	5699(4)	2539(5)	6277(2)	49(1)
C(44)	10472(5)	4340(7)	6440(3)	68(2)
C(13)	7230(5)	9277(4)	6027(2)	54(2)
C(33)	4756(5)	1729(5)	6457(3)	60(2)
C(55)	8752(5)	8663(5)	7867(2)	48(1)
C(24)	6675(5)	7404(5)	4580(2)	56(2)
C(25)	7029(5)	10698(4)	6835(2)	55(2)
C(34)	4303(5)	2095(6)	6919(3)	58(2)
C(21)	7529(5)	8034(5)	5141(2)	70(2)
C(23)	8152(5)	7389(7)	5194(3)	95(3)
C(45)	10474(5)	5114(8)	6188(4)	88(3)
Li(1)	6908(7)	6242(8)	5951(3)	45(2)
C(22)	8436(9)	9243(7)	5092(4)	168(7)
P(2)	2556(1)	5216(1)	8711(1)	37(1)
O(2)	-411(3)	3899(3)	9536(1)	40(1)
N(2)	1539(3)	3889(4)	8410(2)	40(1)
C(66)	-1997(4)	2620(4)	8748(2)	33(1)
C(61)	-1214(4)	2809(5)	9220(2)	41(1)
C(76)	-1970(4)	3648(4)	8590(2)	30(1)
C(91)	3984(4)	5428(4)	8625(2)	36(1)
C(78)	-2120(4)	4459(4)	9100(2)	33(1)
C(77)	-841(4)	4335(4)	8374(2)	37(1)
C(92)	4759(4)	6194(4)	8365(2)	36(1)
C(65)	-2768(4)	1489(4)	8432(2)	41(1)
C(82)	1666(5)	5927(6)	7964(2)	50(1)
C(93)	5848(4)	6332(4)	8333(2)	41(1)
C(79)	-2936(4)	3228(4)	8101(2)	36(1)
C(81)	2493(5)	6305(5)	8438(2)	44(1)
C(106)	350(5)	2077(5)	7677(2)	44(1)
C(64)	-2811(6)	530(5)	8530(2)	55(2)
C(2)	2378(5)	5546(5)	9433(2)	47(1)
C(83)	1533(6)	6735(8)	7791(3)	70(2)
C(101)	1355(4)	3194(5)	7850(2)	39(1)
C(103)	1807(5)	2737(5)	6886(2)	52(1)
C(102)	2072(4)	3495(5)	7434(2)	41(1)
C(96)	4276(5)	4750(5)	8849(3)	49(1)
C(62)	-1279(6)	1826(5)	9340(2)	66(2)
C(104)	830(5)	1657(5)	6728(2)	52(1)
C(94)	6133(5)	5674(5)	8568(3)	51(1)
C(86)	3156(7)	7459(6)	8719(2)	68(2)
C(63)	-2029(7)	737(5)	8980(2)	71(2)
C(105)	97(5)	1335(5)	7132(2)	49(1)
C(95)	5348(5)	4875(6)	8818(3)	61(2)
C(74)	-734(6)	2584(5)	10424(2)	64(2)
C(75)	-3678(6)	-691(5)	8172(2)	65(2)

C(85)	3015(8)	8288(7)	8548(3)	80(2)
C(71)	-502(9)	1959(6)	9863(3)	101(4)
C(84)	2196(8)	7906(8)	8081(3)	81(3)
C(73)	-783(15)	770(8)	9906(4)	222(10)
Li(4)	689(9)	3772(9)	9049(4)	54(2)
C(72)	764(9)	2607(9)	9806(3)	128(5)
Li(3)	879(8)	5460(9)	9796(3)	55(3)
Li(2)	4589(7)	5475(7)	4793(3)	42(2)
C(223)	8260(6)	10019(7)	12498(4)	76(5)
C(222)	7408(8)	9377(7)	12026(3)	68(4)
C(221)	6396(6)	9401(8)	12035(3)	81(4)
C(220)	6234(6)	10067(8)	12517(4)	78(5)
C(225)	7086(8)	10709(7)	12989(4)	74(4)
C(224)	8098(7)	10685(6)	12980(3)	65(4)
C(241)	6855(7)	8407(8)	11217(4)	84(5)
C(242)	5849(9)	8423(8)	11300(4)	88(5)
C(243)	5051(7)	8084(9)	10829(6)	107(7)
C(244)	5259(10)	7730(10)	10274(5)	415(51)
C(245)	6266(11)	7715(9)	10191(4)	96(6)
C(246)	7064(8)	8053(9)	10663(5)	99(6)
C(251)	8371(9)	11476(9)	13709(6)	127(8)
C(252)	7327(8)	11433(8)	13672(5)	101(5)
C(253)	6916(9)	11745(10)	14170(7)	275(22)
C(254)	7549(16)	12101(11)	14706(5)	412(43)
C(255)	8593(14)	12143(9)	14743(6)	220(18)
C(256)	9005(7)	11831(9)	14244(8)	760(64)
C(205)	4512(8)	9019(9)	10416(4)	56(4)
C(204)	4933(9)	9793(9)	10108(4)	60(5)
C(203)	5782(9)	9845(9)	9778(4)	72(5)
C(202)	6211(7)	9122(10)	9754(4)	66(5)
C(201)	5791(9)	8348(9)	10061(4)	79(6)
C(200)	4941(9)	8296(8)	10392(4)	87(8)
C(210)	6657(8)	11821(8)	14623(4)	72(6)
C(211)	5515(7)	11079(9)	14602(4)	54(4)
C(212)	5191(6)	10302(8)	14907(4)	55(4)
C(213)	6009(8)	10267(8)	15232(4)	65(5)
C(214)	7151(7)	11009(9)	15253(3)	53(4)
C(215)	7475(6)	11786(8)	14948(4)	54(4)

Table A.23a Crystal data and structure refinement for (40).

Identification code	(40)
Empirical formula	C35 H43 O P
Formula weight	510.66
Temperature	120(2) K
Wavelength	0.71073 A
Crystal system	Monoclinic
Space group	P 21/n
Unit cell dimensions	a = 9.0633(2) A alpha = 90 deg. b = 18.2098(4) A beta = 99.2210(10) deg. c = 18.9012(4) A gamma = 90 deg.
Volume	3079.16(12) A^3
Z	4
Density (calculated)	1.102 Mg/m^3
Absorption coefficient	0.113 mm^-1
F(000)	1104
Crystal size	0.43 x 0.22 x 0.21 mm
Theta range for data collection	1.56 to 25.50 deg.
Index ranges	-10<=h<=10, -22<=k<=20, -22<=l<=22
Reflections collected	27796
Independent reflections	5721 [R(int) = 0.0516]
Absorption correction	None
Refinement method	Full-matrix least-squares on F^2
Data / restraints / parameters	5721 / 0 / 506
Goodness-of-fit on F^2	1.027
Final R indices [I>2sigma(I)]	R1 = 0.0475, wR2 = 0.1247
R indices (all data)	R1 = 0.0693, wR2 = 0.1390
Largest diff. peak and hole	0.940 and -0.562 e.A^-3

Table A.23b Atomic coordinates (x 10^4) and equivalent isotropic displacement parameters (A^2 x 10^3) for (40). U(eq) is defined as one third of the trace of the orthogonalized Uij tensor.

	x	y	z	U(eq)
P(1)	260(1)	2970(1)	482(1)	24(1)
O(1)	-2848(2)	3186(1)	-1180(1)	25(1)
C(1)	267(3)	3621(1)	-219(1)	30(1)
C(2)	-1539(2)	3003(1)	781(1)	28(1)
C(3)	-1988(2)	3756(1)	1012(1)	27(1)
C(4)	-1719(2)	3959(1)	1732(1)	31(1)
C(5)	-2235(3)	4626(1)	1945(1)	36(1)
C(6)	-3000(3)	5105(1)	1451(2)	39(1)
C(7)	-3238(3)	4913(1)	733(2)	37(1)
C(8)	-2738(2)	4244(1)	509(1)	30(1)
C(9)	1755(2)	3130(1)	1199(1)	22(1)
C(10)	1676(2)	2885(1)	1893(1)	23(1)
C(11)	2877(2)	2989(1)	2433(1)	27(1)
C(12)	4168(2)	3325(1)	2286(1)	30(1)
C(13)	4267(2)	3558(1)	1597(1)	31(1)
C(14)	3058(2)	3468(1)	1053(1)	26(1)
C(15)	447(2)	2065(1)	115(1)	26(1)
C(16)	1522(3)	1566(1)	440(1)	32(1)
C(17)	1627(3)	880(1)	136(1)	40(1)
C(18)	621(3)	688(1)	-480(1)	40(1)
C(19)	-452(3)	1172(1)	-784(1)	36(1)
C(20)	-547(3)	1866(1)	-498(1)	31(1)
C(21)	-3867(2)	3339(1)	-1730(1)	24(1)
C(22)	-5317(2)	2986(1)	-1831(1)	25(1)
C(23)	-6372(2)	3159(1)	-2435(1)	30(1)
C(24)	-6095(3)	3659(1)	-2955(1)	33(1)
C(25)	-4712(3)	3999(1)	-2858(1)	33(1)
C(26)	-3593(2)	3866(1)	-2273(1)	27(1)
C(27)	-2094(3)	4279(1)	-2192(1)	32(1)
C(28)	-1897(3)	4740(1)	-1497(1)	36(1)
C(29)	-783(3)	3745(1)	-2183(1)	33(1)
C(30)	-2010(4)	4827(2)	-2808(2)	48(1)
C(31)	-5714(2)	2445(1)	-1264(1)	28(1)
C(32)	-4674(3)	1775(1)	-1190(1)	33(1)
C(33)	-5587(3)	2844(2)	-537(1)	36(1)
C(34)	-7316(3)	2152(2)	-1448(1)	38(1)
C(35)	-7291(3)	3855(2)	-3587(2)	44(1)

Table A.24a Crystal data and structure refinement for (41)

Identification code	(41)
Empirical formula	C36 H30 N O P
Formula weight	523.58
Temperature	150(2) K
Wavelength	0.71073 A
Crystal system	Triclinic
Space group	P -1
Unit cell dimensions	a = 13.3921(1) A alpha = 87.657(1) deg. b = 13.7417(1) A beta = 70.415(1) deg. c = 18.5718(1) A gamma = 61.213(1) deg.
Volume, Z	2791.86(3) A^3, 4
Density (calculated)	1.246 Mg/m^3
Absorption coefficient	0.128 mm^-1
F(000)	1104
Crystal size	0.40 x 0.20 x 0.15 mm
Theta range for data collection	1.18 to 30.51 deg.
Limiting indices	-19<=h<=18, -17<=k<=18, -22<=l<=25
Reflections collected	22635
Independent reflections	14642 [R(int) = 0.0464]
Absorption correction	Multi-scan
Max. and min. transmission	0.970459 and 0.693488
Refinement method	Full-matrix least-squares on F^2
Data / restraints / parameters	14556 / 0 / 719
Goodness-of-fit on F^2	1.082
Final R indices [I>2sigma(I)]	R1 = 0.0649, wR2 = 0.1133
R indices (all data)	R1 = 0.1380, wR2 = 0.1602
Largest diff. peak and hole	0.404 and -0.479 e.A^-3

Table A.24b Atomic coordinates (x 10^4) and equivalent isotropic displacement parameters (A^2 x 10^3) for (41). U(eq) is defined as one third of the trace of the orthogonalized Uij tensor.

	x	y	z	U(eq)
P(1)	8022(1)	5783(1)	1787(1)	21(1)
O(1)	8965(2)	6521(1)	-381(1)	25(1)
N(1)	8700(2)	5303(2)	875(1)	24(1)
C(1)	8948(2)	5947(2)	2231(1)	23(1)
P(2)	533(1)	9382(1)	3193(1)	22(1)
O(2)	-1908(2)	10530(1)	5372(1)	23(1)
N(2)	307(2)	9237(2)	4095(1)	24(1)
C(2)	10213(2)	5229(2)	1937(2)	29(1)
C(3)	10926(3)	5308(3)	2303(2)	38(1)
C(4)	10391(3)	6096(3)	2952(2)	45(1)
C(5)	9149(3)	6815(3)	3232(2)	46(1)
C(6)	8420(3)	6752(2)	2878(2)	35(1)
C(11)	6684(2)	7128(2)	1938(1)	21(1)
C(12)	6785(2)	7925(2)	1472(2)	28(1)
C(13)	5765(2)	8969(2)	1564(2)	30(1)
C(14)	4655(2)	9226(2)	2136(2)	30(1)
C(15)	4563(2)	8452(2)	2614(2)	28(1)
C(16)	5569(2)	7400(2)	2519(2)	26(1)
C(21)	7560(2)	4830(2)	2280(1)	24(1)
C(22)	7288(2)	4199(2)	1892(2)	30(1)
C(23)	6866(3)	3506(2)	2282(2)	39(1)
C(24)	6717(3)	3446(2)	3057(2)	39(1)
C(25)	6991(2)	4069(2)	3444(2)	36(1)
C(26)	7419(2)	4757(2)	3061(2)	31(1)
C(31)	10039(2)	7837(2)	-129(2)	29(1)
C(32)	10416(3)	6996(2)	326(2)	31(1)
C(33)	11505(3)	6611(3)	449(2)	36(1)
C(34)	12263(3)	7051(3)	108(2)	42(1)
C(35)	11918(3)	7879(3)	-352(2)	42(1)
C(36)	10824(3)	8269(2)	-469(2)	37(1)
C(41)	8382(2)	7616(2)	-376(1)	25(1)
C(42)	8848(2)	8307(2)	-239(2)	28(1)
C(43)	8182(3)	9472(2)	-215(2)	35(1)
C(44)	7085(3)	9988(2)	-338(2)	41(1)
C(45)	6657(3)	9322(2)	-507(2)	35(1)
C(46)	7264(2)	8157(2)	-527(2)	28(1)
C(51)	6717(2)	7520(2)	-715(2)	30(1)
C(52)	6183(3)	7824(3)	-1277(2)	40(1)
C(53)	5587(3)	7312(3)	-1430(2)	48(1)
C(54)	5518(3)	6464(3)	-1027(2)	45(1)
C(55)	6059(3)	6128(3)	-478(2)	38(1)
C(56)	6654(2)	6643(2)	-323(2)	32(1)
C(61)	628(2)	10612(2)	2918(1)	22(1)
C(62)	62(2)	11265(2)	2423(2)	29(1)
C(63)	210(2)	12177(2)	2197(2)	32(1)
C(64)	926(2)	12431(2)	2457(2)	32(1)
C(65)	1482(2)	11791(2)	2949(2)	32(1)
C(66)	1332(2)	10885(2)	3183(2)	25(1)
C(71)	1966(2)	8194(2)	2623(1)	24(1)
C(72)	2592(2)	8278(2)	1874(2)	29(1)
C(73)	3694(2)	7364(2)	1429(2)	34(1)
C(74)	4176(3)	6372(2)	1726(2)	36(1)
C(75)	3569(3)	6283(2)	2470(2)	37(1)
C(76)	2460(2)	7191(2)	2923(2)	29(1)
C(81)	-687(2)	9464(2)	2948(2)	24(1)
C(82)	-486(3)	8980(3)	2232(2)	36(1)
C(83)	-1474(3)	9191(3)	2027(2)	45(1)
C(84)	-2657(3)	9873(3)	2535(2)	44(1)
C(85)	-2863(3)	10343(3)	3252(2)	40(1)
C(86)	-1887(2)	10155(2)	3455(2)	31(1)
C(91)	-3295(2)	9365(2)	5642(2)	26(1)
C(92)	-2130(2)	8478(2)	5211(2)	29(1)
C(93)	-1780(3)	7377(2)	5338(2)	35(1)
C(94)	-2566(3)	7121(3)	5907(2)	38(1)
C(95)	-3713(3)	7989(3)	6351(2)	37(1)
C(96)	-4064(3)	9090(3)	6220(2)	32(1)
C(101)	-3035(2)	11090(2)	5385(1)	21(1)
C(102)	-3759(2)	10553(2)	5497(1)	25(1)
C(103)	-4946(2)	11157(2)	5489(2)	31(1)
C(104)	-5463(2)	12270(3)	5380(2)	34(1)

C(105)	-4794(2)	12814(2)	5299(2)	29(1)
C(106)	-3609(2)	12257(2)	5311(1)	24(1)
C(111)	-2982(2)	12927(2)	5244(1)	24(1)
C(112)	-3646(3)	14038(2)	5617(2)	31(1)
C(113)	-3122(3)	14713(2)	5529(2)	36(1)
C(114)	-1894(3)	14286(3)	5073(2)	40(1)
C(115)	-1219(3)	13182(2)	4710(2)	36(1)
C(116)	-1746(2)	12513(2)	4795(2)	28(1)

Table A.25a Crystal data and structure refinement for (42)

Identification code	(42)
Empirical formula	C24 H33 N4 O P
Formula weight	424.51
Temperature	293(2) K
Wavelength	0.71073 A
Crystal system	Monoclinic
Space group	P2(1)/n
Unit cell dimensions	a = 12.8520(2) A alpha = 90 deg. b = 42.4786(7) A beta = 103.1920(10) deg. c = 13.49790(10) A gamma = 90 deg.
Volume	7174.5(2) A^3
Z	12
Density (calculated)	1.179 Mg/m^3
Absorption coefficient	0.137 mm^-1
F(000)	2736
Crystal size	? x ? x ? mm
Theta range for data collection	0.96 to 27.50 deg.
Index ranges	-16<=h<=16, -55<=k<=29, -17<=l<=17
Reflections collected	51407
Independent reflections	16453 [R(int) = 0.1061]
Refinement method	Full-matrix least-squares on F^2
Data / restraints / parameters	16380 / 0 / 847
Goodness-of-fit on F^2	1.175
Final R indices [I>2sigma(I)]	R1 = 0.0812, wR2 = 0.1451
R indices (all data)	R1 = 0.1296, wR2 = 0.1731
Largest diff. peak and hole	0.304 and -0.430 e.A^-3

Table A.25b Atomic coordinates (x 10^4) and equivalent isotropic displacement parameters (A^2 x 10^3) for (42). U(eq) is defined as one third of the trace of the orthogonalized Uij tensor.

	x	y	z	U(eq)
P(1)	6149(1)	1700(1)	7203(1)	22(1)
O(1)	5786(2)	2081(1)	4500(2)	21(1)
N(11)	5438(2)	1713(1)	6074(2)	24(1)
N(12)	6192(2)	1352(1)	7726(2)	32(1)
N(13)	5645(2)	1925(1)	7962(2)	30(1)
N(14)	7337(2)	1825(1)	7150(2)	29(1)
C(101)	5257(3)	1209(1)	7993(3)	46(1)
C(102)	7054(3)	1126(1)	7699(3)	40(1)
C(103)	5874(4)	1897(1)	9075(3)	49(1)
C(104)	5229(4)	2234(1)	7587(3)	45(1)
C(105)	8111(3)	1912(1)	8084(3)	45(1)
C(106)	7815(3)	1775(1)	6272(3)	40(1)
C(107)	6056(2)	2368(1)	4331(2)	20(1)
C(108)	6995(2)	2429(1)	3946(2)	22(1)
C(109)	7273(3)	2738(1)	3763(3)	29(1)
C(110)	6682(3)	2994(1)	3964(3)	31(1)
C(111)	5785(3)	2939(1)	4351(3)	26(1)
C(112)	5461(2)	2635(1)	4541(2)	21(1)
C(113)	7686(3)	2165(1)	3743(2)	25(1)
C(114)	7260(3)	1887(1)	3253(3)	27(1)
C(115)	7922(3)	1651(1)	3032(3)	35(1)
C(116)	9028(3)	1683(1)	3312(3)	41(1)
C(117)	9455(3)	1954(1)	3806(3)	41(1)
C(118)	8797(3)	2192(1)	4020(3)	30(1)
C(119)	4505(3)	2596(1)	4982(2)	24(1)
C(120)	3760(3)	2354(1)	4677(3)	26(1)
C(121)	2871(3)	2322(1)	5092(3)	32(1)
C(122)	2695(3)	2531(1)	5833(3)	35(1)
C(123)	3421(3)	2772(1)	6141(3)	32(1)
C(124)	4310(3)	2805(1)	5728(3)	28(1)
P(2)	3685(1)	1634(1)	2364(1)	21(1)
O(2)	4145(2)	1248(1)	5037(2)	22(1)
N(21)	4370(2)	1639(1)	3505(2)	24(1)
N(22)	3553(2)	1979(1)	1810(2)	32(1)
N(23)	4265(2)	1418(1)	1640(2)	31(1)
N(24)	2522(2)	1486(1)	2405(2)	29(1)
C(201)	4486(4)	2147(1)	1609(3)	53(1)
C(202)	2646(4)	2185(1)	1830(3)	47(1)
C(203)	4047(4)	1439(1)	526(3)	53(1)
C(204)	4774(4)	1123(1)	2048(3)	45(1)
C(205)	2008(3)	1535(1)	3258(3)	47(1)
C(206)	1803(3)	1368(1)	1470(3)	48(1)
C(207)	4023(2)	962(1)	5350(2)	20(1)
C(208)	4745(3)	711(1)	5259(2)	22(1)
C(209)	4601(3)	411(1)	5634(3)	29(1)
C(210)	3746(3)	343(1)	6074(3)	34(1)
C(211)	3020(3)	581(1)	6137(3)	31(1)
C(212)	3129(3)	886(1)	5780(2)	23(1)
C(213)	5627(2)	763(1)	4736(2)	20(1)
C(214)	6312(3)	1024(1)	4938(2)	23(1)
C(215)	7153(3)	1063(1)	4455(3)	28(1)
C(216)	7323(3)	844(1)	3743(3)	30(1)
C(217)	6650(3)	587(1)	3520(3)	29(1)
C(218)	5816(3)	547(1)	4012(2)	24(1)
C(219)	2302(2)	1126(1)	5844(2)	25(1)
C(220)	2562(3)	1433(1)	6187(3)	29(1)
C(221)	1775(3)	1648(1)	6281(3)	42(1)
C(222)	704(4)	1564(1)	6014(4)	52(1)
C(223)	431(3)	1264(1)	5658(3)	51(1)
C(224)	1217(3)	1048(1)	5570(3)	37(1)
P(3)	951(1)	89(1)	12475(1)	21(1)
O(3)	1023(2)	-393(1)	10040(2)	22(1)
N(31)	269(2)	-10(1)	11377(2)	22(1)
N(32)	1186(2)	-235(1)	13132(2)	27(1)
N(33)	2065(2)	268(1)	12440(2)	34(1)
N(34)	319(2)	346(1)	13033(2)	26(1)
C(301)	2057(3)	-252(1)	14055(3)	44(1)
C(302)	466(4)	-506(1)	12997(3)	47(1)
C(303)	2634(4)	490(1)	13219(3)	56(1)
C(304)	2739(3)	126(1)	11816(3)	55(1)
C(305)	-371(3)	244(1)	13689(3)	40(1)

C(306)	99(4)	667(1)	12639(3)	41(1)
C(307)	1274(2)	-683(1)	9879(2)	20(1)
C(308)	2215(2)	-754(1)	9506(2)	21(1)
C(309)	2452(3)	-1067(1)	9320(3)	26(1)
C(310)	1828(3)	-1318(1)	9496(3)	28(1)
C(311)	934(3)	-1253(1)	9879(2)	24(1)
C(312)	648(2)	-947(1)	10080(2)	21(1)
C(313)	2931(2)	-504(1)	9270(2)	22(1)
C(314)	2556(3)	-218(1)	8801(3)	27(1)
C(315)	3249(3)	-6(1)	8501(3)	31(1)
C(316)	4337(3)	-66(1)	8685(3)	36(1)
C(317)	4727(3)	-340(1)	9182(3)	35(1)
C(318)	4045(3)	-555(1)	9475(3)	29(1)
C(319)	-330(3)	-902(1)	10494(2)	21(1)
C(320)	-1077(3)	-662(1)	10157(2)	24(1)
C(321)	-1986(3)	-634(1)	10539(3)	29(1)
C(322)	-2181(3)	-844(1)	11269(3)	33(1)
C(323)	-1457(3)	-1081(1)	11612(3)	34(1)
C(324)	-545(3)	-1111(1)	11228(2)	26(1)

Table A.26a Crystal data and structure refinement for (43).

Identification code	(43)
Empirical formula	C30 H29 N P2
Formula weight	465.48
Temperature	150(2) K
Wavelength	0.71073 A
Crystal system	Monoclinic
Space group	P2(1)/n
Unit cell dimensions	a = 9.555(1) A alpha = 90 deg. b = 10.182(1) A beta = 98.75(1) deg. c = 25.711(2) A gamma = 90 deg.
Volume	2472.3(4) A^3
Z	4
Density (calculated)	1.251 Mg/m^3
Absorption coefficient	0.195 mm^-1
F(000)	984
Crystal size	0.3 x 0.2 x 0.06 mm
Theta range for data collection	1.60 to 25.00 deg.
Index ranges	-11<=h<=11, -12<=k<=10, -30<=l<=30
Reflections collected	14385
Independent reflections	4358 [R(int) = 0.0917]
Reflections observed	3030 [I>2sigma(I)]
Absorption correction	None
Refinement method	Full-matrix least-squares on F^2
Data / restraints / parameters	4252 / 0 / 334
Goodness-of-fit on F^2	1.138
Final R indices [I>2sigma(I)]	R1 = 0.0622, wR2 = 0.1055
R indices (all data)	R1 = 0.1068, wR2 = 0.1336
Largest diff. peak and hole	0.306 and -0.311 e.A^-3

Table A.26b Atomic coordinates (x 10^4) and equivalent isotropic displacement parameters (A^2 x 10^3) for (43). U(eq) is defined as one third of the trace of the orthogonalized Uij tensor.

	x	y	z	U(eq)
P(1)	8483(1)	351(1)	1507(1)	21(1)
P(2)	7146(1)	-536(1)	492(1)	23(1)
N	8461(3)	-555(3)	1011(1)	25(1)
C(1)	9402(3)	-512(4)	2079(1)	21(1)
C(2)	10567(5)	-1431(4)	1957(2)	34(1)
C(3)	9199(5)	-1990(4)	2070(2)	31(1)
C(4)	8023(4)	134(4)	-34(1)	26(1)
C(5)	7134(5)	692(5)	-519(2)	39(1)
C(6)	7963(5)	1588(4)	-131(2)	36(1)
C(11)	9460(4)	1866(4)	1460(1)	23(1)
C(12)	10209(4)	1965(4)	1039(1)	27(1)
C(13)	10983(4)	3079(4)	968(2)	34(1)
C(14)	11003(4)	4113(4)	1314(2)	37(1)
C(15)	10262(4)	4039(4)	1740(2)	35(1)
C(16)	9496(4)	2918(4)	1817(1)	28(1)
C(21)	6734(3)	804(3)	1647(1)	20(1)
C(22)	6124(4)	2020(4)	1497(1)	24(1)
C(23)	4709(4)	2272(4)	1545(1)	26(1)
C(24)	3900(4)	1307(4)	1740(1)	29(1)
C(25)	4498(4)	90(4)	1880(1)	29(1)
C(26)	5899(4)	-165(4)	1831(1)	27(1)
C(31)	9615(4)	193(3)	2601(1)	23(1)
C(32)	8568(4)	186(4)	2924(1)	25(1)
C(33)	8772(4)	809(4)	3410(2)	35(1)
C(34)	10027(5)	1471(4)	3578(2)	38(1)
C(35)	11077(5)	1492(4)	3262(2)	37(1)
C(36)	10871(4)	864(4)	2778(2)	31(1)
C(41)	7136(4)	-2257(4)	275(1)	24(1)
C(42)	8149(4)	-3191(4)	478(1)	29(1)
C(43)	8080(4)	-4470(4)	287(2)	36(1)
C(44)	6994(4)	-4833(4)	-106(2)	36(1)
C(45)	5981(4)	-3928(4)	-312(2)	30(1)
C(46)	6048(4)	-2657(4)	-121(1)	28(1)

Table A.27a Crystal data and structure refinement for (44).

Identification code	(44)
Empirical formula	C37 H33 Li N O P3 S2
Formula weight	671.61
Temperature	120(2) K
Wavelength	0.71073 A
Crystal system	Triclinic
Space group	P -1
Unit cell dimensions	a = 9.9256(2) A alpha = 103.56(1) deg. b = 11.4860(2) A beta = 100.02(1) deg. c = 17.0712(3) A gamma = 108.00(1) deg.
Volume	1734.2(6) A^3
Z	2
Density (calculated)	1.286 Mg/m^3
Absorption coefficient	0.322 mm^-1
F(000)	700
Crystal size	0.40 x 0.10 x 0.06 mm
Theta range for data collection	1.27 to 30.33 deg.
Index ranges	-13<=h<=13, -16<=k<=14, -23<=l<=24
Reflections collected	17706
Independent reflections	9183 [R(int) = 0.0543]
Absorption correction	Multi-scan
Max. and min. transmission	0.81 and 1.0
Refinement method	Full-matrix least-squares on F^2
Data / restraints / parameters	9159 / 0 / 518
Goodness-of-fit on F^2	1.047
Final R indices [I>2sigma(I)]	R1 = 0.0633, wR2 = 0.1252
R indices (all data)	R1 = 0.1318, wR2 = 0.1653
Largest diff. peak and hole	0.768 and -0.489 e.A^-3

Table A.27b Atomic coordinates (x 10^4) and equivalent isotropic displacement parameters (A^2 x 10^3) for (44). U(eq) is defined as one third of the trace of the orthogonalized Uij tensor.

	x	y	z	U(eq)
P(1)	5448(1)	8337(1)	2444(1)	22(1)
P(2)	6292(1)	6297(1)	2982(1)	19(1)
P(3)	2174(1)	3145(1)	-45(1)	25(1)
S(1)	4330(1)	7394(1)	1255(1)	27(1)
S(2)	6237(1)	5052(1)	1935(1)	28(1)
O(1)	3611(2)	4139(2)	-10(1)	26(1)
N(1)	6212(3)	7665(3)	2998(2)	29(1)
Li(1)	5163(6)	5635(5)	781(3)	27(1)
C(1)	4240(4)	8919(3)	2988(2)	26(1)
C(2)	2729(4)	8323(4)	2707(3)	37(1)
C(3)	1815(5)	8718(4)	3156(3)	47(1)
C(4)	2422(5)	9746(5)	3874(3)	51(1)
C(5)	3910(6)	10356(6)	4162(4)	79(2)
C(6)	4833(5)	9944(5)	3723(3)	62(2)
C(7)	6907(4)	9805(3)	2499(2)	28(1)
C(8)	6564(5)	10770(4)	2232(3)	44(1)
C(9)	7677(5)	11870(4)	2242(3)	54(1)
C(10)	9136(5)	12006(5)	2518(3)	52(1)
C(11)	9479(5)	11064(4)	2782(3)	45(1)
C(12)	8371(4)	9967(4)	2779(2)	31(1)
C(13)	4925(3)	5489(3)	3455(2)	23(1)
C(14)	4450(4)	4161(4)	3311(3)	35(1)
C(15)	3483(5)	3604(6)	3737(3)	55(1)
C(16)	3013(5)	4338(7)	4308(3)	62(2)
C(17)	3473(5)	5636(6)	4446(3)	54(1)
C(18)	4424(4)	6226(4)	4029(2)	35(1)
C(19)	8005(3)	6679(3)	3757(2)	23(1)
C(20)	8658(4)	7882(4)	4369(2)	29(1)
C(21)	9934(4)	8155(4)	4981(2)	38(1)
C(22)	10576(4)	7255(4)	4989(3)	42(1)
C(23)	9946(4)	6054(4)	4379(3)	41(1)
C(24)	8663(4)	5768(4)	3770(2)	30(1)
C(25)	1031(5)	2448(4)	-1099(2)	36(1)
C(26)	2391(4)	1832(4)	315(3)	39(1)
C(27)	1995(6)	1587(5)	1035(3)	63(1)
C(28)	2232(6)	591(4)	1313(3)	61(1)
C(29)	2756(5)	-192(4)	837(3)	56(1)
C(30)	3116(7)	-8(6)	130(4)	89(2)
C(31)	2936(7)	1027(5)	-120(4)	82(2)
C(32)	1185(4)	3806(3)	607(2)	24(1)
C(33)	1915(4)	4473(3)	1452(2)	28(1)
C(34)	1181(4)	4945(4)	1994(2)	35(1)
C(35)	-275(4)	4781(4)	1701(2)	35(1)
C(36)	-1012(4)	4130(4)	866(3)	36(1)
C(37)	-296(4)	3636(4)	317(2)	31(1)

Table A.28a Crystal data and structure refinement for (45)

Identification code	$[(^tBu)_2MeC_6H_2OLi.thf]_2$
Empirical formula	C39 H62 Li2 O4
Formula weight	608.77
Temperature	100(2) K
Wavelength	0.71073 A
Crystal system	Monoclinic
Space group	P 2(1)/c
Unit cell dimensions	a = 11.4891(4) A alpha = 90 deg. b = 15.6993(5) A beta = 103.292(1) deg. c = 21.4274(7) A gamma = 90 deg.
Volume	3761.3(2) A^3
Z	4
Density (calculated)	1.075 Mg/m^3
Absorption coefficient	0.066 mm^-1
F(000)	1336
Crystal size	0.50 x 0.45 x 0.32 mm
Theta range for data collection	1.86 to 30.44 deg.
Index ranges	-15<=h<=16, -22<=k<=21, -29<=l<=28
Reflections collected	45725
Independent reflections	10515 [R(int) = 0.0477]
Refinement method	Full-matrix least-squares on F^2
Data / restraints / parameters	10515 / 0 / 627
Goodness-of-fit on F^2	1.011
Final R indices [I>2sigma(I)]	R1 = 0.0564, wR2 = 0.1461
R indices (all data)	R1 = 0.0850, wR2 = 0.1673
Largest diff. peak and hole	0.606 and -0.413 e.A^-3

Table A.28b Atomic coordinates (x 10^4) and equivalent isotropic displacement parameters (A^2 x 10^3) for (45). U(eq) is defined as one third of the trace of the orthogonalized Uij tensor.

	x	y	z	U(eq)
O(1)	4086(1)	5445(1)	4572(1)	22(1)
O(2)	6306(1)	4852(1)	3901(1)	35(1)
O(21)	5298(1)	5240(1)	648(1)	20(1)
O(22)	4875(1)	3094(1)	314(1)	28(1)
Li(1)	5555(2)	4936(2)	4596(1)	29(1)
Li(2)	4906(3)	4281(2)	170(1)	27(1)
C(1)	3345(1)	5902(1)	4122(1)	20(1)
C(2)	3528(1)	6800(1)	4062(1)	20(1)
C(3)	2743(1)	7256(1)	3580(1)	23(1)
C(4)	1786(1)	6879(1)	3156(1)	24(1)
C(5)	1611(1)	6009(1)	3220(1)	24(1)
C(6)	2354(1)	5506(1)	3686(1)	22(1)
C(7)	2067(1)	4550(1)	3736(1)	28(1)
C(8)	1753(2)	4380(1)	4387(1)	38(1)
C(9)	3117(2)	3985(1)	3658(1)	37(1)
C(10)	981(2)	4265(1)	3214(1)	46(1)
C(11)	4540(1)	7281(1)	4528(1)	24(1)
C(12)	4548(2)	8239(1)	4366(1)	30(1)
C(13)	4356(2)	7220(1)	5216(1)	33(1)
C(14)	5779(2)	6934(1)	4503(1)	38(1)
C(15)	955(2)	7399(1)	2643(1)	30(1)
C(16)	5773(2)	5155(1)	3258(1)	39(1)
C(17)	6267(2)	4594(1)	2818(1)	42(1)
C(18)	7556(2)	4528(2)	3192(1)	41(1)
C(19)	7451(2)	4476(2)	3893(1)	31(1)
C(18A)	7414(11)	4075(9)	3269(6)	55(3)
C(19A)	7267(8)	4150(6)	3904(4)	29(2)
C(21)	5688(1)	5719(1)	1170(1)	18(1)
C(22)	6940(1)	5880(1)	1405(1)	20(1)
C(23)	7303(1)	6459(1)	1908(1)	25(1)
C(24)	6504(2)	6868(1)	2205(1)	26(1)
C(25)	5299(1)	6666(1)	2002(1)	24(1)
C(26)	4863(1)	6094(1)	1501(1)	20(1)
C(27)	3523(1)	5877(1)	1322(1)	24(1)
C(28)	3334(1)	4904(1)	1349(1)	28(1)
C(29)	2940(2)	6238(1)	656(1)	32(1)
C(30)	2840(2)	6268(1)	1795(1)	38(1)
C(31)	7885(1)	5397(1)	1130(1)	24(1)
C(32)	7757(2)	5586(1)	412(1)	30(1)
C(33)	7754(2)	4436(1)	1231(1)	31(1)
C(34)	9173(2)	5647(2)	1465(1)	44(1)
C(35)	6931(2)	7480(1)	2757(1)	38(1)
C(36)	5258(2)	2713(1)	943(1)	41(1)
C(37)	5471(2)	1777(1)	815(1)	37(1)
C(38)	4484(2)	1613(1)	220(1)	31(1)
C(39)	4485(2)	2431(1)	-162(1)	29(1)

Table A.29a Crystal data and structure refinement for $Ph_2MePNPh$.

Identification code	$Ph_2MePNPh$
Empirical formula	C19 H18 N P
Formula weight	291.31
Temperature	150(2) K
Wavelength	0.71073 A
Crystal system	Monoclinic
Space group	P(2)1/c
Unit cell dimensions	a = 12.107(2) A alpha = 90 deg. b = 24.607(4) A beta = 109.338(4) deg. c = 11.041(2) A gamma = 90 deg.
Volume	3103.7(9) A^3
Z	8
Density (calculated)	1.247 Mg/m^3
Absorption coefficient	0.170 mm^-1
F(000)	1232
Crystal size	? x ? x ? mm
Theta range for data collection	1.66 to 30.50 deg.
Index ranges	-16<=h<=11, -34<=k<=35, -9<=l<=15
Reflections collected	22409
Independent reflections	8572 [R(int) = 0.0408]
Refinement method	Full-matrix least-squares on F^2
Data / restraints / parameters	8572 / 0 / 523
Goodness-of-fit on F^2	1.019
Final R indices [I>2sigma(I)]	R1 = 0.0440, wR2 = 0.0979
R indices (all data)	R1 = 0.0803, wR2 = 0.1129
Largest diff. peak and hole	0.371 and -0.368 e.A^-3

Table A.29b Atomic coordinates (x 10^4) and equivalent isotropic displacement parameters (A^2 x 10^3) for $Ph_2MePNPh$. U(eq) is defined as one third of the trace of the orthogonalized Uij tensor.

	x	y	z	U(eq)
P(1)	5360(1)	962(1)	146(1)	19(1)
P(2)	11159(1)	1959(1)	1054(1)	20(1)
N(2)	11351(1)	1706(1)	2421(1)	24(1)
C(13)	5216(1)	1675(1)	476(2)	21(1)
N(1)	5881(1)	610(1)	1403(1)	22(1)
C(7)	6140(1)	945(1)	-1004(2)	21(1)
C(31)	9829(1)	2347(1)	662(2)	20(1)
C(6)	8016(2)	808(1)	1998(2)	24(1)
C(1)	7031(1)	612(1)	2259(2)	20(1)
C(32)	10994(1)	1468(1)	-219(2)	23(1)
C(18)	5638(2)	1853(1)	1745(2)	23(1)
C(20)	12309(1)	1395(1)	3141(2)	22(1)
C(28)	7785(2)	2957(1)	173(2)	28(1)
C(2)	7222(2)	385(1)	3482(2)	25(1)
C(4)	9296(2)	566(1)	4115(2)	27(1)
C(27)	8044(2)	2549(1)	1089(2)	28(1)
C(25)	12336(2)	1228(1)	4368(2)	27(1)
C(17)	5565(2)	2400(1)	2037(2)	25(1)
C(14)	4694(2)	2051(1)	-495(2)	25(1)
C(5)	9129(2)	785(1)	2912(2)	26(1)
C(30)	9560(2)	2753(1)	-268(2)	26(1)
C(8)	6155(2)	460(1)	-1662(2)	26(1)
C(12)	6851(2)	1375(1)	-1120(2)	24(1)
C(16)	5065(2)	2770(1)	1066(2)	27(1)
C(26)	9052(2)	2243(1)	1332(2)	24(1)
C(19)	3909(2)	725(1)	-674(2)	27(1)
C(38)	12262(2)	2430(1)	937(2)	28(1)
C(15)	4622(2)	2597(1)	-198(2)	28(1)
C(22)	14184(2)	942(1)	3549(2)	32(1)
C(21)	13253(2)	1236(1)	2749(2)	25(1)
C(23)	14205(2)	790(1)	4765(2)	37(1)
C(35)	10761(2)	686(1)	-2121(2)	34(1)
C(34)	10799(2)	1233(1)	-2406(2)	35(1)
C(3)	8334(2)	363(1)	4390(2)	28(1)
C(9)	6868(2)	415(1)	-2420(2)	33(1)
C(11)	7560(2)	1326(1)	-1880(2)	28(1)
C(36)	10821(2)	529(1)	-896(2)	32(1)
C(37)	10926(2)	917(1)	48(2)	26(1)
C(33)	10923(2)	1623(1)	-1467(2)	30(1)
C(29)	8536(2)	3057(1)	-515(2)	28(1)
C(10)	7563(2)	846(1)	-2532(2)	33(1)
C(24)	13270(2)	932(1)	5164(2)	33(1)

Appendix B

Research Colloquia, Lectures and Conferences Attended

Research Colloquia, Lectures and Seminars

1996

October 22 Professor Lutz Gade, Univ. Wurzburg, Germany
Organic transformations with Early-Late Heterobimetallics: Synergism and Selectivity

October 22 Professor B. J. Tighe, Department of Molecular Sciences and Chemistry, University of Aston
Making Polymers for Biomedical Application - can we meet Nature's Challenge?

October 23 Professor H. Ringsdorf (Perkin Centenary Lecture), Johannes Gutenberg-Universitat, Mainz, Germany
Function Based on Organisation

October 29 Professor D. M. Knight, Department of Philosophy, University of Durham.
The Purpose of Experiment - A Look at Davy and Faraday

October 30 Dr Phillip Mountford, Nottingham University
Recent Developments in Group IV Imido Chemistry

November 12 Professor R. J. Young, Manchester Materials Centre, UMIST
New Materials - Fact or Fantasy?
Joint Lecture with Zeneca & RSC

November 18 Professor G. A. Olah, University of Southern California, USA
Crossing Conventional Lines in my Chemistry of the Elements

November 19 Professor R. E. Grigg, University of Leeds
Assembly of Complex Molecules by Palladium-Catalysed Queueing Processes

1997

January 16 Dr Sally Brooker, University of Otago, NZ
Macrocycles: Exciting yet Controlled Thiolate Coordination Chemistry

January 21 Mr D. Rudge, Zeneca Pharmaceuticals
High Speed Automation of Chemical Reactions

January 22 Dr Neil Cooley, BP Chemicals, Sunbury
Synthesis and Properties of Alternating Polyketones

January 29 Dr Julian Clarke, UMIST
What can we learn about polymers and biopolymers from computer-generated nanosecond movie-clips?

February 4 Dr A. J. Banister, University of Durham
From Runways to Non-metallic Metals - A New Chemistry Based on Sulphur

February 12 Dr Geert-Jan Boons, University of Birmingham
New Developments in Carbohydrate Chemistry

February 18 Professor Sir James Black, Foundation/King's College London
My Dialogues with Medicinal Chemists

February 19 Professor Brian Hayden, University of Southampton
The Dynamics of Dissociation at Surfaces and Fuel Cell Catalysts

February 25 Professor A. G. Sykes, University of Newcastle
The Synthesis, Structures and Properties of Blue Copper Proteins

March 4 Professor C. W. Rees, Imperial College
Some Very Heterocyclic Chemistry

March 11 Dr A. D. Taylor, ISIS Facility, Rutherford Appleton Laboratory
Expanding the Frontiers of Neutron Scattering

October 15 Dr R M Ormerod, Department of Chemistry, Keele University
Studying catalysts in action

October 21 Professor A F Johnson, IRC, Leeds
Reactive processing of polymers: science and technology

October 27 Professor W Roper FRS. University of Auckland, New Zealand

October 28 Professor A P de Silva, The Queen's University, Belfast
Luminescent signalling systems"

November 5 Dr M Hii, Oxford University
Studies of the Heck reaction

November 11 Professor V Gibson, Imperial College, London
Metallocene polymerisation

November 25 Dr R Withnall, University of Greenwich
Illuminated molecules and manuscripts

November 26 Professor R W Richards, University of Durham, Inaugural Lecture
A random walk in polymer science

December 2 Dr C J Ludman, University of Durham
Explosions

1998

January 20 Professor J Brooke, University of Lancaster
What's in a formula? Some chemical controversies of the 19th century

February 3 Dr J Beacham, ICI Technology
The chemical industry in the 21st century

February 24 Professor R Ramage, University of Edinburgh
The synthesis and folding of proteins

February 25 Dr C Jones, Swansea University
Low coordination arsenic and antimony chemistry

March 11 Professor M J Cook, Dept of Chemistry, UEA
How to make phthalocyanine films and what to do with them.

March 18 Dr J Evans, Oxford University
Materials which contract on heating (from shrinking ceramics to bullet proof vests)

October 9 Professor M F Hawthorne, Department Chemistry & Biochemistry, UCLA, USA
RSC Endowed Lecture

October 28 Professor J P S Badyal, Department of Chemistry, University of Durham
Tailoring Solid Surfaces, Inaugural Lecture

November 3 Dr C J Ludman, Chemistry Department, University of Durham
Bonfire night Lecture

November 4 Dr N Kaltscoyannis, Department of Chemistry, UCL, London
Computational Adventures in d & f Element Chemistry

November 10 Dr J S O Evans, Chemistry Department, University of Durham
Shrinking Materials

November 12 Professor S Loeb, University of Windsor, Ontario, Canada
From Macrocycles to Metallo-Supramolecular Chemistry

November 17 Dr J McFarlane
Nothing but Sex and Sudden Death!

November 18 Dr R Cameron, Department of Materials Science & Metallurgy, Cambridge University
Biodegradable Polymers

November 24 Dr B G Davis, Department of Chemistry, University of Durham
Sugars and Enzymes

December 9	Dr M Smith Department. of Chemistry, Warwick University Multinuclear solid-state magnetic resonance studies of nanocrystalline oxides and glasses
January 27	Professor K Wade, Department of Chemistry, University of Durham Foresight or Hindsight? Some Borane Lessons and Loose Ends
February 9	Professor D J Cole-Hamilton, St. Andrews University Chemistry and the Future of life on Earth
March 9	Dr Michael Warhurst, Chemical Policy issues, Friends of the Earth Is the Chemical Industry Sustainable?
March 10	Dr A Harrison, Department of Chemistry, The University of Edinburgh Designing model magnetic materials
May 11	Dr John Sodeau, University of East Anglia Ozone Holes and Ozone Hills

Lecture Courses

October 1996 - March 1997

Practical nuclear-magnetic resonance	Dr. A. M. Kenwright
Diffraction and Scattering methods	Dr. C. W. Lehmann
Molecular Modelling	Dr. C. W. Lehmann

Conferences and Symposia

Fourth Anglo/German Inorganic Chemistry meeting, September 14-17, 1997, Marburg, Germany.†

Second International Conference on the Chemistry of the Alkali and Alkaline Earth Metals, September 17-20, 1997, Erlangen, Germany.†

1998 National Congress and Young Researchers' Meeting, April 6-9, Durham, UK. †

Main Group Symposium in Honour of Dr. Arthur Bannister and Profs. Evelyn Ebsworth and Kenneth Wade, June 29, 1998, Durham, UK.

32nd annual Universities of Scotland Inorganic Club Conference, September 15-16, 1998, Strathclyde, UK. †‡

'*The chemists are a strange class of mortals impelled by an almost insane impulse to seek their pleasure among smoke and vapor, soot and flame, poison and poverty. Yet among these evils I seem to live so sweetly...*' (J.J.Becher c.a. 1675).

† Poster presented to these conferences.
‡ Oral contribution presented to this conference.